THE SILENCING OF HER2/*neu* GENE EXPRESSION IN A BREAST CANCER CELL MODEL USING CATIONIC LIPID BASED DELIVERY SYSTEMS

BY

ADHIKA BALGOBIND

Submitted in fulfilment of the academic requirements for the degree of

DOCTOR OF PHILOSOPHY

In the School of Life Sciences,

University of KwaZulu-Natal, Westville Campus.

June 2016

As the candidate's supervisor and co-supervisor respectively, we approve submission of this thesis.

Supervisor: **Dr. Moganavelli Singh**

Signed: _____ Date: _____

Co-Supervisor: **Professor Mario Ariatti**

Signed: _____ Date: _____

ABSTRACT

RNA interference technology, based on the use of siRNA, has emerged as a promising approach in the treatment strategy to suppress disease-causing genes such as those associated with breast cancer (BC). Despite its potential as a form of therapy, instability and poor cellular uptake of the therapeutic nucleic acid have posed daunting challenges. The major hurdle for siRNA-based therapy is the evolution of nontoxic, stable and efficient delivery systems to channel siRNA into target cells. Accordingly, this study assesses the efficacy of two cationic lipid-based delivery systems to deliver intact siRNA which would target the Human Epidermal Growth Factor Receptor 2 (HER2/*neu*) oncogene in a BC cell model.

A series of cationic liposomes were formulated using an equimolar ratio of the respective cytofectins together with the neutral lipid dioleoylphosphatidylethanolamine (DOPE). Sterically stabilized or stealth liposomes contained a 0-5 mol.% 1,2-Distearoyl-*sn*-glycero-3-phosphoethanolamine-N-[methoxy(polyethylene glycol)-2000] (DSPE-PEG_{2000}) grafting.

Cryogenic-transmission electron microscopy (cryo-TEM) and dynamic light scattering measurements revealed that PEGylation generated smaller, defined structures when compared to their non-PEGylated counterparts. The hydrodynamic size ranges of the liposomal formulations and lipoplexes were 65-127 nm and 103-237 nm respectively, with moderate particle size distributions (polydispersity indices were <0.4). Liposomes bound and efficiently compacted pCMV-*luc* plasmid DNA (pDNA) and siRNA as evidenced in band shift and ethidium bromide intercalation assays respectively, while nuclease digestion assays demonstrated that the degradative effect of serum on lipoplex-associated nucleic acid was minimal.

Cytotoxicity studies, involving the reduction of 3-(4, 5-dimethyl-2-thiazolyl)-2, 5-diphenyl-2H-tetrazolium bromide (MTT), indicated that the pDNA and siRNA lipoplexes elicited a dose-dependent cytotoxic effect, with cell viability remaining above 70% and 50% respectively. Effective *in vitro* pCMV-*luc* pDNA and HER2/*neu*-specific siRNA transfections were achieved in all BC cell lines tested in the presence of serum. Gene expression studies indicated that the Chol-T:DOPE (0% PEG)/siRNA complexes induced the highest HER2/*neu* silencing effect at all tested N/P charge ratios, as observed from the significant fold-decrease in gene expression (> 10 000-fold, $P<0.001$). Western blot analysis further confirmed this trend and revealed a dose-dependent decrease in HER2/*neu* protein expression levels as indicated by a

160.28, 163.89 and 212.80-fold decrease in protein expression relative to the untreated SKBR-3 cells. Furthermore, the most active non-PEGylated Chol-T formulations were less cytotoxic and exceeded the knockdown level of Lipofectamine® 3000 control (4.1-fold decrease). Results suggest that these cytofectin-based cationic liposomes with moderate degree of PEGylation have potential as vectors for trans-gene expression and HER2/*neu* siRNA gene silencing in BC cells.

PREFACE

The experimental work described in this thesis was carried out in the School of Life Sciences, University of KwaZulu-Natal (Westville Campus), Durban, South Africa from May 2010 to June 2016, under the supervision of Dr. M. Singh and the co-supervision of Professor M. Ariatti.

These studies represent original work by the author and have not otherwise been submitted in any form for any degree or diploma to any tertiary institution. Where use has been made of the work of others it is duly acknowledged in the text.

DECLARATION 1 - PLAGIARISM

I, Adhika Balgobind declare that

1. The research reported in this thesis, except where otherwise indicated, is my original research.

2. This thesis has not been submitted for any degree or examination at any other university.

3. This thesis does not contain other persons' data, pictures, graphs or other information, unless specifically acknowledged as being sourced from other persons.

4. This thesis does not contain other persons' writing unless specifically acknowledged as being sourced from other researchers. Where other written sources have been quoted, then:

- **a.** Their words have been re-written but the general information attributed to them has been referenced.
- **b.** Where their exact words have been used, then their writing has been placed in italics and inside quotation marks, and referenced.

5. This thesis does not contain text, graphics or tables copied and pasted from the internet, unless specifically acknowledged, and the source being detailed in the thesis and in the Reference Section.

Signed: _____

Declaration Plagiarism 22/05/08 FHDR Approved

DECLARATION 2 - PUBLICATIONS

DETAILS OF CONTRIBUTION TO PUBLICATIONS that form part and/or include research presented in this thesis (include publications in preparation, submitted, *in press* and published and give details of the contributions of each author to the experimental work and writing of each publication).

Manuscripts

Balgobind, A., Ariatti, M., and Singh, M. Cationic lipid based nanosystems associated with siRNA: Enhanced HER2/*neu* gene silencing in a breast cancer cell model in the presence of serum. *In preparation* (**Appendix B**)

Balgobind, A., Ariatti, M., and Singh, M. Silencing breast cancer using siRNA gene knockdown technology: Potential therapeutic impact and progress in developing non-viral nanocarrier systems. *In preparation* (**Appendix B**)

Presentations

Presented a portion of my current doctoral research at the 1st Internatinal Conference and Exhibition on Cancer Science, held in Las Vegas during August 2011.

Presented at a conference hosted by The South African Society of Biochemistry and Molecular Biology SASBMB/FASBMB Congress 2012 held at the Champagne Sport's Resort, Drakensberg, KZN from 29 January to 1 February 2012.

Signed: _____

Declaration Publications FHDR 22/05/08 Approved

TABLE OF CONTENTS

ABSTRACT ii

PREFACE iv

DECLARATION 1 - PLAGIARISM v

DECLARATION 2 - PUBLICATIONS vi

TABLE OF CONTENTS vii

LIST OF FIGURES xii

LIST OF TABLES xvi

ABBREVIATIONS AND SYMBOLS xvii

ACKNOWLEDGEMENTS xxii

CHAPTER ONE

INTRODUCTION

1.1 Background to the Study 1

1.2 Scope of the Present Study 3

1.2.1 Hypothesis tested 4

1.2.2 Objectives 4

1.2.3 Aims 5

1.3 Novelty of Study 5

1.4 Overview of the Thesis 6

CHAPTER TWO

LITERATURE REVIEW

2.1 The Nature of Cancer 8

2.2 Breast Cancer 9

2.3 The Normal Mammary Gland and the Biology of Breast Cancer 9

2.3.1 Development of the mammary gland 9

2.3.2 The biology of breast cancer 12

2.4 Classification of Breast Cancer 14

2.4.1 Immunohistochemical classification 14

2.4.2 Molecular classification 15
2.5 The Human Epidermal Growth Factor Receptor 2 (HER2/*neu*) 15
2.5.1 Physiological role of HER2/*neu* 15
2.5.2 HER2/*neu* receptor biology 16
2.5.3 HER2/*neu* receptor mechanism of action and signaling pathways 18
2.5.4 The role of HER2/*neu* in breast cancer 20
2.5.5 HER2/*neu* as a target for breast cancer therapy 21
2.6 Current Treatment Options for HER2/*neu* 22
2.6.1 Antibody targeting the extracellular domain 22
2.6.2 Tyrosine kinase inhibitors to HER2/*neu* receptor 23
2.7 Overview of Gene Therapy 24
2.8 History, Uniqueness and Mechanism of siRNA Gene Silencing 26
2.8.1 Advances in RNA interference 26
2.8.2 Mechanism of siRNA gene silencing 27
2.9 Therapeutic Potential of siRNA Gene Silencing 30
2.9.1 Identifying targets for siRNA-induced gene silencing 30
2.9.1.1 Inhibition of angiogenesis 30
2.9.1.2 Apoptosis 31
2.9.1.3 Cell cycle regulation 33
2.9.1.4 HER2/*neu* 33
2.9.1.5 Sensitizing drug resistant proteins to conventional therapies 35
2.10 Challenging Pharmacokinetic Characteristics of Synthetic siRNA 36
2.11 Nanocarriers for siRNA Gene Delivery 37
2.11.1 Stealth technology - nanocarrier biological stability 40
2.11.2 Lipid-based systems 43
2.11.2.1 Cationic liposomes 46
2.11.2.2 Anionic and neutral liposomes 48
2.11.3 Polymer systems 49
2.11.3.1 Synthetic polymers 50
2.11.3.2 Natural polymers 52
2.12 Cellular Binding, Uptake and Internalization 54

2.12.1 Cellular binding: Passive and active targeting 54
2.12.2 Cellular uptake and internalization 55

CHAPTER THREE
MATERIALS AND METHODS
3.1 Liposome Formulation 56
3.1.1 Materials, chemicals and reagents 56
3.1.2 Liposome preparation 56
3.2 Physical Characterization of Liposome and Liposome-Nucleic Acid Interactions 58
3.2.1 Materials, chemicals and reagents 58
3.2.2 Plasmid DNA 58
3.2.3 Small interfering RNA (siRNA) duplexes 59
3.2.4 Preparation of Chol-T- and MS09-liposome / pCMV-*luc* or siRNA lipoplexes 60
3.2.5 Imaging and sizing 60
3.2.5.1 Cryogenic-transmission electron microscopy (cryo-TEM) 60
3.2.5.2 Determination of particle size, polydispersity index and zeta potential 61
3.2.6 Nucleic acid binding capacity of cationic liposomes by gel retardation 62
3.2.6.1 Cationic liposome-pDNA interactions 62
3.2.6.2 Cationic liposome-siRNA interactions 63
3.2.7 Serum nuclease protection assay 66
3.2.8 Ethidium bromide dye displacement assay 68
3.3 Cell Lines and Routine Cell Culture Techniques 69
3.3.1 Materials, chemicals and reagents 69
3.3.2 Cell lines and maintenance 70
3.3.3 Cryopreservation and reconstitution of cells 71
3.3.4 Examination of cultures 71
3.4 Transfections 72
3.4.1 Materials, chemicals and reagents 72
3.4.2 MTT cell viability assay 72
3.4.3 Luciferase assay 73

3.5 HER2/*neu* Silencing at mRNA and Protein Levels 74
3.5.1 Materials, chemicals and reagents 74
3.5.2 Transfection of siRNA 75
3.5.3 RNA extraction and qRT-PCR 76
3.5.3.1 RNA extraction 76
3.5.3.2 Quantitative Real-Time PCR (qRT-PCR) 77
3.5.4 Protein extraction and Western blotting 79
3.5.4.1 Protein extraction 79
3.5.4.2 Western blotting 80
3.6 Statistical Analysis 81

CHAPTER FOUR
RESULTS AND DISCUSSION
4.1 Liposome/Lipoplex Formulation 82
4.1.1 Conventional and PEGylated cationic liposome components and formulation 83
4.2 Biophysical Characterization of Liposome and Liposome-Nucleic Acid Interactions 85
4.2.1 Morphological observations using cryo-TEM 85
4.2.2 Particle size distribution and zeta potential analysis 92
4.3 Lipoplex Binding Affinity and Protection Efficiencies 96
4.3.1 Electrophoretic mobility shift assay 96
4.3.2 Nuclease protection assay 100
4.3.3 Ethidium bromide (EtBr) fluorescence quenching assay 104
4.4 *In Vitro* Cell Culture 108
4.4.1 Cell lines 108
4.4.2 MTT cytotoxicity assay 108
4.4.3 Luciferase activity 116
4.4.4 HER2/*neu* Gene Silencing in SKBR-3 Breast Cancer Cells 123
4.4.4.1 Quantitative Real-Time PCR 123
4.4.4.2 HER2/*neu* protein expression 127

CHAPTER FIVE

CONCLUSION

5.1 Concluding Remarks **134**

CHAPTER SIX

REFERENCES

6.1 Cited Literature **138**

APPENDIX A **167**

APPENDIX B **170**

LIST OF FIGURES

Figure 2.1: A diagrammatic representation of human mammary gland development. **(A)** An illustration of the five different stages of human mammary gland development, beginning with pubertal growth, followed by progression from adult to lactating breasts and finally waning at involution. Depicted are mammary fat pads (pink) and ductal epithelium (purple). The circular objects represent lobulo-alveolar units during pregnancy, lactation, and involution. **(B)** A model of mammary epithelial cell hierarchy as proposed by Shore and Rosen (2014). **11**

Figure 2.2: Outline of BC progression. Breast cancer is believed to advance through a series of well-defined stages. This sketch depicts cross-sections of the mammary duct at different stages of BC progression: Normal duct, Atypical ductal hyperplasia (ADH), Ductal carcinoma *in situ* (DCIS), and Invasive ductal carcinoma (IDC) (Mukhopadhyay *et al*., 2011; Shore and Rosen, 2014). **13**

Figure 2.3: Portrait of the HER2/*neu* structure (**A**). The extracellular domain consists of four subdomains (I-IV); two leucine-rich domains (L 1/ I and L 2/ III) which are marked with a stop symbol as they do not participate in ligand binding, and two cysteine-rich domains (CR 1/ II and CR 2/ IV) responsible for receptor dimerization. Depicted are the transmembrane domain; the amino- (NH) and carboxyl-terminal lobes of the kinase domain and the carboxyl-terminal tail containing several tyrosine residues that can be phosphorylated. Inhibitors of HER2/*neu* mediated signalling using monoclonal antibody (Trastuzumab) and small molecule tyrosine kinase inhibitor (Lapatinib) are also indicated. Key HER2/*neu* signalling pathways involved in tumorigenesis are also schematically illustrated (**B**). HER2/*neu* dimerizes with the activated HER receptor resulting in the phosphorylation of the tyrosine residues and signal transduction in the intracellular domain. This activates the lipid kinase phosphatidyl inositol 3 kinase (PI3K), which phosphorylates a phosphatidylinositol that in turn binds and phosphorylates the enzyme Ak transforming factor (Akt). Among the Akt multiple targets is the mammalian target of rapamycin (mTOR), which drives cell survival by promoting cell cycle progression and inhibiting pro-apoptotic members of the Bcl-2 family. On the other hand, the mammalian homologue of the son of sevenless (SOS), a guanine nucleotide exchange factor, activates the rat sarcoma (RAS) enzyme which, in turn, activates the receptor activation factor (RAF) and then mitogen extracellular signal kinase (MEK). MEK then phosphorylates the mitogen-activated protein kinase (MAPK), which results in cell cycle progression and proliferation (Adapted from Colombo *et al*., 2010; Roskoski Jr, 2014; Seliger and Kiessling, 2013; Thery *et al*., 2014; Videira *et al*., 2014). **19**

Figure 2.4: A graphic representation of the widespread application of gene therapy in clinical trials (Wirth *et al*., 2013). **25**

Figure 2.5: A schematic representation of the siRNA-mediated gene silencing pathway. 1) Introduction of exogenous long dsRNA is recognized by Dicer-2 in the cytoplasm; 2) Long dsRNA is cleaved by Dicer-2 into siRNA duplexes of 21-23 nucleotides in length followed by interaction with R2D2; 3) Synthetic siRNAs bypass the requirement for Dicer-2 processing and are recognized by both Dicer-2 and R2D2; 4) Dicer-2 and R2D2 facilitate the transport of siRNA to Ago-2, followed by formation of RISC; 5) Ago-2 protein promotes the unwinding of the duplexed siRNA, and the sense (passenger) strand is rapidly cleaved and dissociated; 6) The anti-sense (guide) strand remains bound to the RISC complex and mediates recognition of the target RNA; 7) Anti-sense RNA strand guides RISC and binds to the complementary site in the target mRNA; 8) RISC engages the endonucleolytic activity of Ago-2, resulting in target mRNA cleavage which shuts off translation of the corresponding protein (Adapted from Yang *et al*., 2013a). **29**

Figure 2.6: Depicted are unilamellar liposomes (bottom) bearing different densities of PEG polymers on their surfaces. Presented from left are total, intermediate and partial surface coverage of the liposomal bilayer. A detailed zoom (top) of the three PEGylated liposomes shows the respective PEG regimens formed as a result of the different surface densities. When the density of PEG on the surface is low, it takes on a heavily coiled flat "pancake" configuration (D > Rf). Increasing PEG densities cause the conformations to switch to low coiled "mushroom" or to extend further into "brush" structures (D < Rf) This figure is adapted from Buyens *et al.* (2012) and Wang and Thanou (2010). **43**

Figure 2.7: A scheme of the typical components of a cationic lipid **(A)** and their spontaneous assembly with neutral co-lipids into liposomes **(B)**. **45**

Figure 3.1: Plasmid map of the pCVM-*luc* vector. The vector comprises cDNA of the firefly luciferase (*luc*) gene and β-lactamase for ampicillin resistance (Amp^r). The vector is driven by the cytomegalovirus promoter (CMV). **59**

Figure 3.2: Diagrammatic representation of the siRNA duplex. **60**

Figure 4.1: Structural representation of the cholesteryl cytofectins. (A) 3β-[*N*-(*N'*, *N'*-dimethyl-aminopropane)-carbamoyl] cholesterol (Chol-T) and (B) *N*, *N*-dimethylaminopropylaminylsuccinyl cholesterylformyl hydrazide (MS09). **82**

Figure 4.2: Transmission electron micrographs of cationic and PEGylated cationic liposomes prepared according to **Table 1**: **A**, Chol-T:DOPE; **B**, Chol-T:DOPE:2% PEG; **C**, Chol-T:DOPE:5% PEG; **D**, MS09:DOPE; **E**, MS09:DOPE:2% PEG; **F**, MS09:DOPE:5% PEG. Bar = 100 nm or 200 nm. **87**

Figure 4.3: Transmission electron micrographs of cationic and PEGylated cationic pCMV-*luc* plasmid DNA complexes (lipid:pCMV-*luc* (+:–) charge ratios): **A**, Chol-T:DOPE (1.6:1); **B**, Chol-T:DOPE:2% PEG (1.7:1); **C**, Chol-T:DOPE:5% PEG (1.6:1); **D**, MS09:DOPE (1.7:1); **E**, MS09:DOPE:2% PEG (1.8:1); **F**, MS09:DOPE:5% PEG (1.7:1). Bar = 200 nm. **89**

Figure 4.4: Transmission electron micrographs of cationic and PEGylated cationic liposome-siGENOME non-targeting siRNA complexes (lipid:siRNA (+:–) charge ratios): **A**, Chol-T:DOPE (3.9:1); **B**, Chol-T:DOPE:2% PEG (6.3:1); **C**, Chol-T:DOPE:5% PEG (8.8:1); **D**, MS09:DOPE (5.4:1); **E**, MS09:DOPE:2% PEG (6.0:1); **F**, MS09:DOPE:5% PEG (7.9:1). Bar = 100 nm or 200 nm. **91**

Figure 4.5: Gel retardation analysis of binding interaction between varying amounts of cationic and PEGylated cationic liposome preparations with pCMV-*luc* plasmid DNA (1 μg) in HBS. **A,** lanes 1-8 (0, 2, 3, 4, 5, 6, 7, and 8 μg Chol-T); **B**, lanes 1-8 (0, 3, 3.5, 4, 5, 6, 7, and 8 μg Chol-T 2% PEG); **C,** lanes 1-8 (0, 3, 4, 5, 6, 7, 8, and 9 μg Chol-T 5% PEG); **D,** lanes 1-8 (0, 2, 3, 4, 5, 6, 7, and 8 μg MS09); **E,** lanes 1-8 (0, 4, 5, 6, 7, 8, 9, and 10 μg MS09 2% PEG); **F,** lanes 1-8 (0, 4, 5, 6, 7, 8, 9, and 10 μg MS09 5% PEG). (➔) indicates end point ratios or point of electroneutrality. **99**

Figure 4.6: Gel retardation analysis of binding interaction between varying amounts of cationic and PEGylated cationic liposome preparations with siRNA (0.32 μg) in HBS. **A,** lanes 1-8 (0, 3.20, 3.52, 3.84, 4.16, 4.48, 4.80, and 5.12 μg Chol-T); **B**, lanes 1-8 (0, 6.08, 6.40, 6.72, 7.04, 7.36, 7.68, and 8.00 μg Chol-T 2% PEG); **C,** lanes 1-8 (0, 10.56, 10.88, 11.20, 11.52, 11.84, 12.16, and 12.48 μg Chol-T 5% PEG); **D,** lanes 1-8 (0, 5.44, 5.76, 6.08, 6.40, 6.72, 7.04, and 7.36 μg MS09); **E,** lanes 1-8 (0, 6.08, 6.40, 6.72, 7.04, 7.36, 7.68, and 8.00 μg MS09 2% PEG); **F,** lanes 1-8 (0, 9.60, 9.92, 10.24, 10.56, 10.88, 11.20, and 11.52 μg MS09 5% PEG). (➔) indicates end point ratios or point of electroneutrality. (●➔) indicates no clear end point. **99**

Figure 4.7: Nuclease protection assay of cationic and PEGylated cationic liposome-pDNA complexes in the presence of 10% FBS. Reaction mixtures (10 μL) contained pCMV-*luc* (1 μg) and varying amounts of liposome suspension. **A,** lanes 3-5 (5, 6, 7 μg Chol-T): lanes 6-8 (6, 7, 8 μg MS09); **B,** lanes 3-5 (6, 7, 8 μg Chol-T 2% PEG): lanes 6-8 (6, 7, 8 μg Chol-T 5% PEG); **C,** lanes 3-5 (7, 8, 9 μg MS09 2% PEG): lanes 6-8 (7, 8, 9 μg MS09 5% PEG). In **A-C**, lane 1: FBS-untreated naked pCMV-*luc* plasmid DNA (1 μg) (control 1) and lane 2: FBS-treated pCMV-*luc* plasmid DNA (1 μg) (control 2). **102**

Figure 4.8: Nuclease protection assay of cationic and PEGylated cationic liposome-siRNA complexes in the presence of 10% FBS. Reaction mixtures (10 μL) contained siRNA (0.2 μg) and varying amounts of liposome suspension. **A,** lanes 3-5 (2.4, 2.8, 3.2 μg Chol-T): lanes 6-8 (3.8, 4.2, 4.6 μg MS09); **B,** lanes 3-5 (4.4, 4.8, 5.2 μg Chol-T 2% PEG): lanes 6-8 (7.0, 7.4, 7.8 μg Chol-T 5% PEG); **C,** lanes 3-5 (4.6, 5.0, 5.4 μg MS09 2% PEG): lanes 6-8 (6.8, 7.2, 7.6 μg MS09 5% PEG). In **A-C**, lane 1: FBS-untreated naked siRNA (0.2 μg) (control 1) and lane 2: FBS-treated siRNA (0.2 μg) (control 2). **102**

Figure 4.9: Schematic representation of preferred intercalation between EtBr and the nucleic acid helix which illustrates the lengthening and untwisting of the helical structure (Bugs and Cornelio, 2001; Nafisi *et al*., 2007; Palchaudhuri and Hergenrother, 2007). **105**

Figure 4.10: Ethidium bromide fluorescence quenching assay of the cationic and PEGylated cationic liposomes in a total of 0.25 mL incubation mixtures containing **(A)** 3 μg pCMV-*luc* plasmid DNA, **(B)** 3.2 μg siRNA and increasing amounts of liposome. **107**

Figure 4.11: Colony morphologies of the three cell lines used in this study. **(A)** and **(B)** SKBR-3, **(C)** and **(D)** MCF-7, **(E)** and **(F)** HEK-293. Cells were viewed as a monolayer at semi-confluency under a 100 × magnification (Nikon TMS-F 6V, Tokyo, Japan). **109**

Figure 4.12: Cell cytotoxicity studies of cationic and PEGylated cationic liposome-pCMV-*luc* plasmid DNA complexes in **(A)** HEK-293, **(B)** MCF-7 and **(C)** SKBR-3 cells *in vitro* using MTT reagent. Incubation mixtures (0.25 mL) contained 0.5 μg of pDNA with varying amounts of liposome from suboptimal to supraoptimal N/P (+:–) charge ratios: Controls - Untreated cells; Lipofectamine® 3000; Chol-T (1.1, 1.6, 2.1); Chol-T 2% PEG (1.2; 1.7, 2.2); Chol-T 5% PEG (1.1, 1.6, 2.1); MS09 (1.2, 1.7, 2.2); MS09 2% PEG (1.4, 1.8, 2.3); MS09 5% PEG (1.3, 1.7, 2.1). The viability percentage of cells was expressed relative to Untreated control cells. Data are presented as means ± SD (n = 3). Statistical analysis among mean values was performed using one-way ANOVA followed by the Tukey-Kramer multiple comparisons test between formulations. Asterisks denote a significant difference compared to the Untreated control cells *P<0.05, **P<0.01, and ***P<0.001. **112**

Figure 4.13: Cell cytotoxicity studies of cationic and PEGylated cationic liposome-siGENOME non-targeting siRNA complexes in **(A)** HEK-293, **(B)** MCF-7 and **(C)** SKBR-3 cells *in vitro* using MTT reagent. Incubation mixtures (0.25 mL) contained 0.32 μg of siRNA with varying amounts of liposome from suboptimal to supraoptimal N/P (+:–) charge ratios: Controls - Untreated cells; Lipofectamine® 3000; Chol-T (3.4, 3.9, 4.4); Chol-T 2% PEG (5.8, 6.3, 6.8); Chol-T 5% PEG (8.3, 8.8, 9.3); MS09 (4.9, 5.4, 5.9); MS09 2% PEG (5.5, 6.0, 6.5); MS09 5% PEG (7.4, 7.9, 8.4). The viability percentage of cells was expressed relative to Untreated control cells. Data are presented as means ± *SD* (n = 3). Statistical analysis among mean values was performed using one-way ANOVA followed by the Tukey-Kramer multiple comparisons test between formulations. Asterisks denote a significant difference compared to the Untreated control cells *P<0.05, **P<0.01, and ***P<0.001. **114**

Figure 4.14: *In vitro* gene transfection data of PEGylated and non-PEGylated lipoplexes studied in **(A)** HEK-293, **(B)** MCF-7, and **(C)** SKBR-3 cell lines. Lipoplexes were formulated with pCMV-*luc* plasmid DNA (1 μg) at various N/P charge ratios (+:–): Control 1 (untreated cells, negative control); Control 2

(pCMV-*luc* DNA alone, negative control) and Lipofectamine® 3000 (positive control); Chol-T (1.1, 1.6, 2.1); Chol-T 2% PEG (1.2; 1.7, 2.2); Chol-T 5% PEG (1.1, 1.6, 2.1); MS09 (1.2, 1.7, 2.2); MS09 2% PEG (1.4, 1.8, 2.3); MS09 5% PEG (1.3, 1.7, 2.1). Transfections were carried out in the presence of 10% foetal bovine serum. Luciferase activity in terms of normalized light units was expressed as RLU mg^{-1} protein. Data are presented as means ± SD (n = 3). Statistical analysis among mean values was performed using one-way ANOVA followed by the Tukey-Kramer multiple comparisons test between formulations. Asterisks denote a significant difference *P<0.05, **P<0.01, and ***P<0.001. **120**

Figure 4.15: Analysis of HER2/*neu* gene expression in SKBR-3 cells by qRT-PCR. Incubation mixtures (1.5 mL) contained 0.64 μg of siRNA with varying amounts of liposome from suboptimal to supraoptimal concentrations: Chol-T:DOPE (7.68, 8.96, 10.24 μg); Chol-T:DOPE:2% PEG (14.08, 15.36, 16.64 μg); Chol-T:DOPE:5% PEG (22.40, 23.68, 24.96 μg); MS09:DOPE (12.16, 13.44, 14.72 μg); MS09:DOPE:2% PEG (14.72, 16.00, 17.28 μg); MS09:DOPE:5% PEG (21.76, 23.04, 24.32 μg). Calibrator (non-treated SKBR-3 cells), NT-siRNA (non-targeting siRNA) and siRNA (HER2/*neu* targeting siRNA alone) served as negative controls. Lipofectamine® 3000-siRNA was included as a positive control. The vertical axis represents the relative quantification of HER2/*neu* normalized against GAPDH mRNA level using the comparative quantification algorithm $2^{-\Delta\Delta Ct}$ (Livak and Schmittgen, 2001). Data shown are the mean ± *SD* of independent experiments (n = 3). Asterisks denote a significant difference ***P<0.001. **125**

Figure 4.16: Analysis of HER2/*neu* oncoprotein expression by Western blotting. **(A)** Non-treated SKBR-3 cells, NT-siRNA (non-targeting siRNA) and siRNA (HER2/*neu* targeting siRNA alone) served as negative controls. Lipofectamine® 3000-siRNA was included as a positive control. **(B)** SKBR-3 cells were treated with HER2/*neu* target siRNA (0.64 μg) with varying amounts of the cationic liposomes from suboptimal to supraoptimal ratios: Chol-T (7.68, 8.96, 10.24 μg); Chol-T 2% PEG (14.08, 15.36, 16.64 μg); Chol-T 5% PEG (22.40, 23.68, 24.96 μg); **(C)** MS09 (12.16, 13.44, 14.72 μg); MS09 2% PEG (14.72, 16.00, 17.28 μg); MS09 5% PEG (21.76, 23.04, 24.32 μg). HER2/*neu* receptor expression was determined in cellular lysates by Western blotting analysis using the HER2/*neu* and β-actin antibodies. Graphs represent the HER2/*neu*/β-actin normalization ratios. **130**

LIST OF TABLES

Table 2.1: Examples of non-viral nanocarriers for siRNA gene delivery into breast cancer cell models **38**

Table 3.1: Composition and mol. ratios of the different cationic liposomal formulations **57**

Table 3.2: Set up for gel retardation assays with varying amounts of cationic and PEGylated cationic liposome preparations with pCMV-*luc* plasmid DNA **64**

Table 3.3: Set up for gel retardation assays with varying amounts of cationic and PEGylated cationic liposome preparations with siGENOME non-targeting siRNA **65**

Table 3.4: Set up for serum nuclease protection assays with varying amounts of cationic and PEGylated cationic liposome preparations with pCMV-*luc* plasmid DNA **67**

Table 3.5: Set up for serum nuclease protection assays with varying amounts of cationic and PEGylated cationic liposome preparations with siGENOME non-targeting siRNA **68**

Table 3.6: Set up for gene expression studies with varying amounts of cationic and PEGylated cationic liposome preparations with ON-TARGETplus SMARTpool HER2/*neu* siRNA **76**

Table 3.7: High Capacity cDNA Reverse Transcription Kit components required to prepare 2× RT master mix **78**

Table 4.1: ZetaSizer measurements of the various cationic/PEGylated cationic liposomes and corresponding DNA/siRNA lipoplexes **95**

Table 4.2: Gel retardation endpoints and charge ratios of the various cationic/ PEGylated cationic liposomes **98**

Table 4.3: EtBr fluorescence quenching by the various cationic/ PEGylated cationic liposomes recorded at points of inflection **106**

ABBREVIATIONS AND SYMBOLS

ADH	Atypical ductal hyperplasia
Ago-2	Argonaute-2
Akt	Ak transforming factor
Amp^r	Ampicillin resistance
anti-EEA1	Primary antibody against early endosomal autoantigen
ATP	Adenosine triphosphate
BC	Breast cancer
BCA	Bicinchoninic acid
bPEI	Branched PEI
BSA	Bovine serum albumin
CCC	Cationic cholesteryl cytofectin
cDNA	Complementary DNA
Chol-T	3β-[*N*-(*N′*, *N′*-Dimethylaminopropyl)-carbamoyl] cholesterol
cm	Centimetre
CMV	Cytomegalovirus promoter
cryo-TEM	Cryogenic-transmission electron microscopy
C_t	Threshold cycle
DC-Chol	3β-[*N*-(*N′*,*N′*-Dimethylaminoethyl) carbamoyl] cholesterol
DCIS	Ductal carcinoma *in situ*
DLS	Dynamic light scattering
DMSO	Dimethyl sulfoxide
DNA	Deoxyribonucleic acid
dNTP	Deoxyribonucleotide triphosphates
DOGS	Dioctadecylamidoglycylspermidine
DOPC	1,2-Dioleoyl-*sn*-glycero-3-phosphocholine
DOPE	Dioleoylphosphatidylethanolamine
DOPG	1,2-Dioleoyl-*sn*-glycero-3-phospho-(1′-*rac*-glycerol)
DOTAP	1,2-Dioleoyl-3-trimethylammonium-propane

DSPE-PEG_{2000}	1,2-Distearoyl-*sn*-glycero-3-phosphoethanolamine-N [methoxy(polyethylene glycol)-2000]
dsRNA	Double stranded RNA
E. coli	*Escherichia coli*
EDTA	*N*, *N*, *N'*, *N'*-Ethylenediaminetetraacetic acid
EGFR	Epidermal Growth Factor Receptors
EMEM	Eagle's Minimum Essential Medium
ER	Estrogen receptors
Erk	Extracellular signal-related kinase
EtBr	Ethidium bromide
EtOH	Absolute ethanol
FBS	Foetal bovine serum
FDA	Food and Drug Administration
FGF	Fibroblast growth factor
F_r	Relative fluorescence
g	Gram
GAPDH	Glyceraldehyde 3-phosphate dehydrogenase
GFP	Green fluorescent protein
g L^{-1}	Gram per litre
g $mol.^{-1}$	Gram per mole
h	Hour
H_{II}	Inverted hexagonal phase
HBS	HEPES buffered saline
HEK-293	Human embryonic kidney cells
HEPES	2-[4-(2-Hydoxyethyl)-1-piperazinyl] ethanesulfonic acid
HER2/*neu*	Human Epidermal Growth Factor Receptor 2
HIF-1	Hypoxia inducible factor-1
HRP	Horseradish peroxide
IAP	Inhibitor of apoptosis proteins
IDC	Invasive ductal carcinoma
IgG	Immunoglobulin G

Kbp	Kilo base pair
kDa	Kilo Dalton
kHz	Kilo Hertz
kV	Kilo Volt
LDV	Laser Doppler Velocimetry
LMWC	Low molecular weight chitosan
luc	Luciferase
L_α	Lamellar phase
M	Molar mass
MAPK	Mitogen-activated protein kinase
MCF-7	Michigan Cancer Foundation breast cancer cells
MDR	Multidrug resistance
MEK	Mitogen extracellular signal kinase
mg/kg	Milli-gram per kilo
min	Minute
mL	Millilitre
mmol.	Millimole
mol.%	Mole percentage
mPHA-g-bPEI	Mono-methoxy-poly(3-hydroxybutyrate-*co*-4-hydroxybutyrate)-graft hyperbranched PEI
MPS	Mononuclear phagocytic system
mP3/4HB-*b*-PEG-*b*-lPEI	Mono-methoxy-poly (3-hydroxybutyrate-*co*-4-hydroxybutyrate)-*block*-polyethylene glycol-*block*-linear PEI
mRNA	Messenger RNA
MS09	*N*, *N*-Dimethylaminopropylaminylsuccinylcholesterylformylhydrazide
mTOR	Mammalian target of rapamycin
MTT	3-(4, 5-Dimethyl-2-thiazolyl)-2, 5-diphenyl-2H-tetrazolium bromide
mV	Milli Volt
M*w*	Molecular weight
MΩ	Megaohm
nm	Nanometers
N/P	Amine to phosphate ratio

OD	Optical density
PAMAM	Poly(amido amine)
PBS	Phosphate buffered saline
PDI	Polydispersity index
pDNA	Plasmid DNA
PEA3	Polyomavirus enhancer activator 3
PEG	Poly(ethylene glycol)
PEI	Polyethyleneimine
P-gp	P-glycoprotein
PgR	Progesterone receptors
PI3K	Phosphatidyl inositol 3 kinase
PLCγ	Phospholipase C-γ
PLL	Poly-L-lysine
P(MDS*co*-CES)	poly(*N*-methyldietheneamine sebacate)-*co*-[(cholesteryloxocarbonylamido ethyl) methyl bis(ethylene) ammonium bromide] sebacate)
PTEN	Phosphatase and tensin homolog
PVDF	Polyvinyldene fluoride
qRT-PCR	Quantitative real time polymerase chain reaction
RAF	Receptor activation factor
RAS	Rat sarcoma
RES	Reticulo-endothelial system
RISC	RNA induced silencing complex
RLU	Relative light units
RNA	Ribonucleic acid
RNAi	RNA interference
ROS	Reactive oxygen species
rpm	Revolution per minute
s	Second
SD	Standard deviation
SDS	Sodium dodecyl sulphate
SDS-PAGE	Sodium dodecyl sulphate-polyacrylamide gel electrophoresis

siRNA	Small interfering RNA
SIS	Soft Imaging System
SKBR-3	Sloan-Kettering breast cancer cells
SOS	Son of sevenless
TAT	Trans-activated transcription
TBST	Tris-buffered saline containing Tween 20
T_m	Transition temperature
TRAIL	TNF-related apoptosis-inducing ligand
Tris base	Tris (hydroxymethyl)-aminomethane
µg	Microgram
µg μL^{-1}	Microgram per microlitre
uPA	Urokinase plasminogen activator
VEGF	Vascular endothelial growth factor
$^{v}/_{v}$	Volume to volume ratio
$^{w}/_{v}$	Weight to volume ratio
$^{w}/_{w}$	Weight to weight ratio
λ	Wavelength (lambda)
ζ	Zeta potential

ACKNOWLEDGEMENTS

I would like to express my deepest gratitude to the following persons:

- My Guru, Swami Ganesh Dutta Shukla (International Religious Preacher) for his blessings, guidance and support.
- My supervisor, Dr. Moganavelli Singh and co-supervisor, Professor Mario Ariatti (Discipline of Biochemistry, UKZN, Westville campus) for their patience, dedication, scientific knowledge, supervision and contribution during the course of this study.
- My dear parents, Mr. Amarjeeth Balgobind and Mrs. Bessie Balgobind for their support and guidance; they have made immense sacrifices and it is through their love and prayers that I have completed this thesis.
- The National Research Foundation (NRF) for financial support during my doctoral studies.
- Dr. James Wesley-Smith (Electron Microscopy) for his expertise and continuous assistance with cryo-TEM required for particle imaging.
- Dr. Thavi Govender (Pharmacy and Pharmacology) for allowing the use of the ZetaSizer Nano-ZS apparatus required for particle size distribution and zeta potential analysis.
- My colleagues of the Discipline of Biochemistry for their support and help throughout my PhD studies.
- My brother and sister-in-law, Yitheen Balgobind and Erin Balgobind for their encouragement and inspiring me to get through tough times during the completion of this thesis.
- My husband, Kiren Roopraj for his love, care, understanding, encouragement and support.
- God, for guiding and granting me the strength to complete the study, without His blessings none of this would have been possible.

JAI SHREE RAAM

To my dear parents

CHAPTER ONE

INTRODUCTION

1.1 Background to the Study

Since its discovery in 1998 as a powerful sequence specific post-transcriptional gene silencing mechanism, RNA interference (RNAi) has opened up a range of opportunities for target gene function validation and therapeutic applications in several genetic disorders. In mammalian cells, transfected synthetic double stranded small interfering RNAs (siRNAs), generally 21-23 nucleotides in length, target messenger RNA (mRNA) sequences with a high degree of specificity, inducing gene silencing. This versatile technique of target specific gene silencing has potential for use against any mRNA transcribed from an organism's genome, thereby offering a unique class of drug molecules comparable to antibody based therapeutics. Based on conceptually simple beginnings, the evolution of siRNA gene silencing technology has inspired a new paradigm of therapeutic intervention strategies for a wide spectrum of disorders, including cancer (Huang *et al*., 2008; Oh and Park, 2009), Huntington's disease (DiFiglia *et al*., 2007), respiratory syncytial virus (Bumcrot *et al*., 2006), and neurodegenerative disorders (Porras and Bezard, 2008).

Malignant tumours, namely cancers, are complex and intrinsically heterogeneous diseases with approximately 8 million people dying from numerous types of cancers in 2008 (Benson and Jatoi, 2012; Graham *et al*., 2012). In South Africa, cancer is an escalating public health problem. The most prevalent malignancy is breast cancer (BC), a major cause of cancer death among women, as is the global trend (DeSantis *et al*., 2011, Núñez *et al*., 2016, Shah and Osipo, 2016). Based on projections of BC incidences and population estimations, the annual global incidence of BC is expected to reach approximately 3.2 million by 2050 (Hortobagyi *et al*., 2005; WPP, 2004). These statistics clearly highlight the increasing threat that BC poses worldwide. Hence there is an urgernt need to investigate the molecular biology of BC to identify alterations associated with malignant behaviour for clinical use as diagnostic markers and as targets for therapy.

Malignant breast tumours form when an individual cell gains and sustains a selective survival advantage, due to a series of somatic alterations that allow the cell to evade the checkpoints that would normally suppress its growth. In particular, overexpression of the Human Epidermal Growth Factor Receptor 2 (HER2/*neu*) oncogene, many researchers believe, is predictive of adverse BC prognosis. Overexpression of HER2/*neu* has been found in

approximately 30% of all invasive BCs and correlates with more unfettered and destructive tumour growth and greater resistance to cancer chemotherapy (Menard *et al*., 2000; Núñez *et al*., 2016; Press *et al*., 2002; Rubin and Yarden, 2001; Slamon *et al*., 1989). Despite recent advances in treatment strategies, most, if not all conventional treatments such as chemotherapy, are limited by a lack of specificity for tumour cells and the cell cycle dependence of many chemotherapeutic agents. This has spurred efforts to develop unique anticancer agents with improved molecular target specificity. In this context, tailored treatments using siRNA to down-regulate the transcription or function of defective genes through specific cleavage of their associated mRNA, introduces an innovative, cutting-edge assemblage of treatment options for BC.

Silencing of the HER2/*neu* oncogene expression using siRNA may be effective in treating patients with HER2/*neu*-overexpressing BCs. Despite the versatility, effectiveness and specificity of siRNAs' use in tumour targeted therapy, the delicate and precise mechanism of action required for gene silencing is the same. However, the delivery of therapeutic siRNA to intracellular targets for the induction of sequence-specific mRNA degradation creates an encumberance which limits the success of siRNA therapy in clinical trials for several reasons. Firstly, the polyanionic nature, hydrophilic character and relatively high molecular weight of siRNA hamper its direct association with the cell membrane. This makes entry into cells via a passive diffusion mechanism difficult for these molecules (Whitehead *et al*., 2009). Furthermore, siRNA molecules in the physiological milieu are prone to degradation by serum nuleases, non-targeted biodistribution and activation of immune response, thereby limiting systemic applications of this powerful tool to perform gene knockdown (Haupenthal *et al*., 2006; Juliano *et al*., 2009; Medarova *et al*., 2007).

The major challenge for siRNA-based gene silencing therapy is the development of non-toxic nanocarriers capable of efficiently transporting siRNAs into target cells. Numerous research efforts focusing on the development of lipid- and polymer-based systems have been directed at meeting this challenge. In particular, cationic liposomes have emerged as the most widely studied non-viral vectors for the transport of negatively charged gene medicines via the formation of lipoplexes. The main component of cationic liposomes, namely the cationic cytofectins, generally comprise four regions: cationic headgroups, hydrophobic lipid tails, spacer segments, and linkers (Ariatti, 2015). Despite progress in cationic liposome-mediated delivery, cell toxicity and the reduced cellular uptake efficiency of siRNA in the presence of serum

nucleases are still major drawbacks for *in vitro* and *vivo* application. The key challenges are to synthesize cytofectins with a unique combination of their domains, which are capable of self-assembling into liposomes. Moreover, a deeper insight into the structure-activity associations of liposomal carriers with siRNA, in order to achieve high transfection performance is imperative.
This leaves BC gene therapy at a point where the need for an optimal gene delivery vector has become the rate limiting step. Therefore, this study aims to develop cationic lipid-based delivery systems for siRNA that can increase serum stability and transfection efficiency. Clearly, the development of an agent with the ability to successfully inhibit cellular growth, migration, and invasion of BC cells is crucial for the suppression of cancer metastasis and progression, thus resulting in reduced mortality.

1.2 Scope of the Present Study

The major challenge for siRNA-based therapy is the development of non-toxic, stable and efficient delivery systems to channel siRNA into target cells. Since their introduction, non-viral vector-mediated nanocarriers have developed to a stage where they have demonstrable advantages over their viral counterparts, in particular where safety issues are concerned, making them an attractive alternative for nucleic acid delivery platforms. Research in this area, however, has to address low levels of gene delivery and transfection efficiency which compromise non-viral gene delivery vector therapy. Undoubtably, non-viral carriers have emerged as essential components in siRNA gene delivery systems. Although research initiatives are being directed at improving current vector technologies, further development of non-viral nanocarrier systems with superior biocompatibility and higher transfection efficiencies is crucial for the success of gene silencing-based therapeutics. Accordingly, this study assesses the ability of two cationic lipid-based delivery systems to efficiently deliver intact siRNA targeting the Her2/*neu* oncogene in a BC cell model.

1.2.1 Hypothesis tested

This study, which examines the efficacy with which liposomes-vehiculated siRNA induces silencing of HER2/*neu* oncogene expression in a BC cell model *in vitro*, hinges on the hypothesis that cationic liposome-based delivery systems that incorporate cytofectins: 3β-[*N*-(*N′*, *N′*-dimethylaminopropane)-carbamoyl] cholesterol (Chol-T) and *N*, *N*-dimethylaminopropyl aminylsuccinylcholesterylformylhydrazide (MS09) increase the serum stability of the nucleic acid in their associated deoxyribonucleic acid (DNA) and ribonucleic acid (RNA) lipoplexes (nucleic acid-liposome complex) and can deliver the cargo nucleic acid into mammalian cells effectively.

1.2.2 Objectives

The following objectives premise the testing of the above hypothesis:

- To prepare and characterize a series of cationic liposomes (PEGylated and non-PEGylated) in terms of imaging and lamellarity by cryogenic-transmission electron microscopy (cryo-TEM), and size and zeta potential using dynamic light scattering (DLS).
- To characterize the formulated liposomes and their interactions with plasmid DNA (pDNA) and small interfering RNA (siRNA) for the purpose of optimizing their bifunctionality.
- To evaluate cytotoxicity *in vitro* using the 3-(4, 5-dimethyl-2-thiazolyl)-2, 5-diphenyl-2H-tetrazolium bromide (MTT) test. To measure transfection activity of the cationic lipoplexes using the luciferase assay as well as HER2/*neu* targeted siRNA.
- To monitor gene expression and silencing using standard reporter gene assays, quantitative Real-Time PCR (qRT-PCR) and Western Blotting.

1.2.3 Aims

- To prepare a series of cationic liposomes (Chol-T and MS09) with and without PEGylation (sterically stable) at two different mole percentages, and to explore and compare the effects these formulations may have on the transfection of pDNA and siRNA.
- To prepare Chol-T- and MS09-liposome/ pDNA- and siRNA-lipoplexes, and to assess these complexes in terms of size, polydispersity index and zeta potential. To further characterize lipoplexes using gel retardation, nuclease protection and ethidium bromide intercalation displacement assays.
- To perform transfection activity studies using both pDNA and siRNA, and to evaluate the results of MTT cytotoxicity tests on various cancer cell lines.
- To extract total RNA and proteins from transfected cells, and to determine their concentration, quality and integrity.
- To conduct qRT-PCR by reverse transcribing total RNA, and then to separate total proteins and check for the presence of HER2/*neu* proteins via Western Blotting.

1.3 Novelty of Study

This study evaluates the ability of two cationic lipid-based carrier systems to efficiently deliver target specific siRNA into breast cancer cells. The two cationic cholesteryl cytofectins (CCCs), Chol-T and MS09, were previously synthesized in our laboratory (Singh and Ariatti, 2006; Singh *et al*., 2001). Liposomes were formulated with an equimolar ratio of the respective cytofectin with dioleoylphosphatidylethanolamine (DOPE); the degree of PEGylation varied from 0-5 mol.%. Although these cationic liposomes have shown potential for nucleic acid delivery into mammalian cells, detailed studies on their ability to bind target specific siRNA have not been conducted. Accordingly, this study aims to assess the ability of these two cationic lipid-based delivery systems to efficiently deliver intact siRNA, which targets the HER2/*neu* oncogene in a BC cell model.

1.4 Overview of the Thesis

- **Chapter One**

This chapter provides an introduction and background to the study. It highlights the challenges encountered in siRNA gene therapy and non-viral gene delivery systems. Finally, it outlines the rationale, scope, objectives and aims of the study.

- **Chapter Two**

This chapter reviews the relevant literature. Firstly, it details the biology and classification of BC with particular reference to the HER2/*neu* receptor and its role in BCs. Secondly, it assesses HER2/*neu* as a target for BC therapy, together with current treatment options and their limitations. Lastly, it explores the therapeutic potential of siRNA gene silencing technology and delivery into cells using non-viral gene delivery systems.

- **Chapter Three**

Chapter Three describes the research design and details the laboratory procedures undertaken. The formulation and preparation of six cationic liposomes (PEGylated and non-PEGylated at two different mole percentages) are detailed, followed by physical characterization of the liposomes and liposome-nucleic acid interactions. These characterizations are based on particle imaging using Cryo-TEM, particle size distribution, and zeta potential analysis. Again, the formulated lipoplexes are comprehensively characterized to establish nucleic acid binding capacity (gel retardation assay), protection from nucleases (serum digestion assay), and condensation capabilities (ethidium bromide intercalation assay) provided by the vector. *In vitro* transfection activities are investigated in the human HEK-293, MCF-7 and SKBR-3 BC cell lines.

- **Chapter Four**

Here, the focus is on the results obtained and a comprehensive report of all experimental work completed. This is followed by a robust interpretation of the results, with detailed discussion which lends shape, contour, and perpective to the study.

- **Chapter Five**

This chapter concludes the study by highlighting findings which are significant to the aims and objectives of the research. Possible limitations and shortcomings of the study are also conceded. Finally, the extent to which the study conceivably contributes to the body of knowledge in this area of research is objectively evaluated, and recommendations for further research initiatives are made.

CHAPTER TWO

LITERATURE REVIEW

2.1 The Nature of Cancer

The human genome, comprising a total length of over 3 billion base pairs, controls the fate of cells in a systematic and precise manner. Genetic material, namely genomic DNA, is under constant attack from both genotoxic and non-genotoxic mechanisms, often resulting in modifications which can potentially transform a normal cell into a premalignant lesion (Nowsheen *et al*., 2014). Eventually, accumulation of dynamic alterations in the genome and a complex network of interactions among mutated cells with multiple distinct cell types lead to metastatic cancer with uncontrolled growth of tissues. According to Hanahan and Weinberg (2000; 2011), cancer may be characterized by six distinctive biological aptitudes: sustained proliferative signaling, insensitivity to growth suppressors, resistance to apoptosis, replicative immortality, induction and sustainment of angiogenesis, invasion through capillary walls and basal membranes and metastasis to other sites of the body.

Globally, cancer rates are escalating at an alarming rate. In developing countries, in particular, an overburdened health sector further exacerbated by economic constraints makes cancer a serious health issue, resulting in the disease being the leading cause of death. Despite considerable advances in diagnostic technology and treatment modalities, the invasive, aggressive growth profile, the complexity of the signaling web involved in cancer development and propagation, coupled with multiple mechanisms to evade apoptosis, pose a formidable challenge to the quest for cancer treatment and a cure (Hanahan and Weinberg, 2000; Li *et al*., 2013). Traditional cancer therapies such as chemotherapy, radiotherapy and surgery are ineffectual in more advanced cases, primarily because these interventions lack specificity and therefore induce adverse side-effects on normal cells. In most cases, these treatment options result in incomplete eradication of the invasive primary tumour or disseminated disease. Furthermore, when cancer treatments fail or when relapse occurs, cross-resistance with several structurally unrelated anticancer agents or multidrug resistance (MDR) is a common occurence (Fatemian *et al*., 2014). These phenotypes are the most prevalent form of tumour resistance, accounting for 90% of cancer treatment failure (Ozben, 2006). The urgency of the quest for innovative anticancer strategies can hardly be over-emphasised.

2.2 Breast Cancer

The estimated global new incidence of BC cases in women was approximately 1.7 million with approximately half a million deaths in 2012, accounting for 25% of all cancer cases and 15% of all cancer deaths among the female population (Torre *et al*., 2015). According to a cancer report by the American Cancer Society, BC is over 100 times more common in women than in men (ACS, 2015). Although there is a higher incidence of BC in industrialized countries, adoption of urbanized lifestyles and changes in reproductive behaviour could possibly be the reasons for the increase of BC in non-industrialized countries (Porter, 2008). Based on BC incidence projections and population estimations, the annual global incidence of BC is expected to reach approximately 3.2 million by 2050 (Hortobagyi *et al*., 2005; WPP, 2004). Clearly, these statistics presage a global BC increase of alarming proportions.

Although BCs are sporadic in nature, approximately, 5-10% of BC cases are genetic in provenance. Generally, BC develops in cells which line the milk ducts and the lobules that supply the ducts with milk, classified as ductal and lobular carcinomas respectively. The most common, invasive ductal carcinomas constitute approximately 80% of BCs; 10-15% are invasive lobular carcinomas; and additional rare types make up less than 5-10% of BCs (Perou *et al*., 2000; Sørlie *et al*., 2003). Breast cancer tumours are heterogeneous, and pathological characteristics such as morphology, grade and hormone-receptor profile stratify tumours into biologically and clinically distinct groups (Simpson *et al*., 2005).

2.3 The Normal Mammary Gland and the Biology of Breast Cancer

2.3.1 Development of the mammary gland

The human mammary gland is a unique organ; it originates in the embryonic stage of human development and undergoes a series of changes post-puberty to senescence (Cowin and Wysolmerski, 2010; Watson and Khaled, 2008). In normal physiological conditions, the mammary gland consists of a branching tubulo-alveolar system composed of a highly dynamic stratified epithelium surrounded by a basement membrane. This glandular structure is embedded

within a matrix of stroma composed of varying amounts of adipose and connective tissue, nerves, blood vessels and lymphatics (Osborne, 2000; Stingl *et al*., 2006).

In newborn infants, the palpable mammary fat pad consists of a simple epithelial ductal structure that quiescently lies beneath the nipple until puberty. In both males and females, pre-pubertal mammary glands are analogous in structure and cellularity with specialized cell biology (Howard and Gusterson, 2000; Javed and Lteif, 2013). Structural modifications of the breast observed at different stages in females (menstrual cycle, pregnancy, lactation and regression) led to the postulation of the existence of progenitor cells that are capable of developing new duct-lobular systems (Raouf *et al*., 2012; Shore and Rosen, 2014; Villadsen *et al*., 2007) **[Figure 2.1]**. In females, the normal range of thelarche is from 8½ to 13 years. During this period, the release of ovarian and pituitary hormones such as estrogen, progesterone and growth hormones stimulate proliferation of the mammary epithelial cells resulting in the generation of an elaborate network of terminal end bud structures (Stingl, 2011). These are dynamic, highly proliferative structures located at the tips of the invading ducts that expand and increase extensively to allow complex branching, ductal elongation and lumen formation (Brisken and O'Malley, 2010; Hennighausen and Robinson, 2001; Sternlicht, 2006). In the adult, the epithelial ducts form into a branched, bilayered ductal structure, comprising an inner layer of polarized luminal epithelial cells and an outer basal layer of cells which are believed to arise from a common bipotent stem cell (Shore and Rosen, 2014; Visvader, 2009). The luminal cells can be further subdivided into luminal progenitors and mature luminal cells, i.e., ductal luminal cells, lining the inside of the ducts, and alveolar luminal cells which are the milk producing cells of the mammary gland. The outer basal layer consists of basal progenitor cells and a population of contractile myoepithelial cells. These are muscle-like cells which, in the presence of oxytocin, contract to force the movement of milk out of the alveoli into the ducts to be ejected from the nipples during lactation (Howard and Gusterson, 2000; Russo and Russo, 2004). Luminal and basal progenitors are believed to produce alveolar progenitors (Visvader, 2009). During pregnancy, these primary ducts that reach the nipple form a complex of auxiliary ducts, which undergo a stepwise process of differentiation to form several alveolar cells or acini (Brisken and Rajaram, 2006). A collection of alveolar cells arising from one terminal duct forms the functional unit of the breast, termed a terminal duct lobular unit. The morphogenesis and systematized differentiation of the mammary gland allow the secretory units of the mammary gland to be inactive, rather than persisting in a functionally

differentiated, milk producing state (Smith *et al*., 2012). During involution, the process when lactation stops and the mammary gland turns in on itself, the majority of differentiated alveolar cells undergo rounds of apoptosis in a controlled manner, reverting the gland to a pubertal state. Importantly, the mammary gland becomes fully differentiated only with the onset of pregnancy, which brings about the next major change in the hormonal environment (Anderson *et al*., 2007).

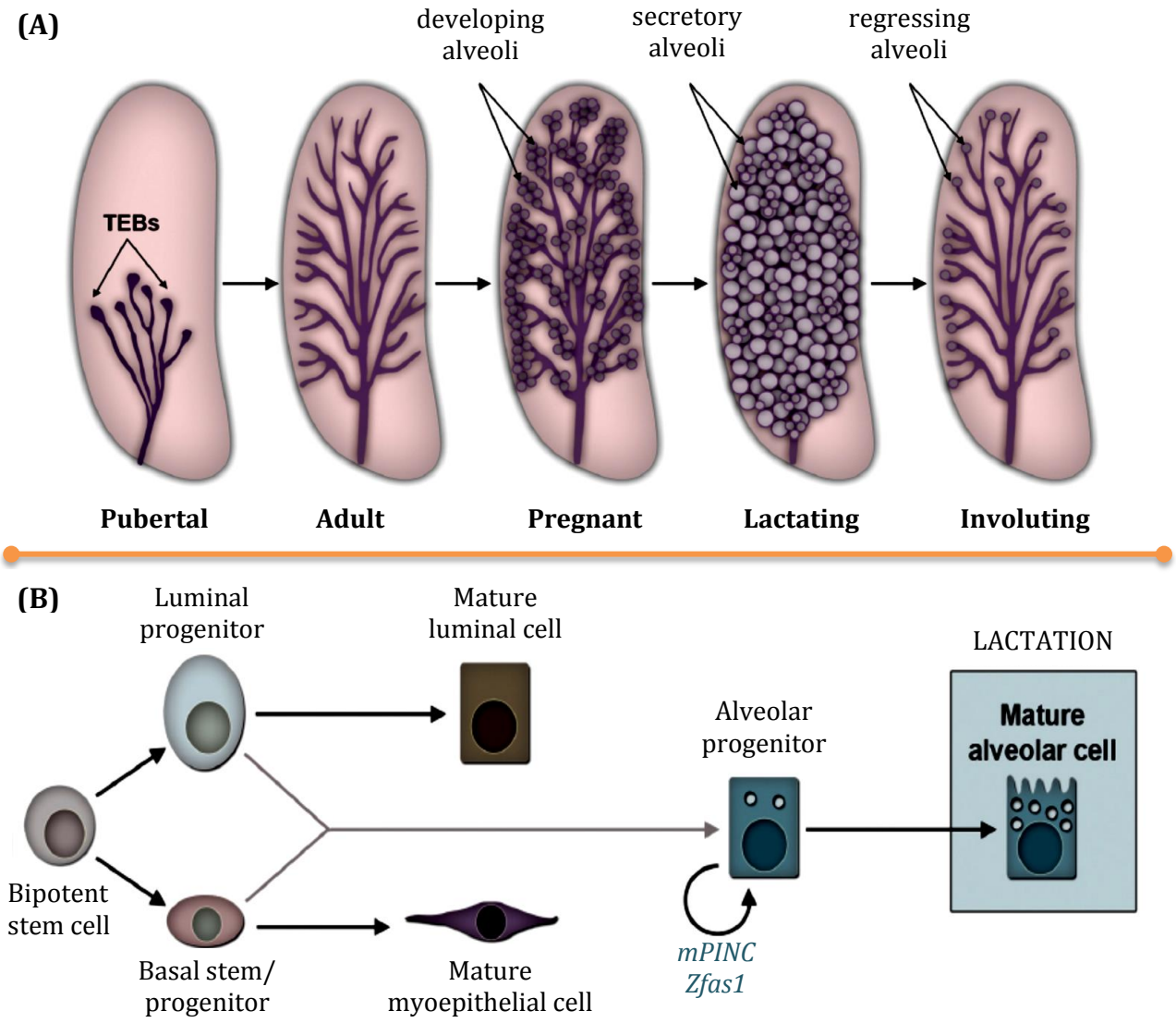

Figure 2.1: A diagrammatic representation of human mammary gland development. **(A)** An illustration of the five different stages of human mammary gland development, beginning with pubertal growth, followed by progression from adult to lactating breasts and finally waning at involution. Depicted are mammary fat pads (pink) and ductal epithelium (purple). The circular objects represent lobulo-alveolar units during pregnancy, lactation, and involution. **(B)** A model of mammary epithelial cell hierarchy as proposed by Shore and Rosen (2014).

2.3.2 The biology of breast cancer

Breast cancer is not a single disease but a highly heterogeneous group of neoplasms (Perou *et al*., 2000). Regardless of the histological type of the tumour, almost all are believed to originate from the epithelial cells lining the milk ducts (Tavassoli and Devilee, 2003). The initiation of BC, i.e., deregulated cell growth and apoptosis, is due to both genetic and epigenetic modifications in a single cell. These changes include: point mutations, duplications, insertions, deletions, translocations, chromosome aberrations, and epigenetic inactivation such as histone deacetylation and promoter hypermethylation (Nowsheen *et al*., 2014). The most well characterized pre-malignant lesions studied and recognized were obtained from the ductal and lobular units of the mammary gland. These are termed atypical ductal or lobular hyperplasias, and ductal or lobular carcinomas *in situ* (Allred *et al*., 2001). The prevailing model focuses specifically on the progression of lesions present within the ductal region of the mammary gland **[Figure 2.2]**. Essentially, the natural history of breast tumourigenesis assumes a sequential progression through defined pathophysiological stages, beginning with atypical ductal hyperplasia (ADH), to ductal carcinoma *in situ* (DCIS), with subsequent evolution into invasive ductal carcinoma (IDC) and metastatic carcinoma (Burstein *et al*., 2004; Polyak, 2007). Collectively, clinical and experimental data suggest that ADH is a pre-malignant tumour and a precursor lesion of DCIS, characterized by abnormal epithelial cells that have proliferated and formed numerous layers within the lumen. Based on molecular and pathological studies, DCIS (also referred to as intraductal carcinoma) is the precursor lesion of invasive BC. DCIS is a clonal proliferation of pre-malignant cells, capable of rupturing the basement membrane surrounding the mammary ducts and invading into the adjacent stroma. Despite being a crucial stage in tumour progression, there is no consensus about its nature. Some researches suggest that it is the result of the accumulation of additional genetic changes coupled with clonal expansion and selection (Place *et al*., 2011). The most prominent changes observed in epithelial cells at both the ADH and DCIS stages are the loss of polarity, abnormal cell morphology, and the ability to hyperproliferate within the mammary duct (Shore and Rosen, 2014). Numerous changes in the cellular composition from normal mammary gland to IDC have been documented. These included loss of epithelial cells, increase in fibroblasts, mast cells, macrophages (immune-competent cells) in the stroma, and enhanced vascularization, which is the most common

(Gudjonsson *et al*., 2005; Lewis and Pollard, 2006; Shekhar *et al*., 2003). Following basement membrane invasion, the spread of malignant mammary epithelial cells to distant organs results in metastatic disease. A range of motility mechanisms facilitate invasion of cancerous breast tissues and metastasis. These include: epithelial mesenchymal transition, structural modifications of the actin cytoskeleton, as well as the control of membrane proteins through endocytosis. These cellular responses within the tumour environment are tightly regulated as each of the constituents within the niche is able to secrete growth factors, chemokines, cytokines and proteins capable of remodelling the extracellular matrix (Jiang *et al*., 2009; Mathias *et al*., 2013; van Zijl *et al*., 2011). Taken together, invasive and metastasized lesions display a variety of morphological features, molecular subtypes, and clinical behaviours which make BC a formidable disease.

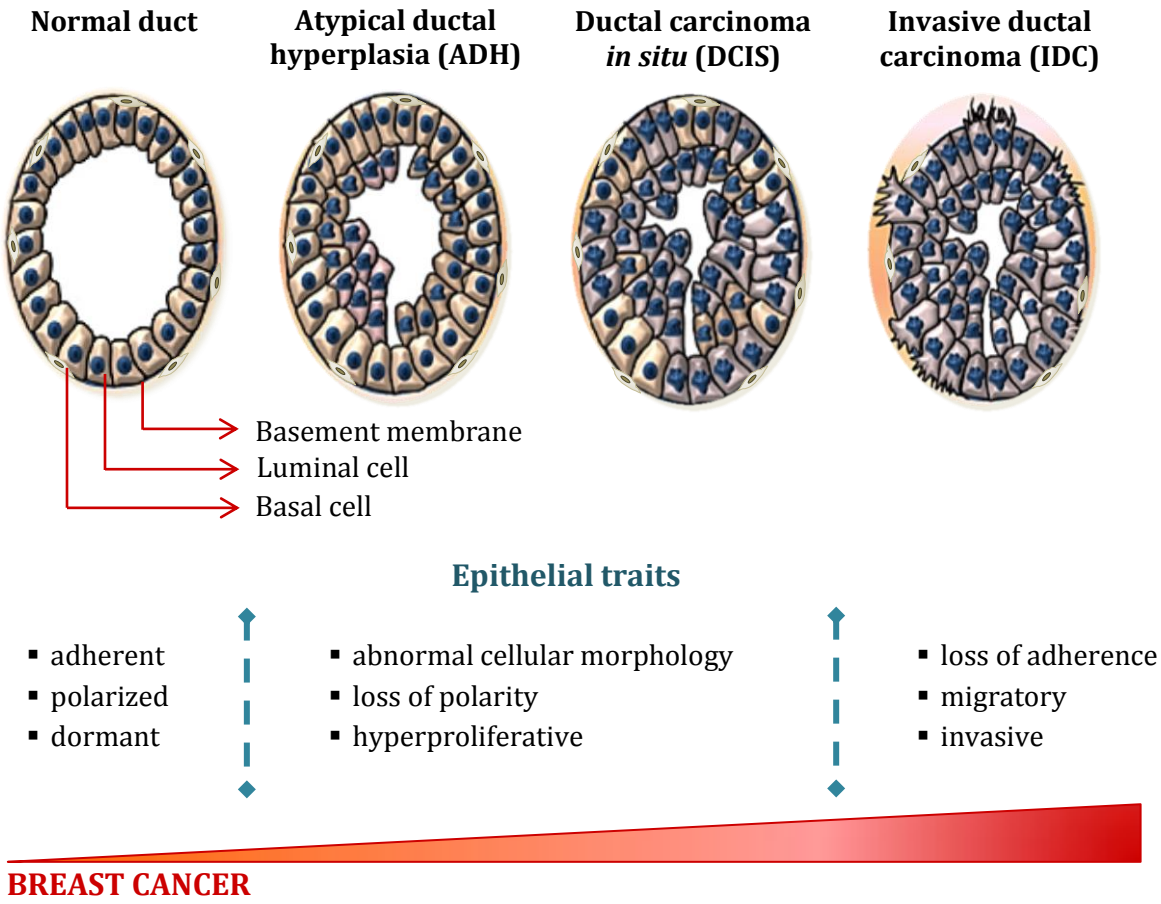

Figure 2.2: Outline of BC progression. Breast cancer is believed to advance through a series of well-defined stages. This sketch depicts cross-sections of the mammary duct at different stages of BC progression: Normal duct, Atypical ductal hyperplasia (ADH), Ductal carcinoma *in situ* (DCIS), and Invasive ductal carcinoma (IDC) (Mukhopadhyay *et al*., 2011; Shore and Rosen, 2014).

2.4 Classification of Breast Cancer

2.4.1 Immunohistochemical classification

Traditional, histopathological subclassification of BCs by immunohistochemistry has resulted in a clinically relevant classification system which contextualizes pathogenesis and therapeutic approaches for its treatment. Typically, this procedure uses the immunostaining technique in paraffin sections of BC (Goldhirsch *et al*., 2009). In clinical practice three predictive biomarkers in BC, not mutually exclusive, have been identified and addressed (Bertos and Park, 2011). These immunohistological biomarkers are categorized on the basis of the amplification/overexpression of the Human Epidermal Growth Factor Receptor 2 (HER2/*neu*), and the presence or absence of expression of the estrogen receptors (ER) and progesterone receptors (PgR) (Hammond *et al*., 2010; Patani *et al*., 2013; Wolff *et al*., 2007). Breast cancers are further sub-classified into four major clinical groups based on cell marker expressions: $ER^+/PgR^+/(HER2/neu)^-$, $ER^+/PgR^+/(HER2/neu)^+$, $ER^-/PgR^-/(HER2/neu)^+$ (HER2/*neu*-enriched), and $ER^-/PgR^-/(HER2/neu)^-$ (triple negative which has none of the abovementioned receptors). Numerous ecological/lifestyle and hereditary risk factors associated with the aetiology of BC also play a role in the hormone-receptor status of the tumour. For example, early menarche, nulliparity, late age at first birth, as well as obesity among postmenopausal women have been more strongly linked to ER and/or PgR^+ than the ER^- tumours (Colditz *et al*., 2004; Cotterchio *et al*., 2003; Rusiecki *et al*., 2005). The majority of BCs express ER and PgR, and the percentage of positive tumours increases with age at diagnoses. Thus in women younger than 35 years, ER^+ varies from 60-70%, whereas in women over 60 years it increases to 80% (Mavaddat *et al*., 2010). In contrast, the fraction of HER2/neu^+ and HER2/neu^- tumours remains approximately the same over all age groups. The issue of heterogeneity which the existing accepted classification posits may explain diversity in tumour proliferative capability and resistance to therapy (Bauer *et al*., 2010; D'Amato *et al*., 2015; Nitta *et al*., 2016).

2.4.2 Molecular classification

Breast cancer classification based on gene expression microarrays has revealed both biologically and clinically meaningful molecular profiles, each with distinct characteristics (Sørlie *et al*., 2001; 2003). Computational systems have enabled the simultaneous gene expression analysis of large cohorts of BC samples in a single experiment in order to generate gene signatures (Rivenbark *et al*., 2013). In 2000, Perou *et al*. were the first to classify BC into intrinsic subtypes based on common gene expression patterns determined by overexpressed genes. In the pivotal study, the group screened 38 BC cases using complementary DNA (cDNA) microarray, and reported a defined list of intrinsic genes. Based on these intrinsic gene signatures, a hierarchical cluster analysis identified four major molecular subtypes of BC: Luminal, HER2/*neu* enriched, Basal-like and Claudin-low (Perou *et al*., 2000; Sørlie *et al*., 2001; 2003; Sotiriou *et al*., 2005). The subsequent expansion of transcription profiling studies in a larger cohort of BC patients provided additional information and created new classifications validated by independent groups. Currently, the Luminal group has been divided into two subcategories, namely, Luminal A and Luminal B. These novel classifications group breast tumours according to their biological characteristics regardless of their prognostic and clinical features (Eroles *et al*., 2012). This study focuses primarily on the HER2/*neu* molecular subtype which is discussed in greater detail below.

2.5 The Human Epidermal Growth Factor Receptor 2 (HER2/*neu*)

2.5.1 Physiological role of HER2/*neu*

The HER2/*neu*, also termed HER2, ErbB-2 or c-erbB2, is a 185 kDa transmembrane glycoprotein ($p185^{HER2/neu}$), encoded by the *ERBB2* gene located at the long arm of human chromosome 17 (17q21-q22) (Burgess, 2008; Coussens *et al*., 1985; Yarden and Sliwkowski, 2001). HER2/*neu* is a member of the HER (ErbB) lineage of proteins, which includes three other structurally related Epidermal Growth Factor Receptors (EGFR): HER1 (EGFR, ErbB-1), HER3 (ErbB-3) and HER4 (ErbB-4). These receptors form part of a group of 90 protein-tyrosine kinases, of which 58 are receptor and 32 are non-receptor kinases (Alonso *et al*., 2004; Klapper

et al., 2000; Roskoski Jr, 2014). Structurally, the ErbB family of receptors is expressed as single-pass integral transmembrane receptor proteins.

Under normal physiological conditions, HER2/*neu* is usually expressed at low levels, anchored in the membrane of epithelial cells in a wide variety of tissues, viz., the placenta, ovary, breast, gastrointestinal tract, endometrium, lung, kidney and the central nervous system (Lemoine *et al*., 1990; Natali *et al*., 1990). In humans, HER2/*neu* is over-expressed on the surface of trophoblasts and foetal epithelial cells during the final stages of trophoblastic differentiation (Mielke *et al*., 1998; Press *et al*., 1990). HER2/*neu* is believed to be an orphan receptor, as none of the epidermal growth factor ligands which are capable of dimerizing with the other HER family members is able to activate it. At the molecular level, HER2/*neu* has no known ligand and its receptors are activated upon homo- or hetero-dimerization with the other members of the HER family or by proteolytic cleavage of their extracellular domain (termed HER2/*neu* shedding) (Olayioye, 2001; Tsé *et al*., 2012). Upon activation, HER2/*neu* is normally involved in the signal transduction pathways leading to cell growth and differentiation.

2.5.2 HER2/*neu* receptor biology

Based upon the primary amino acid structure and cDNA analysis of the HER2/*neu* receptor, three distinct regions have been identified: a glycosylated N-terminal extracellular domain, a single hydrophobic α-helical transmembrane domain, and an intracellular portion with a juxtamembrane segment, a protein tyrosine kinase domain, and a carboxyterminal tail (Ullrich *et al*., 1984; Olayioye *et al*., 2000) **[Figure 2.3A]**. Similar to all HER receptors, the N-terminal extracellular domain of the HER2/*neu* receptor is the largest of the three domains (95-115 kDa), and is organized into four subdomains (I-IV) (Cho *et al*., 2003). Subdomains I and III are related leucine-rich segments that form a binding site for the receptor's potential ligands, and subdomains II and IV, which are cysteine-rich residues, participate in disulfide homo- and hetero-dimerization (Lax *et al*., 1988; Pietras *et al*., 1995). In particular, subdomain II contains a short hairpin loop dimerization arm which protrudes on the outer surface of this subdomain. Therefore, subdomain II is believed to be the main contributor to dimerization, capable of connecting with the dimerization arm of HER family members (Tai *et al*., 2010a). Based on the X-ray crystal structure of the extracellular domain, two conformations are known to exist: a

closed (inactive) configuration and an open (active) configuration (Garrett *et al*., 2003). In the inactive conformation, the interplay between domains II and IV prevents the association with dimerization arms from other HER receptors because these receptors possess a tethered and closed structure. In contrast, binding of its native ligand to the receptor induces the interaction between subdomains I and III, resulting in an extended and open conformation in which the dimerization arm of subdomains II and IV are exposed and not buried, effectively forming an active conformation state. Except the HER2/*neu* receptor, all other members of the HER family of receptors (ErbB-1/3/4), employ a receptor-only mediated dimerization mechanism (Lemmon, 2009). HER2/*neu* receptors in their native form exist in an open configuration, indicating that the dimerization arm remains constitutively extended and capable of dimerizing with the other receptors (Burgess *et al*., 2003; Garrett *et al*., 2003; Tai *et al*., 2010a). Together, the four HER family members are able to form 28 homo- and hetero-dimers, with HER2/*neu* being the preferred dimerization partner for all the other HER (ErbB-1/3/4) receptors (Graus-Porta *et al*., 1997; Pinkas-Kramarski *et al*., 1996).

Connecting the extracellular region to the intracellular protein tyrosine kinase domain is a single α-helical transmembrane domain comprised of 19-25 amino acid residues. Fleishman *et al*. (2002) recognize a molecular activation switch in the HER2/*neu* transmembrane region, and show that there are two motifs with a conserved sequence of approximately 5 residues. Further, these two dimerization motifs play a major role for receptor dimerization. The dimerization is triggered by strong dimerization interactions which are created by hydrogen bonds and van der Waal forces between hydrophobic segments within the dimerization motifs (Bazley and Gullick, 2005). This mechanism has been substantiated by crystallographic analysis of the HER2/*neu* transmembrane homodimers (Tai *et al*., 2010a).

The intracellular protein tyrosine kinase region has approximately 570 residues, and is divided into three major subdomains: (i) a cytoplasmic juxtamembrane linker, (ii) a tyrosine kinase domain, and (iii) a carboxyl-terminal tail. The juxtamembrane is a small flexible segment which links the transmembrane domain and tyrosine kinase domain. The tyrosine kinase domain has several short amino-terminal lobes/loops containing several conserved α-helices and β-stands which form the enzyme active site (Knighton *et al*., 1991; Telesco and Radhakrishnan., 2009). This region is the most complicated of the HER2/*neu* protein receptor. Numerous studies have focused on this segment of the receptor, and it has been extensively reviewed (Jones *et al*., 2006;

Roskoski Jr, 2014; Schulze *et al*., 2005). The carboxyl-terminal tail contains several tyrosine residues which are available for phosphorylation, and serve as docking sites for adaptor proteins or enzymes containing either modular Src homology 2 or phosphotyrosine binding domains (or both) (Roskoski Jr, 2014).

2.5.3 HER2/*neu* receptor mechanism of action and signaling pathways

In the physiological quiescent state, HER2/*neu* receptors are inactive monomers. Receptor dimerization is a fundamental requirement for HER2/*neu* signalling activities that govern essential cellular processes (Olayioye *et al*., 2000). Among the different dimers formed by the HER receptors, HER2/*neu*-containing heterodimers are characterized by the most powerful signal transduction cascade; this markedly reduces the rate of ligand dissociation, allowing potent and prolonged activation of downstream signaling pathways (Rubin and Yarden, 2001).
Dimerization results in the phosphorylation of tyrosine residues which are catalyzed by the juxtaposed cytoplasmic kinase domains leading to protein kinase activation. The response to HER2/*neu* activation depends largely on the different dimeric combinations of HER proteins within the dimers and the pattern of dimerization, mediated by the activation of at least three different pathways, namely, phosphatidyl inositol 3 kinase (PI3K)/ Ak transforming factor (Akt)/ mammalian target of rapamycin (mTOR), mitogenic Ras/ receptor activation factor (RAF)/mitogen-activated protein kinase (MAPK), and phospholipase C-γ (PLCγ) pathways (Citri and Yarden, 2006; Rubin and Yarden, 2001) **[Figure 2.3B]**. Depending on which of the signal cascades are activated, HER2/*neu* receptors can be involved in the regulation of complex cellular processes including proliferation, cell survival, differentiation, adhesion and migration. Typically, induction of the PI3K cascade is stimulated by the (HER2/*neu*)/HER3 heterodimer, this dimerization pair being the most robust of the HER homo- and hetero-dimers (Tzahar *et al*., 1996). On the other hand, HER2/*neu* dimerization with all of the HER (ErbB-1/3/4) members can activate the MAPK pathway (Yarden and Sliwkowski, 2001). Both the PI3K and MAPK pathways are known to provide the key signaling cascades that prevent apoptosis, promote cell growth and proliferation, cellular migration and angiogenesis (Tai *et al*., 2010a).

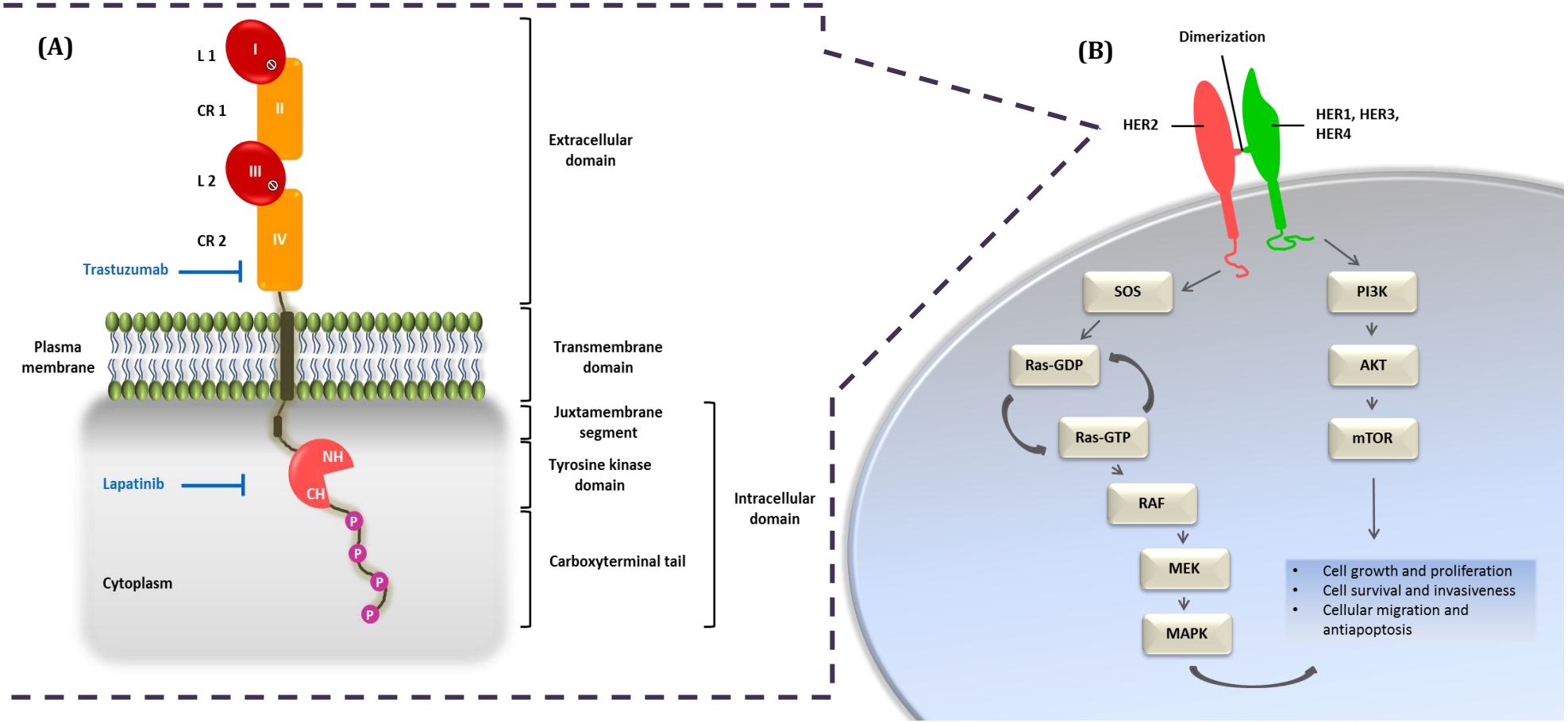

Figure 2.3: Portrait of the HER2/*neu* structure (**A**). The extracellular domain consists of four subdomains (I-IV); two leucine-rich domains (L 1/ I and L 2/ III) which are marked with a stop symbol as they do not participate in ligand binding, and two cysteine-rich domains (CR 1/ II and CR 2/ IV) responsible for receptor dimerization. Depicted are the transmembrane domain; the amino- (NH) and carboxyl-terminal lobes of the kinase domain and the carboxyl-terminal tail containing several tyrosine residues that can be phosphorylated. Inhibitors of HER2/*neu* mediated signalling using monoclonal antibody (Trastuzumab) and small molecule tyrosine kinase inhibitor (Lapatinib) are also indicated. Key HER2/*neu* signalling pathways involved in tumorigenesis are also schematically illustrated (**B**). HER2/*neu* dimerizes with the activated HER receptor resulting in the phosphorylation of the tyrosine residues and signal transduction in the intracellular domain. This activates the lipid kinase phosphatidyl inositol 3 kinase (PI3K), which phosphorylates a phosphatidylinositol that in turn binds and phosphorylates the enzyme Ak transforming factor (Akt). Among the Akt multiple targets is the mammalian target of rapamycin (mTOR), which drives cell survival by promoting cell cycle progression and inhibiting pro-apoptotic members of the Bcl-2 family. On the other hand, the mammalian homologue of the son of sevenless (SOS), a guanine nucleotide exchange factor, activates the rat sarcoma (RAS) enzyme which, in turn, activates the receptor activation factor (RAF) and then mitogen extracellular signal kinase (MEK). MEK then phosphorylates the mitogen-activated protein kinase (MAPK), which results in cell cycle progression and proliferation (Adapted from Colombo *et al*., 2010; Roskoski Jr, 2014; Seliger and Kiessling, 2013; Thery *et al*., 2014; Videira *et al*., 2014).

2.5.4 The role of HER2/*neu* in breast cancer

One of the most common malignant transformations of mammary cells leads to amplification and/or over-expression of the HER2/*neu* oncogene, accounting for ~30% of all invasive BC cases (Menard *et al*., 2000; Press *et al*., 2002; Rubin and Yarden, 2001; Slamon *et al*., 1989). HER2/*neu* mutations are rare in BCs. In a novel study, Bose *et al.* (2013) concluded that approximately 1.6% of BC patients possess an HER2/*neu* gene mutation. These mutations were reported to occur in the extracellular domain, carboxyterminal tail as well as in the protein kinase domain. Gene amplification and transcriptional up-regulation have major roles in HER2/*neu* over-expression. In HER2/*neu*-amplified breast carcinomas, HER2/*neu* expression levels are significantly higher, varying from five hundred thousand to more than two million receptors per tumour cell, compared to twenty-five to one-hundred and eighty-five thousand receptors per tumour cell in non-amplified tumours (Tsé *et al*., 2012; Yarden, 2001). Over-expression of HER2/*neu* receptors is an adverse prognostic marker associated with poor disease-free survival. At the time of diagnosis, patients with HER2/*neu*-enriched subtype are likely to have a higher incidence of advanced disease, coupled with reduced overall survival rate and time of relapse (Kennecke *et al*., 2010; Voduc *et al*., 2010). It has been found to correlate with tumours which are larger in size, of high nuclear grade, and with a decrease in the expression of steroid hormone receptors (Konecny *et al*., 2003; Nielsen *et al*., 2009). They are characterized as a more aggressive tumour phenotype associated with increased cell proliferation, a greater likelihood of lymph node involvement, increased tumour invasiveness, and metastasis (Moasser, 2007; Slamon *et al*., 1987). In addition, HER2/*neu* enhances angiogenesis by increasing vascular endoethelial growth factor production, and reduces apoptosis by increasing the expression of survivin (Siddiqa *et al*., 2008; Zhou *et al*., 2000).

Although HER2/*neu* BCs usually display several genomic aberrations, cell proliferation and survival depend critically on HER2/*neu* activation and signalling. Thus far, two different mechanisms have been described. In the first and more common type, HER2/*neu* permanently forms self-dimerization or partners with one of the other HER family of receptors to form homo- and/or hetero-dimers, whereupon an increase in cell signal transduction cascades is triggered (Graus-Porta *et al*., 1997; Pinkas-Kramarski *et al*., 1996; Warren and Landgraf, 2006; Yarden, 2001). In the second, HER2/*neu* signalling transduction can be induced via formation of

truncated HER2/*neu* carboxy-terminal fragments, which constitutively maintain kinase activity (Anido *et al*., 2006; Pedersen *et al*., 2009). HER2/*neu* hetero-dimers are capable of evading inactivation processes as they contain strong bonds which decrease the rate of ligand dissociation. Moreover, they are able to bypass the degradative pathway by returning to their primary site on the cell surface (Harari and Yarden, 2000).

2.5.5 HER2/*neu* as a target for breast cancer therapy

In recent years, targeted molecular therapeutics for BC has been changing considerably. Research efforts have focused mainly on the identification of the precise molecular abnormalities responsible for tumourigenesis (Workman, 2005). In the late 1980s, Slamon *et al*. (1987) were the first to associate HER2/*neu* amplification with negative clinical outcomes. In addition, they described HER2/*neu* protein over-expression as a likely predictive target for treatment. The discovery of HER2/*neu* and its role in malignant progression constituted a major breakthrough, and led to the development of a number of targets for anticancer drugs.

There are several reasons for the exploitation of the HER2/*neu* receptor as a therapeutic target for BC. Firstly, the identification and molecular characterization of HER2/*neu*, indicated that all three domains are involved in a specific aspect of the signalling cascade responsible for abnormal growth and malignant transformation. Therefore, each domain can be targeted separately to inhibit the HER2/*neu* signalling pathway. Secondly, HER2/*neu* is over-expressed in cancer cells and is present in high numbers in both pre-malignant tumours and metastasized organs (Moasser, 2007). Finally, as mentioned in the previous section, HER2/*neu*-containing hetero-dimers have the greatest mitogenic potential among all HER2/*neu* dimers. Thus, blocking the extracellular domain inhibits HER2/*neu* dimerization and prevents the activation of intracellular signalling pathways involved in the onset and progression of BC. Currently, several novel HER2/*neu* targeted therapies are used in clinical trials to test their efficacy in BC therapeutics. Recent reviews on HER2/*neu* targeted therapies include those published by Figueroa-Magalhães *et al*., 2014; Gullo *et al*., 2013; Hurvitz *et al*., 2013; Nandy *et al*., 2014; Palmieri *et al*., 2014.

2.6 Current Treatment Options for HER2/*neu*

To date, several anti-HER2/*neu* targeted therapies have been developed and approved in the United States and elsewhere based on their role in increasing survival outcomes in patients. Most notably, Trastuzumab and Lapatinib are the main targeted therapies exclusively associated with HER2/*neu* gene amplification and/or over-expression of the protein, which have demonstrable benefits in the clinical setting. Traditionally, these treatments are first administered and analyzed in the metastatic disease state, and then in neoadjuvant trials (Campone *et al*., 2011; Figueroa-Magalhães *et al*., 2014; Shah and Osipo, 2016).

2.6.1 Antibody targeting the extracellular domain

The extracellular domain of HER2/*neu* has been the target of several monoclonal antibodies used to suppress its dimerization with other HER family members. The binding of antibody blocks the activation of all HER2/*neu* dimers, thereby preventing phosphorylation of the tyrosine kinase domain as well as retarding or inactivating its downstream signalling pathway (Tai *et al*., 2010a). In 1998, the recombinant humanized monoclonal antibody Trastuzumab (Herceptin®) (Genentech Inc. San Francisco, CA, USA; Hoffmann-La Roche Ltd. Basel, Switzerland) was approved by the USA Food and Drug Administration (FDA) for the treatment of HER2/*neu* positive BC (Schaefer *et al*., 2006; Shawver *et al*., 2002; Tokunaga *et al*., 2006; Yeon and Pegram, 2005). Trastuzumab is currently recommended as first-line treatment for patients with HER2/*neu* over-expressing metastatic tumours, either as a single agent or in combination with endocrine therapy and/or chemotherapy. It has also been used as a treatment option in early stage BC, as well as in the adjuvant setting (Awada *et al*., 2012). It is recommended that 3+ over-expression or gene amplification by immunohistochemical and fluorescent *in situ* hybridization, respectively, is essential for likely benefits from treatment (Nielsen *et al*., 2009).

Basically, Trastuzumab acts by binding to domain IV on the juxtamembrane region of the extracellular domain **[Figure 2.3A]** of HER2/*neu* protein (Azim and Azim Jr, 2008). Although the precise mechanism of Trastuzumab's anti-tumour action has not been fully elucidated, several proposed mechanisms exist based upon preclinical and clinical trials (Colombo *et al*., 2010). These include: the down-regulation of the HER2/*neu* receptor resulting in the reduction of

available receptors; blockage of HER2/*neu* extracellular proteolysis, thus preventing the formation of truncated highly active receptors; anti-angiogenesis leading to reduced micro vessel development *in vivo*, coupled with decreased cellular migration *in vitro*; induction of apoptosis mediated through the activation of antibody-dependent cellular cytotoxicity; and induction of cell cycle arrest during the G1 phase, followed by reduction of proliferation (Dean-Colomb and Esteva, 2008; Klos *et al*., 2003; Molina *et al*., 2001; Spector and Blackwell, 2009).

There are, however, a number of concerns associated with its use in the clinical setting. For one, cardiac toxicity has raised a major safety concern, and remains the hallmark side effect. This is primarily due to the pivotal role of HER2/*neu* in embryonic cardiac development (Negro *et al*., 2004; Perez, 2008), thus precluding its use in patients with poor cardiac function. Again, not all patients respond positively to Trastuzumab (Tai *et al*., 2010a), with a significant number of patients acquiring intrinsic resistance within a year of treatment. Resistance to Tratuzumab has been shown to develop via several mechanisms, including; (1) impaired receptor-antibody binding, (2) truncated HER2/*neu* protein, (3) gene mutations, (4) signalling via alternative pathways, (5) co-expression of insulin growth factor receptor, (6) loss of phosphatase and tensin homolog (PTEN), and (7) cancer-associated fibroblasts (Browne *et al*., 2011; Mao *et al*., 2015; Nahta *et al*., 2005; 2006; Pohlmann *et al*., 2009; Saini *et al*., 2011). Furthermore, BC recurrence has been observed in early BC, and disease progression has been reported with most metastatic disease cases within a year of administering treatment. Large trials, too, have documented an increase in central nervous system metastasis (primary site of tumour recurrence) (Collins *et al*., 2009; Montemurro *et al*., 2006). Finally, the high cost of Trastuzumab limits its use, and all these constraints have prompted research aimed at developing more efficient and better tolerated HER2/*neu* targeted therapies.

2.6.2 Tyrosine kinase inhibitors to HER2/*neu* receptor

Tyrosine kinase inhibitors are small molecules which constitute another group of agents designed to target the HER2/*neu* receptor. In 2007, the first promising small molecule inhibitor, Lapatinib (GW572016, Tykerb™/Tyverb™) (GlaskoSmithKline, Middlesex, UK), was approved by the FDA and the European Medicines Agency as an effective drug for the treatment of HER2/*neu* and HER1 overexpressing breast carcinomas (Geyer *et al*., 2006; Spector *et al*., 2005). Lapatinib

is a reversible dual HER2/*neu* and HER1 tyrosine kinase inhibitor that has a unique mechanism of action compared to other tyrosine kinase inhibitors. Small molecule inhibitors are designed to compete with adenosine triphosphate (ATP) for the intracellular ATP-binding pocket of the tyrosine kinase domain. The nature of the contact between Lapatinib and the domain results in a very slow dissociation, enabling prolonged inhibition of tyrosine kinase phosphorylation. Lapatinib selectively interrupts signal transduction, which leads to inhibition of downstream pathways that control proliferation and survival of tumour cells (Tevaarwerk and Kolesar, 2009). In addition, Lapatinib inhibits the downstream signalling proteins such as cyclin D, extracellular signal-related kinase (Erk) and Akt (Collins *et al*., 2009; Xia *et al*., 2002).

Unlike Trastuzumab, Lapatinib is able, as a small molecule, to cross the blood brain barrier and could therefore be effective in dealing with brain metastasis. Moreover, cardiac toxicity risks associated with Trastuzumab are considerably lower with Lapatinib (Collins *et al*., 2009; Saini *et al*., 2011). Lapatinib clearly demonstrates significant clinical activity. However, both in the adjuvant and neoadjuvant setting, Lapatinib has been associated with a high incidence of diarrhoea, hepatic toxicity, skin rash, anorexia, fatigue, nausea, headache, and vomiting (Collins *et al*., 2009; Moy and Gross, 2006; 2007; Metzger Filho *et al*., 2012; Vu *et al*., 2014).

2.7 Overview of Gene Therapy

Gene therapy is a unique therapeutic technique which has been developed as an alternative to conventional medicine to favourably modify or cure both contracted and inherited genetic defects (Fischer and Cavazzana-Calvo, 2008). Significant advances in basic gene therapy research are occurring in countries all around the world. To date, gene therapy has been used to address a wide variety of diseases at their root cause, ranging from cancer (Faneca *et al*., 2008; Li and Huang, 2006; Nakase *et al*., 2005; Xing *et al*., 1998) to neurological disorders (Kaplitt *et al*., 2007; Zhang *et al*., 2003). Numerous clinical trials are ongoing worldwide (Edelstein *et al*., 2004; 2007), with the majority focussing on cancer, the latter comprising approximately 64% of all on-going clinical gene therapy trials, followed by monogenic and cardiovascular diseases **[Figure 2.4]**. However, as yet, widespread therapeutic success has remained elusive.

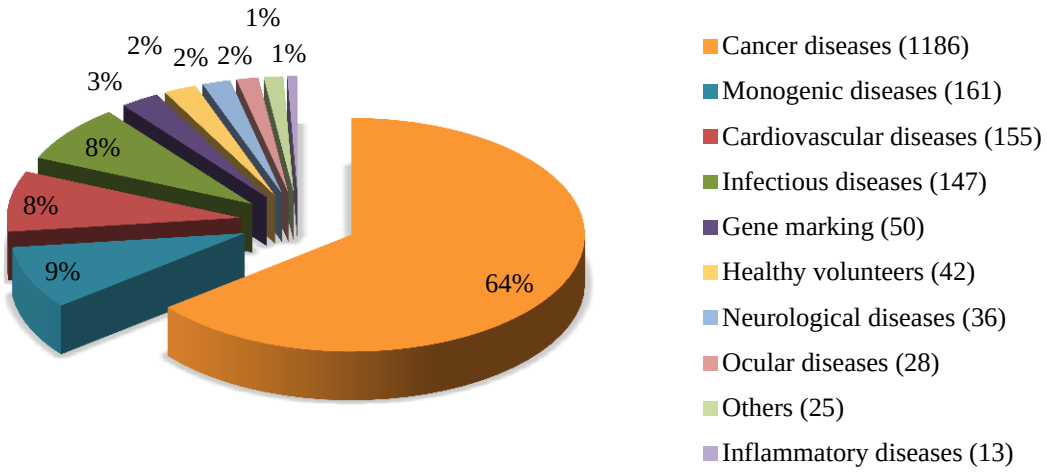

Figure 2.4: A graphic representation of the widespread application of gene therapy in clinical trials (Wirth *et al*., 2013).

Current legislature permits gene therapy only in somatic cells. This means that the genetic material is inserted into some target cells of an individual, and genetic changes occur only in the targeted cells, and cannot be passed on to the next generation. Prior to developing gene therapy for any specific condition, the following challenges need to be addressed: genetic malfunctions must be precisely characterized and the causal gene identified; the specific cells in the host requiring treatment must be identified and accessible; and a functional copy of the gene involved must be available. Furthermore, a gene delivery vehicle must be available to efficiently carry the functional copy of the gene into target cells where it can be stably expressed for an extended period.

The spectrum of gene therapy applications includes the use of nucleic acids (DNAs or RNAs) with regulatory function. Presently, these molecules belong to one of at least six possible classes, namely, DNA oligonucleotides, small regulatory RNAs, long anti-sense RNAs, other molecular binding RNAs, small catalytic RNAs and DNAs and decoy RNAs and DNAs (Giacca, 2010). Unlike traditional pharmaceutical drugs, gene therapy has the potential to treat almost any disease. Due to their diverse biological activities and unique mechanisms of action, gene-based therapeutics has resulted in several approaches for modifying defective genes (Wang *et al*., 2015). These include: 1) replacing an abnormal gene with a normal gene through homologous recombination; 2) replacing a non-functional gene by inserting a normal gene into a non-specific

location within the genome; 3) repairing an abnormal gene through selective reverse mutation; and 4) altering the expression of a particular gene (gene knockdown) (Grimm and Kay, 2007). Plasmid DNA (pDNA) and small interfering RNA (siRNA) are the two major classes of genetic materials which have been applied to mediate their effects at the transcriptional and/or translational level (Bumcrot *et al*., 2006; Gary *et al*., 2007; Park *et al*., 2006). DNA-based gene therapy is founded on the episomal or integrated presence and expression of corrective DNA in the host cell. This entails the delivery of exogenous pDNA encoding a particular gene and the subsequent stable or transient expression of the resulting transgene. The expression of therapeutic proteins thus ameliorates a specific pathological condition (Anderson, 1998; Verma and Somia, 1997). More recently, the field of new therapies based on RNAi has become the focus of the pharmaceutical industry as an attractive approach for investigating physiological gene function validation and for the potential treatment of human disease (de Fougerolles *et al*., 2007; Pecot *et al*., 2011; Wittrup and Lieberman, 2015). RNAi is a biological process which makes use of siRNA to induce sequence-specific post transcriptional gene silencing via the cleavage of homologous mRNA. This leads to the targeted inhibition of gene expression both *in vivo* and *in vitro* (de Fougerolles *et al*., 2007; Kim and Rossi, 2007; Kurreck, 2009; Leung and Whittaker, 2005; Takahashi *et al*., 2009).

2.8 History, Uniqueness and Mechanism of siRNA Gene Silencing

2.8.1 Advances in RNA interference

RNA interference represents an exclusive form of post-transcriptional gene silencing. It is an evolutionarily conserved cellular mechanism which is exploited for RNA-guided regulation of gene expression in mammalian cells and model organisms. This phenomenon was first discovered in Petunia flowers in the late 1980s by Napoli and co-workers (1990). Its molecular mechanism, however, remained unclear for almost a decade until Fire *et al*. (1998), using the nematode *Caenorhabditis elegans*, concluded that RNAi is a natural gene knockdown mechanism. This discovery was lauded by the Science magazine as “Breakthrough of the year” in 2002. Four years later Andrew Fire and Craig Mello were awarded the Nobel Prize for Medicine or Physiology for their pioneering work (Fire *et al*., 1998; Reinhart *et al*., 2000). In

2001, Elbashir *et al*., using synthetic siRNA, demonstrated the occurrence of RNAi in mammalian cell lines. These significant breakthroughs have highlighted the enormous potential of this technology to create selective gene silencing and to develop a new transgenic research field. Spurred by this development, the scientific community has engaged in intensive research efforts focused on siRNA therapeutics and its applications. Numerous scientific and technological breakthroughs in related fields have steered a rapid transition of potential therapeutic siRNAs from *in vitro* studies to clinical trials, resulting in remarkable progress in just over a decade (Davis, 2009; de Fougerolles, 2008).

2.8.2 Mechanism of siRNA gene silencing

Small interfering RNAs belong to a class of macromolecules (oligonucleotides) which are 21-23 nucleotide RNA duplexes derived from the digestion of larger double stranded RNA (dsRNA) trigger duplexes (> 30-50 bp) by an RNase III-like endonuclease known as Dicer-2 (Tuschl *et al*., 1999; Zhang *et al*., 2004). Alternatively, chemically or enzymatically synthesized siRNAs may be used as precursors to trigger the pathway (Amarzguioui *et al*., 2005; Elbashir *et al*., 2001). In each case, these siRNAs are characterized as 'small' dsRNA molecules with 2-nucleotides unpaired in the 5'-phosphorylated ends and with 3'-unphosphorylated ends (Elbashir *et al*., 2001; Hannon, 2002). **Figure 2.5** depicts the siRNA-mediated gene silencing pathway. In mammalian cells, within the cytoplasm, siRNA duplexes are incorporated into RNA induced silencing complex (RISC). Contained within the core of RISC is the multifunctional protein-RNA endonuclease, Argonaute-2 (Ago-2), which is involved in RISC activation (Liu *et al*., 2004a). Ago-2 is composed primarily of three domains, namely, the PAZ, MID and PIWI domains. The PAZ and MID domains are involved in the anchoring and docking of RNA, whereas PIWI functions in the mRNA silencing activity (Kim *et al*., 2009). ATP-dependent helicase unwinds the duplex, followed by Ago-2 mediated cleavage of the passenger (sense) strand (Matranga *et al*., 2005; Rand *et al*., 2005). The guide (anti-sense) strand remains bound to RISC via the divalent ion Mg^{2+} (Ma *et al*., 2005a), and guides it to anneal to complementary target mRNA molecules in the mid region between nucleotide bases ten and eleven relative to the 5'-phosphorylated end of the anti-sense siRNA strand (Elbashir *et al*., 2001; Matranga *et al*., 2005). Following this, the PIWI domain cleaves the target phosphodiester bond of the mRNA,

thereby rendering mRNA dysfunctional (Elbashir *et al*., 2001). mRNA silencing may be achieved via two mechanisms depending on the degree of complementarity between the anti-sense strand and the cognate mRNA: 1) site-specific cleavage of the message in the region of the siRNA-mRNA duplex leading to sequence-specific degradation, or 2) through translational repression (Caudy *et al*., 2003; Doench *et al*., 2003). The guide strand is recycled, thus permitting cleavage of numerous mRNA copies. The degree to which this process occurs depends mostly on the dissociation rate of the cleaved mRNA from the RISC assembly (Haley and Zamore, 2004). RISC recycling is a feature which distinguishes siRNA from other nucleic acid therapeutics such as anti-sense oligonucleotides, as it may demonstrate a silencing effect for up to seven days in dividing cells and for several weeks in non-dividing cells. Additionally, repeated administration of siRNA can result in stable long term target gene knockdown (Bartlett and Davis, 2006). The intrinsic capacity of siRNAs to selectively silence mRNA in a temporal and spatial modus is cause for optimism in the field of human BC therapeutics.

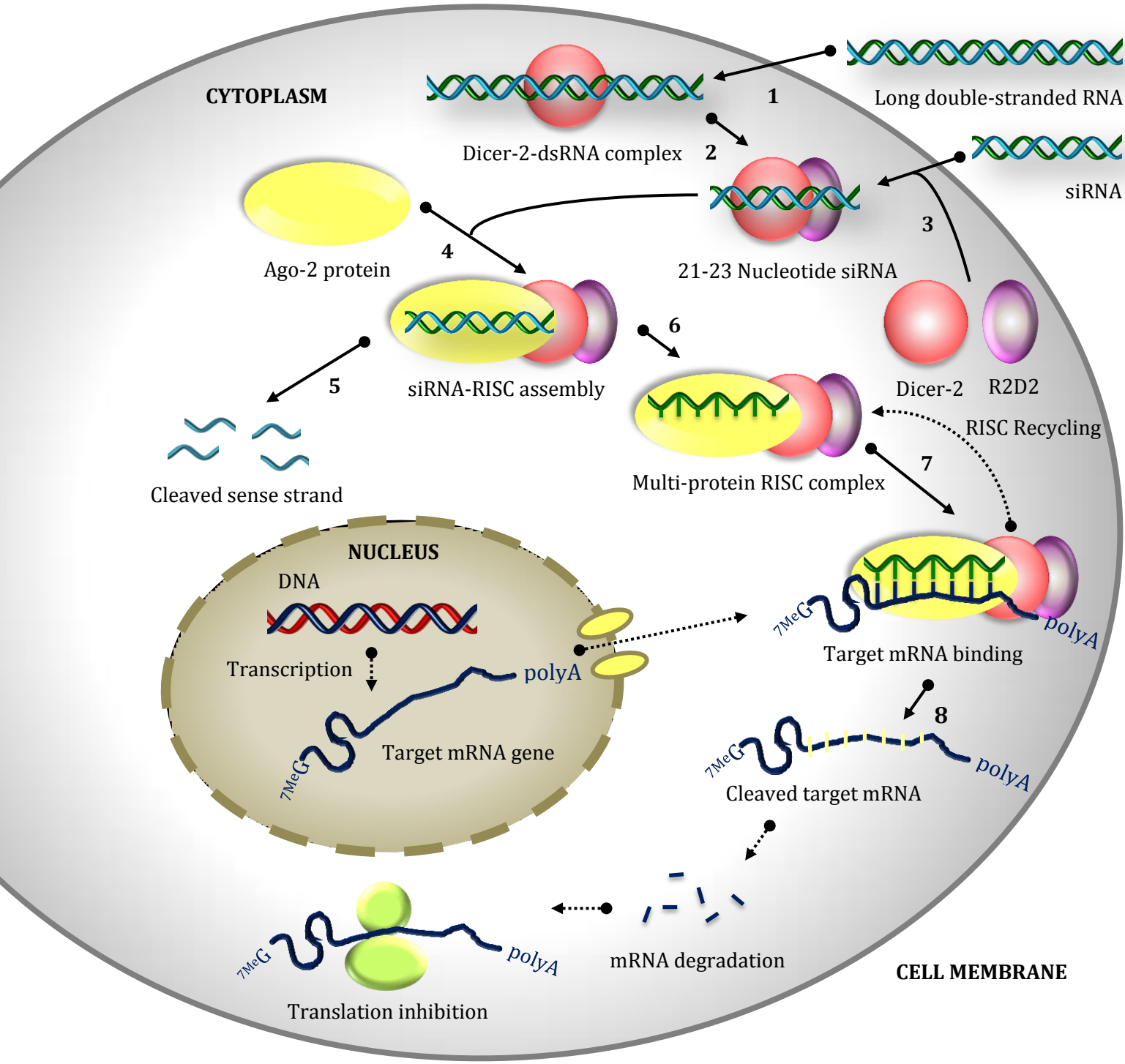

Figure 2.5: A schematic representation of the siRNA-mediated gene silencing pathway. 1) Introduction of exogenous long dsRNA is recognized by Dicer-2 in the cytoplasm; 2) Long dsRNA is cleaved by Dicer-2 into siRNA duplexes of 21-23 nucleotides in length followed by interaction with R2D2; 3) Synthetic siRNAs bypass the requirement for Dicer-2 processing and are recognized by both Dicer-2 and R2D2; 4) Dicer-2 and R2D2 facilitate the transport of siRNA to Ago-2, followed by formation of RISC; 5) Ago-2 protein promotes the unwinding of the duplexed siRNA, and the sense (passenger) strand is rapidly cleaved and dissociated; 6) The anti-sense (guide) strand remains bound to the RISC complex and mediates recognition of the target RNA; 7) Anti-sense RNA strand guides RISC and binds to the complementary site in the target mRNA; 8) RISC engages the endonucleolytic activity of Ago-2, resulting in target mRNA cleavage which shuts off translation of the corresponding protein (Adapted from Yang *et al*., 2013a).

2.9 Therapeutic Potential of siRNA Gene Silencing

2.9.1 Identifying targets for siRNA-induced gene silencing

The mapping of the human genome in the new millennium paved the way for scientists Perou *et al*. (2000) to classify human BC tumours based on their molecular portraits and unique gene expression profiles. They described four distinct BC subtypes: HER2/*neu*-positive, luminal, basal, and normal breast-like. A critical event in the progression of each of these BC subtypes is the initiation of specific gene expression patterns as a consequence of gene aberrations or upstream activation. The ability to selectively silence the expression of an activated oncogene at the mRNA level inhibits the production of abnormal proteins. This novel therapeutic strategy may be exploited in BC to modulate the expression of any protein, even undruggable target proteins (e.g., transcription factors) which are involved in tumour initiation, growth, and metastasis formation, thus providing an attractive, useful and promising technique for targeted therapeutics in gene therapy (Scherr *et al*., 2005). The identification of molecular targets is a prime research area in the pursuit of 'personalized' therapies for metastatic types of BC. The heterogeneous nature of BC and its attendant diversity in gene expression patterns present a range of specific targets for siRNA therapeutics. Furthermore, different signalling pathways have been determined and incorporated within the BC network. These will help identify key molecular relays which may be exploited to discover surrogate biomarkers for prognosis and siRNA therapy assessment. In the main, siRNA mediated BC therapies include: inhibition of tumour survival and induction of apoptosis (Huang *et al*., 2008) via HER2/*neu* gene silencing (Tan *et al*., 2007); Bcl-2 gene silencing (Beh *et al*., 2009); p53 gene silencing (Martinez *et al*., 2002) or inhibiting Wnt pathway (Wieczorek *et al*., 2008); angiogenesis (Xie *et al*., 2004); and chemoresistance (Creixell and Peppas, 2012).

2.9.1.1 Inhibition of angiogenesis

The development of new blood vessels from the existing vascular network (angiogenesis) significantly regulates tumour growth, invasion and metastasis of BC (Boudreau and Myers, 2003; Hobday and Perez, 2005; Sobel *et al*., 1992). Irrespective of cellular origin, initiation of

tumour angiogenesis at the molecular level is mediated by either a switch between up-regulation of inducers/activators or suppression of inhibitors of angiogenesis. Some key angiogenic activators include the vascular endothelial growth factor (VEGF), fibroblast growth factor (FGF), and transcription factor for hypoxia inducible factor-1 (HIF-1), whereas inhibitors include thrombospondin-1, angiostatin, interferon α/β and endostatin (Hanahan and Weinberg, 2000; Klagsbrun and Moses, 1999; Şalva *et al*., 2015). Research suggests that the VEGF (glycoprotein) family in particular is a vital angiogenesis oncogene target, and high levels of VEGF produced by tumour cells are attested as key contributors to tumour angiogenesis and growth (Davidoff and Nathwani, 2004; Dvorak *et al*., 1999; Sledge *et al*., 2006; Zelnak and O'Regan, 2007). In breast carcinoma cells, high VEGF levels are thought to act in an autocrine manner for cell survival (Bachelder *et al*., 2001), to induce disruption of endothelial cell basement membrane, contributing to metastasis (Weis and Cheresh, 2005), and decreasing response to conventional hormonal- and chemo-therapies (Toi *et al*., 1995). In addition, tumour cells overexpressing VEGF have been associated with poor prognosis and decreased survival rates (Linderholm *et al*., 1998; 2000). Intratumoural delivery of siRNA targeting VEGF was reported to inhibit breast tumour growth in an MDA-435 xenograft model (Xie *et al*., 2004). Some transcription factors such as ER-α (Stoner *et al*., 2004), HIF-1 (Forsythe *et al*., 1996) and polyomavirus enhancer activator 3 (PEA3) (Hua *et al*., 2009) can influence the activation VEGF transcription. In a study conducted by Hua *et al*. (2009), chromatin immunoprecipitation and luciferase assays were used to demonstrate the binding of PEA3 to the VEGF promoter, and PEA3 activation of VEGF promoter activity in cells overexpressing PEA3, respectively. PEA3 siRNA was reported to reduce VEGF promoter activity as well as attenuate the binding of PEA3 to the VEGF promoter in SKBR-3 cells. These researches suggest that PEA3 siRNA provides a possible means to demarcate potential targets for inhibiting or preventing cancer development and progression.

2.9.1.2 Apoptosis

The apoptotic system comprises an organization of sensors that detect pro-apoptotic stimuli, a signal transduction network, and execution machinery. This complex system is effected by the activation of a well-defined family of caspase proteases that influence cells through proteolytic

activity (Kerr *et al*., 1972). Activation of caspases mainly occurs through one of two pathways, namely, the intrinsic pathway which includes cell stress such as DNA damage or growth factor withdrawal, or the extrinsic pathway which is triggered by death ligands such as TNF-related apoptosis-inducing ligand (TRAIL). In normal cells, programmed cell death is closely controlled by a balance between pro-apoptotic and anti-apoptotic factors. At each level of pro-apoptotic stimulation, specific proteins are able to negatively regulate caspases and block apoptosis (Liu *et al*., 2004b). These include several members of the Bcl-2 family, nuclear factor-kB family of transcription factors, and inhibitor of apoptosis proteins (IAP) (Fulda, 2007; Hunter *et al*., 2007; Yang *et al*., 2003). These proteins and their regulators act in combination during "programmed" cell death. On the other hand, dysregulation due to aberrations in many genes that regulates the apoptotic system results in a blockage of cell death which ultimately leads to disease progression, and to chemio- and radio-resistance. Abnormalities have been identified in many genes that regulate the apoptotic cascade; these include Bcl-2 (Piché *et al*., 1998), bax (Su *et al*., 1998), and p53 (Elledge and Allred, 1994). Bcl-2 and Bcl-XL from the Bcl-2 anti-apoptotic family, for example, are overexpressed in cancer cells and have a strong anti-apoptotic effect. Basically, they counteract the activity of Bid, Bax and Bak (pro-apoptotic molecules), thereby supressing pro-apoptotic signalling in the mitochondria. The expression levels of Bcl-2 generally correlate with chemotherapy resistance (Buchholz *et al*., 2005; Ferlini *et al*., 2003; Tophkhane *et al*., 2007). siRNA-mediated down-regulation of Bcl-2 in MCF-7 cells results in an increase in apoptosis by 9% (at 72 h) and 11% (at 96 h) in comparison with the positive control (Lima *et al*., 2004). Foster *et al*. (2009) reported that siRNA-based depletion of a member of the IAP family XIAP increased apoptosis in response to Trastuzumab, Lapatinib or Gefitinib in Her2/*neu*-overexpressing BT-474 cells. Moreover, depleting the cells of XIAP overcomes the intrinsic resistance of BT-20 and MDA-MB-468 cells to TRAIL. Another frequent genetic abnormality is the elevated expression of c-Myc which is also involved in the apoptotic casade (Doisneau-Sixou *et al*., 2003; Liao and Dickson, 2000). Wang *et al*. (2005) found that 31.1% of MCF-7 cells transfected with p*Silencer*-c-Myc (short hairpin RNAs ligated into p*Silencer*) underwent apoptosis after serum starvation. Furthermore, they showed that on the 5^{th} day of transfection the plasmids endogenously expressing siRNA could successfully deplete up to 80% of c-Myc expression in MCF-7 cells. Tumour inhibition effects persisted for at least 12 days after transfection *in vitro* and for 2 months in nude mice respectively.

2.9.1.3 Cell cycle regulation

Silencing of certain genes associated with the development of tumours, poor prognosis, as well as resistance to anticancer agents can halt cell division and regulate the cell to enhance apoptosis. An example is the Akt pathway which is constitutively activated in BC cells (Nicholson and Anderson, 2002). In a report by Santi and Lee (2011), siRNA down-regulation of the Akt2 isoform in MDA-MB-231 BC cells showed a pronounced decrease in cell proliferation. The authors further reported that this was due, in part, to the unique role of Akt2 in the promotion of cell cycle progression, as the silencing of Akt2 decreases the levels of Cdk2 and cyclin D (responds to oncogenes and various growth factors). Since complexes are formed between Cdk2 and cyclin A or E, and between cyclin D with Cdk4 or Cdk6 (Rivard *et al*., 1996), the down-regulation of only two proteins (Cdk2 and cyclin D) in Akt2-siRNA transfected cells ensured the effective cell cycle arrest in the G0/G1 phase. Futher, upregulation of the E2F3 transcription factor also plays a role in controlling cell cycle progression (Vimala *et al*., 2012). More specifically, siRNA targeting cyclin E overexpression in SKBR-3, MDA-MB-157 and MDA-MB-436 cell lines promoted apoptosis, blocking their proliferation and transformation phenotypes. In addition, cyclin E siRNA synergistically enhanced the cell killing effects of doxorubicin in cell culture, and this combination significantly suppressed tumour growth in mice (Liang *et al*., 2010). In a comprehensive study utilizing E2F3 overexpressed BC cell lines, E2F3-siRNA markedly blocked the expression of the E2F3 proteins in the MCF-7 cell line, thus controlling rapid tumour cell proliferation (Vimala *et al*., 2012). In another study, siRNA mediated silencing of the anterior-gradient 2 (an estrogen-responsive secreted protein) in an ER-α positive BC cell line resulted in down-regulation of ER and cyclin D1 (Vanderlaag *et al*., 2010). These findings presage the likelihood of positive outcomes of the therapeutic application of siRNA in BC models and ER-positive cell lines in particular.

2.9.1.4 HER2/*neu*

Overexpression of growth factor receptors results in an increase of hetero-dimers, which in turn leads to an overall increase in intracellular signalling and activation of genes involved in cell proliferation (Fernández Val *et al*., 2002; Ross and Fletcher, 1999). This is naturally concomitant

with unabated aggressive tumour growth and death. As mentioned before, HER2/*neu* is associated with more aggressive tumour phenotypes, a greater likelihood of lymph node involvement, and increased resistance to cancer endocrine/chemotherapy (Bartsch *et al*., 2007; Engel and Kaklamani, 2007; Menard *et al*., 2000; Moasser, 2007; Slamon *et al*., 1987).

In response, scientists have therefore focussed on HER2/*neu* as a logical target for siRNA based BC therapies (Tan *et al*., 2007; Urban-Klein *et al*., 2005). Complications which arise are attributed to the primary resistance of HER2/*neu* gene-amplified breast carcinomas to HER-targeted therapies. This has been explained in the context of overactive HER2/*neu*-independent downstream pro-survival pathways by Oliveras-Ferraros *et al*. (2011). These authors addressed a specific role of the IAP survivin on the molecular efficacy of HER2/*neu* targeting drugs, and discovered that the up-regulation of survivin contributed to the enhanced survival of JIMT-1 cells, intrinsically displaying cross-resistance to HER1/2-targeted molecular therapies. Moreover, siRNA down-regulation of survivin (up to 80% survivin reduction 72 h after siRNA transfection) was sufficient to competently inhibit cell growth and survival as well as allow a combined anti-proliferative effect with HER antagonists. Wong *et al*. (2010) investigated the effects of siRNA knockdown of the PP2A catalytic subunit in two HER2/*neu*-positive BC cell lines, BT-474 and SKBR-3. PP2A-siRNA down-regulation demonstrably caused the silenced HER2/*neu* BC cells to undergo apoptosis, which was mediated by p38 MAPK-caspase 3/PARP activation. In a clinical study reported by Konecny *et al*. (2004), 87.7% of HER2/*neu* positive BCs were associated with overexpressed VEGF. Tai *et al*. (2010b) examined the effect of dual silencing of HER2/*neu* and VEGF genes on tumour growth and invasiveness. Their comprehensive study included nine HER2/*neu* and ten VEGF siRNAs which were capable of silencing the target genes by up to 75-83.5%. Furthermore, dual silencing of HER2/*neu* and VEGF resulted in significant change in cell morphology, substantial suppression of migration, cell adhesion, and proliferation. These observations suggested that HER2/*neu*-positive breast carcinomas may be more effectively treated by dual silencing of HER2/*neu* and VEGF gene expressions using siRNA (Tai *et al*., 2010b).

2.9.1.5 Sensitizing drug resistant proteins to conventional therapies

Chemotherapy entails the use of cytotoxic drugs commonly implemented in the treatment of many cancer types, including BC (Tack *et al*., 2004). A significant variety of cells, however, demonstrate suboptimal therapeutic responses associated with MDR. In essence, cancerous cells present altered strategies to prevent apoptosis induced by chemotherapy. Two main mechanisms exist, which enable cells to become multidrug resistant; firstly by increasing drug efflux pumps present on the cell membrane, and secondly by upregulating anti-apoptotic pathways (Gottesman, 2002). Using siRNA to down-regulate the activity of overexpressed genes encoding efflux pump proteins has become a feasible approach to sensitize cells to chemotherapeutic agents. The P-glycoprotein (P-gp), a 170 kDa membrane-associated drug efflux transporter, is often overexpressed, thereby impeding the permeability of several cytotoxic drugs such as doxorubicin, paclitaxel, and anthracycline, amongst others. Patil *et al*. (2010) encapsulated paclitaxel into a biodegradable polymer poly(D,L-lactide-coglycolide) mixed with polyethyleneimine (PEI) to form micelles. siP-gp was complexed to the nanoparticle via electrostatic interactions and the nanoplex was transfected into drug resistant JC cells. P-gp gene knockdown increased intracellular paclitaxel accumulation *in vitro* and enhanced *in vivo* cytotoxicity of paclitaxel, ultimately resulting in a reduction of tumour growth. Li *et al*. (2010) analyzed gene expression profiles of 115 breast carcinomas from women and conducted a neoadjuvant chemotherapy trial. Overexpression of YWHAZ (an anti-apoptotic gene) and LAPTM4B (a lysosomal gene) was associated with poor tumour response to anthracycline administration. They demonstrated the synergistic effect of co-delivering target specific siRNA and anthracycline using a lipid-mediated siRNA vector, and reported that the down-regulation of these genes enhanced the drug concentrations within the nucleus. Similarly, cationic biodegradable polymeric nanoparticles were reported to encapsulate siRNA targeting Plk1, MDR-1, and Bcl-2 into MDA-MB-435 and MDA-MB-231 breast carcinoma cell lines, thereby sensitizing the cells to paclitaxel and doxorubicin respectively (Sun *et al*., 2011; Wang *et al*., 2006; Xiong and Lavasanifar, 2011).

2.10 Challenging Pharmacokinetic Characteristics of Synthetic siRNA

By definition, pharmacokinetic characteristics refer to the process by which a drug is internalized, distributed, metabolized and eliminated by the body. Synthetic siRNAs have been intensively investigated in basic and pre-clinical science as a versatile gene expression silencer. However, most published research on pre-clinical animal models concern siRNA's low biological stability, i.e., rapid degradation by nucleases (~15 min half-life in serum) (Aagaard and Rossi, 2007; Bumcrot *et al*., 2006; Kuhn *et al*., 2007; Ozpolat *et al.*, 2014), and non-specific organ accumulation and rapid elimination through glomerular filtration (Aigner, 2006; Akhtar and Benter, 2007; Braasch *et al*., 2004; de Fougerolles *et al*., 2007; Kawakami and Hashida, 2007; van de Water *et al*., 2006; Xie *et al*., 2006). Overall, these investigations suggest that siRNAs, with their relatively large molecular weight (~13 kDa), behave as typical macromolecules of less than 50 kDa and 7 nm, thereby limiting their use in naked form. At the level of target cells, *in vitro* applications of siRNA demonstrated a short serum half-life and limited binding to and passive diffusion across lipophilic cell membranes because of their anionic surface charge (~40 negative phosphate charges) and hydrophilic nature (Moreira *et al*., 2008; Paroo and Corey, 2004). Additionally, within the cytoplasm, siRNA has to escape from the endocytic pathway and avoid lysosomal destruction prior to being incorporated into the RNAi machinery (Dams *et al*., 2000; Knop *et al*., 2010).

Moreover, major concerns were raised regarding the adverse effects of siRNA therapeutics, which include off-target silencing (Svoboda, 2007), saturation of the RNAi machinery (Grimm *et al*., 2006) and unwanted immune activation (Judge and Maclachlan, 2008). The intertwining of cellular anti-viral systems with the siRNA system leads to greater complexity and unpredictability in the action of siRNA. Synthetic siRNAs may thus induce type I interferon responses and stimulate the production of pro-inflammatory cytokines. The development of an appropriate and efficient delivery system for synthetic siRNA to target sites in the body is consequently the main hurdle preventing successful clinical applications. Delivery systems should be designed to address the vagaries of the pharmacokinetic and biodistribution properties of siRNA. The resolution of these issues, clearly, would pave the way for the envisioned role of siRNA as a powerful therapeutic agent.

2.11 Nanocarriers for siRNA Gene Delivery

Delivery vectors employed in gene therapy applications are broadly classified as viral or non-viral. Viral vectors are generally able to transfect target cells efficiently following systemic administration. Their development for application in humans, however, is still limited by inherent immune responses to the vector envelope and potential toxicity. Therefore, research efforts increasingly focus on non-viral vectors which, although currently less efficient, have a superior safety profile (Al-Dosari and Gao, 2009). Non-viral vectors are relatively easy to produce in large scale and provide a cost effective alternative to deliver large amounts of siRNA to target cells. Nanocarrier engineering is employed to enhance the stability, specificity and efficiency of non-viral nucleic acid delivery systems. An important advantage of this approach is that it makes use of naturally occurring or synthetic materials that may eliminate immune responses and exhibit low toxicity. Additionally, the unique morphological and phenotypic features of BC cells or tissues may be exploited to achieve tumour targeted delivery. Moreover, non-viral vectors may be designed to protect siRNA cargoes from nuclease digestion, avoid endosomal compartmentalization, and promote localization in the cytoplasm where the siRNA can be recognized by the RISC. In summary, nanocarrier engineering of non-viral vectors offers superior pharmacodynamic and pharmacokinetic characteristics **(Table 2.1)**. However, ensuring the successful expression of these design features in non-viral delivery systems is both challenging and arduous. For the purposes of this study, the literature review focuses on lipid and polymer based siRNA delivery systems in BC cell models.

Table 2.1: Examples of non-viral nanocarriers for siRNA gene delivery into breast cancer cell models

Composition of delivery systems	Particles' size[b] (nm)	Particles' charge[c] (mV)	PDI	Coating PEG	Targeting ligands	Applications[d]	Cell line	Reference
Cationic lipids								
DOGS/DOPE	~120	Not informed	~0.20	[a]	[a]	siRNAs directed against cyclin D1	MCF-7 (*in vitro*)	Lavigne and Thierry (2007)
DC-Chol/DOPE	130 - 150	+30 - +65	Not informed	PEG	[a]	anti-HER-2 siRNA	SKBR-3 (*in vitro*)	Zhang *et al.* (2010)
BHEM-Chol	170	+13.8	0.216	mPEG-PLA	[a]	siRNA directed against Plk1	MDA-MB-435s murine xenograft model (*in vivo:* i. v. administration)	Yang *et al.* (2011)
DOTAP/CHOL/ePC	105.9	−42.8	Not informed	PEG-PE	N-terminal fusion peptide DMPGTVLP	siRNA directed against PRDM14	MCF-7 (*in vitro*)	Bedi *et al.* (2011)
DDAB/CHOL/TPGS/HSA	79.5 ± 5.5	+15.3	Not informed	[a]	[a]	phrGFP siRNA	MCF-7, MDA-MB-231 and SKBR-3- phrGFP (*in vitro*)	Piao *et al.* (2013)
Stabilized nucleic acid lipid particles (SNALP)								
DODAP/DSPC/CHOL	194.7 - 254.4	Not informed	0.144 - 0.149	$CerC_{16}$-PEG_{2000}	DSPE-PEG-MAL-F3	anti-eGFP siRNA	MDA-MB-435s-eGFP (*in vitro*)	Gomes-da-Silva *et al.* (2012)
Anionic lipids								
DOPG/DOPE/Ca^{2+}	324.2 ±19.6	-22.9 ± 0.1	Not informed	[a]	[a]	anti-eGFP siRNA	MDA-MB-231-eGFP (*in vitro*)	Kapoor and Burgess (2012)
Polymers								
$mPEG_{2000}$-PLA_{3000}-*b*-R_{15}	54.30 ± 3.48	+34.8 ± 1.77	Not informed	PEG	[a]	anti-EGFR siRNA	MCF-7 nude mice xenograft model (*in vivo:* i. v. administration)	Zhao *et al.* (2012)
mPHA-*g*-bPEI	<200	+33 - +43	0.16 - 0.22	[a]	[a]	anti-*luc* siRNA	MCF-7-*luc* (*in vitro*)	Zhou *et al.* (2012)
mPEG-*b*-PCL-*b*-PPEEA	~60	+48	Not informed	PEG	[a]	siRNA directed against acid ceramidase	BT-474 murine xenograft model (*in vivo:* i. v. administration)	Mao *et al.* (2011)
mP3/4HB-*b*-PEG-*b*-lPEI	158	+28	<0.33	PEG	[a]	anti-*luc* siRNA	MCF-7-*luc* (*in vitro*)	Zhou *et al.* (2013)
P(MDS*co*-CES)	<250	+70	1.57	PEG	[a]	siRNA directed against Bcl-2	MDA-MB-231 (*in vitro*)	Beh *et al.* (2009)
Chitosan								
TAT-*g*-CS	212.2	+18.58	0.121	[a]	TAT ligand	siRNA directed against survivin	4T1-*luc* mice xenograft model (*in vivo*: i. t. administration)	Yang *et al.* (2013b)
CS/QD NPs	80	-35	Not informed	[a]	HER-2 antibody	siRNA directed against HER2/*neu*	SKBR-3 (*in vitro*)	Tan *et al.* (2007)
CS	130	Not informed	Not informed	[a]	[a]	anti-*luc* siRNA	MDA-MB-231-*luc* (*in vitro*)	Kong *et al.* (2012)

Single-chain antibody (fusion proteins)								
F5-P	N/A	N/A	N/A	N/A	HER-2 antibody	siRNA directed against DNMT	BT-474 murine xenograft model (*in vivo*: i. v. administration)	Dou *et al*. (2012)
RNA aptamers								
HER-2 aptamer	N/A	N/A	N/A	N/A	HER-2	siRNA directed against Bcl-2	N202.1A (*in vitro*: HER2/*neu* transgenic mouse)	Thiel *et al*. (2012)
Immunoliposomes								
Lyophilized PIL	~400	~35	Not informed	PEG	anti-HER-2 Fab'	anti-RhoA siRNA	SKBR-3 (*in vitro*)	Gao *et al*. (2010)
TLPD-FCC	150	<12	Not informed	DSPE-PEG-Mal	anti-EGFR antibody	anti-*luc* siRNA	MDA-MB-231-*luc* nude mice xenograft model (*in vivo*: i. v. administration)	Gao *et al*. (2011)
Gold nanoparticles								
PEI-C-AuNPs	15.3	+5	Not informed	[a]	[a]	anti-GFP siRNA	MDA-MB-435-GFP (*in vitro*)	Lee *et al*. (2011)

Abbreviations: PDI: polydispersity index; siRNA: small interfering RNA; i. v.: intravenous; i. t.: intratumourally; PEG: polyethylene glycol; DOGS: dioctadecylamidoglycylspermidine; DOPE: 1,2-dioleoyl-*sn*-glycero-3-phosphoethanolamine; DC-Chol: 3*β*-[*N*-(*N*′,*N*′-dimethylaminoethane) carbamoyl] cholesterol; BHEM-Chol: *N*,*N*-bis(2-hydroxyethyl)-*N*-methyl-*N*-(2-cholesteryloxycarbonyl aminoethyl) ammonium bromide; mPEG-PLA: poly(ethylene glycol)-*b*-poly(*d*,*l*-lactide); *Plk1*: polo-like kinase 1; DODAP: 1,2-dioleoyl-3-dimethylammonium-propane; DSPC: 1,2-distearoyl-*sn*-glycero-3-phosphocholine; CHOL: cholesterol; $CerC_{16}$-PEG_{2000}: *N*-palmitoyl-sphingosine-1-[succinyl(methoxypolyethylene glycol)$_{2000}$]; DSPE-PEG-MAL/F3: 1,2-distearoyl-*sn*-glycero-3-phosphoethanolamine-*N*-[maleimide(polyethylene glycol)2000] ammonium salt; ePC: L-α-phosphatidylcholine; DPPG: 1,2-dipalmitoyl-*sn*-glycero-3-[phospho-*rac*-(1-glycerol)] sodium salt; DOTAP: 1,2-dioleoyl-3-trimethylammonium-propane chloride salt; PEG-PE: 1,2-distearoyl-*sn*-glycero-3-phosphoethanolamine-N-[amino(polyethylene glycol)$_{2000}$] ammonium salt; DDAB: Dimethyl dioctadecyl ammonium bromide; TPGS: D-α-tocopheryl-polyethylene glycol 1000 succinate; HSA: human serum albumin; Ca^{2+}: calcium ions; DOPG: 1,2-dioleoyl-*sn*-glycero-3-phospho-(1′-*rac*-glycerol); $mPEG_{2000}$-PLA_{3000}: monomethoxy poly(ethylene glycol)-block-poly(*d*,*l*-lactide); *b*-R15: polyarginine; EGFR: Epidermal growth factor receptor; mPHA: monomethoxy-poly(hydroxyalkanoates); bPEI: branched poly(ethyleneimine); mPEG: monomethoxy poly(ethylene glycol); *b*-PCL: *block*-poly(ϵ-caprolactone); *b*-PPEEA: *block*-poly(2-aminoethyl ethylene phosphate); mP3/4HB-*b*-PEG-*b*-lPEI: mono-methoxy-poly (3-hydroxybutyrate-*co*-4-hydroxybutyrate)-*block*-polyethylene glycol-*block*-linear polyethyleneimine; P(MDS*co*-CES): poly(*N*-methyldietheneamine sebacate)-*co*-[(cholesteryl oxocarbonylamido ethyl) methyl bis(ethylene) ammonium bromide] sebacate); CS: chitosan; QD: quantum dot; NP: nanoparticle; F5-P: anti-HER-2 single-chain antibody fragment with protamine; DNMT: DNA methyltransferase; PIL: PEGylated DC-Chol/DOPE immunoliposomes; anti-HER-2 Fab': Fab' of recombinant humanized anti-HER-2 monoclonal antibody; TLPD-FCC: targeted DOTAP/Chol liposome-polycation-DNA complex conjugated with anti-EGFR Fab'; PEI-C-AuNPs: polyethyleneimine-coated gold nanoparticles using catechol-conjugated PEI.

[a]: Absence

[b]: Depending on the methodology

[c]: Depending on the ± charge ratio

[d]: The application to breast cancer therapy is indicated when it exists; otherwise, reporter genes were used as mentioned (eGFP: enhanced green fluorescent protein; *luc*: firefly luciferase reporter gene.

2.11.1 Stealth technology - nanocarrier biological stability

When systemically applied, nanocarriers have to overcome several biological barriers within the bloodstream and the extracellular matrix. Blood plasma is rather complex, containing approximately 3700 identified proteins, i.e., 60-80 g L^{-1} serum total protein. In particular, liposomes are not inert with respect to blood components and they may interact with proteins and lipoproteins resulting in substantial changes in liposome identity. Unfavourable pharmacokinetic profiles follow, mainly due to the rapid clearance of particles by the tissues of the mononuclear phagocytic system (MPS) (Sharma and Sharma, 1997). Following introduction, nanocarriers are immediately surrounded by free protein, a process which is initiated either by a diffusion mechanism or an energy gradient (Caracciolo, 2015). Under thermodynamically favourable conditions, delivery systems are subject to unspecific interactions with the serum proteins (opsonins), influencing their fate *in viv*o (Scholz and Wagner, 2012; Walkey and Chan, 2012). In particular, liposomes bearing charged (anionic or cationic) phospholipid headgroups may have more efficiency to adsorb more proteins than those bearing neutral surfaces (Kabanov, 1999). Cationic lipids have a tendency to activate complement adsorption with acidic plasma proteins, whereas their anionic counterparts preferentially adsorb the basic proteins (Caracciolo, 2015). The tight binding of selected proteins on the surface of the liposomes forms a protein-corona which is recognized by the organism's biological system. Therefore, it is not the liposomes themselves that are recognized by the MPS, but rather the opsonins on the interface of the liposome. As such, liposomes are efficiently taken up by the macrophages and consequently eliminated from circulation by the reticulo-endothelial system (RES) or by renal excretion, depending on the size of the particle (Reischl and Zimmer, 2009). In addition, protein binding may promote liposomal aggregation, as well as hinder cellular uptake of the lipoplex (Zhang *et al*., 2012).

These major obstacles in the field of liposome technology have prompted research to progress from conventional liposomal delivery vehicles to the field of "second-generation liposomes". Here, conventional liposomes are surface modified by the incorporation of biocompatible, hydrophilic moieties (Allen, 1989; Sen and Mandal, 2013; Wang and Thanou, 2010). The polymer most often employed is poly(ethylene glycol) (PEG) as it is neither toxic nor immunogenic, and is easily excreted from the biological system (Ishida and Kiwada, 2008;

Zalipsky, 1995). PEGylation involves PEG grafting on functionalized lipids or the integration of PEG conjugated phospholipid molecules into the liposomal bilayer (Klibanov *et al*., 1990; Torchilin *et al*., 1994). PEG polymers (ethylene oxide monomers) are inert and biocompatible, and have been FDA approved for use in humans (Harris *et al*., 2001).

PEGylation has become the best and most commonly employed strategy to impart promising pharmacodynamic and pharmacokinetic properties to increase the longevity of lipoplexes in circulation (Drummond *et al*., 1999; Immordino *et al*., 2006; Kolate *et al*., 2014; Perche and Torchilin, 2013). When tethered to the surface of liposomes, resulting vesicles are referred to as PEGylated-stealth or sterically stabilized liposomes, and are often depicted displaying a protective "cloud". PEG chains hinder the close association or aggregation of lipid nanoparticles, thereby providing steric stabilization to the liposomes. In addition, PEG 'masks' the liposome surface (charge density), which obstructs opsonin protein adsorption and reduces recognition and uptake by macrophages of the RES (Papahadjopoulos *et al*., 1991; Yan *et al*., 2005). Together, these factors aid in prolonging their plasma circulation time thus improving localization of the liposomes at the tumour site (passive targeting) (Gaumet *et al*., 2008), with the caveat that the presence of PEG chains may impede liposomal binding and internalization by cancer cells.

A typical PEG polymer comprises an anchor connected via ethylene glycol repeats to a distal terminal group. The anchor portion penetrates the liposome surface and the terminal group extends and interacts with the environment. The ethylene glycol repeats may vary in number and therefore determine the length and molecular weight of the PEG molecule. Strategies to immobilize PEG onto liposomal surfaces include simple direct adsorption, chemical and radiation cross-linking and self-assembled monolayers (Thalla *et al*., 2013). A technique, widely used is to anchor the polymer on the liposome bilayer through coupling to a phospholipid, e.g., 1,2-distearoyl-*sn*-glycero-3-phosphoethanolamine-*N*-[methoxy(polyethylene glycol)] (Allen *et al*., 1991). The arrangement and the activity of the PEG layer is dependent on three prime factors; PEG molecular weight, PEG chain length, and the concentration of PEG chains (surface densities) (Ho *et al*., 2010; Vonarbourg *et al*., 2006). Lipids containing covalently linked PEG_{2000} have been the focus of attention, as the molecular weight of PEG was found to optimize blood circulation times of liposomes (Zhang *et al*., 2012). Ideally, a liposome layered by a near perfect PEG coat would be necessary to ensure suitable steric stabilization and reduced protein

adsorption. The volume which each flexible PEG chain occupies (Rf) and the distance between each PEG molecule (*D*) on the liposomal surface affect the resultant conformation of the PEG chains **[Figure 2.6]**. Low PEG densities allow the PEG chains to self-assemble into tightly coiled, "flat pancake"-like structures (*D* > Rf). An increase in PEG density creates a moderate lateral pressure between the PEG chains, forcing the pancake regimen to extend into an intermediate random coil-like "mushroom" conformation. A higher PEG density increases the lateral pressure between PEG "mushrooms" even further. This forces the PEG chains to uncoil and extend away from the liposomal surface, forming low-coiled, more linear "brush" structures (*D* < Rf). These findings have suggested that the PEG density is somewhat more important than the size of the polymer (Buyens *et al*., 2012; Dos Santos *et al*., 2007; Wang and Thanou, 2010).

PEG polymers used in these applications are characterized by low polydispersity and solubility in aqueous solutions and numerous organic solvents. The solubility of PEGs is facilitated by the directional bonds formed between the PEG and water molecules (Sofia *et al*., 1998). This favourable polymer-solvent contact creates a "hydration shell" around the PEG chains. The PEG chain entangles 2-3 water molecules per oxyethylene unit, increasing its apparent molecular weight to 5-10 times that of a globular protein of similar molecular weight (Kolate *et al*., 2014). Upon hydration, the PEG chain swells, and this plays an important role in stabilizing PEG-grafted liposomes. Tirosh *et al*. (1998) reported that grafting PEG-lipid at concentrations of about 5 to 7 mol.% onto the surface of liposomes compresses the liposomal lipid bilayer as water is being released from the lipid head group region. This enhances the lateral packaging of the phospholipid acyl chains, and, at the same time, decreases bilayer defects resulting in good stealth liposomes. In general, an 8-10 mol.% of PEG-lipid present in the liposomal formulation equates to the formation of a "brush" regime (Buyens *et al*., 2012); this generates greater protein repulsion. However, higher PEG-lipid concentrations result in lateral repulsion of the PEG chains (simultaneous micelle formation) which acts as a liposomal destabilization agent (Li and Huang, 2009). Moreover, high mol.% of PEG-lipid densities apparently hamper the release of siRNA cargo into the cytoplasm of transfected cells (Buyens *et al*., 2012).

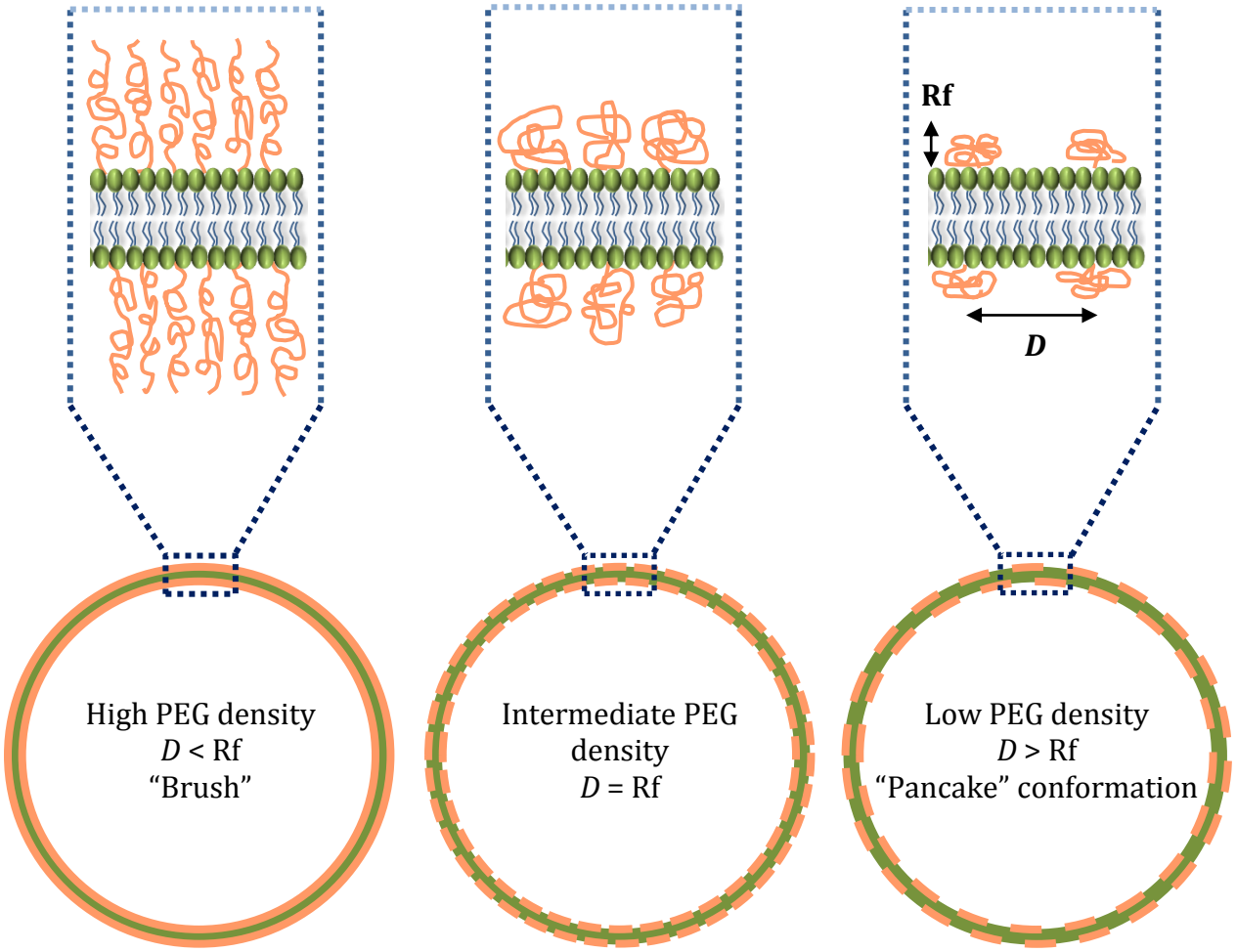

Figure 2.6: Depicted are unilamellar liposomes (bottom) bearing different densities of PEG polymers on their surfaces. Presented from left are total, intermediate and partial surface coverage of the liposomal bilayer. A detailed zoom (top) of the three PEGylated liposomes shows the respective PEG regimens formed as a result of the different surface densities. When the density of PEG on the surface is low, it takes on a heavily coiled flat "pancake" configuration (D > Rf). Increasing PEG densities cause the conformations to switch to low coiled "mushroom" or to extend further into "brush" structures (D < Rf) This figure is adapted from Buyens *et al.* (2012) and Wang and Thanou (2010).

2.11.2 Lipid-based systems

In the biological milieu, the inherent properties of phospholipids (e.g. phosphatidylcholine) and cholesterol allow them to self-assemble into flexible biological bilayers forming an integral feature of membrane systems, which enables the trafficking of biomolecules within as well as

among cells. Many lipid-based systems designed for siRNA delivery are based on this natural phenomenon and make use of natural or synthetic biocompatible materials for interaction with the cell membrane to promote efficient delivery. Typically, lipid systems comprise a neutral, anionic or cationic lipid, a fusigenic helper/co-lipid [such as DOPE and 1,2-dioleoyl-sn-glycero-3-phosphocholine (DOPC)] and, in some cases, a PEG-lipid, which together form self-closed spherical particles, referred to as liposomes **[Figure 2.7B]**.

Liposomes are vesicular colloidal particles which have gained interest and popularity as efficient siRNA delivery vehicles. Comprising natural membrane constituents, these vesicles, with an aqueous core, are biocompatible and biodegradable *in vivo*, and their by-products are non-toxic (Kesharwani *et al*., 2012; Oh and Park, 2009; Shim *et al*., 2013). Importantly, liposomes are readily prepared, as they form spontaneously when the constituent lipid mixture is dispersed in an aqueous solution. In addition, they may be prepared controllably to form structures varying in size, number of bilayers and entrapped aqueous phase. Liposome formulations may also include target-specific ligands that enhance their selectivity for tumour delivery (Guo *et al*., 2010). Pirollo and Chang (2008) reported specific knockdown of HER2/*neu* expression in BC animal models using siRNA immunolipoplexes containing an anti-transferrin receptor antibody ligand. Based on the molecular make-up of the polar head component, liposomes are categorized as anionic, cationic, zwitterionic and non-ionic in nature. Generally, cationic and anionic-lipidic nanoscaled vehicles have shown promise for successful siRNA delivery in BC therapeutics. Their unique characteristics in respect of their interactions with siRNA and the cell membrane will be discussed below.

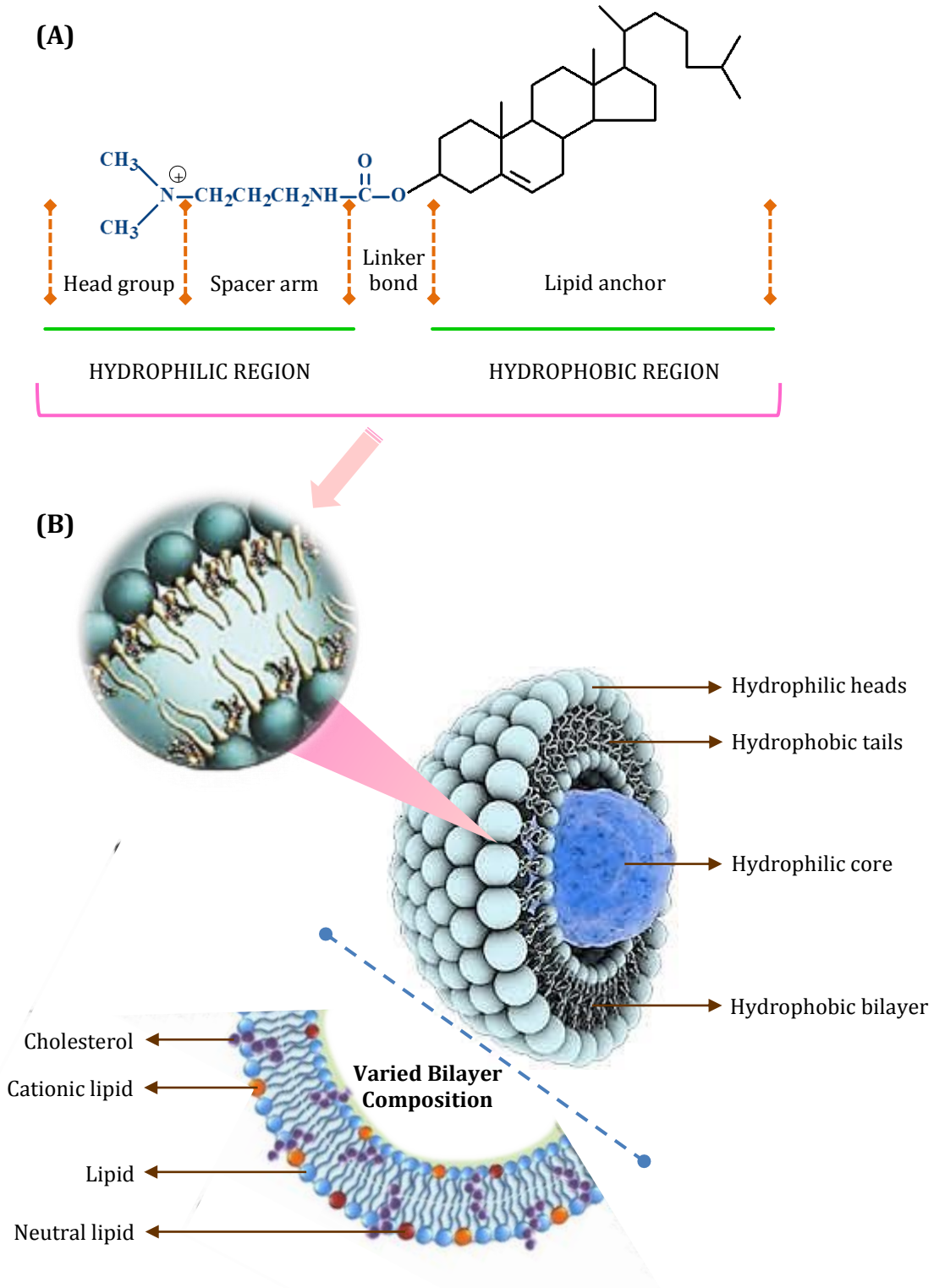

Figure 2.7: A scheme of the typical components of a cationic lipid **(A)** and their spontaneous assembly with neutral co-lipids into liposomes **(B)**. Adapted from Hong and Nam (2014); Natarajan *et al*. (2014).

2.11.2.1 Cationic liposomes

Cationic liposomes comprise cationic lipids which are amphiphilic molecules displaying a net positive charge. In general, these cationic lipid molecules are composed of three basic modules: a hydrophilic positively charged head group which functions as a binding site for siRNA; a lipid hydrophobic tail moiety which anchors the head group to the liposomal membrane bilayer; and a linker which connects the hydrophilic and hydrophobic regions (Gao and Hui, 2001; Li and Jr Szoka, 2007; Liu and Huang, 2010; Schroeder *et al*., 2010) **[Figure 2.7 (A)]**. In general, head groups fall into the following categories: primary, secondary and tertiary amines, quaternary ammonium moieties, lipoamines, guanidinium or amidine salts, and heterocyclic rings (Heyes *et al*., 2002; Niculescu-Duvaz *et al*., 2003). The lipophilic tail domain is mainly comprised of aliphatic chains of lengths ranging from 12 to 20 carbons or cholesteryl groups (Wasungu and Hoekstra, 2006). The connecting linker bonds are usually ether, ester (Leventis and Silvius, 1990), amide (Behr *et al*., 1989), urethane (Lee *et al*., 1996), or carbamate groups (Koynova and Tenchov, 2010). The nature of each of these components influences directly or indirectly the cohesive charge-charge interactions in siRNA-liposome complexes (lipoplexes). This, in turn, affects both transfection efficiency and degree of toxicity. Enhanced endosomal escape and efficient transfection are properties associated with lipoplexes formulated with cytofectins containing a bulky alkyl chain and a small hydrophilic head group (Tseng *et al*., 2009). For improved transfection *in vitro* and *in vivo*, cationic lipids are often mixed with neutral lipids, such as DOPE or cholesterol to form liposomes (Dass, 2004; Ramezani *et al*., 2009; Xu and Anchordoquy, 2008). Combinations and relative amounts of cationic lipids and co-lipids profoundly influence toxicity and transfection efficiency (Gao and Huang, 1995; Plank *et al*., 1996). It is worth noting that some cationic lipids only function effectively as transfecting agents upon formulation with DOPE or cholesterol (Banerjee *et al*., 1999). DOPE seemingly enhances fusion of a lipoplex membrane with an endosomal membrane (Fletcher *et al*., 2006; Hoekstra *et al*., 2007), while cholesterol conceivably stabilizes lipoplexes and reduces interaction with serum proteins (Dass, 2004; Xu and Anchordoquy, 2008). Cationic liposome morphology with respect to lamellarity and size is largely determined by the method of preparation and, to a lesser extent, by lipid composition (Gabizon *et al*., 2006; Khuller *et al*., 2004). The facility and reproducibility of the electrostatic interaction between the polyanionic phosphate backbone of the siRNA and the

positively charged head groups of the cationic liposome to form the vector lipoplex (Felgner *et al*., 1997) have firmly established cationic liposomes as attractive delivery vehicles.

Lavigne and Thierry (2007) formulated a highly stable and reproducible preparation of dioctadecylamidoglycylspermidine (DOGS) and DOPE with a low cationic net charge and termed these vectors DLS. As determined by dynamic light scattering, DLS liposome suspensions were homogeneous in size (~120 nm) with a low polydispersity. Rhodamine-labelled siRNA targeting cyclin D1 was allowed to form stable lipoplexes with the DLS formulation in sterile RNase-free water, prior to transfection. MCF-7 BC cells were transfected with DLS lipoplexes (50 nM with respect to siRNA). Thereafter, the cells were fixed to decrease non-specific binding of the antibodies and permeabilized for immunocytochemical analysis using FITC-conjugated primary antibody against early endosomal autoantigen (anti-EEA1). Delivery by the DLS vector system and subcellular distribution of rhodamine-labelled siRNAs directed against cyclin D1 were examined. Results indicated that the rhodamine-labelled siRNA, vectorized by the DLS system, was localized to perinuclear regions within the cytoplasm, independent of the presence or absence of serum, in areas more distinct than early endosomal vesicles. Furthermore, the siRNA did not co-localize with anti-EEA1, as this antibody was shown to be specifically associated with the early endosomal membrane. This confirmed that the DLS:siRNA lipoplexes were not trapped in the endosomes, but were efficiently delivered into the cytoplasm where they enter the RNAi pathway.

Cationic liposomes composed of 3β-[*N*-(*N*′,*N*′-dimethylaminoethane) carbamoyl] cholesterol (DC-Chol) and DOPE (DC-Chol/DOPE liposomes) were reported to stably transfect FAM-siRNA into SKBR-3 BC cells at an optimized equimolar DC-Chol/DOPE ratio of 1 (Zhang *et al*., 2010). Moreover, siRNA transfection efficiency of DC-Chol/DOPE liposomes improved with increased DC-Chol/DOPE:siRNA weight ratio, until a plateau was reached. Zhang *et al*. (2010) observed that an increase in lipoplex concentration was accompanied by increased internalization and more efficient transfection. Although DC-Chol/DOPE:antiHER-2 siRNA lipoplex was successfully internalized into the HER-2 overexpressing SKBR-3 cells, low levels (< 25%) of HER-2 gene silencing were achieved. Interestingly, siRNA transfection efficiency was not significantly affected by the presence of foetal bovine serum. Gene silencing competence, however, was greatly reduced to < 6% in the presence of serum. DC-Chol/DOPE liposomes exhibited stability in the presence of serum, a property which is desirable *in vitro* as it

ensures increased cell survival and lowers DC-Chol/DOPE:siRNA toxicity. In the same study, PEGylation was seen to reduce the size and the surface charge density of the liposomes, resulting in considerable reduction of siRNA transfection efficiency compared to their non-PEGylated counterparts. Furthermore, DC-Chol/DOPE liposomes containing even a small quantity of PEG (1 mol.%) significantly impaired siRNA silencing efficiency. PEGylation is often adopted as it prolongs the half-life of the lipoplexes in serum by providing a surface layer that minimizes the binding of serum proteins (Ross and Hui, 1999). However, this is sometimes partially offset by unfavourable interactions with the cell surface (Masson *et al*., 2004).

2.11.2.2 Anionic and neutral liposomes

The feasibility of anionic, neutral or zwitterionic lipids as potentially safe siRNA delivery agents has also been explored (Kapoor and Burgess, 2012; Pulford *et al*., 2010; Srinivasan and Burgess, 2009). These systems, however, showed poor and variable nucleic acid entrapment or encapsulation and very low delivery efficiency when transfected as independent entities (Foged *et al*., 2007). It is theorized that the anionic head group prevents efficient siRNA compaction due to the lack of complexation-enhancing electrostatic forces that occur between the anionic phosphate backbone of the siRNA and the neutral/negatively charged head groups of the lipids. Therefore, to negate electrostatic repulsion and to facilitate intense association and lipoplex assembly, a third moiety, typically a divalent cation (Ca^{2+}, Mg^{2+} and Mn^{2+}), is incorporated into the anionic delivery vehicles. Research efforts have focussed on the use of Ca^{2+} as a bridging agent for siRNA delivery, as higher transfection efficiencies have been observed with calcium for DNA deliveries (Srinivasan and Burgess, 2009). These authors reported that the strong DNA and Ca^{2+} binding affinities are potentially due to the calcium which possesses a small hydrodynamic radius and renders a larger charge per unit surface area.

Ideally, an optimized formulation represents the best charge balance between the anionic lipid and siRNA, with a slight excess of Ca^{2+} to facilitate binding between the cellular membrane and the lipoplexes. Kapoor and Burgess (2012) conducted formulation optimization studies on anionic liposomes composed of 1,2-dioleoyl-*sn*-glycero-3-phospho-(1′-*rac*-glycerol) (DOPG)/ DOPE and calcium. These researchers reported ~70% protein knockdown in MDA-MB-231 BC cells using anionic formulations composed of 40:60 DOPG/DOPE, 1 µg/mL lipid, 2.4 mM Ca^{2+}

and 10 nM anti-eGFP siRNA. Notably, anionic liposome formulations containing > 40 mol.% DOPG resulted in no further increment in silencing efficiency as the concentration of DOPG reached a point of saturation for DOPG-Ca^{2+}-siRNA bridging. Optimal formulations were in the size range of 324.2 ± 19.6 nm with a surface charge of -22.9 ± 0.1 mV and an encapsulation efficiency of 98.5 ± 1.4%. These optimized anionic lipoplexes were highly stable in the presence of serum, and were able to achieve an effective endosomal escape mechanism which resulted in increased silencing efficiency. In addition, lipoplexes were several-fold safer than the commercial cationic liposome Lipofectamine^{TM} 2000.

2.11.3 Polymer systems

Polymeric delivery systems have evolved into a dominant strategy for siRNA gene delivery as they are biocompatible, biodegradable and offer increased stability and low polydispersity. As is the case with lipid based delivery systems, polymers usually comprise cationic moieties which allow for self-assemblage with the polyanionic backbone of siRNA forming polyplexes with a robust non-covalent interaction. While siRNA molecules are typically 2 nm in diameter and 7 nm in length, polyplexes may range from < 100 nm to several 100 nm in size due to siRNA-induced aggregation. A variety of polycations or polycation-containing block co-polymers have been employed to condense siRNA via electrostatic interactions into polyplexes or other polymeric carriers such as micelles (de Martimprey *et al*., 2009). Cationic polymers can be classified into natural and synthetic polymeric delivery systems. Natural polymers include chitosan, atelocollagen and cationic polypeptides, whereas synthetic polymers include polyethyleneimine (PEI), poly-L-lysine (PLL), poly(amido amine) (PAMAM) and cyclodextrin-based polycations. Physicochemical properties such as molecular weight, solubility, charge density and functional groups of both biological and synthetic polymers may be appropriately manipulated for a particular therapeutic application, due to their structural flexibility. Research efforts which have focussed on efficient polymeric siRNA delivery systems will now be discussed.

2.11.3.1 Synthetic polymers

PEI is an organic linear or branched polymer which can be synthesized in various lengths with a wide range of molecular weights (1 to over 1000 kDa), and can be substituted with different functionalized degradable moieties and co-polymers. This protects siRNA from enzymatic degradation, reduces cytotoxicity, and enhances transfection efficacy (Meyer *et al*., 2008; Mintzer and Simanek, 2009; Neu *et al*., 2005; Philipp *et al*., 2009; Park *et al*., 2010; Zintchenko *et al*., 2008). PEIs harbour many amino groups, making them highly protonable polymers which exhibit a buffering 'proton sponge effect' on the cell endosomes. In essence, the amine groups in the PEIs have a buffering capability in the low pH environment of the endosome, stimulating the rupturing of the endosomal membrane which results in an increased release of siRNA from the complex into the cytoplasm (Howard, 2009). PEI transfection efficiency depends largely on its molecular weight, size and the amine/phosphate (N/P) ratio of the polyplexes. The N/P ratio is a prime formulation factor used to obtain PEI-siRNA polyplexes within a desired size range. It is defined as the number of amine groups of the polycation divided by the number of phosphate groups of the nucleic acid. In general, polyplexes attain a net positive charge when the N/P ratio is above 1. Furthermore, it has been reported that high N/P ratios correspond to a smaller mean diameter of the polyplex and *vice versa* (Grzelinski *et al.*, 2006; Schiffelers *et al*., 2004). To promote cellular uptake, PEIs and similar polycationic polymers deliver nucleic acid material across the cell membrane via the formation of transient nanoscale holes. It has been speculated that the same destabilizing mechanism of action on cell membranes has a cytotoxic effect, suggesting that more efficient polymers are often also more cytotoxic (Hong *et al*., 2006; Lungwitz *et al*., 2005). High molecular weight PEI (> 25 kDa) polyplexes have been extensively explored for highly efficient siRNA transfection (Bologna *et al*., 2003; Jere *et al*., 2009; Urban-Klein *et al*., 2005). However, high molecular weight PEIs are also characterized by appreciable cytotoxicity through cellular mechanisms such as necrosis and apoptosis (Boeckle *et al*., 2004; Hunter, 2006; Nimesh *et al*., 2006; Swami *et al*., 2007; Xie *et al*., 2006). Numerous modifications of PEIs have been investigated with the aim of reducing the potential cytotoxicity induced by high molecular weight PEIs. These include; PEGylation, conjugation of butyrate or alkanoates, and hydrophobic modifications (Aliabadi *et al*., 2012; Mao *et al*., 2006; Schiffelers *et al*., 2004; Zhou *et al*., 2012; Zhou *et al*., 2013). A range of PEG moieties have been used as

block elements, i.e., incorporated onto PEIs for production of block co-polymers to specifically reduce cytotoxicity (Mao *et al*., 2006). In addition, the combination of PEI-PEG is also able to coat (PEGylate) the siRNA polyplex structure and prevent non-specific binding to cells or proteins in the physiological milieu (Schiffelers *et al*., 2005).

Polymer micelles are generated as a result of self-assemblage of amphiphilic block polymers i.e. from either di-block co-polymer AB, or tri-block co-polymers ABC or ABA. Generally, part A includes polycations such as PEI and PLL and part B is a highly hydrophilic polymer such as PEG or dextran. In a study conducted by Zhou *et al*. (2012), mono-methoxy-poly(3-hydroxybutyrate-co-4-hydroxybutyrate)-graft-hyperbranched PEI (25 kDa) (mPHA-g-bPEI) co-polymers displayed higher optimal transfection efficiencies (with low cytotoxicity) compared to the unmodified branched PEI (bPEI) in MCF-7-*luc* cells. In brief, the co-polymers were synthesized with various block length poly(hydroxyalkanoates) from 1300 to 2900 Da, through Michael addition between acrylated monomethoxy-poly(hydroxyalkanoates) and bPEI. Above a $^{w}/_{w}$ ratio of 1:1, bPEI/siRNA complexes were not able to mediate knockdown of luciferase (*luc*) expression without marked cytotoxic effects of bPEI/siRNA complexes. Notably, *in vitro* knockdown of *luc* expression in this cell line, using an mPHA-g-bPEI (mAP2) complex, was comparable (up to 85%) to that of the commercially available transfection agent Lipofectamine^{TM} 2000. In a recent study, Zhou *et al*. (2013) synthesized a mono-methoxy-poly (3-hydroxybutyrate-*co*-4-hydroxybutyrate)-*block*-polyethylene glycol-*block*-linear PEI (mP3/ 4HB-*b*-PEG-*b*-lPEI) using 1800 Da linear polyethyleneimine. They demonstrated that mP3/4HB-*b*-PEG-*b*-lPEI co-polymers could effectively bind siRNA, protect it from degradation by nucleases, and efficiently release the complexed siRNA under polyanionic heparin competition. However, the *luc* gene silencing efficiency of these micelles was unsatisfactory in MCF-7-*luc* cells, even at high N/P ratios of 70. The researchers deduced that the use of these co-polymers as efficient siRNA gene delivery vehicles for exogenous gene silencing depended largely on cell type and N/P ratios. Cationic micelles composed of the amphiphilic copolymer poly(*N*-methyldietheneamine sebacate)-*co*-[(cholesteryl oxocarbonylamido ethyl) methyl bis(ethylene) ammonium bromide] sebacate) (P(MDS*co*-CES) were shown to complex with Bcl-2-targeted siRNA and efficiently deliver it into the MDA-MB-231 BC cell line (Beh *et al*., 2009). After transfection with P(MDS*co*-CES):siRNA micelles, low levels of Bcl-2 mRNA expression were reported. Consistent with the down-regulation of Bcl-2 mRNA levels, Bcl-2

protein expression was down-regulated by 36-66% in cells treated with micelles. Furthermore, the Bcl-2 mRNA down-regulation efficiency was comparable to that mediated by Lipofectamine^{TM} 2000, but higher than that induced by PEI alone. Increasing the concentration of siRNA resulted in a lower Bcl-2 protein expression level; siRNA concentrations of 22 nM and 1100 nM resulted in approximately 36 and 66% down-regulation respectively.

Hydrophobic moieties are incorporated onto polymeric carrier systems to enhance the interaction with the lipophilic cell membrane to enable more efficient cellular uptake of the polymer associated siRNA. Aliabadi *et al*. (2011) reported the toxicity profile of modified polymers in a P-gp over-expressing BC cell line (MDA-MB-435/MDR). Lipid substitution on low molecular weight PEI (2 kDa) increased the toxicity of the complexes; however, the level of toxicity was significantly lower than the high molecular weight PEI (25 kDa) polymers. In another study which explored the feasibility of lipid-substituted low molecular weight (2 kDa) PEI as a delivery vector for siRNA-mediated BCRP down-regulation, a significant increase in siRNA delivery as a function of lipid substitution for a range of lipids ranging from C8 to C18, was reported (Aliabadi *et al*., 2012). Lipid-substituted polymers that enhanced the cellular uptake were most effective in BRCP gene silencing, which effectively lasted for 5 days after a single treatment of siRNA. This trend was corroborated by examining the correlation between cellular uptake and down-regulation level with a sigmoidal profile that plateaued after a certain level of cellular uptake.

2.11.3.2 Natural polymers

Properties of natural polymers which favour their potential application as siRNA delivery vehicles include biodegradability, low toxicity and immunogenicity (Frohlich and Wagner, 2010). Among the biological polymers, chitosan, a linear polysaccharide polymer composed of repeating β-(1-4)-linked D-glucosamine and N-acetyl-D-glucosamine units derived from the deacetylation of chitin (Rudzinski and Aminabhavi, 2010), is perhaps the most prominent. It forms compact polyplexes with siRNA through electrostatic interactions and provides effective protection against enzymatic degradation (Katas and Alpar, 2006; Liu *et al*., 2007). The molecular weight and concentration of the polymer, its degree of deacetylation, and the N/P ratio of polyplexes and chitosan salt are important parameters that must be considered as they strongly

influence the resulting charge of the polyplexes (Mao *et al*., 2010). Kong *et al*. (2012) reported that low molecular weight chitosan (LMWC) (2 and 5 kDa) tends to form smaller particle size chitosan/siRNA complexes with a more favourable siRNA transporting capability compared to the higher molecular weight chitosan (20 to 80 kDa). However, poor functional ability to induce target *luc* mRNA knockdown was observed in MDA-MB-231-*luc* human BC cells. The authors suggested that the strong electrostatic interaction between the LMWC and siRNA facilitated cellular uptake of the LMWC/siRNA complex, but prevented effective intracellular unpacking of siRNA from its LMWC carrier. To overcome this obstacle, the authors utilized a phosphorylatable short peptide conjugated LMWC which led to improved intracellular siRNA disassociation and increased the target gene silencing effect of the chitosan/siRNA. Yang *et al*. (2013b) assessed the gene silencing level of trans-activated transcription (TAT) surface-modified chitosan/siRNA-*luc* nanoplexes in an endogenous MCF-7-*luc* cell line. Gene knockdown was similar to that achieved with Lipofectamine^{TM} 2000; moreover, the gene silencing efficiency of TAT-g-chitosan/siRNA-*luc* nanoparticles (69.2%) was 3.7-fold higher than that of chitosan/siRNA-*luc* nanoparticles (18.8%). In this case, the introduction of TAT into chitosan molecules increased the cell penetrating ability of chitosan, and further resulted in the higher uptake efficiency of TAT-g-chitosan/siRNA nanoparticles than chitosan/siRNA nanoparticles. In another study, Tan *et al*. (2007) investigated chitosan nanoparticles encapsulating quantum dots, complexed to HER2/*neu* siRNA. The entrapped fluorescent quantum dots allowed the investigators to track the nanoparticles and determine the degree of internalization of siRNA complexes into SKBR-3 BC cells. HER-2 antibody-labelled chitosan nanoparticles provided specific delivery of siRNA to HER-2-overexpressing SKBR-3 BC cells. Gene knockdown of HER2/*neu* siRNA was observed following treatment of the cells. Chitosan, when used as a coating material, has also been shown to improve the transfection efficiency of other vectors in siRNA delivery. Pille *et al*. (2006) demonstrated the efficacy of intravenously administered anti-RhoA siRNA encapsulated in chitosan-coated polyisohexylcyanoacrylate nanoparticles in nude mice bearing aggressive BC (MDA-MB-231) xenographs. The authors reported that after 3 consecutive days of administering the chitosan-coated nanoparticles to mice at a dose of 0.15 or 1.5 mg/kg body weight, the growth of tumours was inhibited by 90% in the 0.15 mg/kg group. Moreover, an even greater inhibition was observed in the 1.5 mg/kg group, signifying the potential efficiency of this carrier system.

2.12 Cellular Binding, Uptake and Internalization

2.12.1 Cellular binding: Passive and active targeting

Characteristically, newly formed tumour blood vessels are usually irregular in form and architecture and are highly permeable due to rapid and defective angiogenesis. Passive targeting of tumour cells by siRNA-containing liposomes employs this dysfunctional lymphatic drainage system present within tumours. Liposomes are designed with the premise that they will avoid clearance by the RES, thus prolonging their circulation in the peripheral blood. They are therefore expected to accumulate in tumours due to the enhanced permeability and retention effect (Sen and Mandal, 2013; Wang and Thanou, 2010). This phenomenon was identified by Maeda and Matsumura (1989) as a means to target anticancer agents onto tumours. Based on this effect, the liposomal delivery systems ranging in size from tens to hundreds of nanometers can passively escape through the fenestrations of the leaky vasculature into the tumour tissue. This is followed by increased accumulation of the liposome in the tumour tissue, i.e., an increased proximity to tumour cells compared to the normal tissue (Xu and Wang, 2015), allowing for the subsequent internalization of the siRNA-containing liposomes into the cytoplasm by a non-targeted passive diffusion mechanism.

On the other hand, liposomes can be formulated with targeting ligand agents such as protein (antibody or antibody fragments), and peptides and vitamins which can bind to respective receptors that are (over)expressed by target cells. This strategy allows for active targeting interactions and improves the therapeutic index by expanding the therapeutic window by increasing delivery to the target tissue and reducing toxic side effects. Two prime factors determine the binding and targeting efficiency, namely, the receptor density at the cell surface, and the affinity and avidity of the coupled ligands (Park *et al*., 2002; van der Meel *et al*., 2014). The urokinase plasminogen activator, uPA, is a natural protein ligand which targets the urokinase plasminogen activator receptor and shows potential as a BC targeting agent. In particular, protein fragments containing only the binding region of uPA have been used for targeting the over-expressed receptors on BC (Yang *et al*., 2009). In general, depending on the approach adopted, tumour targeting liposomes can accumulate in tumour tissues at levels

approximately 10-100 -fold greater than those achieved by passive delivery (Ozpolat *et al*., 2014).

2.12.2 Cellular uptake and internalization

Following efficient passive or active target cell binding of the carrier, siRNA must be internalized into the cytoplasm of the cell (Zhou *et al*., 2014). A multitude of internalization mechanisms are known to exist, although there is no consensus on how these operate. Classically, the uptake mechanisms are divided into two groups: the endocytic and non-endocytic pathways (David *et al*., 2010; Xiang *et al*., 2012). Endocytosis represents the major mechanism of entry via which lipoplexes and polyplexes mediate the delivery of siRNA cargo into the target cells (ur Rehman *et al*., 2013a). Within the endocytic group, there are a variety of entry pathways, including both clathrin- and caveolae-mediated endocytosis, phagocytosis and macropinocytosis, as well as entry portals that are clathrin- and caveolae-independent (Doherty and McMahon, 2009; Hillaireau and Couvreur, 2009; Juliano *et al*., 2008; Resnier *et al*., 2013).
Non-endocytic pathways encompass two categories; invasive and non-invasive pathways. In particular, the naturally existing non-invasive pathways which include fusion and penetration mechanisms are deemed as being more useful to enhance the intracellular availability of non-viral gene complexes (Xiang *et al*., 2012). Three fundamental factors are known to influence the uptake mechanism: the particle size; surface charge; and the presence of targeting ligands. For siRNA-containing liposomes ranging in size from 50 to 150 nm, the preferred uptake mechanism is the endocytic pathway. Complexes with a net positive charge show favoured binding to heparansulfate proteoglycan-containing negatively charged cell membranes. Alternatively, the presence of targeting ligands on the carrier may direct complexes to those cells expressing the corresponding receptor on the surface, leading to facilitated internalization of the siRNA-containing delivery system (Scholz and Wagner, 2012).

CHAPTER THREE

MATERIALS AND METHODS

3.1 Liposome Formulation

3.1.1 Materials, chemicals and reagents

Dioleoylphosphatidylethanolamine (DOPE, $C_{41}H_{78}NO_8P$) were obtained from the Sigma-Aldrich Chemical Co. (St. Louis, MO, USA). Chloroform ($CHCl_3$), absolute ethanol (EtOH, C_2H_6O), sodium chloride (NaCl) and 2-[4-(2-hydoxyethyl)-1-piperazinyl] ethanesulfonic acid (HEPES, $C_8H_{18}N_2O_4S$) were purchased from Merck (Darmstadt, Hesse, Germany). 1,2-Distearoyl-*sn*-glycero-3-phosphoethanolamine-N-[methoxy(polyethylene glycol)-2000] (DSPE-PEG_{2000}), hereafter referred to as PEG, was acquired from Avanti Polar Lipids (Alabaster, AL, USA). The two CCCs namely; Chol-T and MS09, were previously synthesized and obtained from the Non-viral Gene Delivery Laboratory, Department of Biochemistry, University of KwaZulu-Natal, Durban, South Africa. Nuclear magnetic resonance spectroscopy (NMR spectra) and electrospray mass spectra were captured using a Gemini 300 instrument and a Waters APIQ-TOF Ultima instrument (ES-TOF) respectively (^1H and ^{13}C, **Appendix A**). All other chemicals and reagents were of analytical grade or higher, and purchased commercially. Ultrapure deionized 18 MΩ water (Milli-Q50) was used throughout.

3.1.2 Liposome preparation

The composition and molar ratio of six liposomal formulations used in the present study are outlined in **Table 3.1.** Cationic liposomes and PEGylated cationic liposomes were prepared according to the commonly used thin film evaporation method adapted from that of Gao and Huang (1991). The two CCCs, Chol-T and MS09, were previously synthesized in our laboratory (Singh and Ariatti, 2006; Singh *et al*., 2001). Stock solutions of the cytofectins (10 μg μL^{-1}), DOPE (10 μg μL^{-1}) and PEG (1 μg μL^{-1}) were prepared separately in $CHCl_3$. Appropriate volumes from the respective stock solutions were added to clean quickfit tubes to obtain 2 μmol. of total lipid in each case and a constant 1 μmol. cytofectin in each preparation. PEGylated liposomes were formulated with 2 or 5 mol.% of PEG, whilst DOPE was adjusted to accommodate changes in PEGylation. The lipid mixture was vortexed for 10 s and the $CHCl_3$ solvent was removed by evaporation (Büchi RE121 Rotavapor, Büchi, Switzerland) at reduced

pressure. Pressure equilibration was accomplished using a thin flow of moisture-free nitrogen gas at 25 °C. The residual solvent was removed by vacuum-desiccation in a Büchi TO-50 pistol drier for at least half-an-hour. The lipid film formed was hydrated overnight at 4 °C in 500 µL of filter-sterilized (0.2 µm pore size, Nucleopore, Pleasanton, USA) HEPES Buffered Saline (HBS, 20 mM HEPES, 150 mM NaCl; pH 7.5). To achieve small unilamellar vesicles, the hydrated opalescent lipid film was vigorously vortexed (Vortex Genie 2, Scientific Industries, Bohemia, USA), and then sonicated to clarity using a temperature-controlled Transsonic T 460/H bath type sonicator (Elma GmbH & Co., Singen, Germany) for 5 min at 21 °C at a frequency of 35 kHz. The resulting unilamellar liposome preparations were stored at 4 °C. Liposomal suspensions were routinely subjected to DNA/ siRNA binding analyses and, with regular sonication, the preparations remained stable for several months.

Table 3.1: Composition and mol. ratios of the different cationic liposomal formulations

Formulation type	**Mol. ratios of the respective cationic liposome components (µmol. 500 µL^{-1})**			**Total lipid content (µg µL^{-1})**
	Cytofectin	**DOPE**	**PEG**	
Chol-T:DOPE	1.00	1.00	-	2.517
Chol-T:DOPE:2% PEG	1.00	0.96	0.04	2.684
Chol-T:DOPE:5% PEG	1.00	0.90	0.10	2.938
MS09:DOPE	1.00	1.00	-	2.746
MS09:DOPE:2% PEG	1.00	0.96	0.04	2.914
MS09:DOPE:5% PEG	1.00	0.90	0.10	3.168

Abbreviations: Chol-T: 3β-[*N*-(*N'*, *N'*-dimethylaminopropane)-carbamoyl] cholesterol; **MS09:** *N*, *N*-dimethylaminopropylaminylsuccinylcholesterylformylhydrazide; **DOPE:** Dioleoylphosphatidylethanol-amine; **PEG:** 1,2-distearoyl-*sn*-glycero-3-phosphoethanolamine-N-[methoxy(polyethylene glycol)-2000].

3.2 Physical Characterization of Liposome and Liposome-Nucleic Acid Interactions

3.2.1 Materials, chemicals and reagents

Escherichia coli strain JM109 was sourced from Promega Corp. (Dübendorf, Zürich, Switzerland). Plasmid pCMV-*luc* was purchased from Plasmid Factory (Bielefeld, North Rhine-Westphalia, Germany). The various siRNAs were obtained from Thermo Scientific Dharmacon Products (Lafayette, CO). Agarose was purchased from Bio-Rad Laboratories (Richmond, CA, USA). The components of the gel loading buffer (glycerol, bromophenol blue, and xylene cyanol) were obtained from Merck (Darmstadt, Hesse, Germany), Sigma-Aldrich Chemical Co. (St. Louis, MO, USA), and Saarchem (Muldersdrift, Gauteng, RSA), respectively. Ethidium bromide (*M* 394.3 g mol.$^{-1}$, EtBr) was purchased from Promega Corp. (Madison, WI, USA). Tris (hydroxymethyl)-aminomethane (*M* 121.2 g mol.$^{-1}$, Tris base) and sodium dihydrogen phosphate (*M* 120 g mol.$^{-1}$, NaH_2PO_4) were acquired from Merck (Darmstadt, Hesse, Germany). *N*, *N*, *N′*, *N′*-ethylenediaminetetraacetic acid (*M* 372.2 g mol.$^{-1}$, EDTA disodium salt) was purchased from Saarchem (Wadeville, Gauteng, RSA), and sodium dodecyl sulphate (*M* 288.4 g mol.$^{-1}$, SDS) from Bio-Rad Laboratories (Richmond, WV, USA). HyClone® Research Grade Foetal Bovine Serum (triple 0.1 μm sterile filtered, FBS) was purchased from Thermo Scientific (Northumberland, UK). Formvar-coated copper grids were prepared by the Electron Microscopy Unit, University of KwaZulu-Natal (Durban, KZN, RSA). Ultrapure deionized 18 MΩ water (Milli-Q50) was used throughout. All other chemicals and reagents were of analytical purity grade or higher, and purchased commercially.

3.2.2 Plasmid DNA

The plasmid used in this study was the pCMV-*luc* DNA [6.2 kbp] that codes for the firefly luciferase (*luc*) gene and carries the cytomegalovirus promoter (CMV) **[Figure 3.1]**. The plasmid was amplified in *E. coli* strain JM109 and isolated and purified according to the standard protocol. Plasmid purity was confirmed by 1% agarose gel electrophoresis followed by EtBr staining. Plasmid preparations with an $OD^{260}/_{280}$ value of more than 1.8 were utilized in this study. Short-term working stock concentrations of 1 μg μL^{-1} were prepared with ultrapure

deionized 18 MΩ water (Milli-Q50) and stored at -20 °C. Plasmid concentrations were confirmed using the NanoDrop 2000c spectrophotometer (Thermo Scientific, Wilmington, DE, USA).

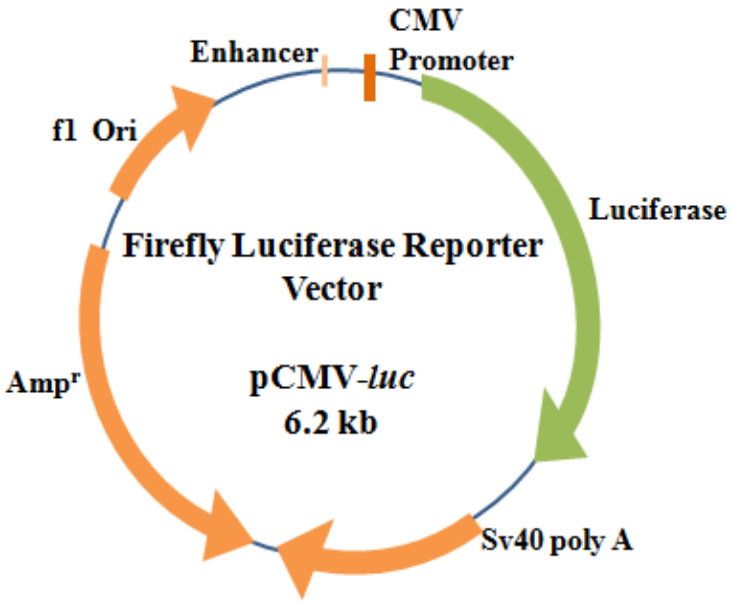

Figure 3.1: Plasmid map of the pCVM-*luc* vector. The vector comprises cDNA of the firefly luciferase (*luc*) gene and β-lactamase for ampicillin resistance (Amp^r). The vector is driven by the cytomegalovirus promoter (CMV).

3.2.3 Small interfering RNA (siRNA) duplexes

siGENOME non-targeting siRNA #1 (D-001210-01-20), sequence: UAGCGACUAAACACAUCAA; ON-TARGETplus SMARTpool, and Human ERBB2 (2064) (L-003126-00-0020), target sequences: UGGAAGAGAUCACAGGUUA (J-003126-17), GAGACCCGCUGAACAAUAC (J-003126-18), GGAGGAAUGCCGAGUACUG (J-003126-19), GCUCAUCGCUCACAACCAA (J-003126-20) were utilized in this study. siRNA duplexes **[Figure 3.2]** were resuspended according to the manufacturer's specifications in 1× RNA buffer to a final concentration 20 µM. Stock solutions were stored at -80 °C and concentrations were routinely confirmed using the NanoDrop 2000c spectrophotometer (Thermo Scientific, Wilmington, DE, USA).

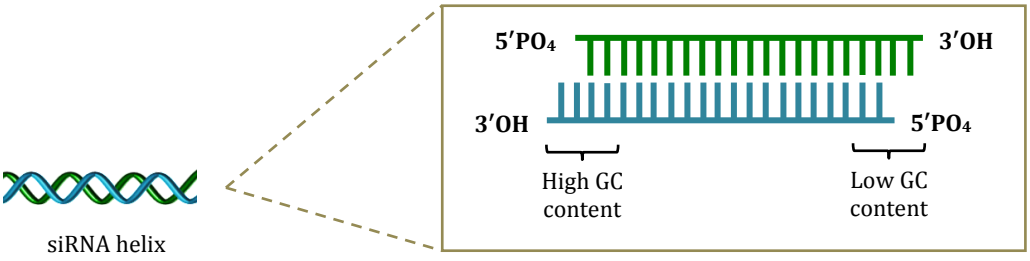

Figure 3.2: Diagrammatic representation of the siRNA duplex.

3.2.4 Preparation of Chol-T- and MS09-liposome / pCMV-*luc* or siRNA lipoplexes

Lipoplexes were freshly prepared for use in each of the assays. Chol-T and MS09 liposome suspensions were vortexed for 1 min and sonicated for 2 min prior to use. The nucleic acids (1 µg of pCMV-*luc* or 0.32 µg siRNA) were mixed directly with various amounts of the appropriate cationic liposome suspensions to achieve specific ranges of mass ($^{w}/_{w}$) or N/P (+:–) ratios. The reaction mixtures were brought up to volume (8 µL) with sterile HBS, gently vortexed for 30 s and incubated at room temperature for 30 min to allow for the development of complexes. The formation of lipolexes was confirmed by nucleic acid binding capacity studies.

3.2.5 Imaging and sizing

3.2.5.1 Cryogenic-transmission electron microscopy (cryo-TEM)

The morphology of the cationic liposomes and lipoplexes (pCMV-*luc*/ siRNA:liposome complexes according to optimal binding capacities) was examined by cryogenic-transmission electron microscopy (cryo-TEM) which employed the combined negative staining (uranyl acetate)-vitrification protocol. A 2 µL aliquot of liposome:HBS (1:5; $^{v}/_{v}$) or freshly prepared lipoplexes:HBS (1:5; $^{v}/_{v}$) was deposited onto a 200-mesh copper grid bearing a carbon coated Lacey Formvar film (Ted Pella Inc. Redding, CA, USA) and contrasted 1:1 ($^{v}/_{v}$) with 4% saturated acidic uranyl acetate negative stain. The aqueous suspensions were allowed to stand for 2 min at room temperature. Excess fluid was then wicked off with Whatman No. 5 filter paper (Sigma-Aldrich Chemical Co., St. Louis, MO, USA) until a very thin layer of fluid formed on

the grid surface. For vitrificaion of the ultrathin specimens, the prepared grids were immediately plunge-frozen in liquid nitrogen at -180 °C (cryo-protectant against freeze thaw damage and ice crystal formation) using an injector system (Leica Microsystems EM CPC, Illinois, USA). The grids were maintained at -180 °C in a Cryostation 626 single tilt liquid nitrogen cryo-transfer holder (Gatan Inc., München, Bavaria, Germany) equipped for low temperature transfer and subsequent recording of electron beam sensitive, frozen hydrated specimens in the cryogenic-TEM. The ultra-structure of liposomes and lipoplexes was then examined under a cryogenic-TEM JEOL JEM-1010 electron microscope (Jeol, Tokyo, Japan) operating at an accelerating voltage of 100 kV under low electron dose. The images were then captured using a Soft Imaging System (SIS) MegaView III, bearing a side mounted 3 mega pixel digital camera and analyzed using SIS iTEM software (Olympus, Münster, North Rhine-Westphalia, Germany).

3.2.5.2 Determination of particle size, polydispersity index and zeta potential

The hydrodynamic size (Z-average) and the size distribution (polydispersity index, PDI) of the liposomes and lipoplexes were determined by dynamic light scattering using the photon correlation spectroscopy technique. The light scattering was measured by a Malvern Nano-ZS ZetaSizer instrument (Malvern Instruments, Worcestershire, UK) which was equipped with a 5 mW He-Ne laser beam (633 nm, fixed backscattering detection optics positioned at 173 °) at 25 °C. Zeta potential (ζ) values of nanoparticles indirectly reflect the surface net charge acquired by the vesicle in a given medium. These values can therefore be used to assess the extent of interaction of the cationic liposomal surface charges with the anionic charges of DNA or siRNA. The zeta potential of the liposomes/lipoplex was measured by the Laser Doppler Velocimetry (LDV) electrophoresis technique. The liposome/lipoplex dispersions in filter-sterilized HBS (1:99, $^{v}/_{v}$, 1 mL) were prepared as in the biological studies under dust-free conditions to obtain appropriate viscosities for measurement, and loaded into 1.5 mL semi-micro disposable quartz cuvettes and universal ‘dip’ cells for particle size analysis and zeta potential studies respectively. Liposomes were allowed to equilibrate to room temperature prior to measurement and lipoplex preparation. The instrument was programmed within the following parameters: sample refractive index, 1.59; viscosity, 0.89 cP; and temperature, 25 °C. Measurements were conducted in automatic mode. The particle size of the liposome/lipoplex was measured in triplicate and data

was expressed as mean hydrodynamic diameter vs. intensity, i.e., results were reported in terms of the intensity distribution. Average diameters were calculated using a monoclonal method (NNLS cumulant or cumulative analysis) and reported as mean ± SD (n = 3) of 12 recorded runs. Zeta potentials were calculated from the mean electrophoretic mobility by applying the Smoluchowski approximation; data represent average and standard deviation (SD) values from measurements carried out in triplicate. Width at half peak height is indicative of the homogeneity of size and charge distribution. All data was analyzed using the ZetaSizer software version 6.30.

3.2.6 Nucleic acid binding capacity of cationic liposomes by gel retardation

3.2.6.1 Cationic liposome-pDNA interactions

Complexation of cationic lipid dispersions with pDNA retards pDNA electrophoretic mobility thus enabling an evaluation of the charge ratio equivalent to complete pDNA binding. pCMV-*luc* Plasmid DNA:cationic liposome complexes with various increasing mass ratios were freshly prepared before use by vortexing a mixture of pCMV-*luc* plasmid DNA (1 µg) and cationic liposome (3-10 µg) at 2500 rpm for 1 min. The complex suspension was brought up to a total volume of 8 µL with HBS at pH 7.4 **(Table 3.2)**. After 30 min incubation at room temperature, 3 µL gel loading buffer (50% glycerol, 0.05% bromophenol blue, 0.05% xylene cyanol, 72 mM Tris-HCl, 60 mM NaH_2PO_4, 20 mM EDTA, pH 7.5) was added to the lipoplex suspensions and mixed. Agarose (1%) gels were prepared (0.2 g agarose, 18 mL ultrapure deionized 18 MΩ water, 2 mL 10× running buffer, $^{w}/_{v}$), moulded and allowed to form for a minimum of 45 min. The gels were submerged in 1× Tris-acetate-EDTA running buffer (36 mM Tris-base, 30 mM NaH_2PO_4, 10 mM EDTA, pH 7.5), and a total volume of 11 µL of each sample was loaded onto the gels. Electrophoresis was conducted at room temperature for 90 min at 50 V cm^{-1} (Bio-Rad PowerPac™ Basic, USA) in a Mini-Sub Cell® GT apparatus (Bio-Rad, Richmond, CA, USA). Naked pCMV-*luc* plasmid DNA (DNAc) loaded into the outermost lane served as a positive control. Following electrophoresis, the agarose gel was stained in an ethidium bromide solution (1 µg mL^{-1}) for 30 min, visualized under UV_{300} transillumination, and images digitally photographed on a Vacutec Syngene G:Box BioImaging System (Syngene, Cambridge, UK) using GeneSnap Imaging Software version 7.05 (Syngene).

3.2.6.2 Cationic liposome-siRNA interactions

siGENOME non-targeting siRNA:cationic liposomes (0.32:2 - 12; $^{w}/_{w}$) were combined in microcentrifuge tubes and diluted to 8 µL with HBS **(Table 3.3)**. The suspensions were vortexed at 2500 rpm for 2 min to ensure proper mixing, and incubated at room temperature for 30 min prior to adding 3 µL gel loading buffer (50% glycerol, 0.05% bromophenol blue, 0.05% xylene cyanol, 72 mM Tris-HCl, 60 mM NaH_2PO_4 and 20 mM EDTA, pH 7.5). Naked siRNA loaded into the outermost lane served as a positive control. Samples were loaded into the wells of a 2% agarose gel and analyzed electrophoretically as described in **Section 3.2.6.1.** Migration patterns were visualized and images were captured as in **Section 3.2.6.1** above.

Table 3.2: Set up for gel retardation assays with varying amounts of cationic and PEGylated cationic liposome preparations with pCMV-*luc* plasmid DNA

Components	Volume (µL)							
	1	**2**	**3**	**4**	**5**	**6**	**7**	**8**
Chol-T:DOPE	0	1 (2.5 µg)	1.19 (3 µg)	1.59 (4 µg)	1.99 (5 µg)	2.38* (6 µg)	2.78 (7µg)	3.18 (8 µg)
HBS	7	6	5.81	5.41	5.01	4.62	4.22	3.82
Chol-T:DOPE:2% PEG	0	1.12 (3 µg)	1.30 (3.5 µg)	1.49 (4 µg)	1.86 (5 µg)	2.24 (6 µg)	2.61* (7 µg)	2.98 (8 µg)
HBS	7	5.88	5.70	5.51	5.14	4.76	4.39	4.02
Chol-T:DOPE:5% PEG	0	1.02 (3 µg)	1.36 (4 µg)	1.70 (5 µg)	2.04 (6 µg)	2.38* (7 µg)	2.72 (8 µg)	3.06 (9 µg)
HBS	7	5.98	5.64	5.30	4.96	4.62	4.28	3.94
MS09:DOPE	0	0.73 (2 µg)	1.09 (3 µg)	1.46 (4 µg)	1.82 (5 µg)	2.18 (6 µg)	2.55* (7 µg)	2.91 (8 µg)
HBS	7	6.27	5.91	5.54	5.18	4.82	4.45	4.09
MS09:DOPE:2% PEG	0	1.37 (4 µg)	1.72 (5 µg)	2.06 (6 µg)	2.40 (7 µg)	2.75 (8 µg)*	3.09 (9 µg)	3.43 (10 µg)
HBS	7	5.63	5.28	4.94	4.60	4.25	3.91	3.57
MS09:DOPE:5% PEG	0	1.26 (4 µg)	1.58 (5 µg)	1.89 (6 µg)	2.21 (7 µg)	2.53* (8 µg)	2.84 (9 µg)	3.16 (10 µg)
HBS	7	5.74	5.42	5.11	4.79	4.47	4.16	3.84

Abbreviations: Chol-T: 3β-[*N*-(*N'*, *N'*-dimethylaminopropane)-carbamoyl] cholesterol; **MS09:** *N*, *N*-dimethylaminopropylaminylsuccinylcholesterylformylhydrazide; **DOPE:** Dioleoylphosphatidylethanol-amine; **PEG:** 1,2-distearoyl-*sn*-glycero-3-phosphoethanolamine-N-[methoxy(polyethylene glycol)-2000]; **HBS:** HEPES Buffered Saline.
Note: In each reaction mixture pCMV-*luc* plasmid DNA was used at a constant concentration of (1µg). The volume of liposome required to reach the respective end-points is indicated by an *.

Table 3.3: Set up for gel retardation assays with varying amounts of cationic and PEGylated cationic liposome preparations with siGENOME non-targeting siRNA

Components	Volume (µL)							
	1	**2**	**3**	**4**	**5**	**6**	**7**	**8**
Chol-T:DOPE	0	1.27 (3.20 µg)	1.40 (3.52 µg)	1.53 (3.84 µg)	1.65 (4.16 µg)	1.78* (4.48 µg)	1.91 (4.80 µg)	2.03 (5.12 µg)
HBS	7	5.73	5.60	5.47	5.35	5.22	5.09	4.97
Chol-T:DOPE:2% PEG	0	2.27 (6.08 µg)	2.39 (6.40 µg)	2.50 (6.72 µg)	2.62 (7.04 µg)	2.74 (7.36 µg)	2.86* (7.68 µg)	2.98 (8.00 µg)
HBS	7	4.73	4.61	4.50	4.38	4.26	4.14	4.02
Chol-T:DOPE:5% PEG	0	3.59 (10.56µg)	3.70 (10.88µg)	3.81 (11.20µg)	3.92 (11.52µg)	4.03* (11.84µg)	4.14 (12.16µg)	4.25 (12.48µg)
HBS	7	3.41	3.30	3.19	3.08	2.97	2.86	2.75
MS09:DOPE	0	1.98 (5.44 µg)	2.10 (5.76 µg)	2.21 (6.08 µg)	2.33 (6.40 µg)	2.45* (6.72 µg)	2.56 (7.04 µg)	2.68 (7.36 µg)
HBS	7	5.02	4.90	4.79	4.67	4.55	4.44	4.32
MS09:DOPE:2% PEG	0	2.09 (6.08 µg)	2.20 (6.40 µg)	2.31 (6.72 µg)	2.42 (7.04 µg)	2.53 (7.36 µg)	2.64 (7.68 µg)	2.75* (8.00 µg)
HBS	7	4.91	4.80	4.69	4.58	4.47	4.36	4.25
MS09:DOPE:5% PEG	0	3.03 (9.60 µg)	3.13 (9.92 µg)	3.23 (10.24µg)	3.33 (10.56µg)	3.43 (10.88µg)	3.54 (11.20µg)	3.64* (11.52µg)
HBS	7	3.97	3.87	3.77	3.67	3.57	3.46	3.36

Abbreviations: Chol-T: 3β-[*N*-(*N'*, *N'*-dimethylaminopropane)-carbamoyl] cholesterol; **MS09:** *N*, *N*-dimethylaminopropylaminylsuccinylcholesterylformylhydrazide; DOPE: Dioleoylphosphatidylethanol-amine; **PEG:** 1,2-distearoyl-*sn*-glycero-3-phosphoethanolamine-N-[methoxy(polyethylene glycol)-2000]; **HBS:** HEPES Buffered Saline.
Note: In each reaction mixture siGENOME non-targeting siRNA was used at a constant concentration of (0.32µg).
The volume of liposome required to reach the respective end-points is indicated by an *.

3.2.7 Serum nuclease protection assay

Protection of nucleic acid from serum nucleases is essential for efficient gene delivery both *in vitro* and *in vivo*. For serum resistance assays, liposome:pDNA/siRNA complexes containing pCMV-*luc* plasmid DNA (1 μg) or siRNA (0.2 μg) were assembled according to three weight ratios based on binding values obtained for gel retardation studies described in **Section 3.2.6 (Tables 3.4** and **3.5)** and incubated at room temperature for 30 min. Serum stabilities of liposome:pDNA/siRNA mixtures were investigated by adding foetal bovine serum (FBS) to the complexes at a final concentration of 10% (1 μL, $^{v}/_{v}$). The reaction mixtures were then incubated at 37 °C for a further 4 h in a 14 L digital temperature-controlled water bath (TriLab Scientific, Johannesburg, Gauteng, RSA). The enzymatic digestion reaction was terminated with 10 mM EDTA (1.1 μL, $^{v}/_{v}$, pH 8) and lipoplexes disassociated using 0.5% SDS (1.33 μL, $^{w}/_{v}$). After an incubation of 20 min at 55 °C, the gel loading buffer (4 μL) was added. The following control samples were tested: naked pDNA/siRNA containing an equal volume HBS instead of the cationic liposome not treated with FBS, and naked pDNA/siRNA in the presence of FBS. The pDNA/siRNA samples were carefully added to the wells of a 1% or 2% agarose gel respectively, and subjected to electrophoresis and visualized as described in **Sections 3.2.6.1** and **3.2.6.2** for the nucleic acid binding capacity assays.

Table 3.4: Set up for serum nuclease protection assays with varying amounts of cationic and PEGylated cationic liposome preparations with pCMV-*luc* plasmid DNA

Components	Volume (µL)							
	Control 1	Control 2	Chol-T:DOPE			MS09:DOPE		
			1	2	3	1	2	3
Liposome	0	0	1.99 (5 µg)	2.38 (6 µg)	2.78 (7 µg)	2.18 (6 µg)	2.55 (7 µg)	2.91 (8 µg)
HBS	10	9	7.01	6.62	6.22	6.82	6.45	6.09
FBS (10%)	0	1	1	1	1	1	1	1
	Control 1	Control 2	Chol-T:DOPE:2% PEG			Chol-T:DOPE:5% PEG		
			1	2	3	1	2	3
Liposome	0	0	2.24 (6 µg)	2.61 (7 µg)	2.98 (8 µg)	2.04 (6 µg)	2.38 (7 µg)	2.72 (8 µg)
HBS	10	9	6.76	6.39	6.02	6.96	6.62	6.28
FBS (10%)	0	1	1	1	1	1	1	1
	Control 1	Control 2	MS09:DOPE:2% PEG			MS09:DOPE:5% PEG		
			1	2	3	1	2	3
Liposome	0	0	2.40 (7 µg)	2.75 (8 µg)	3.09 (9 µg)	2.21 (7 µg)	2.53 (8 µg)	2.84 (9 µg)
HBS	10	9	6.60	6.25	5.91	6.79	6.47	6.16
FBS (10%)	0	1	1	1	1	1	1	1

Abbreviations: Chol-T: 3β-[*N*-(*N'*, *N'*-dimethylaminopropane)-carbamoyl] cholesterol; **MS09:** *N*, *N*-dimethylaminopropylaminylsuccinylcholesterylformylhydrazide; **DOPE:** Dioleoylphosphatidylethanol-amine; **PEG:** 1,2-distearoyl-*sn*-glycero-3-phosphoethanolamine-N-[methoxy(polyethylene glycol)-2000]; **HBS:** HEPES Buffered Saline; **FBS:** Foetal Bovine Serum.
Note: In each reaction mixture, pCMV-*luc* plasmid DNA was used at a constant concentration of 1µg.

Table 3.5: Set up for serum nuclease protection assays with varying amounts of cationic and PEGylated cationic liposome preparations with siGENOME non-targeting siRNA

Components	Volume (µL)							
	Control 1	Control 2	Chol-T:DOPE			MS09:DOPE		
			1	2	3	1	2	3
Liposome	0	0	0.95 (2.4 µg)	1.11 (2.8 µg)	1.27 (3.2 µg)	1.38 (3.8 µg)	1.53 (4.2 µg)	1.68 (4.6 µg)
HBS	8.50	7.50	6.55	6.39	6.23	6.12	5.97	5.82
FBS (10%)	0	1	1	1	1	1	1	1
	Control 1	Control 2	Chol-T:DOPE:2% PEG			Chol-T:DOPE:5% PEG		
			1	2	3	1	2	3
Liposome	0	0	1.64 (4.4 µg)	1.79 (4.8 µg)	1.94 (5.2 µg)	2.38 (7.0 µg)	2.52 (7.4 µg)	2.65 (7.8 µg)
HBS	8.50	7.50	5.86	5.71	5.56	5.12	4.98	4.85
FBS (10%)	0	1	1	1	1	1	1	1
	Control 1	Control 2	MS09:DOPE:2% PEG			MS09:DOPE:5% PEG		
			1	2	3	1	2	3
Liposome	0	0	1.58 (4.6 µg)	1.72 (5.0 µg)	1.85 (5.4 µg)	2.15 (6.8 µg)	2.27 (7.2 µg)	2.40 (7.6 µg)
HBS	8.50	7.50	5.92	5.78	5.65	5.35	5.23	5.10
FBS (10%)	0	1	1	1	1	1	1	1

Abbreviations: Chol-T: 3β-[*N*-(*N'*, *N'*-dimethylaminopropane)-carbamoyl] cholesterol; **MS09**: *N*, *N*-dimethylaminopropylaminylsuccinylcholesterylformylhydrazide; **DOPE:** Dioleoylphosphatidylethanol-amine; **PEG:** 1,2-distearoyl-*sn*-glycero-3-phosphoethanolamine-N-[methoxy(polyethylene glycol)-2000]; **HBS:** HEPES Buffered Saline; **FBS:** Foetal Bovine Serum.
Note: In each reaction mixture, siGENOME non-targeting siRNA was used at a constant concentration of 0.2 µg.

3.2.8 Ethidium bromide dye displacement assay

Fluorescence titrations of pDNA/siRNA-ethidium bromide (EtBr) complexes with cationic liposomes were adapted from the method previously described by Singh and Ariatti (2006). A solution of EtBr (10 µL, 100 µg mL^{-1}) was added to 0.25 mL HBS in 96-well black flat-bottom FluorTrac plates, and a standard baseline reading of 0% relative fluorescence was established.

Subsequently, 3 µL pCMV-*luc* plasmid DNA (1 µg μL^{-1}) or 10 µL siRNA (0.32 µg μL^{-1}) was added to the mixture, and the fluorescence taken was set to represent 100% relative fluorescence intensity. Thereafter 1 µL aliquots of the complexation agents were sequentially added, the mixture was agitated for 30 s, and the fluorescence of the solution measured at excitation and emission wavelengths of 520 nm and 600 nm respectively using an automated spectrofluorometric microplate reader (SynergyMx ELX 800, BioTek Instruments, Winooski, VT, USA). Binding of the cationic liposomes to the nucleic acids caused condensation and displacement of intercalated EtBr, resulting in reduced fluorescence emission intensity until a plateau in readings was reached. All measurements were conducted in triplicate at 25 °C and relative fluorescence (F_r) was plotted against liposome lipid mass. Normalized fluorescence was calculated using the following equation:

$$F_r\ (\%) = (F - F_0) / (F_{100} - F_0) \times 100$$

where F represents the fluorescence of nucleic acid + EtBr + cationic liposome, F_0 the fluorescence of EtBr alone, and F_{100} the fluorescence of nucleic acid + EtBr.

3.3 Cell Lines and Routine Cell Culture Techniques

3.3.1 Materials, chemicals and reagents

Eagle's Minimum Essential Medium (EMEM) containing L-glutamine (4.5 g L^{-1}), Trypsin-EDTA mixture [Versene (EDTA) 200 mg L^{-1} and Trypsin 170.000 U L^{-1}] and antibiotics (100×) containing penicillin G (10 000 U mL^{-1}), streptomycin sulphate (10000 µg mL^{-1}) and amphotericin B (25 µg mL^{-1}) mixtures were purchased from Lonza BioWhittaker (Verviers, Liège, Belgium). Gamma-irradiated foetal bovine serum (FBS) and dimethyl sulfoxide (DMSO) were purchased from Hyclone, Thermo Scientific (Northumberland, UK). SKBR-3 cell line was purchased from American Tissue Culture Collection (ATCC) [HTB 30, University Boulevard, Manassas, VA, USA]. MCF-7 cells were supplied by the Department of Therapeutic and Medicines Mangement, Medical School, University of KwaZulu-Natal, Durban, South Africa, and the HEK293 cells were provided by the Anti-viral Gene Therapy Unit, Medical School,

University of the Witwatersrand, South Africa. Calbiochem® phosphate buffered saline (PBS) tablets were obtained from Merck (Darmstadt, Hesse, Germany). All sterile tissue culture plastic consumables were obtained from Corning Incorporated (Corning, NY, USA). Milli-Q50 ultrapure deionized 18 MΩ cm water was used throughout. All other chemicals and reagents were of analytical purity grade or higher, and purchased commercially.

3.3.2 Cell lines and maintenance

The SKBR-3 cell line is well known for the overexpression of the Her2/*neu* gene product. The SKBR-3 cell line was first isolated by G. Trempe and L.J. Old in 1970 from the malignant pleural effusion of a 43-year-old caucasian female with metastatic ductal adenocarcinoma of the breast. This cell line served as a positive BC cell line for Her2/*neu* gene knockdown using target specific siRNA. The MCF-7 cell line was also first isolated in 1970 from the malignant pleural effusion of a 69-year-old caucasian woman with adenocarcinoma of the breast tissue. In this BC cell line the Her2/*neu* gene product is not overexpressed, and was therefore used in this study as a negative control cell line together with the non-Her2/*neu* expressing human embryonic kidney cells (HEK-293). All routine cell culture procedures, including complete culture media prepararion, mammalian cell line propagation and maintenance, were carried out in a class II Airvolution biological safety cabinet (United Scientific (Pty) Ltd.) Cells were propagated in 25 cm^2 gas permeable screw-capped cell culture flasks containing 5 mL EMEM supplemented with 10% ($^{v}/_{v}$) FBS and Pen./Strep. antibiotics. The cultures were incubated at 37 °C in a saturated humidified atmosphere containing 95% air and 5% CO_2 (Labotec, ThermoElectron Corp., Steri-Cult CO_2 incubator, HEPA Class 100). Cells were maintained in monolayer culture, and were routinely trypsinized using 1 mL trypsin-EDTA and split at a 1:3-1:5 ratio every 3-4 days. The cells were then stored in a Nuaire Ultralow freezer at -80 °C in 0.9 mL complete medium containing 10% ($^{v}/_{v}$) dimethyl sulfoxide (DMSO).

3.3.3 Cryopreservation and reconstitution of cells

The cells were cryopreserved by first washing the confluent cells twice with 2 mL phosphate buffered saline (PBS), followed by addition of 1 mL trypsin-EDTA to dislodge the cells and 2 mL complete medium (EMEM, 10% FBS, antibiotics). The cells were then transferred to a microcentrifuge tube and pelleted by centrifugation (Eppendorf Centrifuge 5415D, Germany) at 1000 rpm for 5 min. The supernatant was decanted; the pellet was resuspended in 0.9 mL complete medium and 0.1 mL DMSO (10%), and then dispensed into 2 mL sterile cryogenic storage vials. To achieve a -1 °C min^{-1} rate of cooling, the sealed cryogenic vials were placed into a Nalgene™ Cryo 1 °C freezing container containing 2-propanol, and the latter in turn placed overnight in an ultralow biofreezer. The next day the vials were transferred to cryo-boxes and stored in a -86 °C ultralow biofreezer (Nuaire, Lasec Laboratory and Scientific Equipment).
When required, the cells were reconstituted by removing the required cryogenic vial from the bio-freezer (-80 °C) and immediately allowing it to thaw out in a 37 °C water bath. The vial was then wiped with alcohol and the cells pelleted by centrifugation at 3000 rpm for 2 min. The supernatant containing the DMSO was decanted, and the cells resuspended in 1 mL complete medium and transferred to a 25 cm^2 screw-capped cell culture flask. An additional 5 mL of complete growth medium was added to the reconstituted cell suspension to dilute traces of DMSO and to facilitate cellular growth. The flask was incubated at 37 °C overnight under a humidified atmosphere with 5% CO_2. The following day, the medium was replaced with fresh culture medium to further remove residual DMSO which is toxic to cells above 4 °C. The cells were monitored daily with frequent medium changes until they reached confluency. Prior to each experiment, cells were freshly cultured and plated to maintain the correct pH balance and to eliminate cellular waste.

3.3.4 Examination of cultures

Cell cultures were examined daily under an inverted phase contrast microscope (Nikon TMS-F 6V, Tokyo, Japan) to monitor the general appearance of cells. Key features inspected were the cell shape and general health condition, as well as any signs of contamination. Cultures were also examined during trypsinization to observe the rounding-off and detachment of cells.

3.4 Transfections

3.4.1 Materials, chemicals and reagents

3-(4, 5-Dimethyl-2-thiazolyl)-2, 5-diphenyl-2H-tetrazolium bromide (MTT) salt and Calbiochem® phosphate buffered saline (PBS) tablets were obtained from Merck (Darmstadt, Germany). Dimethyl sulfoxide (DMSO) was obtained from Highveld Biological (Pty) Ltd., Kelvin, South Africa. The luciferase assay kit was purchased from Promega Corporation (Madison, WI). The bicinchoninic acid (BCA) assay reagents and the protein standard bovine serum albumin (BSA) protein standards were purchased from Sigma-Aldrich (St. Louis, MI). The 48-well microtiter plates and all other tissue culture plastic consumables were from Corning Incorporated (Corning, New York, USA).

3.4.2 MTT cell viability assay

The cytotoxicity of pDNA/siRNA lipoplexes was determined to indicate the viability and proliferation of cells against transfection complexes. MTT [3-(4, 5-dimethyl-2-thiazolyl)-2, 5-diphenyl-2H-tetrazolium bromide, a yellow tetrazole] is reduced in the mitochondria of viable cells to a purple formazan product. These reductions take place only when reductase enzymes are active, and are often used as a measure of viable cells. The cytotoxicity of cationic liposomes (steric stabilized and non-steric stabilized MS09 and Chol-T liposomal formulations) was assessed using the MTT viability assay against HEK-293, MCF-7 and SKBR-3 cells. Confluent HEK-293, MCF-7 and SKBR-3 cells were separately trypsinized, harvested and then seeded into 48-well microtiter plates at the following densities: 1.9×10^4, 1.8×10^4 and 2.0×10^4 cells per well respectively. Cell counts were conducted using a haemocytometer. To allow attachment and growth to semi-confluency, the cells were incubated in 0.25 mL of EMEM supplemented with 10% ($^{v}/_{v}$) FBS and antibiotics at 37 °C in a 5% CO_2 atmosphere for 24 h. The following day, pDNA/siRNA lipoplexes were prepared in triplicate volumes (30 µL) based on various optimized end-point ratios ($^{w}/_{w}$) in HBS, and incubated at room temperature for 30 min. The medium in the cell culture microtiter plates was then replaced with fresh EMEM (0.25 mL), and 10 µL of the various lipoplexes were pipetted into the wells in triplicate. The plates were then

incubated at 37 °C for 48 h. The cells of positive control were incubated with EMEM (10% FBS, antibiotics) only and the cell viability was assumed to be 100%. After 48 h, the complete medium was removed from each well and replaced with 0.2 mL of a MTT stock solution (5 mg mL^{-1} in PBS) and 0.2 mL complete EMEM. Thereafter, the plates were incubated for an additional 4 h at 37 °C until the purple precipitates were visible. Following incubation, the MTT-containing medium was carefully aspirated to avoid disturbing any formazan crystals formed by living cells, and 0.2 mL DMSO was added to each well. The plates were gently agitated at room temperature to dissolve the formazan crystals. Finally, the UV_{570} absorbance of the formazan products was measured by a Vacutec, Mindray MR-96A microplate reader using DMSO as a blank. The cell viability (%) was then calculated using the following equation:

% Cell Survival (CS) = Average of treated cells / Average of control cells × 100

3.4.3 Luciferase assay

A day before transfection, HEK-293, MCF-7 and SKBR-3 cells were trypsinized and evenly seeded into 48-well microtiter plates at a density of 2.1×10^4, 2.4×10^4 and 2.2×10^4 cells per well in 0.25 mL complete medium. The cells were allowed to attach to the bottom of the wells and grow to semi-confluence at 37 °C in a 5% CO_2 atmosphere. The following day, pCMV-*luc* plasmid DNA lipoplexes were prepared in triplicate volumes (30 µL) based on various optimized end-point ratios ($^{w}/_{w}$) in HBS and incubated at room temperature for 30 min. The cells were prepared by decanting the medium from each well and replacing it with 0.25 mL complete medium. The lipoplexes (10 µL) were then added to each well and mixed gently by rocking the plate back and forth. The cells were incubated at 37 °C with 5% CO_2 for 4 h. The medium was then removed and replaced with complete growth medium and further cultured for 48 h at 37 °C with 5% CO_2. Following the incubation period, relative *luc* activity was assessed using a Glomax™ Multi+ Detection System (Promega Biosystems, Sunnyvale, USA). The cells were prepared by gently aspirating the medium from each well and carefully washing twice with 0.2 mL PBS. Thereafter, 80 µL cell lysis reagent was added to each well and the microtiter plate was placed on a platform shaker (Stuart Scientific Platform Shaker STR6, UK) for 15 min at 30 rev min^{-1}. To facilitate cell lysis, each well was manually 'scraped', and the resultant cell lysates

were transferred to microcentrifuge tubes and briefly centrifuged (5 s at 12 000 rpm) to pellet cellular debris. The cell-free extracts were transferred into a 96-well white GLOMAX plate followed by the addition of 50 μL Promega luciferase assay reagent. The reaction mixture was briefly vortexed and the *luc* activity of each sample was immediately measured in relative light units (RLU) for a period of 10 s in a Promega GLOMAX® MULTI+ Detection system. Luciferase activity was expressed as RLU mg^{-1} protein. Protein determinations were performed on the cell-free extracts using the BCA protein assay.

3.5 HER2/*neu* Silencing at mRNA and Protein Levels

3.5.1 Materials, chemicals and reagents

The ReadyPrep™ protein extraction kit (total protein), 10× Tris/Glycine/SDS buffer, 5× transfer buffer, blotting-grade blocker (non-fat dry milk), Tween 20, Trans-Blot® Turbo™ transfer system RTA transfer kit, Mini-PROTEAN® TGX™ long shelf life precast gels, 2× Laemmli sample buffer, Precision Plus Protein™ dual extra standards, clarity Western ECL substrate and RT-PCR strip tubes were purchased from Bio-Rad Laboratories (Richmond, CA, USA). Tris (hydroxymethyl)-aminomethane (*M* 121.2 g $mol.^{-1}$, Tris base), sodium chloride (*M* 58.44 g $mol.^{-1}$, NaCl), hydrochloric acid (HCl), absolute ethanol (EtOH, C_2H_6O), chloroform ($CHCl_3$), and isopropanol ($CH_3CHOHCH_3$) were acquired from Merck (Darmstadt, Hesse, Germany). TRIzol® Reagent, Lipofectamine® 3000, High Capacity cDNA Reverse Transcription Kit with RNase inhibitor, MicroAmp® Fast optical 96-well reaction plates, MicroAmp® Optical Adhesive Films, and distilled water DNase/RNase free were purchased from Life Technologies (Carlsbad, CA, USA). For all materials, chemicals and reagents used for the siRNA gene transfection refer to **Section 3.1.1.** The following antibodies were used for Western blotting: Neu (0.N.211); sc-71667, a mouse monoclonal antibody raised against a synthetic peptide corresponding to amino acids 1242-1255 of human Neu (M*w* 185 kDa), β-Actin (C4); sc-47778, a mouse monoclonal antibody raised against gizzard Actin of avian origin (M*w* 43 kDa); and goat anti-mouse IgG-HRP; sc-2005, an affinity purified secondary antibody raised in goat against mouse IgG and conjugated to horseradish peroxide (HRP). These antibodies were purchased from Santa Cruz

Biotechnology, Inc. (CA, USA). Ultrapure deionized 18 MΩ water (Milli-Q50) was used throughout.

3.5.2 Transfection of siRNA

Four different sequences of 19 nucleotides (ON-TARGETplus SMARTpool) were used as potential siRNAs targeting the HER2/*neu* gene (refer to **Section 3.2.3**). A non-targeting sequence siRNA was used as a non-specific siRNA control. For *in vitro* analysis, SKBR-3 cells were seeded into 6-well plates at a density of 1×10^5 cells per well. This was conducted 24 h prior to transfection to allow the cells to attach and grow to semi-confluency. The following day, the culture medium was replaced with 1.5 mL fresh EMEM supplemented with 10% ($^{v}/_{v}$) FBS and antibiotics. Thereafter, 10 µL of pre-assembled siRNA lipoplexes (prepared according to end-point ratios) in HBS were added into each well in triplicate **(Table 3.6)**. Lipofectamine® 3000 (Life Technologies, Carlsbad, CA, USA) was included as a positive transfection control and lipoplexes were assembled according to the manufacturer's instructions. The cationic lipid complexes were prepared by incubating 5 µL Lipofectamine® 3000 Reagent and 2.5 µL siRNA in 250 µL EMEM medium for 5 min at room temperature. After 48 h and 72 h of transfection, the complete medium was removed from each well and cells were harvested for assessing HER2/*neu* gene knockdown status, using quantitative real time polymerase chain reaction (qRT-PCR) and Western blotting analysis respectively.

Table 3.6: Set up for gene expression studies with varying amounts of cationic and PEGylated cationic liposome preparations with ON-TARGETplus SMARTpool HER2/*neu* siRNA

Components	Volume (µL)								
	Chol-T:DOPE			**Chol-T:DOPE:2% PEG**			**Chol-T:DOPE:5% PEG**		
	1	**2**	**3**	**1**	**2**	**3**	**1**	**2**	**3**
Liposome	3.05 (7.7 µg)	3.56 (9.0 µg)	4.07 (10.2µg)	5.25 (14.1µg)	5.72 (15.4µg)	6.20 (16.6µg)	7.62 (22.4µg)	8.06 (23.7µg)	8.50 (25.0µg)
HBS	4.45	3.94	3.43	2.25	1.78	1.30	4.88	4.44	4.00
siRNA	2.5	2.5	2.5	2.5	2.5	2.5	2.5	2.5	2.5
	MS09:DOPE			**MS09:DOPE:2% PEG**			**MS09:DOPE:5% PEG**		
	1	**2**	**3**	**1**	**2**	**3**	**1**	**2**	**3**
Liposome	4.43 (12.2µg)	4.89 (13.4µg)	5.36 (14.7µg)	5.05 (14.7µg)	5.49 (16.0µg)	5.93 (17.3µg)	6.87 (21.8µg)	7.27 (23.0µg)	7.68 (24.3µg)
HBS	3.07	2.61	2.14	2.45	2.01	1.57	5.63	5.23	4.82
siRNA	2.5	2.5	2.5	2.5	2.5	2.5	2.5	2.5	2.5

Abbreviations: Chol-T: 3β-[*N*-(*N'*, *N'*-dimethylaminopropane)-carbamoyl] cholesterol; **MS09**: *N*, *N*-dimethylaminopropylaminylsuccinylcholesterylformylhydrazide; **DOPE:** Dioleoylphosphatidylethanol-amine; **PEG:** 1,2-distearoyl-*sn*-glycero-3-phosphoethanolamine-N-[methoxy(polyethylene glycol)-2000]; **HBS:** HEPES Buffered Saline.
Note: In each reaction mixture, ON-TARGETplus SMARTpool HER2/*neu* siRNA was used at a constant concentration of 0.64 µg.

3.5.3 RNA extraction and qRT-PCR

3.5.3.1 RNA extraction

For qRT-PCR analysis, total cellular RNA from transfected cells was extracted using TRIzol® Reagent (Life Technologies, Carlsbad, CA, USA), following the manufacturer's detailed protocol. The RNA isolation procedure was conducted at room temperature in a class II biohazard laminar flow cabinet under sterile RNase free conditions, and involved four primary steps: cellular homogenization, RNA precipitation, RNA wash and RNA resuspension. Firstly, the growth medium was removed from the culture plates and 1 mL TRIzol reagent was added directly to the cells in each well. The cells were lysed manually by homogenizing the samples

several times (35-40 strokes) using a pipette. To allow complete dissociation of the nucleoprotein complex, the homogenate was incubated at room temperature for 5 min. Samples were transferred into sterile 2 mL polypropylene microcentrifuge tubes prior to the addition of 0.2 mL chloroform. The tubes were securely capped and shaken vigorously by hand for 15 seconds; the samples were then left to stand at room temperature for 3 min before centrifuging (Eppendorf centrifuge 5424R) at 12,000 × *g* for 15 min at 4 °C. The mixture separated into a lower red phenol chloroform phase, an interphase, and a colourless upper aqueous phase. RNA remains exclusively in the upper aqueous phase which makes up ~50% of the total volume of the sample. The aqueous phase was gently removed by angling the tube at 45 ° and pipetting out the solution. Care was taken to avoid contamination with the inter- and organic phases. The aqueous solution was transferred into a new 2 mL tube and treated with 0.5 mL of 100% isopropanol for 10 min at room temperature before centrifuging at 12,000 × *g* for 10 min at 4 °C. The supernatant was removed and the gel-like RNA pellet formed on the side of the tube was washed by briefly vortexing the sample in 75% ethanol followed by centrifugation at 7500 × *g* for 5 min at 4 °C. The pellet was allowed to air dry. The RNA pellet was resuspended in 30 μL RNase free water (Life Technologies, Carlsbad, CA, USA) by pipetting the solution up and down several times and incubating the suspension for 15 min at 55 °C. The concentration and quality of the cellular RNA were assessed by the absorbance ratio at 260 nm and 280 nm on the NanoDrop 2000c spectrophotometer (Thermo Scientific, Wilmington, DE, USA). The integrity of the RNA was analyzed by electrophoresis on a 2% agarose gel, following the method described in **Section 3.2.6.2**.

3.5.3.2 Quantitative Real-Time PCR (qRT-PCR)

The efficiency of HER2/*neu* siRNA interference was evaluated by qRT-PCR which serves to indicate the gene knockdown at the mRNA level. The total RNA was converted into cDNA by reverse transcriptase PCR using the High Capacity cDNA Reverse Transcription (RT) Kit with RNase inhibitor (Life Technologies, Carlsbad, CA, USA), following the manufacturer's protocol. The kit components were mixed to afford a 2× RT master mix per 20 μL reaction (**Table 3.7**). The cDNA RT reactions were prepared by mixing 10 μL 2× RT master mix and 10 μL (~0.2 μg μL^{-1}) total RNA sample in RT-PCR strip tubes. The tubes were sealed and briefly

centrifuged to spin down the contents and to eliminate any air bubbles. Reactions with no MultiScribe™ reverse transcriptase were included as negative controls in each run. The reverse transcription was performed in three phases: step 1 - 25 °C (10 min); step 2 - 37 °C (120 min); and step 3 - 85 °C (5 min) on a Bio-Rad C1000 Touch™ Thermal Cycler. Thereafter the cDNA products were stored at 4 °C.

Table 3.7: High Capacity cDNA Reverse Transcription Kit components required to prepare 2× RT master mix

Component	**Volume per reaction (µL)**
10× RT buffer	2.0
25× dNTP mix (100 mM)	0.8
10× RT random primers	2.0
MultiScribe™ reverse transcriptase	1.0
RNase inhibitor	1.0
Nuclease-free H_2O	3.2
Total per reaction	**10.0**

Abbreviations: RT: Reverse Transcription; **dNTP:** deoxyribonucleotide triphosphate.

Next, gene expression was quantified by qRT-PCR using the TaqMan® gene expression assays which are FAM™ dye-labelled and possess minor-groove binding (MGB) probe. The primers and probe used were the gene of interest HER2/*neu* (Assay ID Hs01001580_m1) and the endogenous control glyceraldehyde 3-phosphate dehydrogenase (GAPDH) (Assay ID Hs03929097_g1) (Life Tachnologies, Carlsbad, CA, USA). Singleplex PCR reactions were conducted as triplicates for all samples tested. Each reaction mixture (20 µL) contained 10 µL TaqMan® gene expression master mix [AmpliTaq Gold® DNA polymerase, deoxyribonucleotide triphosphates (dNTPs) with deoxyuridine triphosphate (dUTP), UP (Ultra Pure), Uracil-DNA Glycosylase (UDG), ROX™ Passive Reference, as well as buffer components optimized for specificity, sensitivity and precision], 1 µL 20× TaqMan® gene expression assay mix, and 9 µL sample cDNA. Reaction mixtures were prepared and mixed in MicroAmp® Fast optical 96-well reaction plates and covered with MicroAmp® Optical Adhesive Films. The qRT-PCR

amplification was performed under the following conditions: initial setup 95 °C for 10 min (hold), followed by 40 cycles of 95 °C for 15 s (denature) and 60 °C for 1 min (anneal/extend) on a CFX 96™ Real-Time System, C1000 Touch™ Thermal Cycler using CFX Manager Software version 3.0 (Bio-Rad). Relative expression values of HER2/*neu* mRNA normalized to the level of GAPDH mRNA were determined using the $2^{-\Delta\Delta Ct}$ method (Livak and Schmittgen, 2001).

$$\text{Fold difference} = 2^{-\Delta\Delta Ct}$$

$$\Delta C_{t\ sample} - \Delta C_{t\ calibrator} = \Delta\Delta C_t$$

$$C_{t\ GOI}{}^{s} - C_{t\ norm}{}^{s} = \Delta C_{t\ sample}$$

$$C_{t\ GOI}{}^{c} - C_{t\ norm}{}^{c} = \Delta C_{t\ calibrator}$$

In the above equation, s represents the sample, c the calibrator (untreated cells), GOI the gene of interest HER2/*neu*, and norm the normalizer gene GAPDH.

3.5.4 Protein extraction and Western blotting

3.5.4.1 Protein extraction

The extraction of total cellular proteins was performed 72 h after transfection, using the ReadyPrep™ Protein Extraction Kit (Total Protein), following the manufacturer's specifications (Bio-Rad, Hercules, CA, USA). The complete growth medium was aspirated from each well and 1 mL of complete 2-D rehydration/sample buffer 1 [7 M urea, 2 M thiourea, 1% ($^{w}/_{v}$) ASB-14 detergent, 40 mM Tris base, and 0.001% Bromophenol Blue] containing 10 µL of ReadyPrep tributylphosphine (TBP, 200 mM) reducing agent were added. The cells were lysed by gently 'scraping' the bottom surface of the plate and then manually mixing the solution with a pipette several times. The samples were transferred into pre-cooled 2 mL microcentrifuge tubes and placed on ice for 1 min. To facilitate disruption of the cells and fragmentation of the genomic DNA, the suspension was vortexed for a total of 15 min and routinely chilled on ice every 3 min. The tubes were then centrifuged at 16 000 × *g* for 30 min at 18 °C to pellet cell debris. The supernatant, containing cellular proteins, was aspirated and transferred to clean microcentrifuge

tubes, and then quantified using a NanoDrop 2000c spectrophotometer (Thermo Scientific, Wilmington, DE, USA).

3.5.4.2 Western blotting

The Western blotting technique was used to analyze HER2/*neu* protein expression in SKBR-3 cells. For the sample preparation, ~20 µg of protein from total cell lysate were treated with an equal volume of 2× Laemmli sample buffer (4% SDS, 10% 2-mercaptoethanol, 20% glycerol, 0.004% bromophenol blue, and 125 mM Tris-HCl, pH 6.8) and heated at 95 °C for 5 min in a 14 L digital temperature-controlled water bath (TriLab Scientific, Johannesburg, Gauteng, RSA). The preparation was then allowed to cool down. Prior loading, Mini-PROTEAN® TGX™ (10%) long shelf life pre-cast gel cassettes (Bio-Rad Laboratories, Richmond, CA, USA) were placed in a Bio-Rad Mini-PROTEAN® Tetra System, and the integrated upper buffer chamber was filled with chilled 1× Tris/Glycine/SDS running buffer [25 mM Tris, 190 mM Glycine and 0.1% ($^{w}/_{v}$) SDS, pH 8.3 (Bio-Rad Laboratories, Richmond, CA, USA)]. Each well was washed twice with running buffer. Thereafter, the lower buffer tank was filled with chilled 1× Tris/Glycine/SDS running buffer to the marked fill line. The protein samples were loaded into the wells and electrophoresis was conducted at room temperature for 30 min at 200 V cm^{-1} (Bio-Rad PowerPac™ Basic, USA). Three µL of the molecular weight marker (Precision Plus Protein™ Dual Extra Standards) was loaded into the first well.

Following electrophoresis, protein transfer (blotting) was conducted using the Bio-Rad Trans-Blot® Turbo™ transfer system and RTA transfer kits following the manufacturer's protocol. The PVDF membranes were immersed in absolute ethanol until the membranes were translucent, and then equilibrated for 3 min in a gel tray containing 30 mL of 1× transfer buffer (Bio-Rad Trans-Blot® Turbo™ transfer buffer). Two transfer stacks (7 layers of filter pads each) were soaked in 50 mL of 1× transfer buffer for 3 min. The transfer cassettes were assembled in sandwich like order: one wetted stack was placed on the bottom of the cassette [serves as bottom ion reservoir on cassette electrode (anode)], PVDF membrane and gel, and the second wetted transfer stack on top of the gel [serves as top ion reservoir on cassette electrode (cathode)]. The assembled sandwich was made even and trapped air bubbles were expelled using a blot roller. The cassettes were tightly locked and placed in the instrument blotter bay. Transfer was

conducted at 2.5 A, 25 V for 10 min to promote high M*w* transfer (> 150 kDa). After the transfer, the blotting sandwich was dissembled and both the blot and the gel were placed in deionized water.

Prior to antibody incubation, unoccupied sites on the blot were saturated in a solution of 3% blotting-grade blocker (non-fat dry milk) in Tris-buffered saline (20 mM Tris-HCl, pH 7.5, 150 mM NaCl) containing 0.1% Tween 20 (TBST) for 1 h at room temperature. The membranes were incubated overnight at 4 °C in TBST containing either Neu, a mouse monoclonal antibody raised against a synthetic peptide corresponding to amino acids 1242-1255 of human Neu (1:5000) for HER2/*neu* protein detection, or β-Actin, a mouse monoclonal antibody raised against gizzard Actin of avian origin (1:200) used as an internal control for protein loading. The following day, the primary antibody was poured out and the membranes were washed in 20 mL TBST with continuous agitation for 5 min (total of 5 washes). Thereafter, the membranes were incubated at room temperature in goat anti-mouse IgG-HRP secondary antibody (1:2000) prepared in TBST. After 1 h, the secondary antibody solution was poured out and the membranes were washed again in 20 mL TBST with continuous agitation for 5 min (total of 5 washes).

The membranes were developed using the commercially available Clarity™ Western ECL substrate kit (Bio-Rad Laboratories, Richmond, CA, USA) following the manufacturer's instructions. The membranes were placed, protein side up, on a clear surface and the substrate kit components [mixed in a 1:1 ratio (12 μL)] were gently added onto the blot ensuring that no air bubbles were formed and that the blot was completely covered with substrate. The blots were incubated for 5 min at room temperature and then visualized using the Bio-Rad digital imager ChemiDoc™ MP system. Band intensity was determined using Image Lab Software version 5.2.2.

3.6 Statistical Analysis

Data are presented as means ± SD (n = 3). Statistical analysis among mean values was performed using one-way ANOVA followed by the Tukey-Kramer multiple comparisons test between formulations. All statistics were performed using a 95% confidence interval and was considered significant when the P value was less than 0.05 (P<0.05).

CHAPTER FOUR

RESULTS AND DISCUSSION

4.1 Liposome/Lipoplex Formulation

Two previously synthesized amphiphilic cholesterol derivatives bearing cationic charges were used to formulate the cationic liposomes (Singh and Ariatti, 2006; Singh *et al*., 2001). As illustrated in **Figure 4.1 (A)** and **(B)**, cytofectins comprise four functional units: (1) a lipophilic anchorage system which is a large hydrocarbon moiety referred to as the non-polar or lipid tail; (2) a hydrophilic cationic head group capable of binding with the negatively charged phosphate backbone of the nucleic acids; (3) a spacer arm for the distancing of an anchor and cationic head group; and (4) a linker group connecting these modules (hydrophobic and hydrophilic domains). Both CCCs, Chol-T and MS09, were previously synthesized from cholesteryl chloroformate. They were designed to harbour a common cationic amine (R_3NH^+) functionalized head group and a fused lipophilic ring system, but differed in the length of the cytofectin spacer elements between the two domains.

(A)

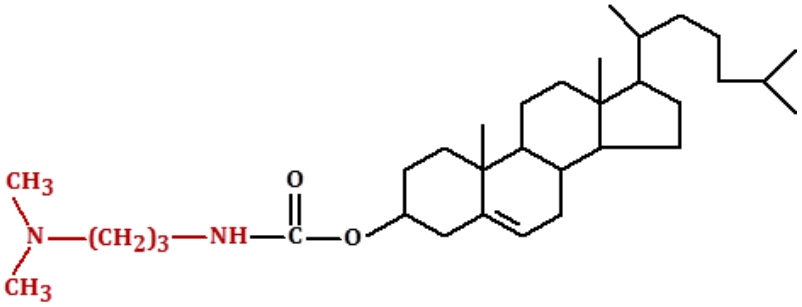

(B)

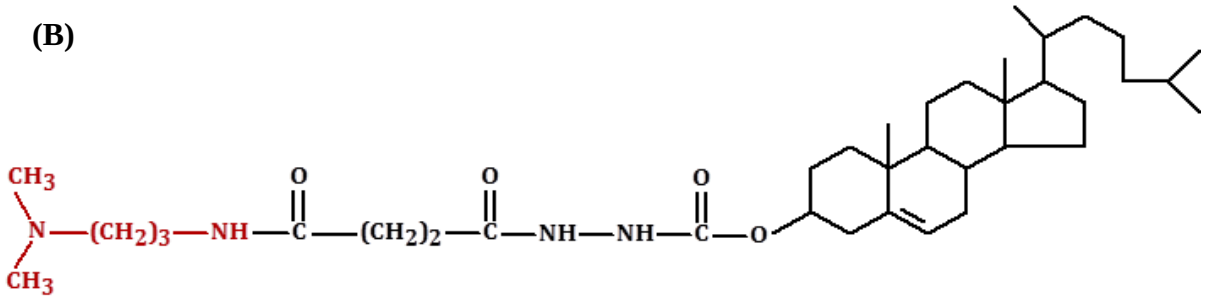

Figure 4.1: Structural representation of the cholesteryl cytofectins. (A) 3β-[*N*-(*N'*, *N'*-dimethyl-aminopropane)-carbamoyl] cholesterol (Chol-T) and (B) *N*, *N*-dimethylaminopropylaminylsuccinyl cholesterylformyl hydrazide (MS09).

4.1.1 Conventional and PEGylated cationic liposome components and formulation

Liposome preparation techniques and the delicate physicochemical interactions amongst the various synthetic lipid classes are fundamental steps that govern the properties of cationic liposomes. Recently, in a review by Patil and Jadhav (2014), procedures for liposome preparation were divided into: (a) film methods which involved the deposition of lipids from an organic solvent onto a substrate and subsequent hydration of the film resulting in the formation of liposomes, and (b) bulk methods where liposomes are attained by transfer of phospholipids from an organic phase into an aqueous phase. In this study, six liposome formulations which included a synthetic CCC (Chol-T or MS09) for binding the negatively-charged nucleic acid (siRNA or pDNA) and a helper lipid (DOPE) were prepared using the dry-film method, first described by Bangham *et al*. (1965). The procedure involved dry-filming the phospholipids from solution in chloroform onto the sides of glass quickfit tubes, followed by hydration in sterile HBS. A constant concentration (2 mM) of the cytofectin (Chol-T or MS09) was retained in the preparation of all liposomes. The choice of bilayer components and optimization of formulation aspects determine the molecular fluidity or rigidity, interfacial elasticity and hydration of the resultant liposomes. In general, the bilayer thickness and T_m depend on the acyl chain length, and the bilayer fluidity is controlled by the acyl chain saturation (Kohli *et al*., 2014). With regard to cholesterol and cholesterol-containing derivatives, they do not readily form lipidic bilayer assemblies on their own. These molecules, due to their amphipathic structural property, permit their insertion into liposomes. Cholesterol is able to promote and stabilize homogeneous liposomal bilayers, thereby offering some degree of protection from mechanical fracture and protein binding (Yang *et al*., 2013c). Incorporation of cholesterol into liposome preparations was found to enhance the resistance of lipid-based carriers to serum-induced aggregation (Han *et al*., 2008). In addition, formulations containing elevated quantities of cholesterol are not prone to metabolic degradation (Pozzi *et al*., 2012; Zhang *et al*., 2008).

Cellular uptake and endosomal escape are two major barriers which need to be overcome in order to achieve efficient transgene expression. In a number of publications, Ewert *et al*. (2002; 2004; 2005; 2006) expatiated on the relationship between transfection efficacy and the supramolecular structures of lipoplexes using small angle X-ray scattering (SAXS). The merging of two lipid membranes (e.g. liposomal and endosomal membrane fusion) is mediated by a

lamellar phase (L_α) to inverted hexagonal phase (H_{II}) transition (Gruner *et al*., 1985). This is accomplished by the amphiphile's capacity to assume certain geometries when suspended in an aqueous environment. The phase structure of cationic lipids can be predicted as a function of their packing parameter; defined by the ratio of the hydrocarbon volume over the product of the hydrophilic head group area, and the critical length of the hydrophobic tail (Wasungu and Hoekstra, 2006). Lipids possessing a small hydrocarbon cross section area with a large head group (P < ½), form typical cone-shaped monomers, and self-assemble into micelles corresponding to a structure exhibiting positive membrane curvature. The formation of lipid bilayers or L_α structures is enhanced when the curvature of the self-assembled amphiphiles is negligible (½ < P > 1). In contrast, when P exceeds 1, the lipid tends to display a negative curvature, adopting the inverted hexagonal phases or inverted micelles (i.e., bilayer destabilizing structure) (Hsu *et al*., 2005; Šmisterová *et al*., 2001). Research suggests that liposomal formulations supplemented with the neutral or zwitterionic phospholipid, DOPE can significantly improve the transfection efficiency of cationic lipids (Farhood *et al*., 1995; Felgner *et al*., 1987; 1994; Zuhorn *et al*., 2002). DOPE is therefore referred to as a 'helper' co-lipid. In this study, DOPE was employed to further enhance the membrane fusion capacity of the cationic liposomes. Importantly, cationic liposomes that require DOPE as a helper do not exhibit H_{II} formation when the lipids are mixed; they form ordered L_α structures. In addition, supportive lipids like DOPE contribute to bilayer assemblies with cationic lipids that do not naturally display such properties (cationic lipids that repel each other) (ur Rehman *et al*., 2013a). Owing to its zwitterionic head, DOPE is pH sensitive; above pH 9.0 DOPE monomers form spherical micelles. However, when exposed to an acidic pH, a structural transition occurs forming an inverted hexagonal phase (Mochizuki *et al*., 2013). Internal endosomal environments (generally encountered on the transfection route) are characteristic of low pH ranges, allowing DOPE to undergo this phase change. Due to the propensity of DOPE to adopt an inverted hexagonal phase, this cone-shaped neutral lipid is known to play a critical role in membrane fusion within endosomes, thereby inducing strong destabilizing effects on the barrier properties of the endosomal membranes. Therefore, cationic liposomes containing DOPE promise effective lipid-mediated siRNA gene delivery.

In addition to formulating conventional liposomes featuring the CCCs (Chol-T and MS09), this study also investigated steric stabilization of the liposomes. Polyethylene glycol

(PEG) is arguably the most common hydrophilic, biocompatible and inert polymer currently employed to improve water solubility; prevent unspecific interactions with charged serum proteins (aggregation); and increase serum stability of cationic liposomes. PEGylated cationic liposomes were prepared by simply mixing solutions of the commercially available PEG-conjugated lipid (DSPE-PEG_{2000}), with the cationic cytofectin (Chol-T or MS09) and DOPE. Liposomes were formulated with 2 or 5 mol.% DSPE-PEG_{2000}, Chol-T and MS09 were kept constant at 50 mol.%, and DOPE was adjusted to accommodate changes in PEGylation. This method of preparing PEGylated complexes is termed pre-PEGylation. The procedure entails inclusion complexation formation, as PEGylation occurs prior to lipoplex formation with pDNA or siRNA. PEGylation of conventional liposomes can occur with PEG chains of varying graft densities and length. DSPE-PEG_{2000} was incorporated into the liposomal mixture as this molecular weight PEG has been reported to optimize blood circulation times of liposomes (Pozzi *et al*., 2014; Zhang *et al*., 2012).

4.2 Biophysical Characterization of Liposome and Liposome-Nucleic Acid Interactions

4.2.1 Morphological observations using cryo-TEM

Morphological and architectural characterization of liposomes and lipoplexes leads to a clearer understanding of their relative structure, orientation of the nucleic acid molecules, and arrangement of the complexes. The ultrastructure of cationic liposomes and lipoplexes was visualized by cryo-TEM, which enables direct examination of colloidal carriers in the vitrified, frozen-hydrated state. Transmission electron microscopy uses an electron gun and a system of electromagnetic lenses to focus an electron beam on a sample. Since electrons are easily refracted, the microscope column is maintained under high vacuum to avoid deflection of electrons by gas molecules (Kuntsche *et al*., 2011). The contrast is obtained by the interaction of the electrons with the specimen, during which the electrons are transformed to unscattered electrons, elastically scattered or inelastically scattered electrons. A series of electromagnetic lenses is then used to focus the unscattered or scattered electrons on a screen in order to generate a phase-contrast image (Lin *et al*., 2014). The sample preparation for cryo-TEM imaging is a rather sensitive process since electrons do not easily penetrate matter. To provide high contrast, a

negative stain containing a heavy metal salt (uranyl acetate) was used to stain the sample (Kuntsche *et al*., 2011). Basically, the stain allows the indicative evaluation of the liposomal structure by binding to the phosphate groups of phospholipids and poorly penetrating the lipid bilayer. Therefore, the outer surface of the liposome or lipoplex is black whilst the inner aqueous core is white (Ruozi *et al*., 2011). After drying, the sample was plunge frozen in liquid nitrogen; this technique preserves the biological material in the liposome/lipoplex inner core and also limits the formation of amorphous ice crystals (Friedrich *et al*., 2010).

Figure 4.2 presents selected cryo-TEM micrographs of the Chol-T liposomes **[(A)** to **(C)]** and MS09 liposomes **[(D)** to **(F)]**. The images revealed a heterogeneous population of typically spherical or ellipsoidal shaped structures with a distinct bilayered membrane surrounding the internal aqueous core. The cationic liposomes appeared well dispersed with little aggregation. The majority of the liposomes appeared electron dense (dark regions), while some were associated with low-density lipid membranes (light regions).

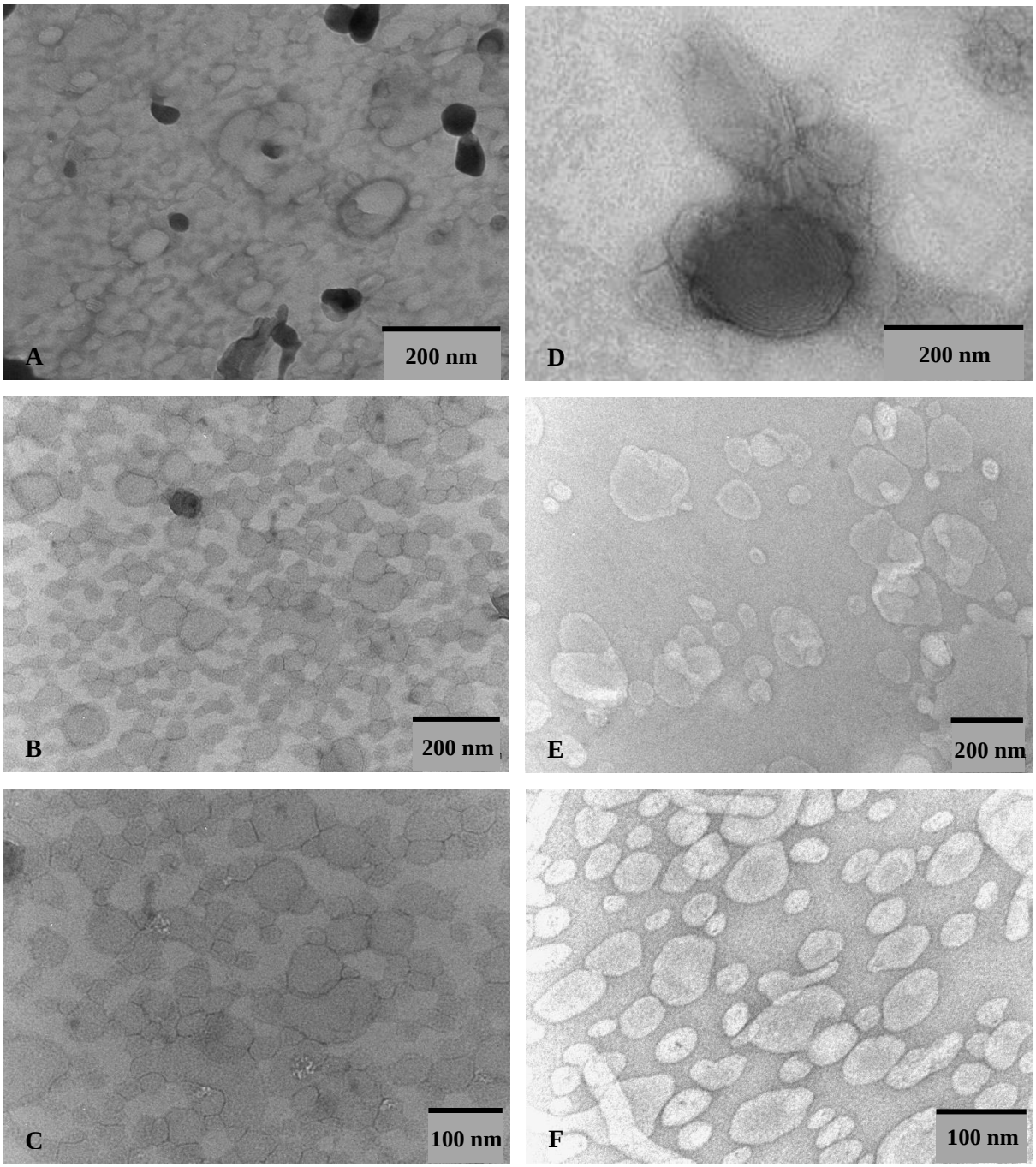

Figure 4.2: Transmission electron micrographs of cationic and PEGylated cationic liposomes prepared according to **Table 1**: **A**, Chol-T:DOPE; **B**, Chol-T:DOPE:2% PEG; **C**, Chol-T:DOPE:5% PEG; **D**, MS09:DOPE; **E**, MS09:DOPE:2% PEG; **F**, MS09:DOPE:5% PEG. Bar = 100 nm or 200 nm.

In particular, two factors influence the bright/dark contrast in cryo-TEM images; (1) the atom positioning in the crystalline structure, and (2) the atomic number (Belletti *et al*., 2013; Rao and Biswas, 2009). In these samples it can be hypothesized that the presence of looped, twisted and invaginated structures is due largely to the amorphous nature or flexibility of the liposomal membranes (i.e., lipid reorganization). Moreover, liposomes formulated with cationic lipids bearing a longer spacer (MS09) revealed multi-lamellar liposomal vesicles, indicating that the morphology of the liposomes was influenced by the spacer length. A certain degree of distortion of the original vesicular structure was also observed. Although this electron microscopic technique allows direct investigations of thin transparent samples in their frozen-hydrated state, processes like staining, freezing and drying may result in possible artifacts and morphological changes accompanied by a reorganization of the fragile liposome vesicle (Kuntsche *et al*., 2010; 2011; Wessman *et al*., 2010). Dehydration of the samples under vacuum may result in an osmotic imbalance between the liposome core and the outer aqueous phase causing vesicle deformation and bilayer invaginations (Kuntsche *et al*., 2011). All liposome preparations containing increasing mol.% of PEGylation (0% to 5%) were similar with no obvious effects on liposomal morphology. It is important to note, however, that surface modifications of liposomal vesicles with PEG-chains are not visible in cryo-TEM images due to the low contrast of polyethylene glycol (Kuntsche *et al*., 2011). The PEGylated liposomes appeared as defined structures which are well separated. This implies that the PEG coating provided physical stability to the liposomes, thereby aiding in dispersing the particles and preventing close contact between the vesicles.

Figure 4.3 represents cryo-TEM images of pCMV-*luc*-associated liposomes. The combination of non-PEGylated cationic liposomes and DNA **[Figure 4.3, (A)** and **(D)]** appeared as predominantly large dense non-spherical multi-lamellar aggregates with a varying number of individual lipoplex per aggregate. These heterogeneous assemblies with a twisted reorganization revealed a particulate surface coating as well as small cavities in the interior of lipoplexes, which are absent in the corresponding liposome micrographs. These observations suggest that the DNA has in fact compacted on the surface of the liposomes via electrostatic interactions.

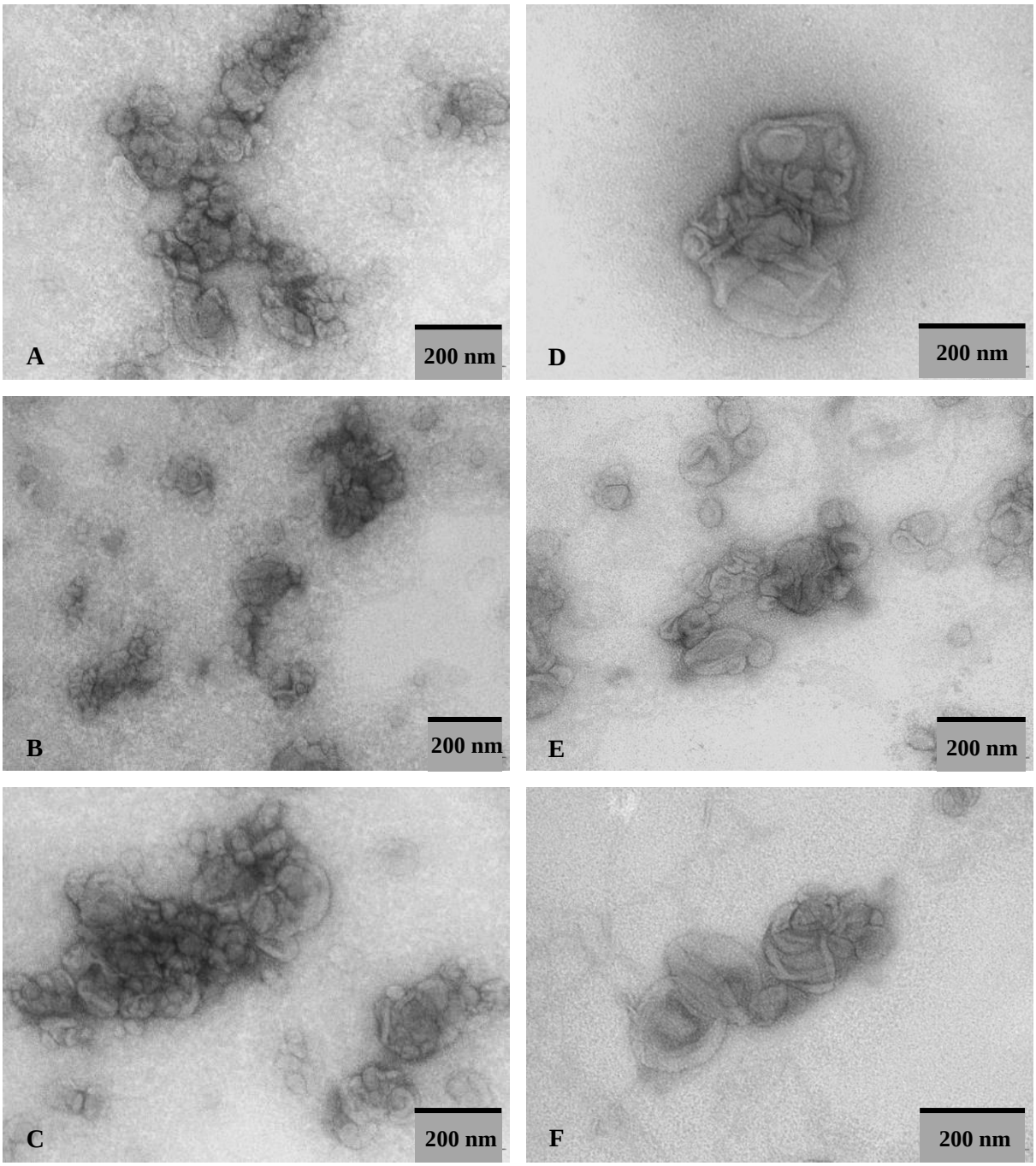

Figure 4.3: Transmission electron micrographs of cationic and PEGylated cationic pCMV-*luc* plasmid DNA complexes (lipid:pCMV-*luc* (+:–) charge ratios): **A**, Chol-T:DOPE (1.6:1); **B**, Chol-T:DOPE:2% PEG (1.7:1); **C**, Chol-T:DOPE:5% PEG (1.6:1); **D**, MS09:DOPE (1.7:1); **E**, MS09:DOPE:2% PEG (1.8:1); **F**, MS09:DOPE:5% PEG (1.7:1). Bar = 200 nm.

Moreover, these findings correlate with reports that have illustrated incongruent distribution of anionic DNA between bilayer membranes that tend to form concentric multi-layered structures or inverted hexagonal structures leading to the formation of small cavities on the surface of lipoplexes (Kapoor *et al*., 2012; Li *et al*., 2011). PEGylated pDNA lipoplexes appeared to have hazy indistinct edges and tended to aggregate to a lesser extent. This can be observed clearly in **Figure 4.3 (E)**; the micrograph depicts few solitary uni-lamellar structures located at the periphery of aggregative structures. As mentioned previously, PEGylation provides steric stabilization by generating hydrated surfaces which ultimately reduces the surface-surface interactions and the aggregation of liposome-DNA complexes (Rangelov *et al*., 2010).

As opposed to pDNA lipoplexes, both PEGylated and non-PEGylated siRNA-liposome complexes appeared as well defined spherical shaped structures with steady phase contrast **[Figure 4.4]**. The cryo-TEM images also revealed uni-lamellar complexes with distinct bilayered membranes. All lipoplexes appeared well dispersed and colloidally stable. The morphology of PEGylated liposome/siRNA complexes correlates with previous work in which PEGylated preformed liposomes formed small uni-lamellar vesicles with siRNA (Fenske and Cullis, 2008; Kim *et al*., 2010). However, micrographs obtained with the combination of siRNA and preformed non-PEGylated cationic liposomes differed from a previous report in which the siRNA self-assembled into multi-layered complexes (Desigaux *et al*., 2007; Weisman *et al*., 2004). Therefore, it can be assumed that the siRNA was bound via electrostatic interactions to the outer surface of the liposomes and not stacked between lipid bilayers.

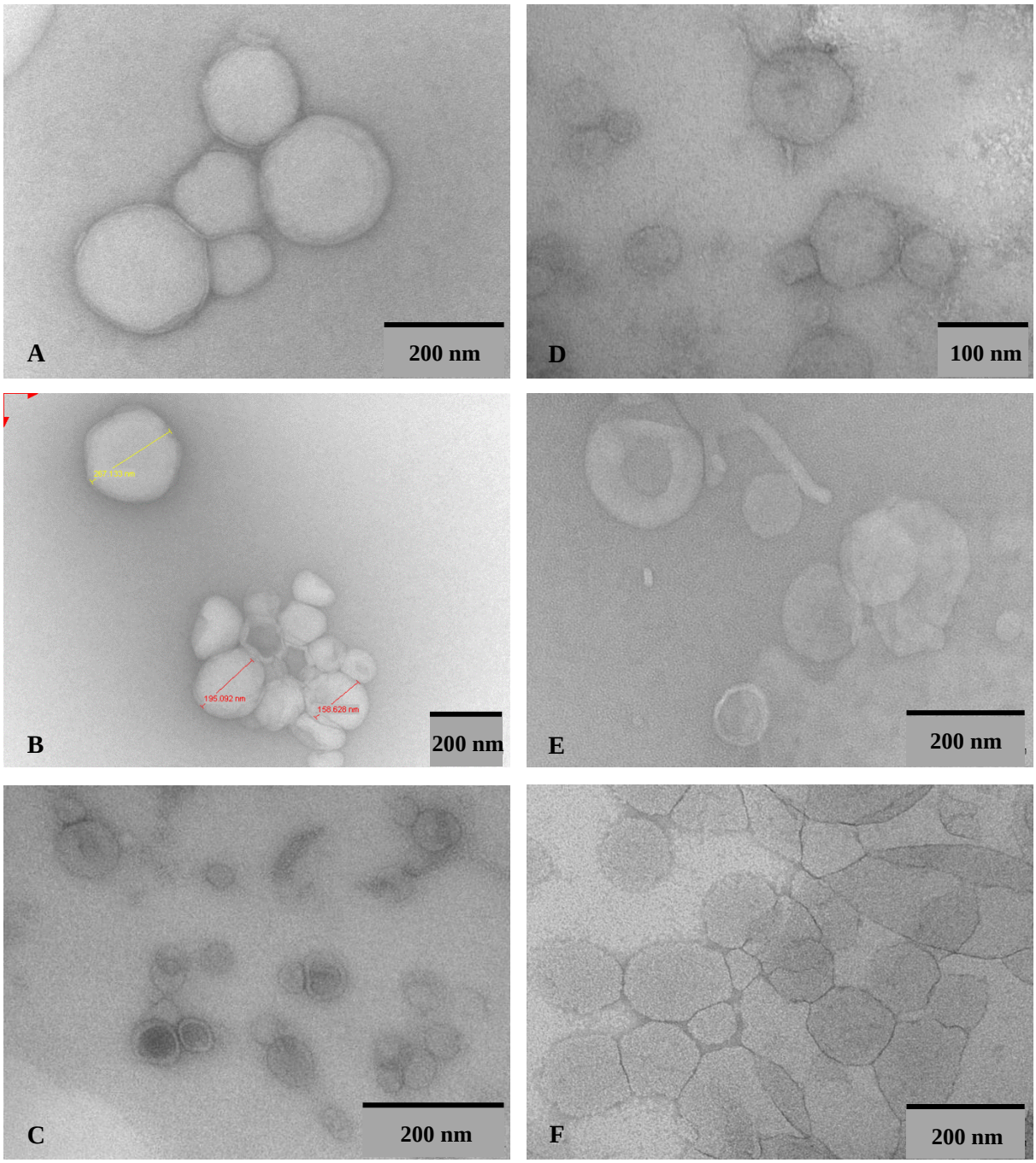

Figure 4.4: Transmission electron micrographs of cationic and PEGylated cationic liposome-siGENOME non-targeting siRNA complexes (lipid:siRNA (+:–) charge ratios): **A**, Chol-T:DOPE (3.9:1); **B**, Chol-T:DOPE:2% PEG (6.3:1); **C**, Chol-T:DOPE:5% PEG (8.8:1); **D**, MS09:DOPE (5.4:1); **E**, MS09:DOPE:2% PEG (6.0:1); **F**, MS09:DOPE:5% PEG (7.9:1). Bar = 100 nm or 200 nm.

4.2.2 Particle size distribution and zeta potential analysis

The route of circulation and navigation of any lipid-based nanoparticle being developed for *in vivo* application is almost exclusively determined by the particle size distribution, lipid component variation and the physicochemical surface properties. The size of the particle has a great influence on its intrinsic propensity for site- and cell-specific localization as well as cellular interaction and uptake. Moreover, optimal particle size (50 - 250 nm) is a prerequisite to bypass elimination and clearance by the RES (Lorenzer *et al*., 2015; Resnier *et al*., 2013).

Dynamic light scattering (*DLS*) using the Photon Correlation Spectroscopy (PCS) technique was used to determine three principal physical characteristics of liposomal formulations alone, and of their lipoplexes formed with pDNA or siRNA: hydrodynamic size of the particles (diameter); particle size distribution (polydispersity index, PDI); and zeta potential (overall charge exhibited by a particle in suspension). The principle of *DLS* is based on the measurement of the time-dependent intensity fluctuations of laser light scattered from particles experiencing Brownian motion. Brownian motion is defined as the random movement of particles in solution, which results from collisions between suspended particles and surrounding solvent molecules. The intensity fluctuation trace comprises a combination of constructive and destructive interferences of the scattered light at a given angle. The hydrodynamic diameter and size distribution can be derived from analysis of the motion-dependent autocorrelation function according to the Stokes-Einstein equation (Brar and Verma, 2011; Lin *et al*., 2014; Troiber *et al*., 2013). The zeta potential of the liposome/lipoplex was measured by the LDV technique, and the values were calculated from the mean electrophoretic mobility by applying the Smoluchowski approximation equation. The main strengths of *DLS* for physicochemical characterization, include its ability to make measurements in native environments in a non-invasive manner, precision in determining the hydrodynamic size of particles in an entire monodisperse suspension, analyzing samples in a wide range of concentrations as well as measuring diluted samples, with the added advantage of being more reproducible than other methods (Laouini *et al*., 2012; Lin *et al*., 2014).

Table 4.1 summarizes the mean particle size, polydispersity indices and zeta potential profiles of the liposomes and lipoplexes [prepared at optimal lipoplex (N/P) ratio (+:–)]. With regard to hydrodynamic diameters, *DLS* characterization of all liposome compositions and

lipoplexes revealed nanometer (nm) sized particles which were accompanied by moderate to narrow PDI (in brackets) as follows: 65.47 nm (0.269) to 127.07 nm (0.321) liposome samples; 114.55 nm (0.229) to 237.31 nm (0.149) pDNA lipoplex samples; and 103.24 nm (0.128) to 187.97 nm (0.127) siRNA lipoplex samples. These measurements indicate that the colloidal suspensions are fairly stable and homogeneous and are within the range generally considered ideal for both cellular uptake and systematic circulation (Kapoor *et al*., 2012; Mével *et al*., 2010). Prior to complex formation with pDNA or siRNA, both Chol-T and MS09 liposomes had a particle size below 130 nm. However, the sizes of the lipoplexes were much larger (up to 237.31 nm) than their corresponding liposomes. This might be due to the binding of the nucleic acid on the liposome surface which is in contrast with the entrapment of nucleic acid inside the liposomes. Of particular interest, the siRNA lipoplexes were smaller in size (except Chol-T 5% PEG) and had a lower PDI than the corresponding pDNA complexes. The largest lipoplexes were formed with non-PEGylated Chol-T liposomes at the following charge ratios: pDNA (1.6:1, +:–) and siRNA (3.9:1, +:–), with pDNA lipoplexes exhibiting greater hydrodynamic diameters than siRNA lipoplexes. This suggests that the formation of large lipoplexes occurred when the charge of the liposome was neutralized. Zhang *et al*. (2010) observed a similar trend with cationic complexes at various N/P ratios and reported larger lipoplexes at near neutral charge (low N/P ratio).

Confirmed size measurements also suggested a significant decrease in particle size and narrow size distributions of Chol-T and MS09 liposomes when PEGylation was introduced at 2%, and then increased to 5% in liposomal formulations. The primary role of PEG is to facilitate the self-assembly of lipid molecules, thereby stabilizing the liposome bilayers. The decrease in size may be attributed to the strong inter-bilayer repulsion that can overcome the attractive van der Waals forces, thus providing a steric barrier at the surface of nascent liposomes. PEG chains on the liposomal surface provide steric stabilization, which is known to prevent vesicle aggregation and encourage the formation of a homogeneous population of smaller liposomes with colloidal stability and biocompatibility (Kenworthy *et al*., 1995; Needham *et al*., 1992). Complex formation with pDNA or siRNA to form lipoplexes shifted the population toward larger vesicle sizes and wider size distributions compared to the non-PEGylated preparations. Once more, lipoplexes containing PEG afforded significantly smaller vesicles indicating the stabilization effect offered by PEG. Many formulation optimization studies have demonstrated

that the capacity of PEGylated liposomes to prevent inter-particle aggregation depends largely on the degree of surface coverage and the distance between graft sites. This, in turn, hinges on the molecular mass and concentration of the polymer, as well as the graft density (de Gennes, 1980; 1987; Dos Santos *et al*., 2007; Immordino *et al*., 2006).

Interestingly, with both Chol-T and MS09 siRNA lipoplexes PEGylation at 2 mol.% formed complexes which were stable (PDI ~0.2) and slightly smaller in diameter than lipoplexes containing a 5 mol.% of DSPE-PEG_{2000}. As described in **Section 2.11.1**, when tethered on the surface of liposomes, PEG chains display various conformations depending on the PEG chain density. It has been documented that the PEG_{2000} chain extends ~5.6 nm from the surface of a liposome, and at polymer concentrations below 4 mol.% intermediate random coil-like "mushroom" structures are favoured that, span a distance of ~3.5 nm (Garbuzenko *et al*., 2005; Gjetting *et al*., 2010; Wang and Thanou, 2010). Increasing the concentration (> 5 mol.%) of PEG, results in larger surface coverage and an increase in the lateral pressure between PEG mushrooms; favouring low-coiled "brush" conformations (lengthening between 10 nm to 15 nm) (Garbuzenko *et al*., 2005, Perrier *et al*., 2010; Yao *et al*., 2013). Hence, the influence of grafted PEG polymers on the hydrodynamic size of a liposome particle is mainly due to changes in the spatial organization of the PEG, which is reliant on the type of configuration favoured, i.e., "mushroom" or "brush" (Chen *et al*., 2011). In the case of Chol-T pDNA lipoplexes, those formulated with 2 mol.% PEG formed larger complexes. This is probably due to the "mushroom-structured" PEG arrangement, which does not shield the cationic liposome as effectively as the 5% "brush" configuration, leading to some aggregation of complexes.

The measurement of zeta potential (ζ) is generally used to predict the long-term stability of colloidal systems and provides a very good index of the interaction magnitude between charged particles (Honary and Zahir, 2013; Wiese and Healy, 1970). In a colloidal suspension, the liquid layer surrounding the charged particle consists of two regions: an inner thin liquid layer termed the Stern layer, where the ions are strongly bound to the surface of the particle; and an outer diffuse layer containing loosely associated ions (Clogston and Patri, 2011). In the interior of the diffuse layer there is a notional margin in which the ions form a stable shear plane. When particles experience tangential motion (e.g., Brownian motion), the movement of charged particle shears ions migrating with the charged particles in the diffuse layer, and ions beyond the "margin" stay with the bulk dispersant. The electrokinetic potential on the shear plane (surface of

hydrodynamic shear) is the zeta potential, which is usually determined by measuring the velocity of the charged particle towards the electrode using methods such as the LDV electrophoresis technique (Lin *et al*., 2014; Sapsford *et al*., 2011).

Table 4.1: ZetaSizer measurements of the various cationic/PEGylated cationic liposomes and corresponding DNA/siRNA lipoplexes

Cationic liposome	Liposome		DNA lipoplex		siRNA lipoplex	
	Size (nm), (PDI)	**ζ Potential (mV) ± SD**	**Size[a] (nm), (PDI)**	**ζ Potential (mV) ± SD**	**Size[a] (nm), (PDI)**	**ζ Potential (mV) ± SD**
Chol-T	127.07 (0.321)	44.09 ± 10.56	237.31 (0.149)	49.15 ± 1.539	187.97 (0.127)	47.26 ± 5.39
Chol-T 2% PEG	71.64 (0.304)	32.51 ± 11.02	162.11 (0.358)	38.60 ± 6.212	149.61 (0.227)	39.05 ± 8.16
Chol-T 5% PEG	74.18 (0.136)	–1.12 ± 4.818	120.22 (0.113)	19.03 ± 10.94	153.24 (0.109)	9.78 ± 1.13
MS09	113.02 (0.348)	53.21 ± 4.329	206.08 (0.411)	35.22 ± 13.62	169.13 (0.326)	44.61 ± 7.56
MS09 2% PEG	66.68 (0.136)	39.43 ± 1.185	114.55 (0.229)	27.46 ± 5.093	103.24 (0.218)	20.88 ± 3.052
MS09 5% PEG	65.47 (0.269)	16.08 ± 3.799	156.19 (0.475)	40.84 ± 2.816	138.64 (0.337)	41.26 ± 9.79

Abbreviations: Chol-T: 3β-[*N*-(*N′*, *N′*-dimethylaminopropane)-carbamoyl] cholesterol; **MS09:** *N*, *N*-dimethylaminopropylaminylsuccinylcholesterylformylhydrazide; **PEG:** Polyethylene glycol; **DNA:** Deoxyribonucleic acid; **siRNA:** Small interfering RNA; **PDI:** Polydispersity index; **SD:** Standard deviation.
Note: Values are represented as mean, $n = 3$

The zeta potential of the cationic liposomes was also measured, and formed part of the pharmacokinetic prolife. As indicated in **Table 4.1,** the zeta potential of the cationic liposomes was highly positive, Chol-T 44.09 ± 10.56 mV and MS09 53.21 ± 4.329 mV. There seemed to be no obvious effects or differences elicited by the specific CCCs on the zeta potential between liposomes or lipoplexes formulated with Chol-T and MS09. A zeta potential value of ± 30 mV is generally a prognostic of satisfactory particle stability, with sufficient barrier to prevent aggregation and flocculation (Laouini *et al*., 2012). Interestingly, the zeta potential of the cationic liposomes gradually decreased with increasing content of the negatively charged PEG lipid. A decrease of 11.58 mV (Chol-T) and 13.78 mV (MS09) was observed upon 2% PEGylation, and a further decrease of 33.63 mV (Chol-T) and 23.35 mV (MS09) was recorded

when PEGylated with 5% PEG. Upon complexation with anionic charged nucleic acids, the zeta potential of the lipoplexes maintained a relatively high positive charge ranging from 19.03 ± 10.94 to 49.15 ± 1.539 (pDNA lipoplexes) and 9.78 ± 1.13 to 47.26 ± 5.39 (siRNA lipoplexes). There was no significant difference in zeta potential between each liposome and its corresponding lipoplex. With regard to cationic lipid based delivery systems, *in vivo* results have suggested that high levels of positive charge on the surface favour interaction with negatively charged plasmatic proteins forming aggregates which are recognized by the innate immune system (Resnier *et al*., 2013). PEG has been incorporated into liposomal surfaces to create artificially a negative hydrophilic and flexible shroud to mask the positive charges of the cationic head groups. Moreover, PEG is able to form dipole interactions with water which alters the zeta potential of lipid carriers (Vonarbourg *et al*., 2005). As observed, the change in zeta potential of the cationic liposomes containing PEG lipids confirms the presence of the polymer layer on the liposomal surface.

It is also important for the carrier system to maintain some degree of positive charge to enable interaction with the anionic nucleic acid. The zeta potential of the liposomes containing 2% PEG still remained highly positive (above 30 mV), indicating that the tethering of PEG on the liposomal surface offers good stability and also provides a suitable milieu for nucleic acid attachment. Sonoke *et al*. (2008) developed PEGylated cationic liposomes bearing highly positive charges which allowed prolonged *in vivo* circulation and protection of siRNA. They attributed the efficient delivery of siRNA to the effectual steric repulsion due to the high flexibility and hydrophilicity of PEG.

4.3 Lipoplex Binding Affinity and Protection Efficiencies

4.3.1 Electrophoretic mobility shift assay

The pDNA or siRNA condensation induced by a nanocarrier system is a prerequisite for successful gene transfection. The capacity to condense nucleic acids and form lipoplexes with a minimum amount of cationic liposome was assessed by the conventional gel electrophoretic mobility technique, across a range of N/P (+:–) charge ratios. When a constant amount of the anionic nucleic acid is efficiently bound to the cationic liposomal carrier, the formation of a

complex reduces the electrophoretic mobility of the nucleic acid through the gel matrix. During the run, the electric field enables unbound nucleic acid to migrate towards the cathode; whereas nucleic acids that have been completely incorporated into the structure of cationic liposomes result in an increase in the size and neutralization of their negative charge within the complexes, and are therefore unable to migrate into the gel matrix (lipoplexes remain within the wells). In order to optimize the charge ratio for transfection, positively charged liposomes were mixed with negatively charged pCMV-*luc* plasmid DNA or siRNA to form lipoplexes via electrostatic interaction at various lipid:pDNA/siRNA ($^{w}/_{w}$) or N/P (+:–) ratios. The agarose gel migration patterns illustrated that all liposomal formulations were effective in binding both pDNA and siRNA, as evidenced by the retardation of the electrophoretic mobility of nucleic acids. **Figure 4.5** (pCMV-*luc*) and **4.6** (siRNA) show the nucleic acid complexation profiles of the various cationic liposomal preparations.

The pDNA control lane containing 1 µg of uncomplexed pCMV-*luc* DNA produced three distinctive conformations: nicked circular (least migration from well), linearized and supercoiled helical (migrates the furthest). The siRNA control lane containing 0.32 µg of naked siRNA, on the other hand, appeared as a single band. The lipid:pDNA/siRNA or N/P (+:–) charge ratios at which the cationic liposomes were able to fully retard nucleic acid mobility are summarized in **Table 4.2.** As can be seen in **Figure 4.5**, between N/P ratios of 6:1 and 8:1 (+:–), the anionic pDNA was entirely neutralized by the gradual increase in cationic liposome, resulting in complete DNA condensation. At these N/P ratios, lipoplexes were retained in the wells and no further migration of the pDNA was observed. This is known as the point of electroneutrality and commonly referred to as the end-point. The migration pattern of siRNA **[Figure 4.6]** changed at a charge ratio (+:–) of 3.9:1 (Chol-T) and 5.4:1 (MS09). Below these ratios, the band fluoresced brightly and then gradually lightened until the band completely disappeared, signifying that the negatively charged siRNA was neutralized entirely at the respective N/P charge ratios. Beyond these charge ratios, no migration of siRNA was detected for non-PEGylated lipoplexes. Interestingly, all lipoplexes were capable of retarding the same amount of pDNA (1 µg) and siRNA (0.32 µg) at various N/P ratios despite the concentration of the cationic cytofectin (Chol-T or MS09) remaining constant (2 mM) in all liposome formulations.

Table 4.2: Gel retardation endpoints and charge ratios of the various cationic/ PEGylated cationic liposomes

Cationic liposome	Cationic liposome : nucleic acid endpoint ($^{w}/_{w}$)		Charge ratio [N/P (+:–)]	
	DNA	**siRNA**	**DNA**	**siRNA**
Chol-T	6 : 1	14 : 1	1.6 : 1	3.9 : 1
Chol-T 2% PEG	7 : 1	24 : 1	1.7 : 1	6.3 : 1
Chol-T 5% PEG	7 : 1	37 : 1	1.6 : 1	8.8 : 1
MS09	7 : 1	21 : 1	1.7 : 1	5.4 : 1
MS09 2% PEG	8 : 1	25 : 1	1.8 : 1	6.0 : 1
MS09 5% PEG	8 : 1	36 : 1	1.7 : 1	7.9 : 1

Abbreviations: Chol-T: 3β-[*N*-(*N'*, *N'*-dimethylaminopropane)-carbamoyl] cholesterol; **MS09:** *N*, *N*-dimethylaminopropylaminylsuccinylcholesterylformylhydrazide; **PEG:** Polyethylene glycol; **DNA:** Deoxyribonucleic acid; **siRNA:** Small interfering RNA.
The theoretical N/P (+:–) ratio represents the charge ratio of cationic lipid to nucleotide. Values were calculated assuming one positive charge per cytofectin molecule at pH 7.5 and one negative charge per nucleotide (average mass 330 Da).

The inference, therefore, is that the differences in binding affinities among the various lipoplex suspensions were most likely due to the incorporation of PEG polymers. As described previously in **Section 4.2.2** the reduced zeta potential values indicate that PEGylation reduced the surface charge of liposomes. The partial masking of the positive charges by PEGylation thus resulted in a reduction of cationic charge available for nucleic acid binding. This phenomenon can be observed clearly with the siRNA lipoplexes that had a far higher N/P charge ratio [from 6.3:1 to 8.8:1 (Chol-T) and 6.0:1 to 7.9:1 (MS09); 2% to 5% PEG, respectively]. Ultimately, greater amounts of the PEGylated liposomes were required to fully bind siRNA compared to the non-PEGylated liposomes, demonstrating a relatively weaker affinity toward the siRNA. Interestingly, MS09 cationic liposomes containing 5% PEG were able to gradually retard siRNA migration to a certain extent although no complete end-point was established.

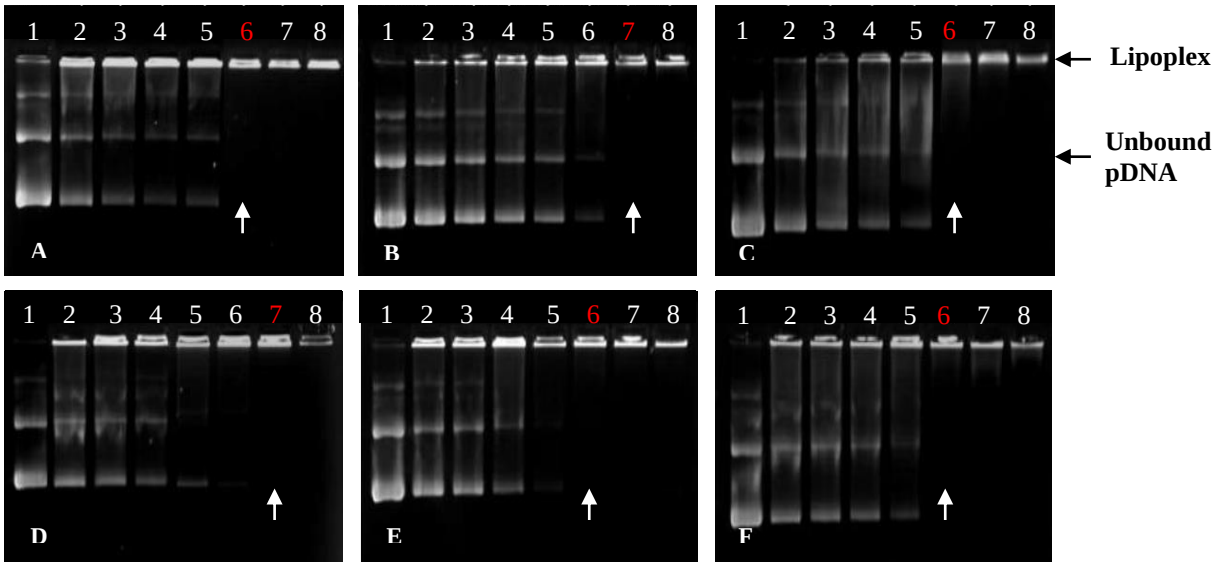

Figure 4.5: Gel retardation analysis of binding interaction between varying amounts of cationic and PEGylated cationic liposome preparations with pCMV-*luc* plasmid DNA (1 µg) in HBS. **A,** lanes 1-8 (0, 2, 3, 4, 5, 6, 7, and 8 µg Chol-T); **B**, lanes 1-8 (0, 3, 3.5, 4, 5, 6, 7, and 8 µg Chol-T 2% PEG); **C,** lanes 1-8 (0, 3, 4, 5, 6, 7, 8, and 9 µg Chol-T 5% PEG); **D,** lanes 1-8 (0, 2, 3, 4, 5, 6, 7, and 8 µg MS09); **E,** lanes 1-8 (0, 4, 5, 6, 7, 8, 9, and 10 µg MS09 2% PEG); **F,** lanes 1-8 (0, 4, 5, 6, 7, 8, 9, and 10 µg MS09 5% PEG). (➔) indicates end point ratios or point of electroneutrality.

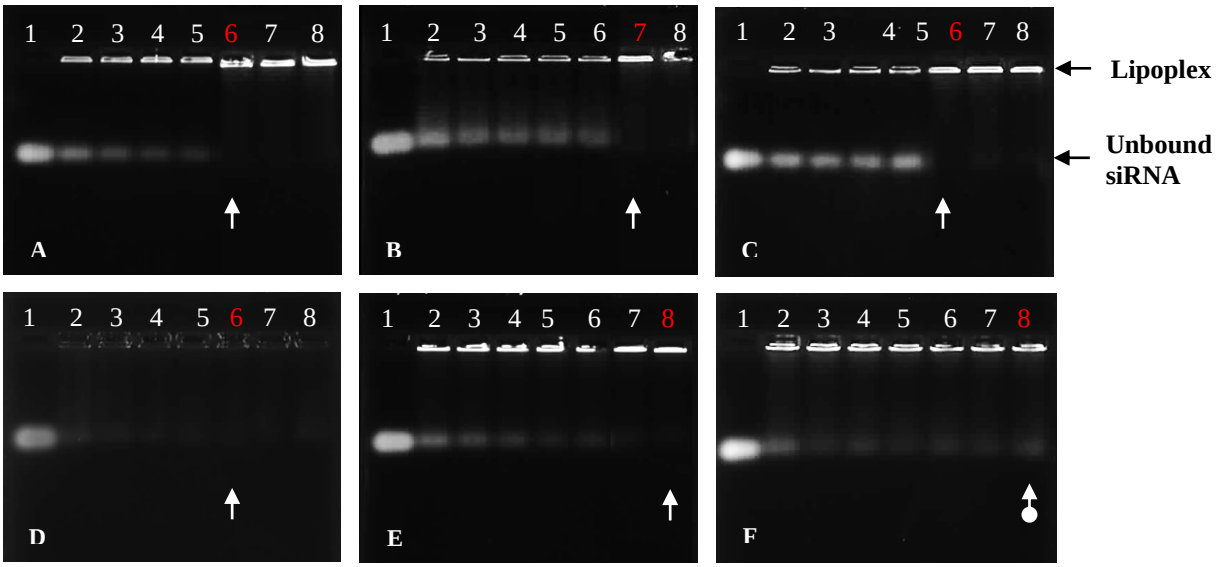

Figure 4.6: Gel retardation analysis of binding interaction between varying amounts of cationic and PEGylated cationic liposome preparations with siRNA (0.32 µg) in HBS. **A,** lanes 1-8 (0, 3.20, 3.52, 3.84, 4.16, 4.48, 4.80, and 5.12 µg Chol-T); **B**, lanes 1-8 (0, 6.08, 6.40, 6.72, 7.04, 7.36, 7.68, and 8.00 µg Chol-T 2% PEG); **C,** lanes 1-8 (0, 10.56, 10.88, 11.20, 11.52, 11.84, 12.16, and 12.48 µg Chol-T 5% PEG); **D,** lanes 1-8 (0, 5.44, 5.76, 6.08, 6.40, 6.72, 7.04, and 7.36 µg MS09); **E,** lanes 1-8 (0, 6.08, 6.40, 6.72, 7.04, 7.36, 7.68, and 8.00 µg MS09 2% PEG); **F,** lanes 1-8 (0, 9.60, 9.92, 10.24, 10.56, 10.88, 11.20, and 11.52 µg MS09 5% PEG). (➔) indicates end point ratios or point of electroneutrality. (●➔) indicates no clear end point.

It has been suggested that mixing preformed cationic liposomes with a siRNA solution to form lipoplexes negatively impacts cationic liposomes containing higher PEG densities on their surfaces. The likely explanation is that high PEG densities form 'brush borders' on the surface of liposomes. This structural feature of highly PEGylated liposomes prevents the formation of siRNA sandwiching lipid multilayers since the siRNA becomes loosely bound to the outer surface of such PEGylated liposomes (Buyens *et al*., 2009; 2012; Desigaux *et al*., 2007).

4.3.2 Nuclease protection assay

Following systemic administration, the protection of nucleic acids (DNA or siRNA) against enzymes in circulation, is crucial to maintain the integrity of the genetic material, so that their effects can be met at the transcriptional and/or translational level. Upon *in vivo* administration, lipoplexes are immediately surrounded by high concentrations of free charged serum components that interact with the particles (Caracciolo, 2015; Kawakami and Hashida, 2007; Tranchant *et al*., 2004). Such interactions are driven either by a potential energy gradient or by diffusion, resulting in a variety of dynamic changes (Lynch and Dawson, 2008; Rocks and Dawson, 2014; Walkey and Chan, 2012). The serum proteins interacting with the complexes establish a protein rich environment around the surface of each particle, termed the protein-corona (refer to **Section 2.11.1**). A number of studies have detailed the various ways in which serum components affect nucleic acid containing nanocarriers. The protein corona can lead to changes in size through aggregation, zeta potential due to surface charge neutralization, and other related surface characteristics which destabilize the lipoplex structure (Li *et al*., 1999; Lundqvist *et al*., 2008; Scholz and Wagner, 2012; Zelphati *et al*., 1998). Furthermore, the presence of charged serum components may induce dissociation of the lipoplexes, leading to irregularities in the lipid bilayers or to vesicle disruption. This in turn exposes the nucleic acid to intrinsic enzymatic degradation or rapid opsonization (Audouy *et al*., 2000; Buyens *et al*., 2008). Despite their importance, studies on *in vitro* transfection behaviour in the presence of biological fluids (serum, for example) are limited, resulting in inconclusive extrapolations and poor correlations between *in vitro* and *in vivo* transfection efficiencies.

Therefore, assessing the ability of a liposomal carrier system to protect its nucleic acid consignment is of paramount importance, since any factor which increases its circulation time is

critical for high transfection efficiencies. To examine the protective capabilities of the formulated cationic liposomes against serum nucleases *in vitro*, the lipoplexes were incubated in FBS (10%, $^{v}/_{v}$) at physiological temperature for 4 h and subjected to an electrophoretic analysis. FBS is a heterogeneous fluid prepared from blood plasma in which the blood cells and fibrinogens have been extracted. It contains various biological macromolecules: albumin, immunoglobulins, apolipoproteins, glycoproteins, lipases, nucleases, fibronectin as well as small molecules such as amino acids, vitamins and inorganic salts. In particular, albumin (the most abundant protein) has been reported to destabilize both charged and neutral liposomes (Chonn *et al*., 1992). In general, siRNA is more sensitive to nucleolytic degradation owing to the 2' OH group of ribose, whereas DNA is less prone to alkaline hydrolysis (Kapoor *et al*., 2012). Naked siRNAs exposed to plasmatic enzymes having a dsRNA binding domain were completely degraded within 30 min into the bloodstream (White, 2008). As mentioned previously, despite the fact that liposomes offer protection to their gene cargo, disruption of the lipoplex structure will trigger release of the bound nucleic acid and subsequent degradation. Therefore, liposomes have to not only safeguard their gene cargo from serum, but also to form a strong enough interaction with the nucleic acids to enable delivery in a serum-resistant manner.

Results from nuclease protection assays are presented in **Figure 4.7** (pCMV-*luc* plasmid DNA) and **Figure 4.8** (siRNA). In these studies two controls were included, viz., control 1 = untreated naked pCMV-*luc*; untreated naked siRNA (**Figure 4.7** and **4.8 A, B, C;** lane 1) and control 2 = naked pCMV-*luc* treated with 10% FBS; naked siRNA treated with 10% FBS (**Figure 4.7** and **4.8 A, B, C;** lane 2]. These were assigned positive and negative controls respectively and were used to assess the degree of serum nuclease digestion of both treated and untreated nucleic acids compared to those in association with cationic liposomes. From the gel patterns, untreated naked pDNA preparation produced three species of DNA in the plasmid, viz. low mobility nicked circular form, linearized form and high mobility compact supercoiled helical form. The untreated naked double stranded siRNA appeared as a single band. Based on EtBr staining intensity, all undigested controls reveal relative quantities of each species.

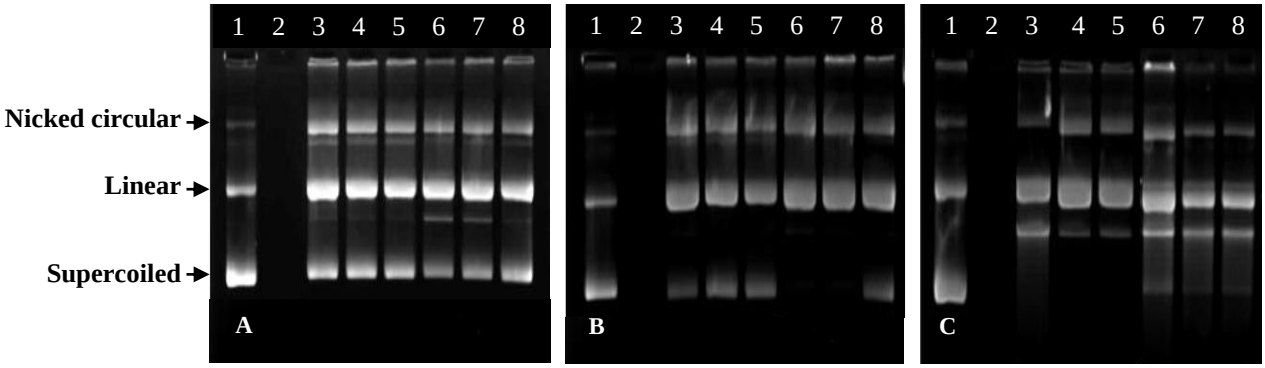

Figure 4.7: Nuclease protection assay of cationic and PEGylated cationic liposome-pDNA complexes in the presence of 10% FBS. Reaction mixtures (10 µL) contained pCMV-*luc* (1 µg) and varying amounts of liposome suspension. **A,** lanes 3-5 (5, 6, 7 µg Chol-T): lanes 6-8 (6, 7, 8 µg MS09); **B,** lanes 3-5 (6, 7, 8 µg Chol-T 2% PEG): lanes 6-8 (6, 7, 8 µg Chol-T 5% PEG); **C,** lanes 3-5 (7, 8, 9 µg MS09 2% PEG): lanes 6-8 (7, 8, 9 µg MS09 5% PEG). In **A-C**, lane 1: FBS-untreated naked pCMV-*luc* plasmid DNA (1 µg) (control 1) and lane 2: FBS-treated pCMV-*luc* plasmid DNA (1 µg) (control 2).

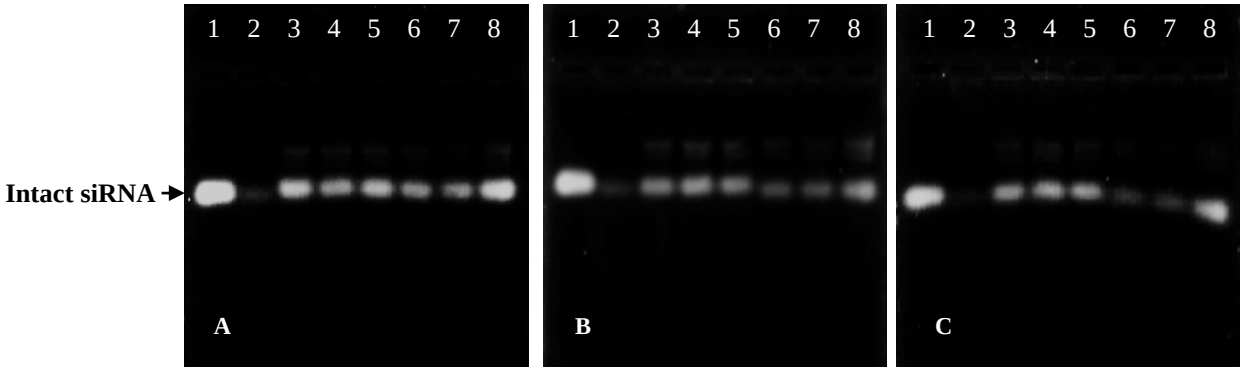

Figure 4.8: Nuclease protection assay of cationic and PEGylated cationic liposome-siRNA complexes in the presence of 10% FBS. Reaction mixtures (10 µL) contained siRNA (0.2 µg) and varying amounts of liposome suspension. **A,** lanes 3-5 (2.4, 2.8, 3.2 µg Chol-T): lanes 6-8 (3.8, 4.2, 4.6 µg MS09); **B,** lanes 3-5 (4.4, 4.8, 5.2 µg Chol-T 2% PEG): lanes 6-8 (7.0, 7.4, 7.8 µg Chol-T 5% PEG); **C,** lanes 3-5 (4.6, 5.0, 5.4 µg MS09 2% PEG): lanes 6-8 (6.8, 7.2, 7.6 µg MS09 5% PEG). In **A-C**, lane 1: FBS-untreated naked siRNA (0.2 µg) (control 1) and lane 2: FBS-treated siRNA (0.2 µg) (control 2).

With regard to pCMV-*luc* plasmid DNA, there was an increase in band intensities form each well, indicating that the pDNA existed mainly in the supercoiled helical form, followed by linearized, and then nicked circular. On the other hand, the naked FBS-treated (pDNA and siRNA) controls were completely digested within 4 h following exposure to serum enzymes. Compared to the fully digested controls, the pDNA associated with cationic liposomes remained relatively intact in the presence of FBS for all lipid:pDNA mass ratios ($^{w}/_{w}$) tested, indicating that the various liposomal formulations were able to sustain the integrity of the bound nucleic acids and offered some degree of protection to the relatively intact nucleic acid structure.

A number of studies have reported the benefits of incorporating cholesterol and cholesterol-containing derivatives into nanocarrier systems (Ma *et al*., 2005b; Miyawaki-Shimizu *et al*., 2006; Morrissey *et al*., 2005, Zimmermann *et al*., 2006). The inclusion of cholesterol and its derivatives into liposomal formulations increases the packaging densities of the phospholipid molecules, thus forming solid-ordered membranes and thereby reducing the penetration behaviour of solutes and ions (Arouri and Mouritsen, 2013; Mady, 2004; Pozzi *et al*., 2012). Owing to the tight lipid arrangement facilitated by cholesterol, these membranes appear thicker and mechanically more stable. This maintained the liposomal integrity, by counteracting the disruptive effect of high density lipoproteins present in serum (Kraske and Mountcastle, 2001; Mayer *et al*., 2000). However, findings related to pDNA confirm that the DNA underwent partial nicking, as evidenced by the relatively greater proportion of relaxed DNA and an accompanying decline of the supercoiled helical conformation compared to the undigested pDNA control. This has been a controversial issue; it has been shown that digestion of the supercoiled content by nucleases present in serum leads to decreased transfection efficiency (Kawabata *et al*., 1995). In contrast, it has also been reported that relative amounts of supercoiling in reporter plasmids do not significantly affect *in vitro* and *in vivo* gene transfection. Further, the relaxed, covalently closed forms of the plasmid are not less efficient than supercoiled forms in gene delivery (Bergan *et al.,* 2000). In essence this study's assessment of pDNA serum stability confirmed that the cationic liposomes were able to offer substantial protection in a nuclease rich environment.

With regard to siRNA protection from serum nucleases, both non-PEGylated Chol-T and MS09 offered better protection to their siRNA cargo compared to their PEGylated counterparts [clear bands present in each lane, **[Figure 4.8 (A)]**. Han *et al*. (2008) reported an increase in

delivery efficiency of siRNA in serum with cationic liposomes containing an amine-based cholesterol derivative compared to cationic liposomes containing ordinary cholesterol in their structure. Hence, the cholesterol derivatives employed in this study helped preserve liposomal stability in the presence of FBS. Liposomal formulations containing 5% PEGylation offered the least protection as evidenced by lighter bands. However, the bands appeared brighter at the supraoptimal cationic liposome:siRNA ($^{w}/_{w}$) ratios compared to the optimal and suboptimal concentrations for both Chol-T and MS09. ZetaSizer measurements of non-PEGylated liposomes showed that they formed stable lipoplexes with zeta potentials of 47.26 mV (Chol-T) and 44.61 mV (MS09) corresponding to proficient serum protection abilities. With regard to liposomes tethered with 5% PEG, there were variations in zeta potentials; Chol-T 5% PEG (9.78 mV ± 1.13) and MS09 5% PEG (41.26 ± 9.79). The low zeta potential indicates liposomal instability and, therefore, reduced siRNA protection from nucleases. On the other hand, although MS09 5% PEG attained a more positive zeta potential, the PDI (0.337) was higher, suggesting that these lipoplexes do experience a certain degree of instability. Silvander *et al*. (1998) observed a similar trend with liposomes containing 5 mol.% PEG, where the sterically stabilized liposomes did not offer substantial stabilization against serum proteins.

4.3.3 Ethidium bromide (EtBr) fluorescence quenching assay

The EtBr fluorescence quenching assay further quantitatively investigated the electrostatic interactions between the cationic liposomes and nucleic acids (pDNA and siRNA). It also corroborated end-point ratios derived from the gel retardation assay. Intercalation of the classical planar molecule EtBr (an aromatic cationic fluorophore) between nucleic acid base pairs has been explored using various techniques over the past 5 decades (LePecq and Paoletti, 1967, Pohl *et al*., 1972; Celedon *et al*., 2010). Binding of EtBr between contiguous base pairs on the double helix structure results in more intense fluorescence and a ~10-fold higher emission intensity than when in water or buffer (Lakowicz, 1999). The high fluorescence emitted from EtBr intercalation into double stranded nucleic acids is primarily due to the hydrophobic milieu found between the base pairs. By moving into this hydrophobic environment, away from the bulk hydrophilic solvent, the EtBr cation dispels any water molecules that were associated with it. As water is a particularly efficient fluorescent quencher, elimination of these water molecules allows

EtBr to fluoresce. The binding of Et cation results in a decrease in the helical twist (~26 °) causing the distance between bases flanking an EtBr molecule to increase, thus creating an opening of ~0.34 nm (Hayashi and Harada, 2007; Tsai *et al.*, 1975; Wang, 1974). Therefore, the unwinding of the helical twist induces local and structural changes, such as elongation or lengthening of the ds-DNA strand as illustrated in **Figure 4.9** (Bugs and Cornelio, 2001; Nafisi *et al*., 2007; Palchaudhuri and Hergenrother, 2007).

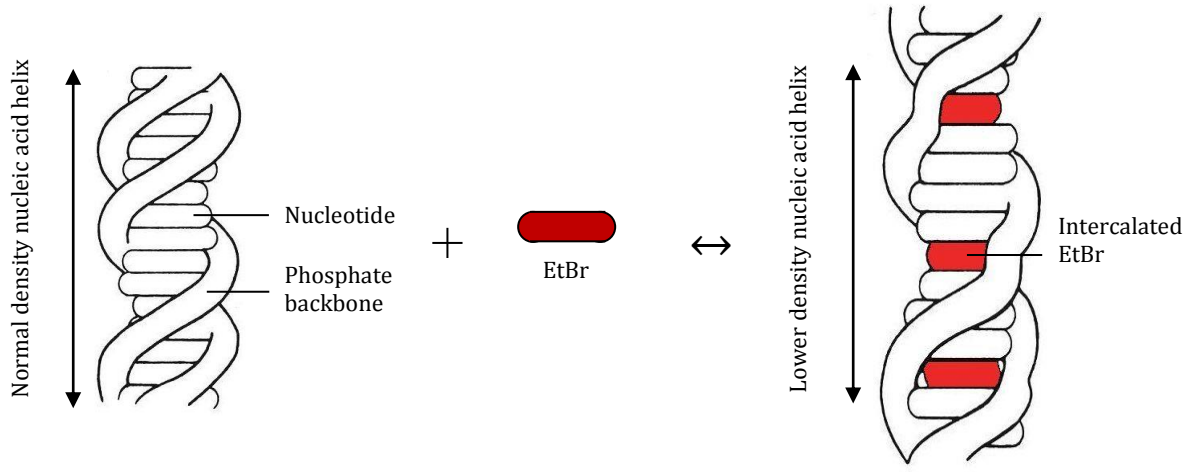

Figure 4.9: Schematic representation of preferred intercalation between EtBr and the nucleic acid helix which illustrates the lengthening and untwisting of the helical structure (Bugs and Cornelio, 2001; Nafisi *et al*., 2007; Palchaudhuri and Hergenrother, 2007).

According to the assay principle, the fluorescence emission intensity of EtBr is greatly enhanced upon intercalative complexation between nucleic acid base pairs. This heightened fluorescence can be quenched, or partly assuaged when displaced upon titration with compounds having a higher affinity for nucleic acid binding (Huang *et al*., 2012). As such, quantification of the cationic liposome-induced compaction of pDNA and siRNA was assessed by determining the relative fluorescence of EtBr intercalation (excitation λ = 520 nm, emission λ = 600 nm) in the double helix when cationic liposomes were added. **Figure 4.10** represents the EtBr fluorescence quenching assay where percentage relative fluorescence (F_r) with pDNA **(A)** and siRNA **(B)** was plotted as a function of the number of micrograms of cationic liposome Chol-T and MS09. Sequential addition of cationic liposomes to EtBr pretreated with pDNA or siRNA caused appreciable diminution of EtBr fluorescence, indicating that the EtBr was displaced by the liposomes. As the lipid:pDNA/siRNA ($^{w}/_{w}$) ratio increased, a decline in fluorescence was recorded until a point of inflection was reached (i.e. maximum nucleic acid compaction and EtBr

displacement by the cationic liposome). The ($^{w}/_{w}$) or N/P (+:–) ratios at which the liposome maximally displaced the EtBr and compacted the respective nucleic acid are presented in **Table 4.3.** All liposomal formulations containing Chol-T or MS09 were able to successfully displace the intercalated EtBr cation and bind the nucleic acid to varying degrees, indicating good compaction abilities. The maximum percentage fluorescence quenching for pDNA was between 42% - 58% (Chol-T based liposomes) and 42% - 68% (MS09 based liposomes), whereas for siRNA fluorescence decay ranged from 29% - 72% (Chol-T based liposomes) and 35% - 49% (MS09 based liposomes). Interestingly, for both pDNA and siRNA, high amounts of EtBr were displaced with the sequential addition of Chol-T (58% and 72% respectively) and MS09 2% PEG (68% and 49% repectively).

Table 4.3: EtBr fluorescence quenching by the various cationic/ PEGylated cationic liposomes recorded at points of inflection

Cationic liposome	Cationic liposome : nucleic acid ($^{w}/_{w}$)		Charge ratio [N/P (+:–)]	
	DNA	siRNA	DNA	siRNA
Chol-T	11 : 1	14.9 : 1	2.9 : 1	4.2 : 1
Chol-T 2% PEG	16 : 1	26 : 1	3.9 : 1	6.8 : 1
Chol-T 5% PEG	15 : 1	38.6 : 1	3.4 : 1	9.2 : 1
MS09	13 : 1	16.3 : 1	3.0 : 1	4.2 : 1
MS09 2% PEG	13 : 1	21.9 : 1	2.9 : 1	5.3 : 1
MS09 5% PEG	13 : 1	43.6 : 1	2.7 : 1	9.6 : 1

Abbreviations: Chol-T: 3β-[*N*-(*N′*, *N′*-dimethylaminopropane)-carbamoyl] cholesterol; **MS09:** *N*, *N*-dimethylaminopropylaminylsuccinylcholesterylformylhydrazide; **PEG:** Polyethylene glycol; **DNA:** Deoxyribonucleic acid; **siRNA:** Small interfering RNA; **EtBr:** Ethidium bromide.
The theoretical N/P (+:–) ratio represents the charge ratio of cationic lipid to nucleotide. Values were calculated assuming one positive charge per cytofectin molecule at pH 7.5 and one negative charge per nucleotide (average mass 330 Da).

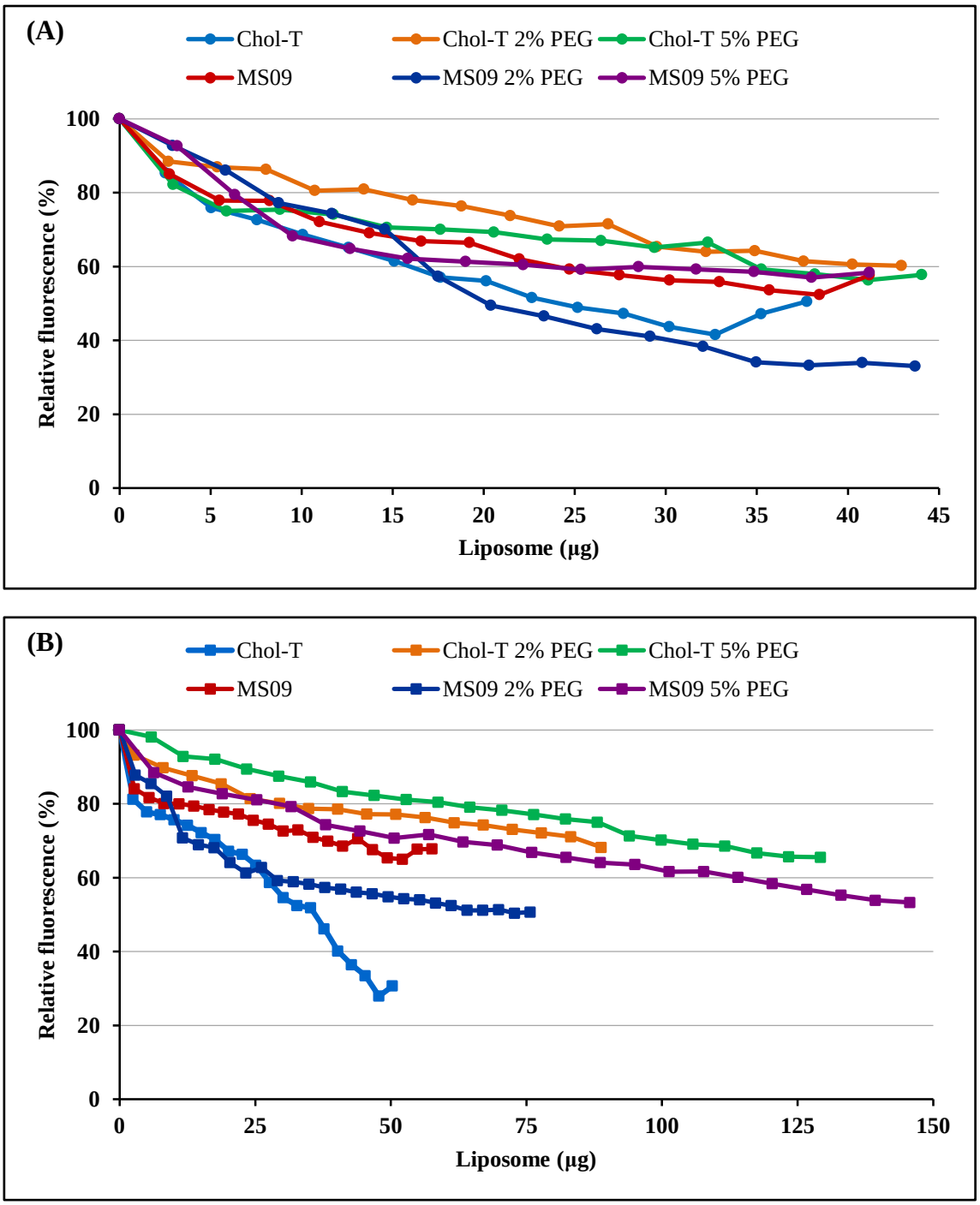

Figure 4.10: Ethidium bromide fluorescence quenching assay of the cationic and PEGylated cationic liposomes in a total of 0.25 mL incubation mixtures containing **(A)** 3 µg pCMV-*luc* plasmid DNA, **(B)** 3.2 µg siRNA and increasing amounts of liposome.

4.4 *In Vitro* Cell Culture

4.4.1 Cell lines

The SKBR-3 (overexpressed HER2/*neu* - positive cell line), MCF-7 and HEK-293 (negative cell lines) were used in this study **[Figure 4.11]**. HEK-293 cells are fibroblastoid semi-adherent cells that grow as monolayer cultures. Colony morphologies of BC cell lines in 3-D culture fall into four distinct classes: round, mass, grape-like and stellate (Kenny *et al*., 2007). SKBR-3 cells appear as spherical structures and form loosely cohesive grape-like colonies displaying poor cell to cell contacts; whereas MCF-7 cells fit into the mass category of cells which form tightly interconnected structures with robust connections among cells. Both these BC cell lines predominantly adopted monolayer morphologies but tended to 'clump' and form small multicellular structures.

4.4.2 MTT cytotoxicity assay

One of the most important features of gene delivery systems is their safety. The 3-(4, 5-dimethyl-2-thiazolyl)-2, 5-diphenyl-2H-tetrazolium bromide (MTT) quantitative colorimetric assay was used to assess the metabolic viability of cell cultures exposed to transfection complexes. This assay is based on the ability of viable cells to produce a dark purple strongly lipophilic fomazan product by reducing the water-soluble yellow coloured tetrazolium dye (van Meerloo *et al*., 2011). These reductions take place only in metabolically active cells when mitochondrial reductase enzymes are active. The quantity of formazan product formed is proportional to the metabolic activity of viable cells, which was determined spectrophotometrically (UV_{570} absorbance), after dissolving the purple formazan crystals in dimethyl sulfoxide. The cytotoxicity of the different lipoplex formulations is depicted in **Figure 4.12** (pCMV-*luc*) and **Figure 4.13** (siRNA). Values are expressed as percentage cell viability against untreated control cells set at 100%, and represented as a function of lipid:nucleic acid N/P charge ratios (+:–).

Cell culture

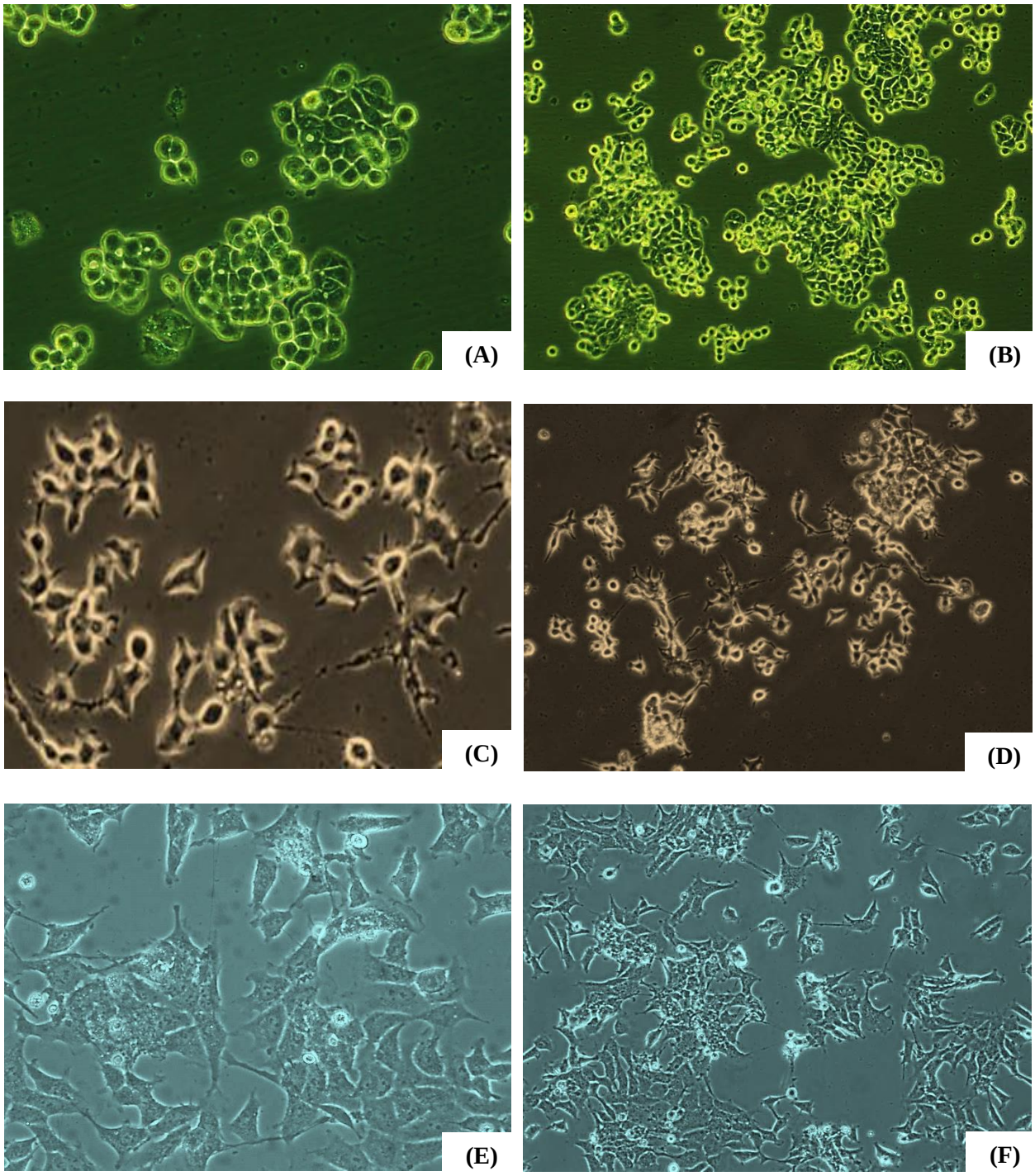

Figure 4.11: Colony morphologies of the three cell lines used in this study. **(A)** and **(B)** SKBR-3, **(C)** and **(D)** MCF-7, **(E)** and **(F)** HEK-293. Cells were viewed as a monolayer at semi-confluency under a 100 × magnification (Nikon TMS-F 6V, Tokyo, Japan).

Cell viabilities of HEK-293 **(A)**, MCF-7 **(B)** and SKBR-3 **(C)** cells treated with pDNA lipoplexes ranged as follows: Chol-T (92 – 86%, 96 – 85% and 96 – 101%), Chol-T 2% PEG (94 – 79%, 96 – 79% and 92 – 91%), Chol-T 5% PEG (83 – 78%, 96 – 74% and 89 – 87%), MS09 (113 – 100%, 99 – 90% and 93 – 86%), MS09 2% PEG (91 – 81%, 96 – 83% and 96 – 98%), MS09 5% PEG (109 – 96%, 95 – 81% and 86 – 80%). As shown in **Figure 4.12**, after 48 h incubation, cell viability with non-PEGylated pDNA lipoplexes remained above 80% when compared with untreated cells. Similarly, pDNA lipoplexes with the incorporation of PEG did not show notable cytotoxicity in all three cell lines either. Cell viabilities of HEK-293, MCF-7 and SKBR-3 cells treated with siRNA lipoplexes ranged as follows: Chol-T (89 – 85%, 89 – 88% and 101 – 102%), Chol-T 2% PEG (84 – 76%, 90 – 81% and 94 – 92%), Chol-T 5% PEG (82 – 74%, 78 – 70% and 96 – 88%), MS09 (101 – 93%, 98 – 91% and 87 – 89%), MS09 2% PEG (87 – 82%, 87 – 85% and 87 – 74%), MS09 5% PEG (84 – 78%, 80 – 76% and 51 – 49%). These results show that the three cell lines maintained a viability of over 70% after treatment with the various siRNA lipoplexes, except for the SKBR-3 cells exposed to MS09 5% PEG lipoplexes which caused a 50% decrease in cell viability (P<0.001). Nevertheless, these findings suggest good biocompatibility with all three cell lines over the range of N/P charge ratios (+:–) tested. Furthermore, these findings on cell viabilities are favourable when compared to that attained using the commercially available transfection reagent, Lipofectamine® 3000. The low cytotoxicities observed could be attributed to the use of monovalent cationic lipids which are known to be less toxic than multivalent cationic lipids (Spagnou *et al*., 2004). It is also very likely that the incorporation of DOPE and cholesterol into the liposomal formulations contributed to the lipoplexes biocompatibility and stability and therefore low levels of cytotoxicity.

As shown in **Figure 4.12** and **Figure 4.13**, HEK-293 **(A)** and MCF-7 **(B)** cells revealed a decrease in cell viability with an increase in lipid:nucleic acid N/P ratios (+:–) for all tested liposomal formulations irrespective of degree of PEGylation, indicating a dose-dependent cytotoxic effect. This trend of visibly reduced cell viability at higher lipid to nucleic acid N/P ratios has been reported in previous studies (Dass, 2002; Lv *et al*., 2006). Research has shown that the cytotoxic effect of cationic liposomes is primarily determined by their cationic nature, since at high charge ratios N/P (+:–) the presence of free or excess cationic liposomes is essentially associated with increased cell toxicity (Xu *et al*., 1999).

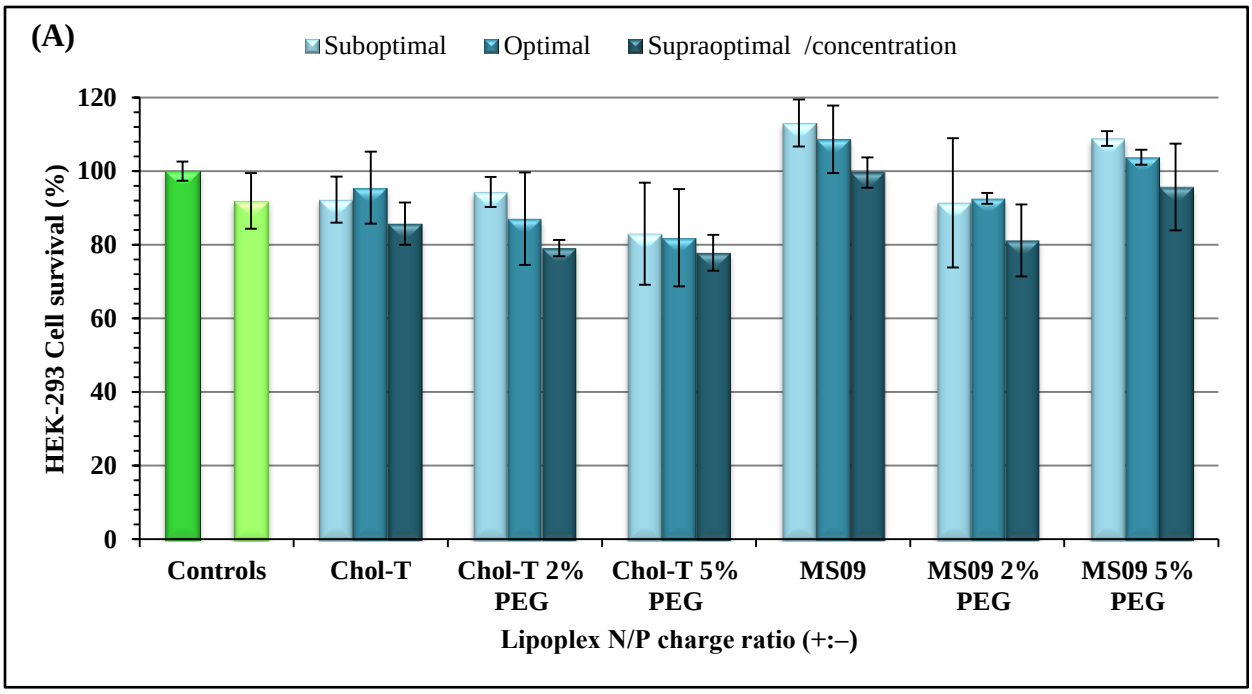
(A)
Suboptimal
Optimal
Supraoptimal /concentration
HEK-293 Cell survival (%)
120
100
80
60
40
20
0
Controls
Chol-T
Chol-T 2% PEG
Chol-T 5% PEG
MS09
MS09 2% PEG
MS09 5% PEG
Lipoplex N/P charge ratio (+:–)

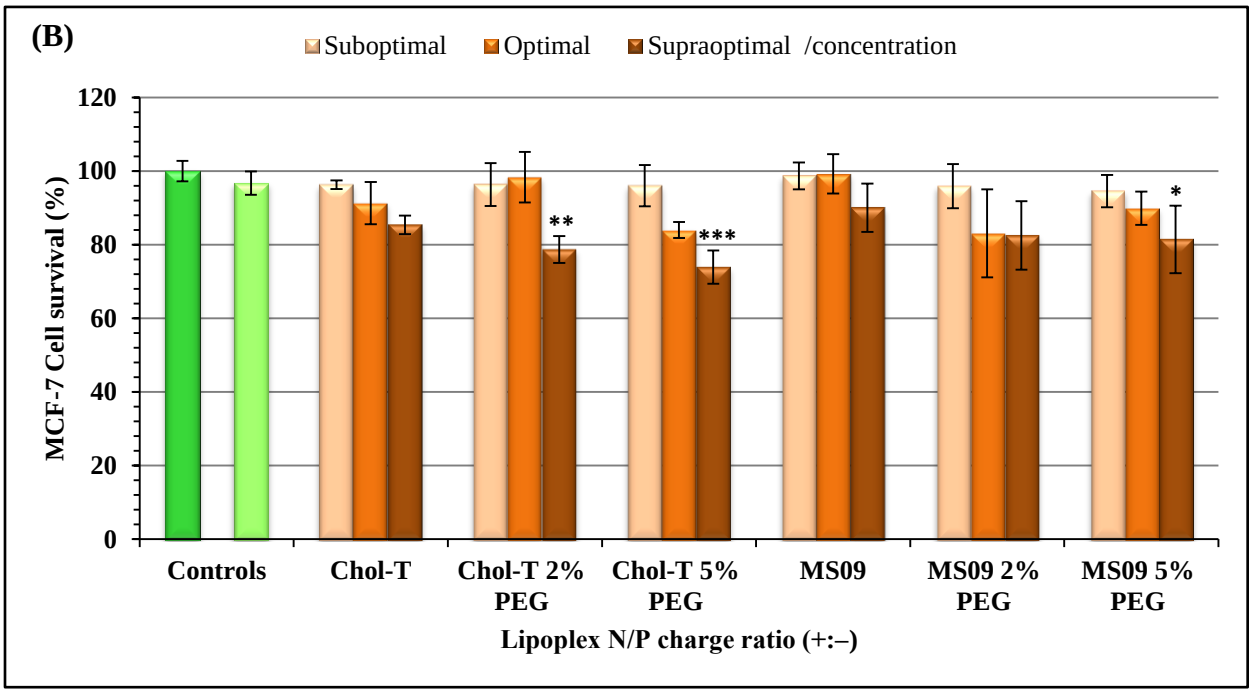
(B)
Suboptimal
Optimal
Supraoptimal /concentration
MCF-7 Cell survival (%)
120
100
80
60
40
20
0
**
***
*
Controls
Chol-T
Chol-T 2% PEG
Chol-T 5% PEG
MS09
MS09 2% PEG
MS09 5% PEG
Lipoplex N/P charge ratio (+:–)

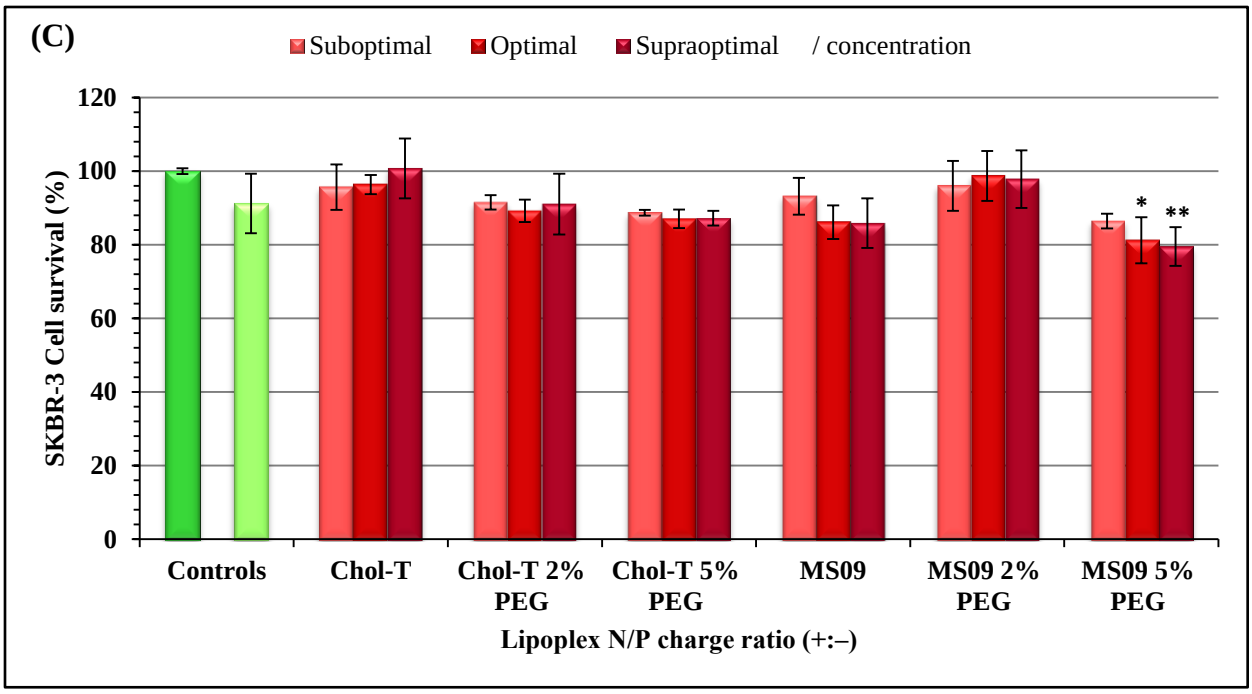

Figure 4.12: Cell cytotoxicity studies of cationic and PEGylated cationic liposome-pCMV-*luc* plasmid DNA complexes in **(A)** HEK-293, **(B)** MCF-7 and **(C)** SKBR-3 cells *in vitro* using MTT reagent. Incubation mixtures (0.25 mL) contained 0.5 μg of pDNA with varying amounts of liposome from suboptimal to supraoptimal N/P (+:–) charge ratios: Controls - Untreated cells; Lipofectamine® 3000; Chol-T (1.1, 1.6, 2.1); Chol-T 2% PEG (1.2; 1.7, 2.2); Chol-T 5% PEG (1.1, 1.6, 2.1); MS09 (1.2, 1.7, 2.2); MS09 2% PEG (1.4, 1.8, 2.3); MS09 5% PEG (1.3, 1.7, 2.1). The viability percentage of cells was expressed relative to Untreated control cells. Data are presented as means ± SD (n = 3). Statistical analysis among mean values was performed using one-way ANOVA followed by the Tukey-Kramer multiple comparisons test between formulations. Asterisks denote a significant difference compared to the Untreated control cells *P<0.05, **P<0.01, and ***P<0.001.

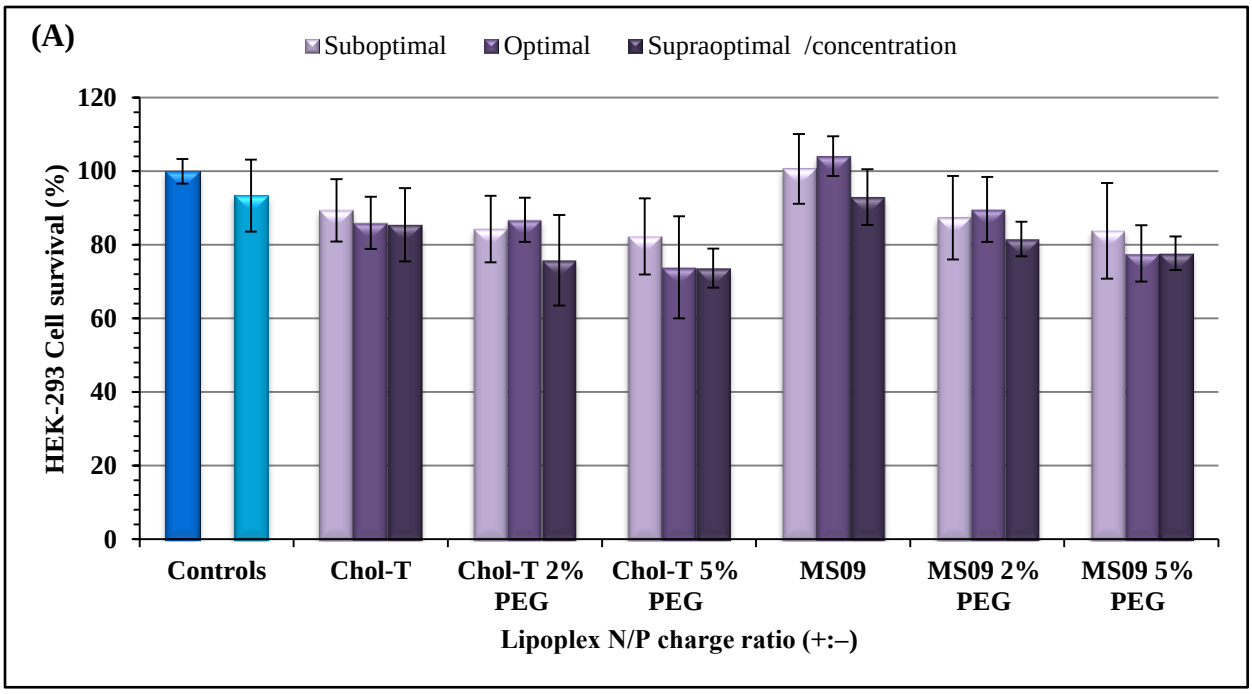
(A)
Suboptimal
Optimal
Supraoptimal /concentration
HEK-293 Cell survival (%)
120
100
80
60
40
20
0
Controls
Chol-T
Chol-T 2% PEG
Chol-T 5% PEG
MS09
MS09 2% PEG
MS09 5% PEG
Lipoplex N/P charge ratio (+:–)

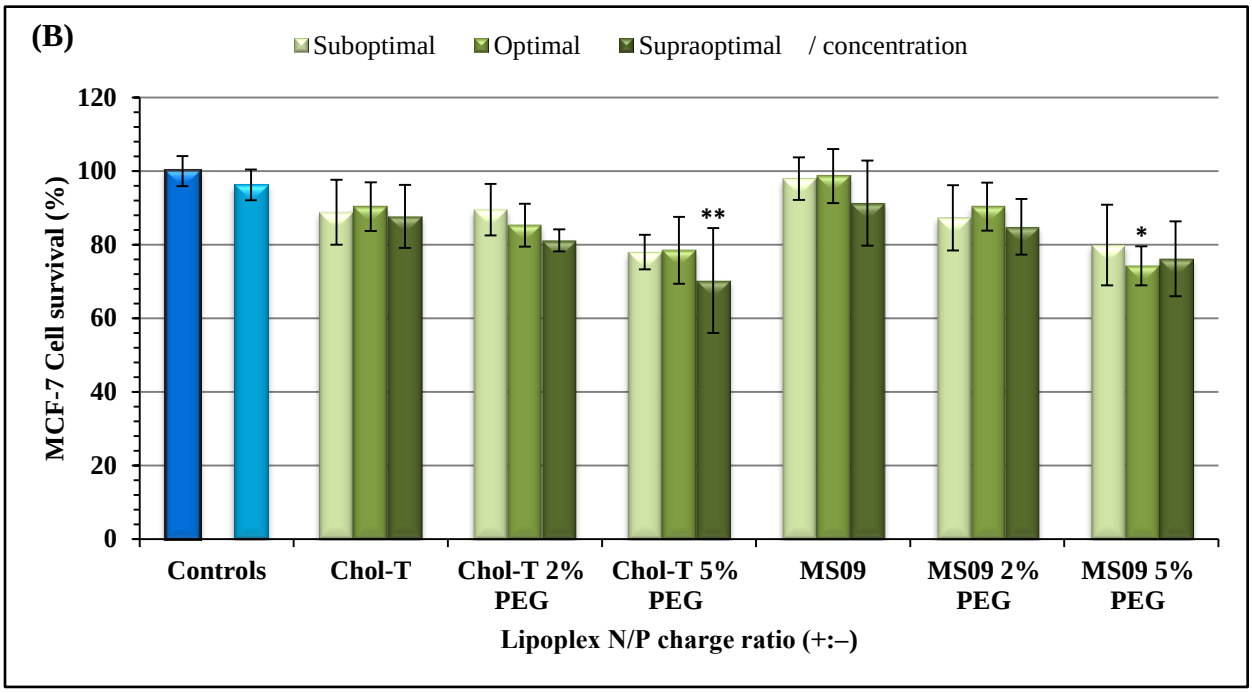
(B)
Suboptimal
Optimal
Supraoptimal / concentration
MCF-7 Cell survival (%)
120
100
80
60
40
20
0
**
*
Controls
Chol-T
Chol-T 2% PEG
Chol-T 5% PEG
MS09
MS09 2% PEG
MS09 5% PEG
Lipoplex N/P charge ratio (+:–)

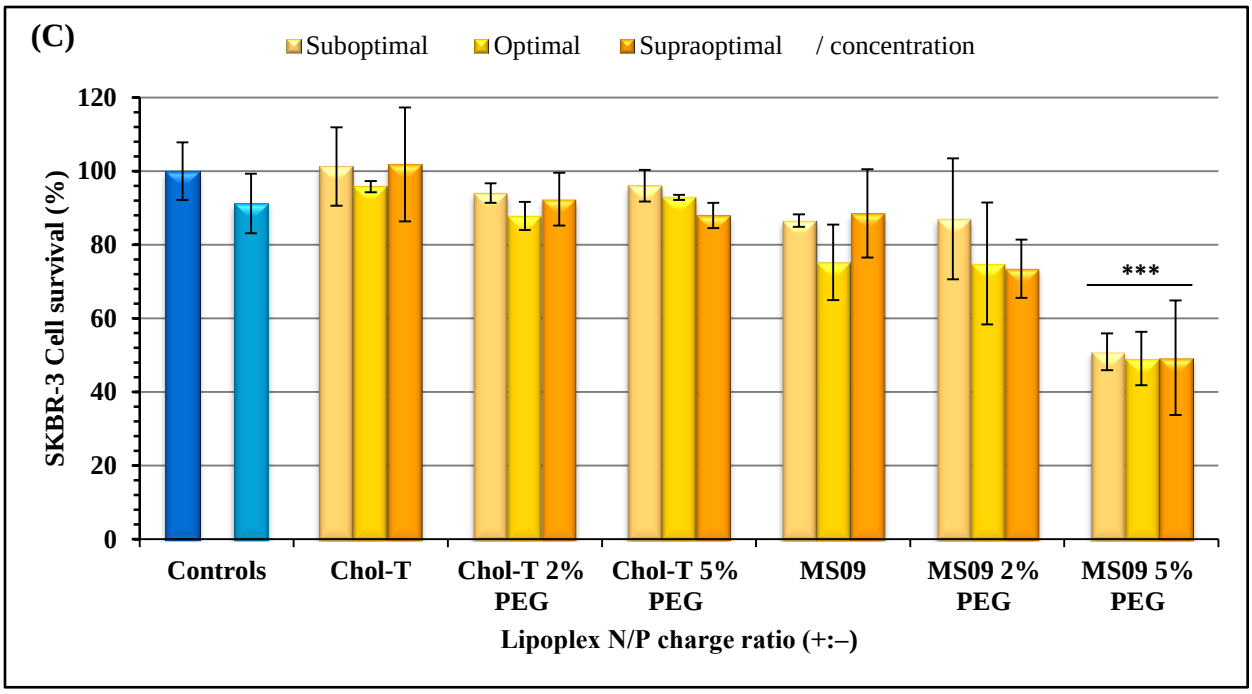

Figure 4.13: Cell cytotoxicity studies of cationic and PEGylated cationic liposome-siGENOME non-targeting siRNA complexes in **(A)** HEK-293, **(B)** MCF-7 and **(C)** SKBR-3 cells *in vitro* using MTT reagent. Incubation mixtures (0.25 mL) contained 0.32 µg of siRNA with varying amounts of liposome from suboptimal to supraoptimal N/P (+:–) charge ratios: Controls - Untreated cells; Lipofectamine® 3000; Chol-T (3.4, 3.9, 4.4); Chol-T 2% PEG (5.8, 6.3, 6.8); Chol-T 5% PEG (8.3, 8.8, 9.3); MS09 (4.9, 5.4, 5.9); MS09 2% PEG (5.5, 6.0, 6.5); MS09 5% PEG (7.4, 7.9, 8.4). The viability percentage of cells was expressed relative to Untreated control cells. Data are presented as means ± *SD* (*n* = 3). Statistical analysis among mean values was performed using one-way ANOVA followed by the Tukey-Kramer multiple comparisons test between formulations. Asterisks denote a significant difference compared to the Untreated control cells **P*<0.05, ***P*<0.01, and ****P*<0.001.

As such, formulated lipoplexes are in general far less cytotoxic than free cationic liposome components (van Gaal *et al*., 2011).

Interestingly, for both the pDNA and siRNA lipoplexes, Chol-T containing treatments were in general slightly more toxic to the HEK-293 and MCF-7 cell lines compared to the MS09 containing lipoplexes. As discussed previously, the structural property of these cytofectins features a cholesterol ring anchor, a monovalent dimethylamino head group, a biodegradable carbamoyl linker and a spacer element. It is well established that each segment of the cationic cytofectin has dramatic effects on cell toxicity (Lv *et al*., 2006). The distinguishing feature between the Chol-T and MS09 cytofectins is the length of the spacer element. The MS09 cytofectin containing the longer spacer element was observed to be slightly less toxic than the Chol-T cytofectin. This trend of reduced cytotoxicity with MS09 compared to Chol-T can be clearly observed with HEK-293 cells exposed to pDNA lipoplexes (viability decrease of 21% and 14%) and siRNA (viability decrease of 12% and 8%), at both low and high charge ratios N/P (+:–) respectively. Interestingly, MS09 N/P 4.9 and 5.4 (siRNA), MS09 N/P 1.2 and 1.7 and MS09 5% PEG N/P 1.3 and 1.7 (pDNA) lipoplexes were non-toxic to HEK-293 cells and in fact led to an increase in cell numbers and therefore increased cell viability above 100% was observed. This pattern of visibly reduced cytotoxicity corroborates previous studies by Floch *et al*. (2000), who reported that an increase in the length of the spacer segment resulted in decreased cytotoxicity in culture format. Moreover, carbamate-linked lipids offer lower cytotoxicity as this bond is stable under neutral conditions, and is prone to acid-catalyzed hydrolysis at low pH values (in the endosome), where lipids may be degraded into less toxic by-products or low molecules within the cell (Boomer *et al*., 2002; Liu *et al*., 2005a; b).

As observed in **Figure 4.13 (A)**, **(B)**, and **(C)**, PEGylated siRNA lipoplexes resulted in an increase in cellular toxicity as evidenced by a decrease in cell viability in all three cell lines tested. At supraoptimal concentrations the non-PEGylated Chol-T siRNA lipoplexes (N/P 4.4) resulted in minimal cytotoxicities in HEK-293 (15%), MCF-7 (12%) and SKBR-3 (0%) cells, compared to their PEGylated counterparts: Chol-T 2% PEG N/P 6.8 (24%, 19% and 8%); Chol-T 5% PEG N/P 9.3 (26%, 30% and 12%). In the same way, the non-PEGylated MS09 siRNA lipoplexes (N/P 5.9) elicited marginal cell deaths in HEK-293 (7%), MCF-7 (9%) and SKBR-3 (11%) cells, compared to their PEGylated counterparts: Chol-T 2% PEG N/P 6.5 (18%, 15% and 26%); Chol-T 5% PEG N/P 8.4 (22%, 24% and 51%). Although the chemical modification of

cationic liposomes with PEG resulted in increased stability (Chol-T and MS09 siRNA lipoplexes at 2 mol.% PEG) as well as smaller particle sizes, PEGylated cationic liposomes were still more cytotoxic than their non-PEGylated equivalents. Zhang *et al*. (2010) reported similar trends with PEGylated DC-Chol/DOPE siRNA lipoplexes. These authors suggested that the increase in cytoxicity was probably due to the higher cationic liposome concentration.

With regard to SKBR-3 cells, a dose-independent decease in cell viability was observed with pDNA (Chol-T and MS09 2% PEG) and siRNA (MS09) lipoplexes, and in some instances MS09 was more toxic than Chol-T. Reports on cationic liposome cytotoxicity have shown that in some instances these lipids generate reactive oxygen species (ROS) (Park *et al*., 2004; Soenen *et al*., 2009), and that cancer cells exhibit greater ROS stress than normal cells. The mechanism of action of ROS within cells has been described as a two-edged sword. In one occurrence ROS activates receptor tyrosine kinases and growth factors, which facilitates cell-cycle progression and cell survival. Conversely, the presence of high levels of ROS can suppress cell growth via continuous activation of cell-cycle inhibitors which leads to apoptosis (Ramsey and Sharpless, 2006; Scherz-Shouval and Elazar, 2007; Takahashi *et al*., 2006). Therefore, the variations in SKBR-3 cell viability may be attributable to the fluctuations of ROS production within these cells. Taken together, these findings indicate that the cationic liposomes synthesized in this study show relatively low cytotoxic effects on HEK-293, MCF-7 and SKBR-3 cell lines, and have the potential for future *in vivo* applications.

4.4.3 Luciferase activity

Plasmids are extra-chromosomal circular DNA molecules which have the ability to replicate autonomously within a suitable host. Moreover, modified plasmids encoding for a particular gene of interest and a promoter have the ability to be expressed within the nucleus of transfected cells in a temporary manner. The reporter gene pCMV-*luc* which comprises a cytomegalovirus promoter and the firefly luciferase (*luc*) gene was used to investigate the ability of the PEGylated and non-PEGylated Chol-T and MS09 cationic liposomes to stably transfect pDNA. The pCMV-*luc* plasmid is a widely used reporter gene since it can be easily identified and gene expression can be measured quantitatively. The pDNA transfection capability of liposomal formulations was evaluated on the three cells lines, namely, HEK-293, MCF-7 and SKBR-3 cells, in an *in vitro*

transfection experiment using the luciferase reporter gene assay. Attached cells were transfected with lipoplexes comprising 1 µg pCMV-*luc* at predetermined N/P charge ratios (+:–) and the RLU measured 48 h after transfection. Luciferase activity was normalized using the BCA protein assay and relative expression was recorded as RLU mg^{-1} protein. The performance of the PEGylated and non-PEGylated Chol-T and MS09 lipid vectors was compared to the established non-viral delivery vector Lipofectamine® 3000 Reagent (positive control). Assay controls also included cells unexposed to liposome or pDNA and cells treated with free pDNA (negative controls). The luciferase reporter assay offers unparalleled sensitivity and versatility to assess or study gene expression (Fan and Wood, 2007). Basically, the reporter technology involves the interaction of the *luc* enzyme with luciferin (luminescent substrate) and, via different chemistries, light is emitted by the process of bioluminescence. Two chemical reactions take place; firstly, D-luciferin is adenylated by Mg-ATP to generate luciferyl adenylate and pyrophosphate. Secondly, luciferyl adenylate is activated by ATP, resulting in oxidation by molecular oxygen to form a dioxetanone ring. A decarboxylation reaction forms oxyluciferin in an electronically excited state, and finally the reaction releases a photon of light as oxyluciferin returns to the ground state (Baldwin, 1996). This reaction is highly energetically efficient as all energy incorporated into the reaction is rapidly converted into light (Allard and Kopish, 2008).
Plasmid DNA transfections of the three cell lines are depicted in **Figure 4.14**; HEK-293 **(A)**, MCF-7 **(B)** and SKBR-3 **(C)**. As expected, the transfection efficiency of free pDNA was very low. Naked or free pDNA is prone to enzymatic degradation in the presence of serum; on the other hand pDNA that is internalized is rapidly destroyed by DNAses present in the endosome or cytoplasm, prior entry into the nucleus (Audouy *et al*., 2000; Buyens *et al*., 2008; Lv *et al*., 2006).

On the other hand, the commercial product Lipofectamine® 3000 increased transfection by about 7.02-fold (HEK-293), 7.30-fold (MCF-7) and 10.90-fold (SKBR-3) compared to free pDNA. As mentioned previously, the incorporation of high levels of cholesterol and/or cholesterol-containing derivatives in liposomal formulations offers several advantages for gene delivery; these include enhanced transfection efficiency as well as resistance to serum-induced aggregation (Islam *et al*., 2009; Pozzi *et al*., 2012; Samadikhah *et al*., 2011; Zhang *et al*., 2008; Zidovska *et al*., 2009). It has been suggested that the increase in transfection offered by cholesterol may be a result of phase transition. Strong repulsive 'hydration forces' exist between

lipid membranes, which forms a major barrier for membrane-membrane interaction and fusion. The presence of cholesterol in the lipid membrane reduces the average hydration repulsion layer of the membrane, prompting phase transition toward a non-lamellar transfecting phase and/or enhanced fusion between the cationic lipoplex membrane and the anionic cell membrane (Pozzi *et al*., 2012; Zidovska *et al*., 2009). As such, the cholesterol containing lipoplexes employed in this study were able to stably transfect the various cell lines tested, albeit at varying degrees, by most likely favouring the interaction with cellular membranes and aiding in fusion-driven cellular uptake and endosomal release.

The pDNA gene transfection efficiencies amongst the different cells lines varied. In general, SKBR-3 cells appeared to be most difficult to transfect amongst the three cells lines, as evidenced by the lower luciferase activity. This difference in transfection between the cell lines is mainly due to the surface charge of the cellular membrane as well as the cells doubling time. The surface charge influences electrostatic interaction between the lipoplexes and the cell membrane affecting the cellular uptake efficiency. On the other hand it could also affect the entry of pDNA into the nucleus (Brunner *et al*., 2000; Obata *et al*., 2010; Zuhorn and Hoekstra, 2002).

Transfection efficiency of non-PEGylated Chol-T and MS09 lipoplexes was considerably limited as compared to pDNA alone (negative control) for almost all N/P (+:–) charge ratios analyzed, except for MS09 tested at suboptimal (N/P 1.2) and supraoptimal (N/P 2.2) ratios against MCF-7 ($P<0.01$) and HEK-293 ($P<0.001$) cells, respectively. It is well established that the first important step for transfection is entry into the cytoplasm. Liposome-mediated transfection is further dependent on the size and surface charge of the cationic liposomes. ZetaSizer measurements indicated that these lipoplexes displayed a highly positive zeta potential, and were larger than their corresponding PEGylated counterparts. Therefore, it can be assumed that although these pDNA containing complexes displayed a cationic charge on their surface which was favourable for binding to the anionic cell membrane and internalization into the cytoplasm, ineffective release of the pDNA from the lipoplex within the cell was most likely associated with low transfection. Reduced pDNA release can be further supported by the EtBr intercalation assay, particularly with regard to Chol-T complexes which demonstrated increased affinity and good compaction capabilities for pDNA.

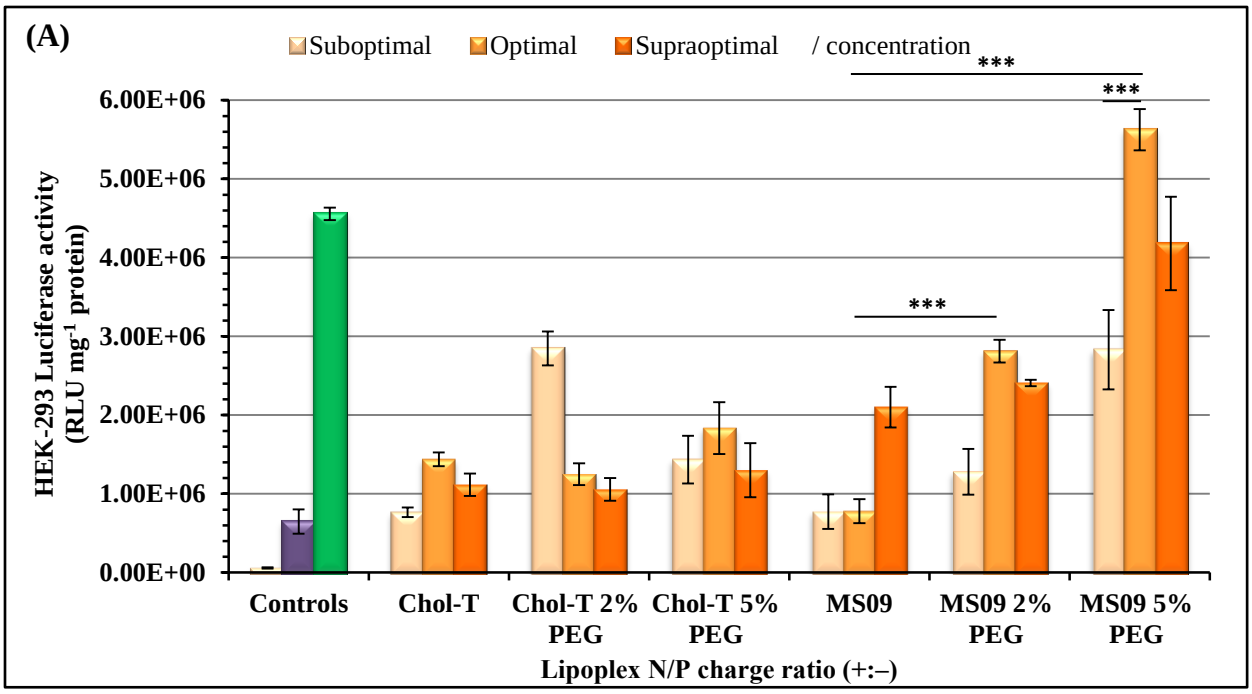
(A)
Suboptimal
Optimal
Supraoptimal
/ concentration
***
***
***
HEK-293 Luciferase activity (RLU mg-1 protein)
6.00E+06
5.00E+06
4.00E+06
3.00E+06
2.00E+06
1.00E+06
0.00E+00
Controls
Chol-T
Chol-T 2% PEG
Chol-T 5% PEG
MS09
MS09 2% PEG
MS09 5% PEG
Lipoplex N/P charge ratio (+:–)

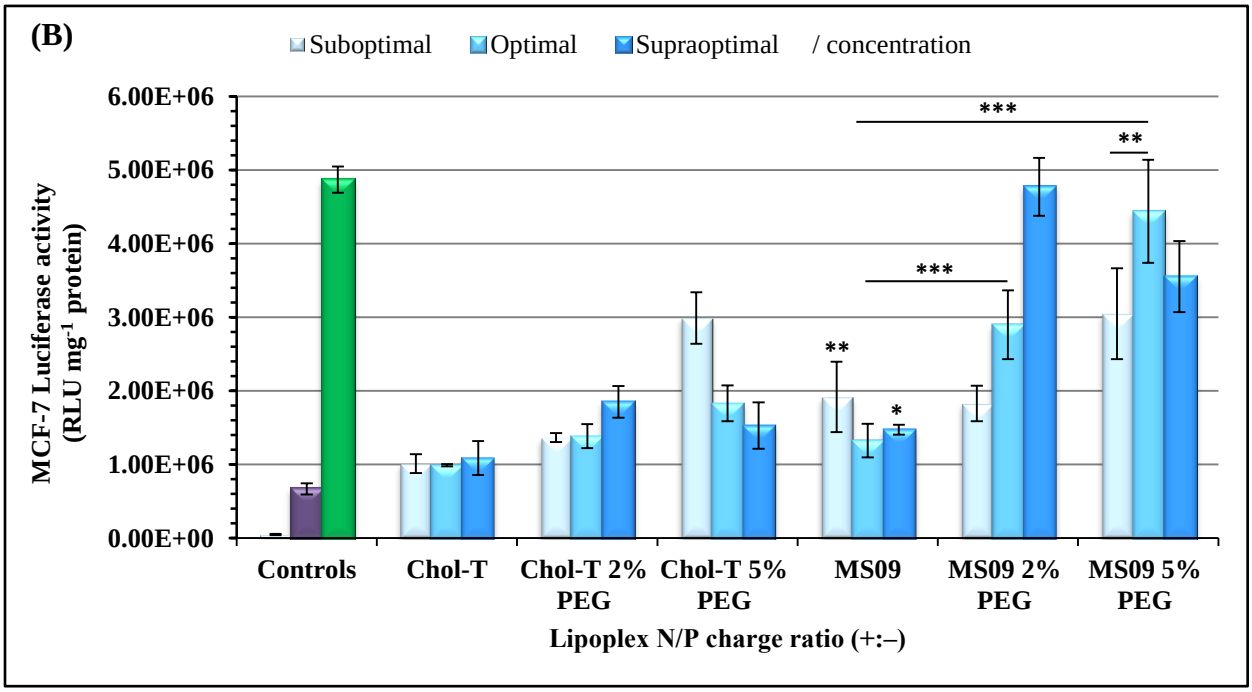
(B)
Suboptimal
Optimal
Supraoptimal
/ concentration
***
**
***
**
*
MCF-7 Luciferase activity (RLU mg-1 protein)
6.00E+06
5.00E+06
4.00E+06
3.00E+06
2.00E+06
1.00E+06
0.00E+00
Controls
Chol-T
Chol-T 2% PEG
Chol-T 5% PEG
MS09
MS09 2% PEG
MS09 5% PEG
Lipoplex N/P charge ratio (+:–)

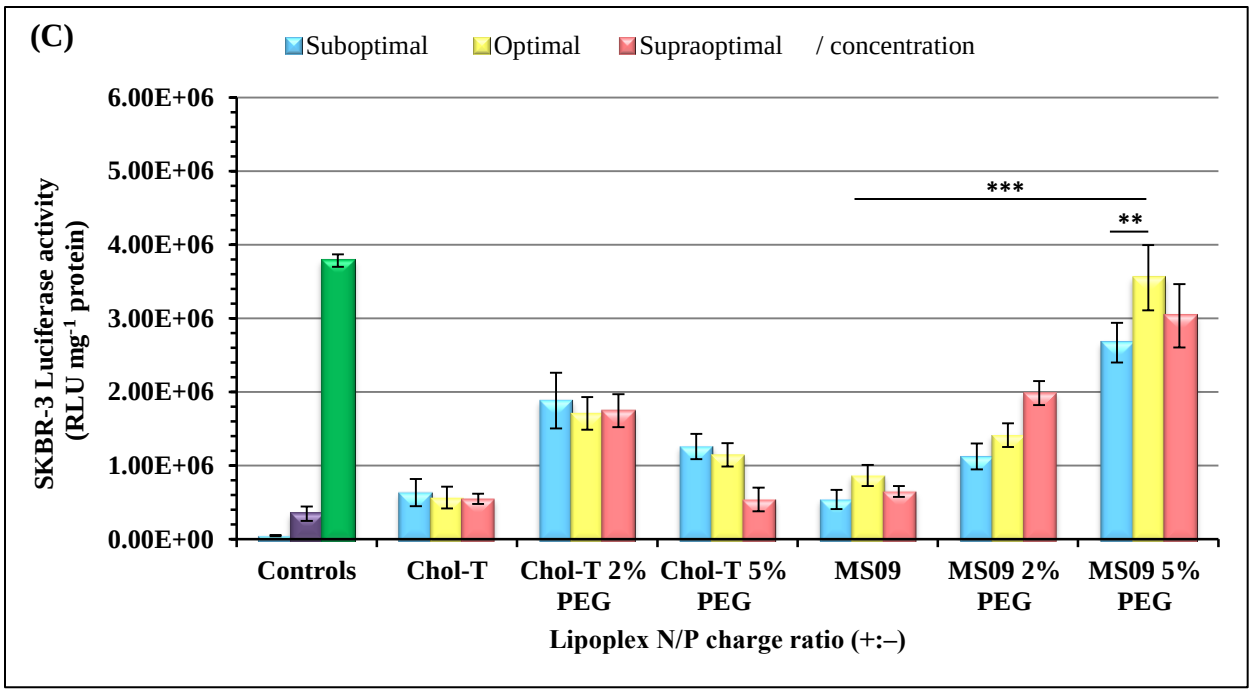

Figure 4.14: *In vitro* gene transfection data of PEGylated and non-PEGylated lipoplexes studied in **(A)** HEK-293, **(B)** MCF-7, and **(C)** SKBR-3 cell lines. Lipoplexes were formulated with pCMV-*luc* plasmid DNA (1 µg) at various N/P charge ratios (+:–): Control 1 (untreated cells, negative control); Control 2 (pCMV-*luc* DNA alone, negative control) and Lipofectamine® 3000 (positive control); Chol-T (1.1, 1.6, 2.1); Chol-T 2% PEG (1.2; 1.7, 2.2); Chol-T 5% PEG (1.1, 1.6, 2.1); MS09 (1.2, 1.7, 2.2); MS09 2% PEG (1.4, 1.8, 2.3); MS09 5% PEG (1.3, 1.7, 2.1). Transfections were carried out in the presence of 10% foetal bovine serum. Luciferase activity in terms of normalized light units was expressed as RLU mg^{-1} protein. Data are presented as means ± SD (n = 3). Statistical analysis among mean values was performed using one-way ANOVA followed by the Tukey-Kramer multiple comparisons test between formulations. Asterisks denote a significant difference *P<0.05, **P<0.01, and ***P<0.001.

Maitani *et al*. (2007) reported similar cellular associations using DC-Chol:DOPE (molar ratio 1/2 and 3/2) liposomes. DC-Chol:DOPE (1/2), however, demonstrated significantly greater transfection efficiency compared to DC-Chol:DOPE (3/2). These authors also suggested that it was the release of the DNA from the lipoplex and not the increase in cellular association that played a crucial role in efficient transfection.

In general, cationic lipoplexes containing DSPE-PEG_{2000} resulted in increased luciferase activity compared to their non-PEGylated counterparts. A comparison of PEGylated Chol-T and MS09 lipoplexes revealed that the latter was more efficient in pDNA-*luc* transfection as indicated by the significant increases in luciferase activity, particularly with lipoplexes containing 5% PEG. The following fold-increases were recorded with MS09 lipoplexes at optimal N/P charge ratios (i.e. end-point) PEGylated at 2% and 5% compared to the non-PEGylated MS09 lipoplexes: HEK-293, 3.6-fold ($P<0.001$) and 7.2-fold ($P<0.001$); MCF-7, 2.4-fold ($P<0.001$) and 3.4-fold ($P<0.001$); SKBR-3, 1.6-fold and 4.1-fold ($P<0.001$), respectively. With regard to PEGylated Chol-T lipoplexes at suboptimal N/P charge ratios, the following findings were observed and recorded: HEK-293, 3.7-fold and 1.9-fold; MCF-7, 1.4-fold and 3.0-fold; SKBR-3, 3.0-fold and 2.0-fold increase in luciferase activity, upon 2% and 5% PEGylation respectively. Although PEGylated Chol-T lipoplexes did result in an increase in luciferase activity, in general, these increases were not clinically significant. As discussed in **Section 4.2.2**, PEGylation induced a size stabilizing effect, forming lipoplexes which were significantly smaller than non-PEGylated lipoplexes. It has also been suggested that when PEGylated lipoplexes are in association with blood plasma or serum, they become restricted, causing a reduction in entropy between PEG chains. This in turn leads to the escalation of a repulsive force, preventing the attachment of plasma proteins as well as other components. *In vitro* transfection experiments performed in the presence of serum, suggested that PEGylation of the lipoplexes did in fact provide a stabilizing effect on the lipoplexes by resisting the formation of a protein corona around their surfaces. Moreover, the DSPE-PEG_{2000} polymer contains a pH sensitive carbamate bond which links the DSPE component to the PEG polymer. Therefore, under reduced pH conditions such as the endosomal compartments, these components are easily disassembled, facilitating the release of the pCMV-*luc* cargo, and thus contributing to increased luciferase gene expression. On the other hand, non-PEGylated lipoplexes formed larger-sized particles, most likely due to the formation of a protein corona and/or aggregation of the lipoplexes. Under these

conditions, the cationic charge of the lipoplexes tends toward neutralization, leading to reduced association between the lipoplexes and the cellular membrane and a consequent decrease in the expression of the luciferase gene.

Interestingly, with regard to N/P charge ratios, a similar trend in luciferase activities was observed in HEK-293 and SKBR-3 cell lines. Basically, an increase in N/P charge ratio from suboptimal to optimal concentrations resulted in escalated luciferase activity for all tested lipoplexes, except Chol-T 2% PEG in HEK-293 cells, and all Chol-T containing lipoplexes in SKBR-3 cells. This result correlates with previous studies which confirmed increase in transfection levels due to increases in lipid/pDNA charge ratios. For example, Candiani *et al*. (2010) reported low transfection levels when using DOPC/DOPE lipid formulations with a charge ratio of 1.25 (close to isoneutrality). However, when the charge ratio was increased to 5, so did the degree of transfection. On the other hand, a further increase from optimal to supraoptimal concentrations led to a decline in luciferase activity. This decrease in luciferase activity was observed with all lipoplex formulations tested excluding MS09 in HEK-293 and Chol-T 2% PEG and MS09 2% PEG in SKBR-3 cells. Balbino *et al*. (2012) reported similar results. Firstly, when lipoplexes are prepared in close proximity to the isoneutrality region, there is an excess of pDNA that may induce the formation of larger particle aggregates via the construction of saturated liposomal surfaces retaining pDNA within their bilayers. Although this offers good pDNA packaging and protection, these multiple bilayers compromise DNA release within cells thus decreasing transfection activity. Secondly, it has been suggested that further increase in N/P charge ratio and the consequent decline in luciferase activity may be a result of the presence of an excess of liposomes. These compete with lipoplexes for cellular internalization thereby limiting the intake of pDNA lipoplxes, and ultimately reducing transfection levels. In most cases, however, the differences in luciferase activity based on N/P charge ratios were not significant. The MS09 5% PEG lipoplexes, in particular, resulted in the abovementioned trends being observed in all three tested cell types; a significant dose-dependent increase in luciferase signals was seen from suboptimal to optimal concentrations: HEK-293 ($P<0.001$); MCF-7 ($P<0.01$); SKBR-3 ($P<0.01$). This result echoes the findings of Gjetting *et al*. (2010). Using DOTAP/cholesterol-based lipoplexes incorporating PEG (range 0 – 10%), they demonstrated that lipoplexes containing 5% PEG-lipid exhibit a threshold in physical properties, and particularly a size-stabilizing effect. Here the stabilizing effect was more pronounced in the

PEGylated MS09 containing lipoplexes than the Chol-T complexes as indicated by a superior PDI obtained with MS09.

4.4.4 HER2/*neu* Gene Silencing in SKBR-3 Breast Cancer Cells

4.4.4.1 Quantitative Real-Time PCR

Quantitative Real-Time PCR (qRT-PCR) is a powerful technique in molecular biology. It is superior to other gene profiling methods because of its facility, sensitivity, precise detection, dynamic range, reliability, robustness and high-throughput potential for gene expression studies. This technology offers several advantages over traditional PCR: monitoring the progress of the qRT-PCR reaction in real time; allowing for an improved dynamic range of detection; enabling highly accurate measurements of the initial quantity of target amplicons; and omitting post-PCR handlings as amplification and detection of the PCR product take place in a single reaction tube (Derveaux *et al*., 2010; Stratford *et al*., 2008; Yuan *et al*., 2006).

In this technique, mRNA is firstly reverse transcribed to generate a single-stranded cDNA template, which is then amplified via PCR. A PCR reaction occurs in three phases, namely, exponential, linear and plateau. In the exponential phase, under ideal conditions assuming 100% reaction efficiency, amplification of the amplicon occurs exponentially, i.e., the kinetics of the reaction favour doubling of the product since reagents are not limited. As the reagents become limited during the linear phase, the reaction starts to slow down, and there is a linear increase of the PCR product. As the reaction continues and the reagents become depleted, the reaction eventually reaches the plateau phase where the quantity of product formed does not change (Heid *et al*., 1996; Yuan *et al*., 2006).

Real-Time PCR exploits the exponential phase for quantification data due to the fact that under ideal conditions initial amplicon doubles after every cycle, producing the most accurate and reproducible data. During this phase two values are calculated: the threshold fluorescence and the threshold cycle (C_t). Threshold fluorescence is defined as the level of signal that reflects a statistically significant increase in fluorescent intensity over the background fluorescent signal, and the C_t refers to the cycle number of the PCR reaction at which the florescent signal of the

reporter dye reaches the threshold. The C_t value is known as the quantitative end-point and it is used in both absolute and relative quantification (Pfaffl, 2001; Schmittgen and Livak, 2008).

The chemically synthesized Chol-T and MS09 cationic liposomal formulations were tested for their ability to efficiently deliver target HER2/*neu* siRNA into SKBR-3 cells. Transfection experiments were conducted using the PEGylated and non-PEGylated cationic liposomes in parallel with the control samples: calibrator, non-targeting siRNA and HER2/*neu* target siRNA alone. Lipofectamine®-3000 Reagent is one of the most common transfection reagents and it is recommended for siRNA gene transfection experiments. Hence the researcher's use of it as a positive control to compare the transfection activity with the liposomes synthesized in this study. Total cellular RNA was isolated from the treated cells 48 h post transfection, and thereafter gene expression and silencing were monitored using qRT-PCR with primers specific for the HER2/*neu* gene. Relative expression of the HER2/*neu* gene was normalized in relation to the GAPDH gene. The concentration of extracted cellular RNA was between 0.32 – 0.38 μg μL^{-1} and of a relatively good quality with $^{260}/_{280}$ ratio between 1.75 – 1.88.

Quantitative RT-PCR results were analyzed using the $2^{-\Delta\Delta Ct}$ method for comparative or relative quantification; the results are presented as the fold-change in gene expression relative to the calibrator (SKBR-3 cells alone). According to the qRT-PCR results depicted in **Figure 4.15**, the calibrator revealed high levels of the HER2/*neu* gene; by definition the fold-change in gene expression of the untreated control is approximately one, since $\Delta\Delta C_t$ equals zero and 2^0 equals one. The non-targeting siRNA (NT-siRNA) showed no knockdown, whereas the uncomplexed HER2/*neu* target siRNA resulted in a slight decrease of the HER2/*neu* gene at the mRNA level. The gene expression levels of the housekeeping normalizer gene GAPDH did not differ significantly among the control and test samples.

Quantitative RT-PCR with HER2/*neu*-spanning primers revealed that each of the liposomal formulations was able to deliver siRNA against the HER2/*neu* gene in the SKBR-3 BC cells in the presence of serum, as indicated by down-regulation of HER2/*neu* at the mRNA level ($P<0.001$). As described in **Section 4.1.2**, the cationic liposomes were formulated with DOPE, a neutral helper fusogenic lipid. Due to the propensity of DOPE to assume an inverted hexagonal phase, this cone-shaped neutral lipid is known to play a critical role in membrane-membrane fusion events (Fletcher *et al*., 2008), thereby inducing strong destabilizing effects on the barrier properties of the endosomal membranes and offering efficient gene delivery into the

cytoplasm. A cationic cholesterol derivative in combination with DOPE has also been reported to provide serum-stable transfection of siRNA (Han *et al*., 2008; Spagnou *et al*., 2004). Also, it has been suggested that the cholesterol moiety may bind to certain ligand components present in the serum, thereby enabling uptake of the delivery system and its gene cargo into cells via ligand-mediated endocytosis (Han *et al*., 2008). In this study, we cannot exclude the possibility that the factors mentioned above have contributed to efficient delivery of HER2/*neu* siRNA by the cationic liposomes.

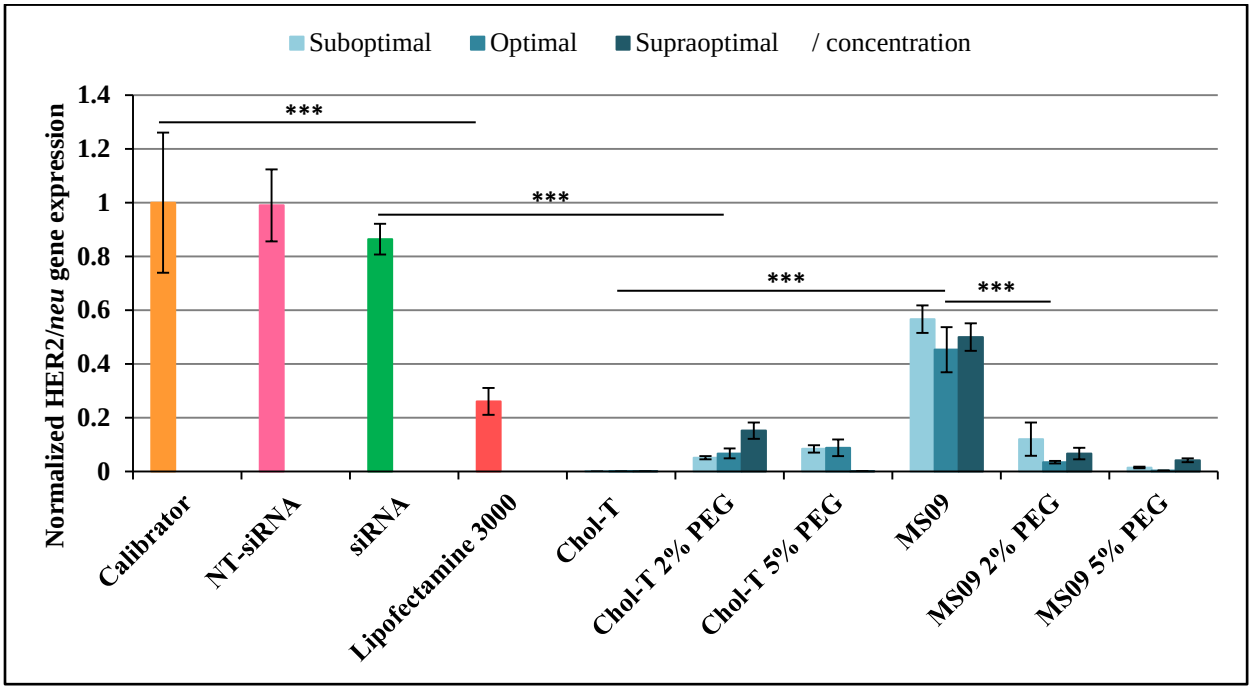

Figure 4.15: Analysis of HER2/*neu* gene expression in SKBR-3 cells by qRT-PCR. Incubation mixtures (1.5 mL) contained 0.64 µg of siRNA with varying amounts of liposome from suboptimal to supraoptimal concentrations: Chol-T:DOPE (7.68, 8.96, 10.24 µg); Chol-T:DOPE:2% PEG (14.08, 15.36, 16.64 µg); Chol-T:DOPE:5% PEG (22.40, 23.68, 24.96 µg); MS09:DOPE (12.16, 13.44, 14.72 µg); MS09:DOPE:2% PEG (14.72, 16.00, 17.28 µg); MS09:DOPE:5% PEG (21.76, 23.04, 24.32 µg). Calibrator (non-treated SKBR-3 cells), NT-siRNA (non-targeting siRNA) and siRNA (HER2/*neu* targeting siRNA alone) served as negative controls. Lipofectamine® 3000-siRNA was included as a positive control. The vertical axis represents the relative quantification of HER2/*neu* normalized against GAPDH mRNA level using the comparative quantification algorithm $2^{-\Delta\Delta Ct}$ (Livak and Schmittgen, 2001). Data shown are the mean ± *SD* of independent experiments (n = 3). Asterisks denote a significant difference ***P<0.001.

A comparison of the non-PEGylated Chol-T and MS09 lipoplexes at different N/P charge ratios (+:–) revealed that the Chol-T/siRNA complexes induced the highest HER2/*neu* silencing effect at all tested concentrations as indicated by the significant fold-difference in gene expression (> 10 000-fold, $P<0.001$). Non-PEGylated MS09 lipoplexes yielded relative HER2/*neu* mRNA levels of 0.57, 0.45 and 0.50 which corresponds to a 1.87, 2.34, and 2.13-fold reduction in mRNA expression compared to the SKBR-3 untreated control ($P<0.001$). Moreover, the level of gene knockdown by Chol-T lipoplexes exceeded the knockdown level of Lipofectamine-3000 (i.e., relative HER2/*neu* gene expression of 0.26 which represents a 4.1-fold decrease). Biophysical characterization of the Chol-T/siRNA complexes showed that these lipoplexes appeared as well-defined, spherical-shaped, uni-lamellar structures with distinct bilayered membranes which appeared well dispersed and colloidally stable **[Figure 4.4 (A)].** These liposomes also formed the largest siRNA lipoplexes [187.97 nm (PDI 0.127)] with the highest zeta potential measurements (47.26 ± 5.39 mV), and were the least cytotoxic in SKBR-3 cells. In addition, the electrophoretic mobility shift assay indicated that the lowest charge ratio at which the liposomes were able to completely condense siRNA was obtained with the non-PEGylated Chol-T liposome [charge ratio (+:–) 3.9:1]. These findings suggest that the Chol-T siRNA complexes formed condensed positively charged structures with low cytotoxic effects at a relatively low charge ratio. These characteristics of lipid based delivery systems have been previously reported to favour efficient gene delivery. In addition, larger lipoplexes have been generally described as being more efficient at gene delivery *in vitro* due to the fact that larger structures settle out from solution easily leading to fast sedimentation and increased contact with cellular membranes, as well as easier dissociation of the lipoplexes post endocytosis (Zhu and Mahato, 2010). Moreover, larger lipoplex formation has been shown to increase serum stability and effectively protect DNA from attack by DNAseI (Almofti *et al*., 2003; García *et al*., 2007).

As shown in **Figure 4.15**, PEGylated Chol-T and MS09 lipoplexes reduced HER2/*neu* mRNA gene level at all concentrations tested (2% and 5% PEG). However, the effect of PEGylation on siRNA gene delivery differed with each of the cytofectins in the liposomal formulation. The following fold-changes in HER2/*neu* gene levels were recorded at different N/P (+:–) charge ratios from suboptimal to supraoptimal concentrations: Chol-T 2% PEG (20.78, 15.86 and 7.00); Chol-T 5% PEG (12.68, 12.14 and 1208.19); MS09 2% PEG (8.86; 31.01 and 16.05) and MS09 5% PEG (72.37, 314.73 and 25.77). From the graph, a clear difference on the

effect of PEGylation can be observed. In the case of Chol-T lipoplexes, the effect of PEGylation at both 2% and 5% reduced the silencing efficiency of the Chol-T liposomes. Results indicated that PEGylation reduced the size and the zeta potential of Chol-T liposomes **(Table 4.1)**. The reduced gene silencing effect, therefore, is most likely a result of the physical changes. This remarkable reduction in gene transfection efficiency accords with a previous report by Zhang *et al*. (2010). They suggested that PEGylation of DC-Chol/DOPE siRNA lipoplexes caused a decrease in particle size and zeta potential, and that the anti-HER2 siRNA DC-Chol/DOPE lipoplexes did not elicit any HER2 silencing in SKBR-3 cells.

On the other hand, PEGylated MS09 lipoplexes significantly increased the HER2/*neu* gene silencing efficiency. An increase of 4.73-fold, 13.23-fold and 7.55-fold was observed upon 2% PEGylation ($P<0.001$), and a further increase of 8.17-fold, 10.15-fold and 1.61-fold was recorded when PEGylated with 5% PEG ($P<0.001$). Interestingly, PEGylation also caused a decrease in particle size and zeta potential of MS09 liposomes. It was shown, however, that the high siRNA gene transfection efficiency of the PEGylated MS09 lipoplexes is concomitant with high cytotoxicity **[Figure 4.13 (C)]**. A comparison of the cell toxicity profiles of PEGylated MS09 siRNA complexes with those of non-PEGylated MS09 lipoplexes showed that there was up to 39.20% reduction in cell viability for the lipoplexes containing 5% PEG.

4.4.4.2 HER2/*neu* protein expression

To evaluate the modulation of HER2/*neu* target siRNA gene delivery into SKBR-3 cells via PEGylated and non-PEGylated Chol-T and MS09 cationic liposomal formulations, HER2/*neu* protein expression levels were analyzed using the Western blotting technique. Total protein lysate was firstly separated via electrophoresis using the sodium dodecyl sulphate-polyacrylamide gel electrophoresis system (SDS-PAGE) and subsequently transferred onto a PVDF membrane. This was followed by specific primary and secondary antibody incubation, either Neu for HER2/*neu* protein detection or β-actin, an internal control for protein loading.

The experimental set-up for Western blotting paralleled that implemented for qRT-PCR, except that protein extraction was conducted 72 h post transfection. The control samples included; SKBR-3 cells alone, non-targeting siRNA, HER2/*neu* target siRNA alone and Lipofectamine®-3000 Reagent. Results were analyzed based on densitometric values, and β-actin

control was used to determine normalization or equivalency of lane loading. Western blot analysis revealed high levels of HER2/*neu* protein expression (ratios) in negative control treatments relative to β-actin (SKBR-3 cells alone - 2.77, non-targeting siRNA - 2.57 and HER2/*neu* target siRNA alone - 1.93) **[Figure 4.16 (A)]**. In contrast, dramatic decreases in HER2/*neu* protein expression levels were observed for all siRNA delivery systems (PEGylated and non-PEGylated Chol-T and MS09) employed in this study.

As indicated in **Figure 4.16 (B)** and **(C)**, Western blot analysis demonstrated that non-PEGylated Chol-T and MS09 liposomes resulted in a dose dependent decease in HER2/*neu* protein expression levels. Normalized HER2/*neu* protein expression levels were 0.017, 0.017 and 0.013 (Chol-T) and 0.880, 0.231 and 0.217 (MS09). These values correspond to a 160.28, 163.89 and 212.80 (Chol-T) and 3.15, 12.02 and 12.77 (MS09)-fold decrease in protein expression relative to the untreated SKBR-3 cells (alone). Comparing free HER2/*neu* target siRNA delivery (control, no liposome treatment) with the cationic liposomal delivery systems, a 111.39, 113.89 and 147.89 (Chol-T) and 2.19, 8.35 and 8.89 (MS09)-fold decrease in protein expression was observed. These results indicate that as the N/P (+:–) charge ratio increased from suboptimal to supraoptimal concentrations, a decrease in protein expression was observed. Reports have indicated that the charge ratio of lipoplexes significantly influences their morphology and capacity to transfect (Zhu and Mahato, 2010). The formation of lipoplexes with excess cationic liposomes (i.e., higher N/P charge ratio) tends toward developing spherical-shaped structures, in which the nucleic acid is effectively condensed and the resulting complexes are relatively more stable, making it easier for cellular internalization (van Gaal *et al*., 2011). To date, there are limited studies which specifically analyze the interaction between siRNA lipoplexes and cells membranes. Since siRNA lipoplexes formed from monovalent cationic liposomes have demonstrated successful gene silencing efficiency *in vitro* (Hattori *et al*., 2015; Xia *et al*., 2016; Zhang *et al*., 2010), two mechanisms have been postulated based on DNA lipoplexes. The first is a non-specific ionic interaction, where the proteoglycans on the cell membrane are involved in the internalization process (Mounkes *et al*., 1998). The second is an ion-pair mechanism where the cationic lipids form ion pairs with anionic lipids (e.g., phosphatidylserine) on the endosomal membrane. Subsequently, the ion-pairs lead to destabilization and disassembly of the lipoplexes and the endosome membrane, which in turn, enables release of the target siRNA into the cytoplasm (Xia *et al*., 2016; ur Rehman *et al*., 2013b).

Comparing the non-PEGylated Chol-T and MS09 HER2/*neu* target siRNA lipoplexes, the Chol-T liposome resulted in a 50.85, 13.64 and 16.67-fold decrease in HER2/*neu* protein expression compared to the MS09 liposome at different N/P charge ratios (+:–). These results corroborate qRT-PCR findings; the Chol-T/siRNA complexes induced the highest HER2/*neu* silencing effect at all tested concentrations as indicated by the significant-fold difference in gene expression **[Figure 4.15]**. Furthermore, there was a 5.61 (N/P 3.4), 5.73 (N/P 3.9) and 7.44 (N/P 4.4)-fold decrease in protein expression levels with non-PEGylated Chol-T lipoplexes compared to Lipofectamine® 3000 Reagent **[Figure 4.16 (A)]**. In a recent publication by Shi *et al*. (2016), cationic liposomes bearing shorter aliphatic chains offered better pDNA transfection efficiency than those containing longer chains. They postulated that increased transfection efficiencies with shorter hydrocarbon chains are due possibly to increased fluidity of the bilayer, leading to a greater degree of inter-membrane transfer and the subsequent mixing of the lipid membrane. These factors could be extrapolated to the siRNA delivery and be the reason why the Chol-T lipoplexes were most effective in gene silencing. Also, the size and zeta potential of a delivery system are important factors which must be considered for transfection. In particular, the size of the lipoplex has been reported to play a significant role in the entry pathway of complexes into the cells. Two main entry pathways have been suggested based on size of the lipoplex, namely, the clathrin coated and the caveolae-mediated pathways. A size range of ~300 nm or less favour the clathrin pathway. On the other hand, complexes which are > 500 nm enter basically via the caveolae-mediated pathways (Caracciolo *et al*., 2010).

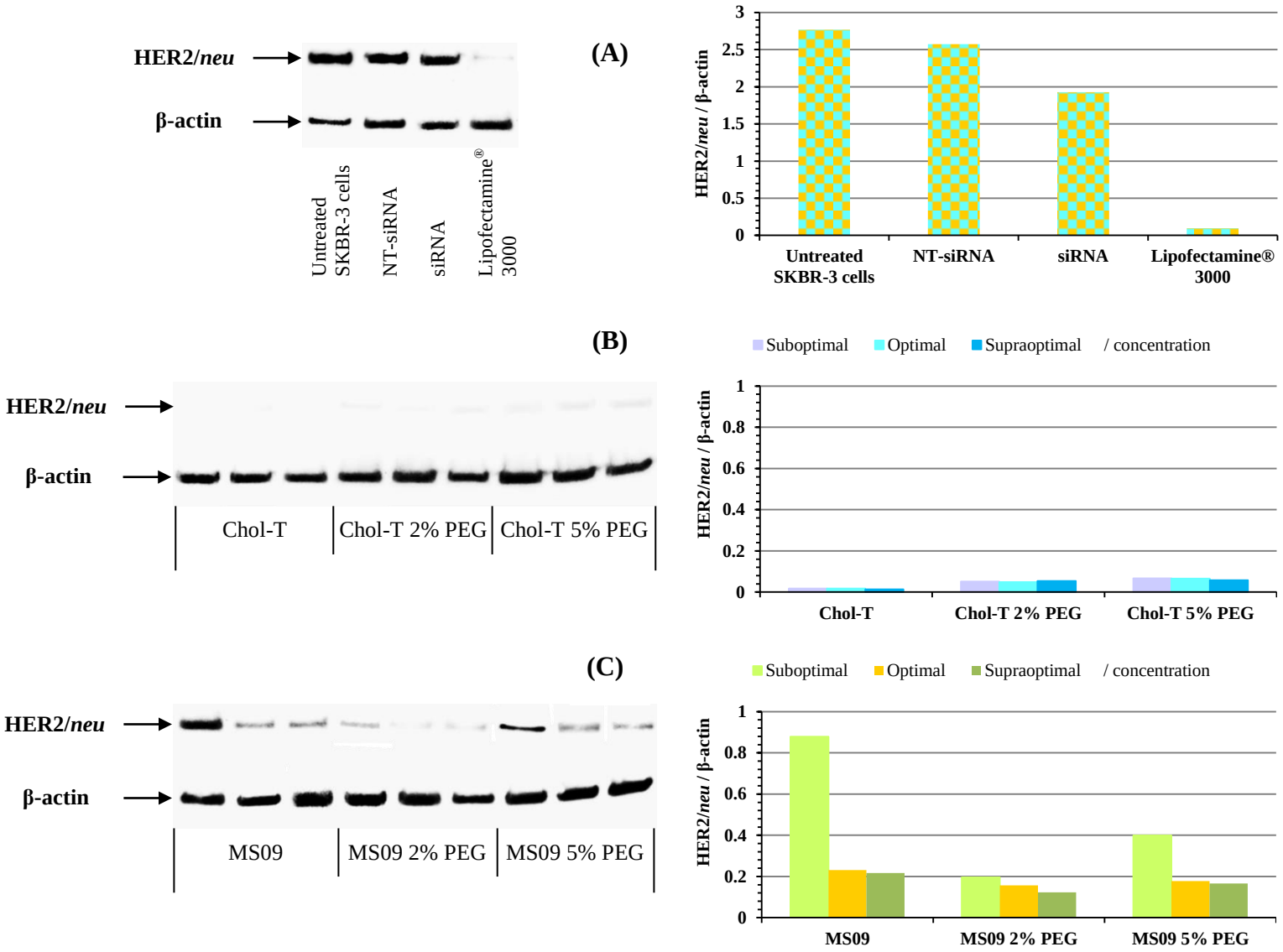

Figure 4.16: Analysis of HER2/*neu* oncoprotein expression by Western blotting. **(A)** Non-treated SKBR-3 cells, NT-siRNA (non-targeting siRNA) and siRNA (HER2/*neu* targeting siRNA alone) served as negative controls. Lipofectamine® 3000-siRNA was included as a positive control. **(B)** SKBR-3 cells were treated with HER2/*neu* target siRNA (0.64 µg) with varying amounts of the cationic liposomes from suboptimal to supraoptimal ratios: Chol-T (7.68, 8.96, 10.24 µg); Chol-T 2% PEG (14.08, 15.36, 16.64 µg); Chol-T 5% PEG (22.40, 23.68, 24.96 µg); **(C)** MS09 (12.16, 13.44, 14.72 µg); MS09 2% PEG (14.72, 16.00, 17.28 µg); MS09 5% PEG (21.76, 23.04, 24.32 µg). HER2/*neu* receptor expression was determined in cellular lysates by Western blotting analysis using the HER2/*neu* and β-actin antibodies. Graphs represent the HER2/*neu*/β-actin normalization ratios.

Interestingly, it has also been suggested that only the latter pathway produces an efficient transfection strategy, since it is capable of supressing lysosomal digestion as well as allowing for an efficient endosomal release mechanism (Rejman *et al*., 2006). In the presence of serum, lipoplexes in general tend to form structurally unstable complexes which lead to reduced or low transfection efficiencies (Cheung *et al*., 2005; Lundqvist *et al*., 2008). In this study, however, the significant gene silencing effect demonstrated by Chol-T/siRNA complexes at both the mRNA and protein levels indicates that these lipoplexes were most efficient at delivering the HER2/*neu* target siRNA into SKBR-3 in the presence of serum. The unusually high transfection efficiency in the presence of serum has been previously described by Caracciolo *et al*. (2010). These researchers used both dynamic light scattering measurements and proteomic experiments to show that in the presence of serum, the size of DC-Chol-DOPE/DNA complexes was regulated by the formation of a protein corona on the surface of the lipoplex which was concomitant with an inherent increase in particle size. They suggested that the formation of a protein-rich layer on the surface of lipoplexes caused the lipoplexes to aggregate due to decreased inter-bilayer electrostatic repulsions between the cationic lipoplexes, and that the larger size was most likely accompanied by caveolae-mediated internalization and an increase in transfection efficiency. With regard to Chol-T and MS09/siRNA lipoplexes, a similar trend is likely as these complexes were relatively larger with a higher ζ potential measurement, thereby enabling greater affinity for serum protein binding. However, MS09/siRNA complexes were less efficient than Chol-T/siRNA in protecting the siRNA cargo from serum nuclease degradation **[Figure 4.8]**. Therefore, although MS09/siRNA lipoplexes possessed larger particle sizes for entry via caveolae-mediated endocytosis, insufficient internalization of the HER2/*neu* target siRNA resulted in low levels of siRNA gene silencing.

As mentioned previously, in order to improve the stability of lipidic complexes *in vivo*, the effect of PEGylation (2 – 5 mol.% of DSPE-PEG_{2000} with respect to CholT:DOPE and MS09:DOPE) on the cationic liposomal delivery system was investigated. Both PEGylated Chol-T and MS09 cationic liposomes resulted in HER2/*neu* gene silencing, as detected at the mRNA and the protein levels. Depicted in **Figure 4.16**, normalized HER2/*neu* protein expression levels decreased by: 53.50, 56.48 and 51.89-fold (Chol-T 2% PEG); 41.29, 41.96 and 48.28 (Chol-T 5% PEG); 14.18, 17.60 and 22.61 (MS09 2% PEG); 6.94, 15.55 and 16.68 (MS09 5% PEG) compared to the untreated SKBR-3 cells (alone). qRT-PCR and Western blot results indicated

that PEGylated Chol-T (2% and 5%) reduced the siRNA gene silencing ability of the Chol-T liposome. Characterization of PEGylated complexes confirmed a decrease in particle size and zeta potential **(Table 4.1)**. The phenomenon observed with PEGylated Chol-T lipoplexes correlates with the above-mentioned premise that a decrease in zeta potential (less cationic charge) most likely reduces the attraction of serum proteins and therefore favours cellular internalization via the clathrin-dependent pathway. It has also been suggested that preformed PEGylated liposomes have a tendency to form unstable complexes with siRNA, as the PEG chains are known to create a hydrophilic barrier that prevents the electrostatic interaction between the siRNA gene material and the cationic lipid carrier (Belletti *et al*., 2016). The siRNA molecules tend to form loose interactions and are usually exposed on the surface of the PEGylated liposomal structure. These siRNA molecules are in most cases unprotected and easily attacked by nucleases present in serum. Characterization of the PEGylated MS09/siRNA complexes indicated that these lipoplexes do experience a certain degree of instability. It was observed, however, that PEGylated lipoplexes were somewhat more efficient in HER2/*neu* gene silencing than their non-PEGylated counterparts, albeit lower than Lipofectamine® 3000 Reagent. Moreover, serum nuclease digestion analysis indicated variations in siRNA gene protection. It can be suggested that during siRNA lipoplex formulation, the high energy transmission induced by vortexing may allow for these rather small siRNA molecules to manoeuver between the PEGs and harmoniously accommodate themselves on the cationic liposome. These siRNAs may then be internalized into the cell, enabling siRNA gene silencing (Barichello *et al*., 2012).

Reports suggest that a 2% - 5% PEG concentration (relative to the lipidic composition) is required to stabilize particles (Belletti *et al*., 2016; Peeters *et al*., 2007). The pre-PEGylated lipoplexes, with only a minimal amount of PEG (2 mol.%), was able to efficiently form lipoplexes, offer adequate protection to their siRNA cargo, and deliver the HER2/*neu* target siRNA into SKBR-3 cells. At the protein expression level the Chol-T 2% PEG demonstrated a 1.30, 1.35 and 1.08-fold decrease while MS09 2% PEG revealed a 2.04, 1.13 and 1.36-fold decrease compared to their 5% PEGylated equivalents. Belletti *et al.* (2016) reported a similar finding using the cationic lipid DOTAP and DSPE-PEG_{2000}. Post-PEGylation at 2 mol.% was capable of effectively stabilizing Blimp-1 siRNA, efficiently delivering it into the BCBL-1 cell line and significantly reducing the BLIMP-1 protein levels. It was also demonstrated that when

the PEG concentration was increased to 5 mol.%, micelles on preformed lipoplexes did not produce the same silencing effect. In fact, a decrease in transfection efficiency resulted.

CHAPTER FIVE

CONCLUSION

5.1 Concluding Remarks

The potential of siRNA to silence the expression of a number of oncogenes at the transcriptional level offers an attractive and powerful therapeutic route for the treatment of BC. The RNAi pathway enables target-specific interference of genes which are expressed at abnormally high levels; these include either pathogenic genes or gene targets involved in cancer progression and/or cell cycle regulation. The application of siRNA-based therapeutics offers several advantages over traditional treatments with minimal side effects. It makes use of an innate cellular pathway, requiring the introduction of either a synthetic siRNA duplex molecule or a dsRNA trigger molecule. Despite recent progress in developing nanocarrier systems, cell toxicity and the reduced cellular uptake efficiency of siRNA in the presence of serum nucleases are still major drawbacks for *in vitro* and *in vivo* applications. This leaves BC gene therapy at a juncture where the need for an optimal gene delivery vector has become the rate limiting step. Further advances in the field of siRNA-gene based therapy depend on the discovery of a competent nanocarrier system which promotes specific tissue and cellular internalization of the therapeutic siRNA, as well as its efficient endosomal escape into the cytoplasm. Therefore, the development of safe nanocarrier delivery systems with the capacity for whole organism application still remains a formidable challenge in the continued quest to optimize the success of siRNA-based therapeutics.

This study evaluated the ability of six cationic lipid-based delivery systems (PEGylated and non-PEGylated) to efficiently deliver intact siRNA which would target the HER2/*neu* oncogene in a BC cell model. Both Chol-T and MS09 cationic cholesterol cytofectins co-formulated (1:1) with the neutral lipid DOPE were able to form liposomes with favourable physicochemical characteristics (particle size and zeta potential measurements) and was capable of binding and protecting nucleic acids (pDNA and siRNA). These delivery systems were reproducible and able to withstand long-term storage at 4 °C. Translation of siRNA lipofection from *in vitro* to *in vivo* applications requires stability of the lipid-based delivery system in the physiological milieu. Noted disadvantages with administration of cationic lipoplexes included: aggregation and poor control of the particle size, adsorption of biomolecules such as plasma proteins, rapid uptake by the reticuloendothelial system, as well as adverse toxicity effects due mainly to the cationic charge. PEGylation has become the most successful and popularly

employed strategy to impart promising pharmacodynamic and pharmacokinetic properties to increase the longevity of lipoplexes in circulation. In this study, grafting DSPE-PEG_{2000} on the surface of liposomal formulations did indeed provide a steric barrier at the surface of nascent liposomes. This prevented vesicle aggregation and encouraged the formation of a homogeneous population of smaller liposomes with colloidal stability and biocompatibility. On the other hand, the partial masking of the positive charges by PEGylation ultimately led to greater amounts of the PEGylated liposome being used to fully bind pDNA or siRNA compared to the non-PEGylated liposomes. This was most apparent with siRNA, as indicated by the EtBr intercalation assay, where greater quantities of the PEGylated liposomes were required to successfully displace the intercalated EtBr cation and bind the siRNA, demonstrating a relatively weaker affinity toward the nucleic acid. As such, PEGylated cationic liposomes were more cytotoxic than their non-PEGylated equivalents due mainly to the higher concentration of the cationic cytofectin.

Preliminary studies testing the ability of these lipid-based delivery systems to transfect pDNA collectively demonstrated that the non-viral cholesterol containing lipoplexes, Chol-T and MS09 (0%, 2% and 5% PEG), were able to stably transfect pDNA into the various cell lines tested, albeit to varying degrees. Results have indicated that PEGylated cationic lipoplexes were more efficient in transfecting the pCMV-*luc* gene and increasing luciferase activity than their non-PEGylated counterparts. Maximal transfection efficiency was attained with MS09 5% PEG (5.62×10^6 RLU mg^{-1} protein) at N/P charge ratio 1.7. Furthermore, these liposomes displayed significant improvement in pCMV-*luc* plasmid DNA transfection [7.2-fold increase, ($P<0.001$)] compared to the non-PEGylated MS09 lipoplexes in the presence of serum. Interestingly, the MS09 5% PEG lipoplexes demonstrated a significant dose-dependent increase in luciferase signals from suboptimal (N/P 1.3) to optimal (N/P 1.7) charge ratios, and then a decrease in activity at supraoptimal ratios (N/P 2.1) in all three tested cell types. Along with mediating improved cellular uptake and transfection efficiency, MS09 5% PEG pDNA lipoplexes also assured their safety and biocompatibility *in vitro* as indicated by low levels of cytotoxicity (> 80% cell survival).

With regard to HER2/*neu* siRNA gene delivery, gene expression studies indicated that the Chol-T:DOPE (0% PEG)/siRNA complexes induced the highest HER2/*neu* silencing effect at all tested N/P charge ratios as indicated by the significant decrease in gene expression (> 10

000-fold, $P<0.001$). In addition, Western blot analysis confirmed the above profile and revealed a dose-dependent decrease in HER2/*neu* protein expression levels as indicated by a 160.28, 163.89 and 212.80-fold decrease in protein expression relative to the untreated SKBR-3 cells (alone). Furthermore, the most active non-PEGylated Chol-T formulations were less cytotoxic and exceeded the knockdown level of Lipofectamine® 3000 control (4.1-fold decrease).

PEGylated Chol-T and MS09 lipoplexes reduced HER2/*neu* mRNA gene level at all concentrations tested (2% and 5% PEG); however, the effect of PEGylation on siRNA gene delivery differed with each of the cytofectins in the liposomal formulations. In the case of Chol-T lipoplexes, qRT-PCR and Western blot results indicated that PEGylated Chol-T (2% and 5%) reduced the siRNA gene silencing ability of the Chol-T liposome. On the other hand, although PEGylated MS09 lipoplexes significantly increased the HER2/*neu* gene silencing efficiency in an N/P charge ratio dependent manner (evidenced by protein expression levels), cytotoxicity was also increased with up to 39.20% reduction in cell viability for lipoplexes containing 5% PEG compared to non-PEGylated MS09 lipoplexes.

These results reflect the immense potential of these PEGylated and non-PEGylated cationic liposomes in HER2/*neu* siRNA gene silencing in the BC cell model utilized in this study. The findings of this study support the hypothesis that these non-viral cationic liposome systems have the ability for future-therapeutic siRNA and DNA gene delivery. However, with the caveat that PEGylated cationic liposomes be used with caution, as their effects varied with each of the cytofectins used in this study. Post-inserting PEG on preformed siRNA lipoplexes is conceivably a viable option to ameliorate some of the negative effects of using PEG. This strategy demonstrably offers better siRNA binding capacity, as well as the potential for masking siRNAs and protecting them from nuclease attack.

Future recommendations may involve optimizing PEGylated liposomal formulations by varying the percentage of PEG derivatives as well as the use of different molecular weights of PEG. Future studies aims at testing the ability of these cationic lipid based nanocarriers to safely and efficiently deliver target siRNA into a HER2/*neu* overexpressed animal model for evaluation *in vivo*. Although the conclusions obtained from this study provide evidence of efficient siRNA gene delivery in the presence of serum, it should be noted that the most efficient nanocarrier in cell culture may not always be the best performer *in vivo*. Additional work to evaluate modes of cell association, as well as, elucidating how the various formulations influence cellular

internalization capacity and endosomal release mechanisms may also be explored. Both pharmacokinetic and pharmacodynamic profiles are necessary to effectively predict the kinetic routes and the association of HER2/*neu* siRNA to its target. To conclude, given their biocompatibility and superior transfection efficiency as compared with the commercial transfection agent, the use of these cationic liposomes offers a promising and attractive alternative for siRNA gene therapy *in vivo*.

CHAPTER SIX

REFERENCES

6.1 Cited Literature

Aagaard, L., and J. J. Rossi. 2007. RNAi therapeutics: principles, prospects and challenges. Advanced Drug Delivery Reviews **59:** 75-86.

Aigner, A. 2006. Delivery systems for the direct application of siRNAs to induce RNA interference (RNAi) *in vivo*. Journal of Biomedicine and Biotechnology **doi** 0.1155/JBB/2006/71659.

Akhtar, S., and I. Benter. 2007. Toxicogenomics of non-viral drug delivery systems for RNAi: Potential impact on siRNA-mediated gene silencing activity and specificity. Advanced Drug Delivery Reviews **59:** 164-182.

Al-Dosari, M. S., and X. Gao. 2009. Nonviral gene delivery: principle, limitations, and recent progress. The AAPS Journal **11:** 671-681.

Aliabadi, H. M., B. Landry, R. K. Bahadur, A. Neamnark, O. Suwantong, and H. Uludağ. 2011. Impact of lipid-substitution on assembly and delivery of siRNA by cationic polymers. Macromolecular Bioscience **11:** 662-672.

Aliabadi, H. M., B. Landry, P. Mahdipoor, Y. M. Charlie, and H. H. Uludağ. 2012. Effective down-regulation of Breast Cancer Resistance Protein (BCRP) by siRNA delivery using lipid-substituted aliphatic polymers. European Journal of Pharmaceutics and Biopharmaceutics **81:** 33-42.

Allard, S. T. M., and K. Kopish. 2008. Luciferase reporter assays: Powerful, adaptable tools for cell biology research. Cell Notes **21:** 23-26.

Allen, T. M. 1989. Stealth liposomes: Avoiding reticuloendothelial uptake. ***In.*** Lopez-Berestein, G., I. Fidler, ed. Liposomes in the therapy of infectious disease and cancer, UCLA symposium in molecular and cellular biology. Boca Raton, Florida: CRC Press; p. 405-415.

Allen, T. M., C. Hansen, F. Martin, C. Redemann, and A. Yau-Young. 1991. Liposomes containing synthetic lipid derivatives of poly(ethylene glycol) show prolonged circulation half-lives *in vivo*. Biochimica et Biophysica Acta **1066:** 29-36.

Allred, D. C., S. K. Mohsin, and S. A. Fuqua. 2001. Histological and biological evolution of human premalignant breast disease. Endocrine-Related Cancer **8:** 47-61.

Almofti, M. R., H. Harashima, Y. Shinohara, A. Almofti, W. Li, and H. Kiwada. 2003. Lipoplex size determines lipofection efficiency with or without serum. Molecular Membrane Biology **20:** 35-43.

Alonso, A., J. Sasin, N. Bottini, I. Friedberg, I. Friedberg, A. Osterman, A. Godzik, T. Hunter, J. Dixon, and T. Mustelin. 2004. Protein tyrosine phosphatases in the human genome. Cell **117:** 699-711.

Amarzguioui, M., J. J. Rossi, and D. Kim. 2005. Approaches for chemically synthesized siRNA and vector-mediated RNAi. FEBS Letters **579:** 5974-5981.

American Cancer Society (ACS), Available at: http://www.cancer.org/acs/groups/cid/documents/webcontent/003090-pdf.pdf. Accessed October 08, 2015.

Anderson, W. F. 1998. Human gene therapy. Nature **392:** 25-30.

Anderson, S. M., M. C. Rudolph, J. L. McManaman, and M. C. Neville. 2007. Key stages in mammary gland development. Secretory activation in the mammary gland: it's not just about milk protein synthesis! Breast Cancer Research **9:** 204.

Anido, J., M. Scaltriti, J. J Bech Serra, B. Santiago Josefat, F. R. Todo, J. Baselga, and J. Arribas. 2006. Biosynthesis of tumorigenic HER2 C-terminal fragments by alternative initiation of translation. The EMBO Journal **25:** 3234-3244.

Ariatti, M. 2015. Liposomal formulation of monovalent cholesteryl cytofectins with acyclic head groups and gene delivery: A systematic review. Current Pharmaceutical Biotechnology **16:** 871-881.

Arouri, A., and O. G. Mouritsen. 2013. Membrane-perturbing effect of fatty acids and lysolipids. Progress in Lipid Research **52:** 130-140.

Audouy, S., G. Molema, L. De Leij, and D. Hoekstra. 2000. Serum as a modulator of lipoplex-mediated gene transfection: Dependence of amphiphile, cell type and complex stability. Journal of Gene Medicine **2:** 465-476.
Awada, A., I. Bozovic-Spasojevic, and L. Chow. 2012. New therapies in HER2-positive breast cancer: A major step towards a cure of the disease? Cancer Treatment Reviews **38:** 494-504.
Azim, H., and H. A. Azim Jr. 2008. Targeting Her-2/*neu* in breast cancer: as easy as this! Oncology **74:** 150-157.
Bachelder, R. E., A. Crago, J. Chung, M. A. Wendt, L. M. Shaw, G. Robinson, and A. M. Mercurio. 2001. Vascular endothelial growth factor is an autocrine survival factor for neuropilin-expressing breast carcinoma cells. Cancer Research **61:** 5736-5740.
Balbino, T. A., A. A. M. Gasperini, C. L. P. Oliveira, A. R. Azzoni, L. P. Cavalcanti, and L. G. de La Torre. 2012. Correlation of the physicochemical and structural properties of pDNA/cationic liposome complexes with their *in vitro* transfection. Langmuir **28:** 11535-11245.
Baldwin, T. O. 1996. Firefly luciferase: the structure is known, but the mystery remains. Structure **4:** 223-238.
Banerjee, R., P. K. Das, G. V. Srilakshmi, A. Chaudhuri, and N. M. Rao. 1999. Novel series of non-glycerol-based cationic transfection lipids for use in liposomal gene delivery. Journal of Medicinal Chemistry **42:** 4292-4299.
Bangham, A. D., M. M. Standish, and J. C. Watkins. 1965. Diffusion of univalent ions across the lamellae of swollen phospholipids. Journal of Molecular Biology **13:** 238-252.
Barichello, J. M., S. Kizuki, T. Tagami, L. A. L. Soares, T. Ishida, H. Kikuchi, and H. Kiwada. 2012. Agitation during lipoplex formation harmonizes the interaction of siRNA to cationic liposomes. International Journal of Pharmaceutics **430:** 359-365.
Bartlett, D. W., and M. E. Davis. 2006. Insights into the kinetics of siRNA-mediated gene silencing from live-cell and live-animal bioluminescent imaging. Nucleic Acids Research **34:** 322-333.
Bartsch, R., C. Wenzel, C. C. Zielinski, and G. G. Steger. 2007. HER-2-positive breast cancer: hope beyond trastuzumab. BioDrugs **21:** 69-77.
Bauer, K., C. Parise, and V. Caggiano. 2010. Use of ER/PR/HER2 subtypes in conjunction with the 2007 St Gallen Consensus Statement for early breast cancer. BMC Cancer **10:** 228.
Bazley, L. A., and W. J. Gullick. 2005. The epidermal growth factor receptor family. Endocrine-Related Cancer **12:** S17-S27.
Bedi, D., T. Musacchio, O. A. Fagbohun, J. W. Gillespie, P. Deinnocentes, R. C. Bird, L. Bookbinder, V. P. Torchilin, and V. A. Petrenko. 2011. Delivery of siRNA into breast cancer cells via phage fusion protein-targeted liposomes. Nanomedicine: Nanotechnology, Biology, and Medicine **7:** 315-323.
Beh, C. W., W. Y. Seow, Y. Wang, Y. Zhang, Z. Y. Ong, P. L. R. Ee, and Y. Y. Yang. 2009. Efficient delivery of Bcl-2-targeted siRNA using cationic polymer nanoparticles: downregulating mRNA expression level and sensitizing cancer cells to anticancer drug. Biomacromolecules **10:** 41-48.
Behr, J. P., B. Demeneix, J. P. Loeffler, and J. Perez-Mutul. 1989. Efficient gene-transfer into mammalian primary endocrine-cells with lipopolyamine-coated DNA. Proceedings of the National Academy of Sciences of the United States of America **86:** 6982-6986.
Belletti, D., M. Tonelli, F. Forni, G. Tosi, M. A. Vandelli, and B. Ruozi. 2013. AFM and TEM characterization of siRNAs lipoplexes: A combinatory tools to predict the efficacy of complexation. Colloids and Surfaces A: Physicochemical and Engineering Aspects **436:** 459-466.
Belletti, D., G. Tosi, F. Forni, I. Lagreca, P. Barozzi, F. Pederzoli, M. A. Vandelli, G. Riva, M. Luppi, and B. Ruozi. 2016. PEGylated siRNA lipoplexes for silencing of BLIMP-1 in Primary Effusion Lymphoma: *In vitro* evidences of antitumoral activity. European Journal of Pharmaceutics and Biopharmaceutics **99:** 7-17.
Benson, J. R., and I. Jatoi. 2012. The global breast cancer burden. Future Oncology **8:** 697-702.

Bergan, D., T. Galbraith, and D. L. Sloane. 2000. Gene transfer *in vitro* and *in vivo* by cationic lipids is not significantly affected by levels of supercoiling of a reporter plasmid. Pharmaceutical Research **17:** 967-973.
Bertos, N. R., and M. Park. 2011. Breast cancer - one term, many entities? The Journal of Clinical Investigation **121:** 3789-3796.
Boeckle, S., K. von Gersdorff, S. van der Piepen, C. Culmsee, E. Wagner, and M. Ogris. 2004. Purification of polyethylenimine polyplexes highlights the role of free polycations in gene transfer. The Journal of Gene Medicine **6:** 1102-1111.
Bologna, J. C., G. Dorn, F. Natt, and J. Weiler. 2003. Linear polyethyleneimine as a tool for comparative studies of antisense and short double-stranded RNA oligonucleotides. Nucleosides, Nucleotides and Nucleic Acids **22:** 1729-1731.
Boomer, J. A., D. H. Thompson, and S. M. Sullivan. 2002. Formation of plasmid based transfection complexes with an acid-labile cationic lipid: characterization of *in vitro* and *in vivo* gene transfer. Pharmaceutical Research **19:** 1292-1301.
Bose, R., S. M. Kavuri, A. C. Searleman, W. Shen, D. Shen, D. C. Koboldt, J. Monsey, N. Goel, A. B. Aronson, S. Li, C. X. Ma, L. Ding, E. R. Mardis, and M. J. Ellis. 2013. Activating HER2 mutations in HER2 gene amplification negative breast cancer. Cancer Discovery **3:** 224-237.
Boudreau, N., and C. Myers. 2003. Breast cancer-induced angiogenesis: multiple mechanisms and the role of the microenvironment. Breast Cancer Research **5:** 140-146.
Braasch, D. A., Z. Paroo, A. Constantinescu, G. Ren, O. K. Oz, R. P. Mason, and D. R. Corey. 2004. Biodistribution of phosphodiester and phosphorothioate siRNA. Bioorganic and Medicinal Chemistry Letters **14:** 1139-1143.
Brar, S. K., and M. Verma. 2011. Measurement of nanoparticles by light-scattering techniques. TrAC Trends in Analytical Chemistry **30:** 4-17.
Brisken, C., and R. D. Rajaram. 2006. Alveolar and lactogenic differentiation. Journal of Mammary Gland Biology and Neoplasia **11:** 239-248.
Brisken, C., and B. O'Malley. 2010. Hormone action in the mammary gland. Cold Spring Harbor Perspectives in Biology **doi** 10.1101/cshperspect.a003178.
Browne, B. C., J. Crown, N. Venkatesan, M. J. Duffy, M. Clynes, D. Slamon, and N. O'Donovan. 2011. Inhibition of IGF1R activity enhances response to trastuzumab in HER-2-positive breast cancer cells. Annals of Oncology **22:**68-73.
Brunner, S., T. Sauer, S. Carotta, M. Cotton, M. Saltik, and E. Wagner. 2000. Cell cycle dependence of gene transfer by lipoplex, polyplex and recombinant adenovirus. Gene Therapy **7:** 401-407.
Buchholz, T. A., A. K. Garg, N. Chakravarti, B. B. Aggarwal, F. J. Esteva, H. M. Kuerer, S. E. Singletary, G. N. Hortobagyi, L. Pusztai, M. Cristofanilli, and A. A. Sahin. 2005. The nuclear transcription factor κB/bcl-2 pathway correlates with pathologic complete response to doxorubicin-based neoadjuvant chemotherapy in human breast cancer. Clinical Cancer Research **11:** 8398-8402.
Bugs, M. R., and M. L. Cornelio. 2001. Analysis of the ethidium bromide bound to DNA by photoacoustic and FTIR spectroscopy. Photochemistry and Photobiology **74:** 512-520.
Bumcrot, D., M. Manoharan, V. Koteliansky, and D. W. Sah. 2006. RNAi therapeutics: a potential new class of pharmaceutical drugs. Nature Chemical Biology **2:** 711-719.
Burgess, A. W. 2008. EGFR family: structure physiology signalling and therapeutic targets. Growth Factors **26:** 263-274.
Burgess, A. W., H. S. Cho, C. Eigenbrot, K. M. Ferguson, T. P. Garrett, and D. J. Leahy. 2003. An open and-shut case? Recent insights into the activation of EGF/ErbB receptors. Molecular Cell **12:** 541-152.
Burstein, H. J., K. Polyak, J. S. Wong, S. C. Lester, and C. M. Kaelin. 2004. Ductal carcinoma *in situ* of the breast. The New England Journal of Medicine **350:** 1430-1441.

Buyens, K., B. Lucas, K. Raemdonck, K. Braeckmans, J. Vercammen, J. Hendrix, Y. Engelborghs, S. C. De Smedt, and N. N. Sanders. 2008. A fast and sensitive method for measuring the integrity of siRNA-carrier complexes in full human serum. Journal of Controlled Release **126:** 67-76.

Buyens, K., J. Demeester, S. C. De Smedt, and N. N. Sanders. 2009. Elucidating the encapsulation of short interfering RNA in PEGylated cationic liposomes. Langmuir **25:** 4886-4891.

Buyens, K., S. C. De Smedt, K. Braeckmans, J. Demeester, L. Peeters, L. A. van Grunsven, X. de Mollerat du Jeu, R. Sawant, V. Torchilin, K. Farkasova, M. Ogris, and N. N. Sanders. 2012. Liposome based systems for systemic siRNA delivery: Stability in blood sets the requirements for optimal carrier design. Journal of Controlled Release **158:** 362-370.

Campone, M., P. Juin, F. André, and T. Bachelot. 2011. Resistance to HER2 inhibitors: Is addition better than substitution? Rationale for the hypothetical concept of drug sedimentation. Critical Reviews in Oncology/Hematology **78:** 195-205.

Candiani, G., D. Pezzoli, L. Ciani, R. Chiesa, and S. Ristori. 2010. Bioreducible liposomes for gene delivery: From the formulation to the mechanism of action. PLoS ONE **5:** 1-8.

Caracciolo, G. 2015. Liposome-protein corona in a physiological environment: Challenges and opportunities for targeted delivery of nanomedicines. Nanomedicine: Nanotechnology, Biology, and Medicine **11:** 543-557.

Caracciolo, G., L. Callipo, S. C. De Sanctis, C. Cavaliere, D. Pozzi, and A. Laganà. 2010. Surface adsorption of protein corona controls the cell internalization mechanism of DC-Chol-DOPE/DNA lipoplexes in serum. Biochimica et Biophysica Acta **1798:** 536-543.

Caudy, A. A., R. F. Ketting, S. M. Hammond, A. M. Denli, A. M. P. Bathoorn, B. B. J. Tops, J. M. Silva, M. M. Myers, G. J. Hannon, and R. H. A. Plasterk. 2003. A micrococcal nuclease homologue in RNAi effector complexes. Nature **425:** 411- 414.

Celedon, A., D. Wirtz, and S. Sun. 2010. Torsional mechanics of DNA are regulated by small-molecule intercalation. The Journal of Physical Chemistry. B. **114:** 16929-16935.

Chen, C. W., D. W. Lu, M. K. Yeh, C. Y. Shiau, and C. H. Chiang. 2011. Novel RGD-lipid conjugate-modified liposomes for enhancing siRNA delivery in human retinal pigment epithelial cells. International Journal of Nanomedicine **6:** 2567-2580.

Cheung, C. Y., P. S. Stayton, and A. S. Hoffman. 2005. Poly(propylacrylic acid)-mediated serum stabilization of cationic lipoplexes. Journal of Biomaterials Science **16:** 163-179.

Cho, H. S., K. Mason, K. X. Ramyar, A. M. Stanley, S. B. Gabelli, D. W. Denney Jr, and D. J. Leahy. 2003. Structure of the extracellular region of HER2 alone and in complex with the Herceptin Fab. Nature **421:** 756-760.

Chonn, A., S. C. Semple, and P. R. Cullis. 1992. Association of blood proteins with large unilamellar liposomes *in vivo*. Relation to circulation lifetimes. The Journal of Biological Chemistry **267:** 18759-18765.

Citri, A., and Y. Yarden. 2006. EGF-ERBB signaling: towards the systems level. Nature Reviews. Molecular Cell Biology **7:** 505-516.

Clogston, J., and A. Patri. 2011. Zeta potential measurement. ***In.*** McNeil, S. E., ed. Characterization of nanoparticles intended for drug delivery. Humana Press; p. 63-70.

Colditz, G. A., B. A. Rosner, W. Y. Chen, M. D. Holmes, and S. E. Hankinson. 2004. Risk factors for breast cancer according to estrogen and progesterone receptor status. Journal of the National Cancer Institude **96:** 218-228.

Collins, D., A. D. K. Hill, and L. Young. 2009. Lapatinib: A competitor or companion to trastuzumab? Cancer Treatment Reviews **35:** 574-581.

Colombo, M., F. Corsi, D. Foschi, E. Mazzantini, S. Mazzucchelli, C. Morasso, E. Occhipinti, L. Polito, D. Prosperi, S. Ronchi, and P. Verderio. 2010. HER2 targeting as a two-sided strategy for breast cancer diagnosis and treatment: Outlook and recent implications in nanomedical approaches. Pharmacological Research **62:** 150-165.

Cotterchio, M., N. Kreiger, B. Theis, M. Sloan, and S. Bahl. 2003. Hormonal factors and the risk of breast cancer according to estrogen- and progesterone-receptor subgroup. Cancer Epidemiology, Biomarkers and Prevention **12:** 1053-1060.

Coussens, L., T. L. Yang-Feng, Y. C. Liao, E. Y. Chen, A. Gray, J. McGrath, P. H. Seeburg, T. A. Libermann, J. J. Schlessinger, U. Francke, A. Levinson, and A. Ullrich. 1985. Tyrosine kinase receptor with extensive homology to EGF receptor shares chromosomal location with *neu* oncogene. Science **230:** 1132-1139.

Cowin, P., and J. Wysolmerski. 2010. Molecular mechanisms guiding embryonic mammary gland development. Cold Spring Harbor Perspectives in Biology **doi** 10.1101/cshperspect.a003251.

Creixell, M., and N. A. Peppas. 2012. Co-delivery of siRNA and therapeutic agents using nanocarriers to overcome cancer resistance. Nano Today **7:** 367-379.

D'Amato, V., L. Raimondo, L. Formisano, M. Giuliano, S. De Placido, R. Rosa, and R. Bianco. 2015. Mechanisms of lapatinib resistance in HER2-driven breast cancer. Cancer Treatment Reviews **41:** 877-883.

Dams, E. T., P. Laverman, W. J. Oyen, G. Storm, G. L. Scherphof, J. W. van DerMeer, F. H. Corstens, and O. C. Boerman. 2000. Accelerated blood clearance and altered biodistribution of repeated injections of sterically stabilized liposomes. The Journal of Pharmacology and Experimental Therapeutics **292:** 1071-1079.

Dass, C. R. 2002. Vehicles for oligonucleotide delivery: therapeutic applicability against tumors. The Journal of Pharmacy and Pharmacology **54:** 3-27.

Dass, C. R. 2004. Lipoplex-mediated delivery of nucleic acids: factors affecting *in vivo* transfection. Journal of Molecular Medicine **82:** 579-591.

David, S., B. Pitard, J. P. Benoît, and C. Passira. 2010. Non-viral nanosystems for systemic siRNA delivery. Pharmacological Research **62:** 100-114.

Davidoff, A. M., and A. C. Nathwani. 2004. Antiangiogenic gene therapy for cancer treatment. Current Hematology Reports **3:** 267-273.

Davis, M. E. 2009. The first targeted delivery of siRNA in humans via a self-assembling, cyclodextrin polymer-based nanoparticle: from concept to clinic. Molecular Pharmaceutics **6:** 659-668.

Dean-Colomb, W., and F. J. Esteva. 2008. Her2-positive breast cancer: Herceptin and beyond. European Journal of Cancer **44:** 2806-2812.

de Fougerolles, A. R. 2008. Delivery vehicles for small interfering RNA *in vivo*. Human Gene Therapy **19:** 125-132.

de Fougerolles, A., H. P. Vornlocher, J. Maraganore, and J. Lieberman. 2007. Interfering with disease: a progress report on siRNA-based therapeutics. Nature Reviews. Drug Discovery **6:** 443-453.

de Gennes, P. G. 1980. Conformations of polymers attached to an interface. Macromolecules **13:** 1069-1075.

de Gennes, P. G. 1987. Polymers at an interface-a simplified view. Advances in Colloid and Interface Science **27:** 189-209.

de Martimprey, H., C. Vauthier, C. Malvy, and P. Couvreur. 2009. Polymer nanocarriers for the delivery of small fragments of nucleic acids: oligonucleotides and siRNA. European Journal of Pharmaceutics and Biopharmaceutics **71:** 490-504.

Derveaux, S., J. Vandesompele, and J. Hellemans. 2010. How to do successful gene expression analysis using real-time PCR. Methods **50:** 227-230.

DeSantis, C., R. Siegel, P. Bandi, and A. Jamal. 2011. "Breast cancer statistics, 2011," CA: A Cancer Journal for Clinicians **61:** 408-418.

Desigaux, L., M. Sainlos, O. Lambert, R. Chevre, E. Letrou-Bonneval, J. P. Vigneron, P. Lehn, J. M. Lehn, and B. Pitard. 2007. Self-assembled lamellar complexes of siRNA with lipidic aminoglycoside derivatives promote efficient siRNA delivery and interference. Proceedings of the National Academy of Sciences of the United States of America **104:** 16534-16539.

DiFiglia, M., M. Sena-Esteves, K. Chase, E. Sapp, E. Pfister, M. Sass, J. Yoder, P. Reeves, R. K. Pandey, K. G. Rajeev, M. Manoharan, D. W. Sah, P. D. Zamore, and N. Aronin. 2007. Therapeutic silencing of mutant Huntingtin with siRNA attenuates striatal and cortical neuropathology and behavioral deficits. Proceedings of the National Academy of Sciences of the United States of America **104:** 17204-17209.

Doench, J. G., C. P. Petersen, and P. A. Sharp. 2003. siRNAs can function as miRNAs. Genes and Development **17:** 438-442.

Doherty, G. J., and H. T. McMahon. 2009. Mechanisms of endocytosis. Annual Review of Biochemistry **78:** 857-902.

Doisneau-Sixou, S. F., C. M. Sergio, J. S. Carroll, R. Hui, E. A. Musgrove, and R. L. Sutherland. 2003. Estrogen and antiestrogen regulation of cell cycle progression in breast cancer cells. Endocrine-Related Cancer **10:** 179-186.

Dos Santos, N., C. Allen, A. M. Doppen, M. Anantha, K. A. K. Cox, R. C. Gallagher, G. Karlsson, K. Edwards, G. Kenner, L. Samuels, M. S. Webb, and M. B. Bally. 2007. Influence of poly(ethylene glycol) grafting density and polymer length on liposomes: Relating plasma circulation lifetimes to protein binding. Biochimica et Biophysica Acta **1768:** 1367-1377.

Dou, S., Y. D. Yao, X. Z. Yang, T. M. Sun, C. Q. Mao, E. W. Song, and J. Wang. 2012. Anti-Her2 single-chain antibody mediated DNMTs-siRNA delivery for targeted breast cancer therapy. Journal of Controlled Release **161:** 875-883.

Drummond, D. C., O. Meyer, K. Hong, D. B. Kirpotin, and D. Papahadjopoulos. 1999. Optimizing liposomes for delivery of chemotherapeutic agents to solid tumors. Pharmacological Reviews **51:** 691-743.

Dvorak, H. K., J. A. Nagy, D. Feng, L. F. Brown, and A. M. Dvorak. 1999. Vascular permeability factor/vascular endothelial growth factor and the significance of microvascular hyperpermeability in angiogenesis. Current Topics in Microbiology and Immunology **237:** 97-132.

Edelstein, M., M. Abedi, J. Wixon, and R. Edelstein. 2004. Gene therapy clinical trials worldwide 1989-2004 - an overview. The Journal of Gene Medicine **6:** 597-602.

Edelstein, M., M. Abedi, and J. Wixon. 2007. Gene therapy clinical trials worldwide to 2007 - an update. The Journal of Gene Medicine **9:** 833-842.

Elbashir, S. M., W. Lendeckel, and T. Tuschl. 2001. RNA interferences is mediated by 21- and 22-nucleotide RNAs. Genes and Development **15:** 188-200.

Elledge, R. M., and D. C. Allred. 1994. The p53 tumor suppressor gene in breast cancer. Breast Cancer Research and Treatment **32:** 39-47.

Engel, R. H., and V. G. Kaklamani. 2007. HER2-positive breast cancer: current and future treatment strategies. Drugs **67:** 1329-1341.

Eroles, P., A. Bosch, J. A. Pérez-Fidalgo, and A. Lluch. 2012. Molecular biology in breast cancer: Intrinsic subtypes and signaling pathways. Cancer Treatment Reviews **38:** 698-707.

Ewert, K., A. Ahmad, H. M. Evans, H. W. Schmidt, and C. R. Safinya. 2002. Efficient synthesis and cell-transfection properties of a new multivalent cationic lipid for nonviral gene delivery. Journal of Medicinal Chemistry **45:** 5023-5029.

Ewert, K., N. L. Slack, A. Ahmad, H. M. Evans, A. J. Lin, C. E. Samuel, and C. R. Safinya. 2004. Cationic lipid-DNA complexes for gene therapy: understanding the relationship between complex structure and gene delivery pathways at the molecular level. Current Medicinal Chemistry **11:** 133-149.

Ewert, K. K., A. Ahmad, H. M. Evans, and C. R. Safinya. 2005. Cationic lipid-DNA complexes for non-viral gene therapy: relating supramolecular structures to cellular pathways. Expert Opinion on Biological Therapy **5:** 33-53.

Ewert, K. K., H. M. Evans, A. Zidovska, N. F. Bouxsein, A. Ahmad, and C. R. Safinya. 2006. A columnar phase of dendritic lipid-based cationic liposome-DNA complexes for gene delivery: hexagonally ordered cylindrical micelles embedded in a DNA honeycomb lattice. Journal of the American Chemistry Society **128:** 3998-4006.

Fan, F., and K. Wood. 2007. Bioluminescent assays for high-throughput screening. Assay and Drug Development Technologies **5:** 127-136.
Faneca, H., A. Faustino, and M.C. Pedroso de Lima. 2008. Synergistic antitumoral effect of vinblastine and HSV-Tk/GCV gene therapy mediated by albumin-associated cationic liposomes. Journal of Controlled Release **126:** 175-184.
Farhood, H., N. Serbina, and L. Huang. 1995. The role of dioleoylphosphatidylethanolamine in cationic liposome mediated gene transfer. Biochimica et Biophysica Acta **1235:** 289-295.
Fatemian, T., L. Othman, and E. H. Chowdhury. 2014. Strategies and validation for siRNA-based therapeutics for the reversal of multi-drug resistance in cancer. Drug Discovery Today **19:** 71-78.
Felgner, P. L., T. R. Gadek, M. Holm, R. Roman, H. W. Chan, M. Wenz, J. P. Northrop, G. M. Ringold, and M. Danielsen. 1987. Lipofection: a highly efficient, lipid-mediated DNA-transfection procedure. Proceedings of the National Academy of Sciences of the United States of America **84:** 7413-7417.
Felgner, J. H., R. Kumar, C. N. Sridhar, C. J. Wheeler, Y. J. Tsai, R. Border, P. Ramsey, M. Martin, and P. L. Felgner. 1994. Enhanced gene delivery and mechanism studies with a novel series of cationic lipid formulations. The Journal of Biological Chemistry **269:** 2550-2561.
Felgner, P. L., Y. Barenholz, J. P. Behr, S. H. Cheng, P. Cullis, L. Huang, J. A. Jessee, L. Seymour, F. Szoka, A. R. Thierry, E. Wagner, and G. Wu. 1997. Nomenclature for synthetic gene delivery systems. Human Gene Therapy **8:** 511-512.
Fenske, D. B., and P. R. Cullis. 2008. Liposomal nanomedicines. Expert Opinion on Drug Delivery **5:** 25-44.
Ferlini, C., G. Raspaglio, S. Mozzetti, M. Distefano, F. Filippetti, E. Martinelli, G. Ferrandina, D. Gallo, F. O. Ranelletti, and G. Scambia. 2003. Bcl-2 down-regulation is a novel mechanism of paclitaxel resistance. Molecular Pharmacology **64:** 51-58.
Fernández Val, J. F., J. Losada, M. A. Arregui Murua, and R. Sarría. 2002. Cell proliferation, nuclear ploidy, and EGFR and HER2/*neu* tyrosine kinase oncoproteins in infiltrating ductal breast carcinoma. Cancer Genetics and Cytogenetics **138:** 69-72.
Figueroa-Magalhães, M. C., D. Jelovac, R. M. Connolly, and A. C. Wolff. 2014. Treatment of HER2-positive breast cancer. The Breast **23:** 128-136.
Fire, A., S. Xu, M. K. Montgomery, S. A. Kostas, S. E. Driver, and C. C. Mello. 1998. Potent and specific genetic interference by double-stranded RNA in *Caenorhabditis elegans*. Nature **391:** 806-911.
Fischer, A., and M. Cavazzana-Calvo. 2008. Gene therapy of inherited diseases. Lancet **371:**2044-2047
Fleishman, S. J., J. Schlessinger, and N. Ben-Tal. 2002. A putative molecular-activation switch in the transmembrane domain of erbB2. Proceedings of the National Academy of Sciences of the United States of America **99:** 15937-15940.
Fletcher, S., A. Ahmad, E. Perouzel, M. R. Jorgensen, and A. D. Miller. 2006. A dialkynoyl analogue of DOPE improves gene transfer of lower-charged, cationic lipoplexes. Organic and Biomolecular Chemistry **4:** 196-199.
Fletcher, S., A. Ahmad, W. S. Price, M. R. Jorgensen, and A. D. Miller. 2008. Biophysical properties of CDAN/DOPE-analogue lipoplexes account for enhanced gene delivery. Chembiochem **9:** 455-463.
Floch, V., S. Loisel, E. Guenin, A. C. Herve, J. C. Clement, J. J. Yaouanc, H. des Abbayes, and C. Ferec. 2000. Cation substitution in cationic phosphonolipids: a new concept to improve transfection activity and decrease cellular toxicity. Journal of Medicinal Chemistry **30:** 4617-4628.
Foged, C., H. M. Nielsen, and S. Frokjaer. 2007. Liposomes for phospholipase A2 triggered siRNA release: preparation and *in vitro* test. International Journal of Pharmaceutics **331:** 160-166.
Forsythe, J. A., B. H. Jiang, N. V. Iyer, F. Agani, S. W. Leung, R. D. Koos, and G. L. Semenza. 1996. Activation of vascular endothelial growth factor gene transcription by hypoxia-inducible factor 1. Molecular and Cellular Biology **16:** 4604-4613.

Foster, F. M., T. W. Owens, J. T. Hughes, R. B. Clarke, K. Brennan, N. J. Bundred, and C. H. Streuli. 2009. Targeting inhibitor of apoptosis proteins in combination with ErbB antagonists in breast cancer. Breast Cancer Research **11:** R41 **doi** 10.1186/bcr2328.

Friedrich, H., P. M. Frederik, G. de With, and N. A. J. M. Sommerdijk. 2010. Imaging of self-assembled structures: interpretation of TEM and cryo-TEM images. Angewandte Chemie International Edition **49:** 7850-7858.

Frohlich, T., and E. Wagner. 2010. Peptide- and polymer-based delivery of therapeutic RNA. Soft Matter **6:** 226-234.

Fulda, S. 2007. Inhibitor of apoptosis proteins as targets for anticancer therapy. Expert Review of Anticancer Therapy **7:** 1255-1264.

Gabizon, A. A., H. Shmeeda, and S. Zalipsky. 2006. Pros and cons of the liposome platform in cancer drug targeting. Journal of Liposome Research **16:** 175-183.

Gao, X., and L. Huang. 1991. A novel cationic liposome reagent for efficient transfection of mammalian cells. Biochemical and Biophysical Research Communications **179:** 280-285.

Gao, X., and L. Huang. 1995. Cationic liposome-mediated gene transfer. Gene Therapy **2:** 710-722.

Gao, H., and K. M. Hui. 2001. Synthesis of a novel series of cationic lipids that can act as efficient gene delivery vehicles through systematic heterocyclic substitution of cholesterol derivatives. Gene Therapy **8:** 855-863.

Gao, J., J. Sun, H. Li, W. Liu, Y. Zhang, B. Li, W. Qian, H. Wang, J. Chen, and Y. Guo. 2010. Lyophilized HER2-specific PEGylated immunoliposomes for active siRNA gene silencing. Biomaterials **31:** 2655-2664.

Gao, J., W. Liu, Y. Xia, W. Li, J. Sun, H. Chen, B. Li, D. Zhang, W. Qian, Y. Meng, L. Deng, H. Wang, J. Chen, and Y. Guo. 2011. The promotion of siRNA delivery to breast cancer overexpressing epidermal growth factor receptor through anti-EGFR antibody conjugation by immunoliposomes. Biomaterials **32:** 3459-3470.

Garbuzenko, O., Y. Barenholz, and A. Priev. 2005. Effect of grafted PEG on liposome size and on compressibility and packing of lipid bilayer. Chemistry and Physics of Lipids **135:** 117-129.

Garrett, T. P., N. M. McKern, M. Lou, T. C. Elleman, T. E. Adams, G. O. Lovrecz, M. Kofler, R. N. Jorissen, E. C. Nice, A. W. Burgess, and C. W. Ward. 2003. The crystal structure of a truncated ErbB2 ectodomain reveals an active conformation, poised to interact with other ErbB receptors. Molecular Cell **11:** 495-505.

Gary, D. J., N. Puri, and Y. Y. Won. 2007. Polymer-based siRNA delivery: perspectives on the fundamental and phenomenological distinctions from polymer-based DNA delivery. Journal of Controlled Release **121:** 64-73.

Gaumet, M., A. Vargas, R. Gurny, and F. Delie. 2008. Nanoparticles for drug delivery: the need for precision in reporting particle size parameters. European Journal of Pharmaceutical and Biopharmaceutics **69:** 1-9.

Geyer, C. E., J. Forster, D. Lindquist, S. Chan, C. G. Romieu, T. Pienkowski, A. Jagiello-Gruszfeld, J. Crown, A. Chan, B. Kaufman, D. Skarlos, M. Campone, N. Davidson, M. Berger, C. Oliva, S. D. Rubin, S. Stein, and D. Cameron. 2006. Lapatinib plus capecitabine for HER2-positive advanced breast cancer. The New England Journal of Medicine **355:** 2733-2743.

Gjetting, T., N. S. Arildsen, C. L. Christensen, T. T. Poulsen, J. A. Roth, V. N. Handlos, and H. S. Poulsen. 2010. *In vitro* and *in vivo* effects of polyethylene glycol (PEG)-modified lipid in DOTAP/cholesterol mediated gene transfection. International Journal of Nanomedicine **5:** 371-383.

Giacca, M. 2010. Gene Therapy. New York, N. Y.: Springer; p. 9-43.

García, L., M. Bũnuales, N. Düzgünes, and T. de Ilarduya. 2007. Serum resistant lipopolyplexes for gene delivery to liver tumour cells. European Journal of Pharmaceutics and Biopharmaceutics **92:** 2373-2385.

Goldhirsch, J. N., R. D. Ingle, A. S. Gelber, B. Coates, H. Thürlimann, and J. SennPanel Members. 2009. Thresholds for therapies: highlights of the St Gallen International Expert Consensus on the primary therapy of early breast cancer. Annals of Oncology **20:** 1319-1329.

Gomes-da-Silva, L. C., A. O. Santos, L. M. Bimbo, V. Moura, J. S. Ramalho, M. C. Pedroso de Lima, S. Simõesa, and J. N. Moreira. 2012. Toward a siRNA-containing nanoparticle targeted to breast cancer cells and the tumor microenvironment. International Journal of Pharmaceutics **434:** 9-19.

Gottesman, M. M. 2002. Mechanisms of cancer drug resistance. Annual Review of Medicine **53:** 615-627.

Graham, A., D. Adeloye, L. Grant, E. Theodoratou, and H. Campbell. 2012. Estimating the incidence of colorectal cancer in Sub-Saharan Africa: a systematic analysis. Journal of Global Health **doi** 10.7189/jogh.02.020204.

Graus-Porta, D., R. R. Beerli, J. M. Daly, and N. E. Hynes. 1997. ErbB-2, the preferred heterodimerization partner of all ErbB receptors, is a mediator of lateral signaling. The EMBO Journal **16:** 1647-1655.

Grimm, D., and M. A. Kay. 2007. RNAi and gene therapy: a mutual attraction. American Society of Hematology **2007:** 473-481.

Grimm, D., K. L. Streetz, C. L. Jopling, T. A. Storm, K. Pandey, C. R. Davis, P. Marion, F. Salazar, and M. A. Kay. 2006. Fatality in mice due to oversaturation of cellular microRNA/short hairpin RNA pathways. Nature **441:** 537-541.

Gruner, S. M., P. R. Cullis, M. J. Hope, and C. P. S. Tilcock. 1985. Lipid polymorphism: the molecular basis of nonbilayer phases. Annual Review of Biophysics and Biophysical Chemistry **14:** 211-238.

Grzelinski, M., B. Urban-Klein, T. Martens, K. Lamszus, U. Bakowsky, S. Höbel, F. Czubayko, and A. Aigner. 2006. RNA interference-mediated gene silencing of pleiotrophin through polyethylenimine-complexed small interfering RNAs *in vivo* exerts antitumoral effects in glioblastoma xenografts. Human Gene Therapy **17:** 751-766.

Gudjonsson, T., M. C. Adriance, M. D. Sternlicht, O. W. Petersen, and M. J. Bissell. 2005. Myoepithelial cells: their origin and function in breast morphogenesis and neoplasia. Journal of Mammary Gland Biology and Neoplasia **10:** 261-272.

Gullo, G., D. Bettio, M. Zuradelli, G. Masci, L. Giordano, C. Bareggi, M. Tomirotti, P. Salvini, L. Runza, N. L. Verde, and A. Santoro. 2013. Level of HER2/*neu* amplification in primary tumours and metastases in HER2-positive breast cancer and survival after trastuzumab therapy. The Breast **22:** 190-193.

Guo, P., O. Coban, N. M. Snead, J. Trebley, S. Hoeprich, S. Guo, and Y. Shu. 2010. Engineering RNA for targeted siRNA delivery and medical application. Advanced Drug Delivery Reviews **62:** 650-666.

Haley, B., and P. D. Zamore. 2004. Kinetic analysis of the RNAi enzyme complex. Nature Structural and Molecular Biology **11:** 599-606.

Hammond, M. E., D. F. Hayes, M. Dowsett, D. C. Allred, K. L. Hagerty, S. Badve, P. L. Fitzgibbons, G. Francis, N. S. Goldstein, M. Hayes, D. G. Hicks, S. Lester, R. Love, P. B. Mangu, L. McShane, K. Miller, C. K. Osborne, S. Paik, J. Perlmutter, A. Rhodes, H. Sasano, J. N. Schwartz, F. C. Sweep, S. Taube, E. E. Torlakovic, P. Valenstein, G. Viale, D. Visscher, T. Wheeler, R. B. Williams, J. L. Wittliff, and A. C. Wolff. 2010. American Society of Clinical Oncology/College of American Pathologists guideline recommendations for immunohistochemical testing of estrogen and progesterone receptors in breast cancer. Journal of Clinical Oncology **28:** 2784-2795.

Han, S. E., H. Kang, G. Y. Shim, M. S. Suh, S. J. Kim, J. S. Kim, and Y. K. Oh. 2008. Novel cationic cholesterol derivative-based liposomes for serum-enhanced delivery of siRNA. International Journal of Pharmaceutics **353:** 260:269.

Hanahan, D., and R. A. Weinberg. 2000. The hallmarks of cancer. Cell **100:** 57-70.

Hanahan, D., and R. A. Weinberg. 2011. Hallmarks of cancer. The next generation. Cell **144:** 646-674.

Hannon, G. J. 2002. RNA interference. Nature **418:** 244-251.
Harari, D., and Y. Yarden. 2000. Molecular mechanisms underlying ErbB2/HER2 action in breast cancer. Oncogene **19:** 6102-6114.
Harris, J. M., N. E. Martin, and M. Modi. 2001. Pegylation: a novel process for modifying pharmacokinetics. Clinical Pharmacokinetics **40:** 539-551.
Hattori, Y., A. Nakamura, S. Arai, K. Kawano, Y. Maitani, and E. Yonemochi. 2015. siRNA delivery to lung-metastasized tumor by systemic injection with cationic liposomes. Journal of Liposome Research **25:** 279-286.
Haupenthal, J., C. Baehr, S. Kiermayer, S. Zeuzem, and A. Piiper. 2006. Inhibition of RNAse A family enzymes prevents degradation and loss of silencing activity of siRNAs in serum. Biochemical Pharmacology **71:** 702-710.
Hayashi, M., and Y. Harada. 2007. Direct observation of the reversible unwinding of a single DNA molecule caused by the intercalation of ethidium bromide. Nucleic Acids Research **35:** e125.
Heid, C. A., J. Stevens, K. J. Livak, and P. M. Williams. 1996. Real time quantitative PCR. Genome Research **6:** 986-994.
Hennighausen, L., and G. W. Robinson. 2001. Signaling pathways in mammary gland development. Developmental Cell **1:**467-475.
Heyes, J. A., D. Niculescu-Duvaz, R. G. Cooper, and C. J. Springer. 2002. Synthesis of novel cationic lipids: effect of structural modification on the efficiency of gene transfer. Journal of Medicinal Chemistry **45:** 99-114.
Hillaireau, H., and P. Couvreur. 2009. Nanocarriers' entry into the cell: relevance to drug delivery. Cellular and Molecular Life Sciences **66:** 2873-2896.
Ho, E. A., E. Ramsay, M. Ginj, M. Anantha, I. Bregman, J. Sy, J. Woo, M. Osooly-Talesh, D. T. Yapp, and M. B. Bally. 2010. Characterization of cationic liposome formulations designed to exhibit extended plasma residence times and tumor vasculature targeting properties. Journal of Pharmaceutical Sciences **99:** 2839-2853.
Hobday, T. J., and E. A. Perez. 2005. Molecularly targeted therapies for breast cancer. Cancer Control **12:** 73-81.
Hoekstra, D., J. Rejman, L. Wasungu, F. Shi, and I. Zuhorn. 2007. Gene delivery by cationic lipids: in and out of an endosome. Biochemical Society Transactions **35:** 68-71.
Honary, S., and F. Zahir. 2013. Delivery Systems - A Review (Part 1). Tropical Journal of Pharmaceutical Research **12:** 255-260.
Hong, C. A., and Y. S. Nam. 2014. Functional nanostructures for effective delivery of small interfering RNA therapeutics. Theranostics **4:** 1211-1232.
Hong, S., P. R. Leroueil, E. K. Janus, J. L. Peters, M. M. Kober, M. T. Islam, B. G. Orr, J. R. Baker Jr., and M. M. Banaszak Holl. 2006. Interaction of polycationic polymers with supported lipid bilayers and cells: nanoscale hole formation and enhanced membrane permeability. Bioconjugate Chemistry **17:** 728-734.
Hortobagyi, G. N., J. de la Garza Salazar, K. Pritchard, D. Amadori, R. Haidinger, C. A. Hudis, H. Khaled, M. C. Liu, M. Martin, M. Namer, J. A. O'Shaughnessy, Z. Z. Shen, and K. S. Albain. 2005. The global breast cancer burden: Variations in epidemiology and survival. Clinical Breast Cancer **6:** 391-401.
Howard, K. A. 2009. Delivery of RNA interference therapeutics using polycation-based nanoparticles. Advanced Drug Delivery Reviews **61:** 710-720.
Howard, B. A., and B. A. Gusterson. 2000. Human breast development. Journal of Mammary Gland Biology and Neoplasia **5:** 119-137.
Hsu, W. L., H. L. Chen, W. Liou, H. K. Lin, and W. L. Liu. 2005. Mesomorphic complexes of DNA with the mixtures of a cationic surfactant and a neutral lipid. Langmuir **21:** 9426-9431.
Hua, D., B. Chen, M. Bai, H. Yu, X. Wu, and W. Jin. 2009. PEA3 activates VEGF transcription in T47D and SKBR3 breast cancer cells. Acta Biochimica et Biophysica Sinica **41:** 63-68.

Huang, C., M. Li, C. Chen, and Q. Yao. 2008. Small interfering RNA therapy in cancer: mechanism, potential targets, and clinical applications. Expert Opinion on Therapeutic Targets **12:** 637-645.
Huang, Q. D., J. Ren, W. J. Ou, Y. Fu, M. Q. Cai, J. Zhang, W. Zhu, and X. Q. Yu. 2012. Cationic lipids containing cyclen and ammonium moieties as gene delivery vectors. Chemical Biology and Drug Design **79:** 879-887.
Hunter, A. C. 2006. Molecular hurdles in polyfectin design and mechanistic background to polycation induced cytotoxicity. Advanced Drug Delivery Reviews **58:** 1523-1531.
Hunter, A. M., E. C. LaCasse, and R. G. Korneluk. 2007. The inhibitors of apoptosis (IAPs) as cancer targets. Apoptosis **12:** 1543-1568.
Hurvitz, S. A., Y. Hu, N. O'Brien, and R. S. Finn. 2013. Current approaches and future directions in the treatment of HER2-positive breast cancer. Cancer Treatment Reviews **39:** 219-229.
Immordino, M. L., F. Dosio, and L. Cattel. 2006. Stealth liposomes: review of the basic science, rationale, and clinical applications, existing and potential. International Journal of Nanomedicine **1:** 297-315.
Ishida, T., and H. Kiwada. 2008. Accelerated blood clearance (ABC) phenomenon upon repeated injection of PEGylated liposomes. International Journal of Pharmaceutics **354:** 56-62.
Islam, R. U., J. Hean, W. A. van Otterlo, C. B. de Koning, and P. Arbuthnot. 2009. Efficient nucleic acid transduction with lipoplexes containing novel piperazine- and polyamine-conjugated cholesterol derivatives. Bioorganic and Medicinal Chemistry Letters **19:** 100-103.
Javed, A., and A. Lteif. 2013. Development of the human breast. Seminars in Plastic Surgery **27:** 5-12.
Jere, D., H. L. Jiang, R. Arote, Y. K. Kim, Y. J. Choi, M. H. Cho, T. Akaike, and C. S. Cho. 2009. Degradable polyethylenimines as DNA and small interfering RNA carriers. Expert Opinion on Drug Delivery **6:** 827-834.
Jiang, P., A. Enomoto, and M. Takahashi. 2009. Cell biology of the movement of breast cancer cells: Intracellular signalling and the actin cytoskeleton. Cancer Letters **284:** 122-130.
Jones, R. B., A. Gordus, J. A. Krall, and G. MacBeath. 2006. A quantitative protein interaction network for the ErbB receptors using protein microarrays. Nature **439:** 168-174.
Judge, A., and I. Maclachlan. 2008. Overcoming the innate immune response to small interfering RNA. Human Gene Therapy **19:** 111-124.
Juliano, R., M. R. Alam, V. Dixit, and H. Kang. 2008. Mechanisms and strategies for effective delivery of antisense and siRNA oligonucleotides. Nucleic Acids Research **36:** 4158-4171.
Juliano, R., J. Bauman, H. Kang, and X. Ming. 2009. Biological barriers to therapy with antisense and siRNA oligonucleotides. Molecular Pharmaceutics **6:** 686-695.
Kabanov, A. V. 1999. Taking polycation gene delivery systems from *in vitro* to *in vivo*. Pharmaceutical Science and Technology Today **2:** 365-372.
Kaplitt, M. G., A. Feigin, C. Tang, H. L. Fitzsimons, P. Mattis, P. A. Lawlor, R. J. Bland, D. Young, K. Strybing, D. Eidelberg, and M. J. During. 2007. Safety and tolerability of gene therapy with an adeno-associated virus (AAV) borne GAD gene for Parkinson's disease: an open label, phase I trial. Lancet 369: 2097-2105.
Kapoor, M., and D. J. Burgess. 2012. Efficient and safe delivery of siRNA using anionic lipids: Formulation optimization studies. International Journal of Pharmaceutics **432:** 80-90.
Kapoor, M., D. J. Burgess, and S. D. Patil. 2012. Physicochemical characterization techniques for lipid based delivery systems for siRNA. International Journal of Pharmaceutics **427:** 35-57.
Katas, H., and H. O. Alpar. 2006. Development and characterization of chitosan nanoparticles for siRNA delivery. Journal of Controlled Release **115:** 216-225.
Kawabata, K., Y. Takakura, and M. Hashida. 1995. The fate of plasmid DNA after intravenous injection in mice: involvement of scavenger receptors in its hepatic uptake. Pharmaceutical Research **12:** 825-830.
Kawakami, S., and M. Hashida. 2007. Targeted delivery systems of small interfering RNA by systemic administration. Drug Metabolism and Pharmacokinetics **22:** 142-151.

Kennecke, H., R. Yerushalmi, R. Woods, M. C. Cheang, D. Voduc, C. H. Speers, T. O. Nielsen, and K. Gelmon. 2010. Metastatic behavior of breast cancer subtypes. Journal of Clinical Oncology **28:** 3271-3277.

Kenny, P. A., G. Y. Lee, C. A. Myers, R. M. Neve, J. R. Semeiks, P. T. Spellman, K. Lorenz, E. H. Lee, M. H. Barcellos-Hoff, O. W. Petersen, J. W. Gray, and M. J. Bissell. 2007. The morphologies of breast cancer cell lines in three-dimensional assays correlate with their profiles of gene expression. Molecular Oncology **1:** 84-96.

Kenworthy, A. K., K. Hristova, D. Needham, and T. J. McIntosh. 1995. Range and magnitude of the steric pressure between bilayers containing phospholipids with covalently attached poly(ethylene glycol). Biophysical Journal **68:** 1921-1936.

Kerr, J. F., A. H. Wyllie, and A. R. Currie. 1972. Apoptosis: a basic biological phenomenon with wide-ranging implications in tissue kinetics. British Journal of Cancer **26:** 239-257.

Kesharwani, P., V. Gajbhiye, and N. K. Jain. 2012. A review of nanocarriers for the delivery of small interfering RNA. Biomaterials **33:** 7138-7150.

Khuller, G. K., M. Kapur, and S. Sharma. 2004. Liposome technology for drug delivery against mycobacterial infections. Current Pharmaceutical Design **10:** 3263-3274.

Kim, D. H., and J. J. Rossi. 2007. Strategies for silencing human disease using RNA interference. Nature Genetics **8:** 173-184.

Kim, V. N., J. Han, and M. C. Siomi. 2009. Biogenesis of small RNAs in animals. Nature Reviews. Molecular Cell Biology **10:** 126-139.

Kim, B. Y., J. T. Rutka, and W. C. Chan. 2010. Nanomedicine. The New England Journal of Medicine **363:** 2434-2443.

Klagsbrun, M., and M. A. Moses. 1999. Molecular angiogenesis. Chemistry and Biology **6:** 217-224.

Klapper, L. N., M. H. Kirschbaum, M. Sela, and Y. Yarden. 2000. Biochemical and clinical implications of the ErbB/HER signaling network of growth factor receptors. Advances in Cancer Research **77:** 25-79.

Klibanov, A. L., K. Maruyama, V. P. Torchilin, and L. Huang. 1990. Amphipathic polyethylene glycols effectively prolong the circulation time of liposomes. FEBS Letters **268:** 235-237.

Klos, K. S., X. Zhou, S. Lee, L. Zhang, W. Yang, Y. Nagata, and D. Yu. 2003. Combined trastuzumab and paclitaxel treatment better inhibits ErbB-2-mediated angiogenesis in breast carcinoma through a more effective inhibition of Akt than either treatment alone. Cancer **98:** 1377-1385.

Knighton, D. R. , J. H. Zheng, L. F. Ten Eyck, V. A. Ashford, N. H. Xuong, S. S. Taylor, and J. M. Sowadski. 1991. Crystal structure of the catalytic subunit of cyclic adenosine monophosphate-dependent protein kinase. Science **253:** 407-414.

Knop, K., R. Hoogenboom, D. Fischer, and U. S. Schubert. 2010. Poly(ethylene glycol) in drug delivery: Pros and cons as well as potential alternatives. Angewandte Chemie (International Edition in English) **49:** 6288-6308.

Kohli, A. G., P. H. Kierstead, V. J. Venditto, C. L. Walsh, and F. C. Szoka. 2014. Designer lipids for drug delivery: From heads to tails. Journal of Controlled Release **190:** 274-287.

Kolate, A., D. Baradia, S. Patil, I. Vhora, G. Kore, and A. Misra. 2014. PEG - A versatile conjugating ligand for drugs and drug delivery systems. Journal of Controlled Release **192:** 67-81.

Konecny, G., G. Pauletti, M. Pegram, M. Untch, S. Dandekar, Z. Aguilar, C. Wilson, H. M. Rong, I. Bauerfeind, M. Felber, H. J. Wang, M. Beryt, R. Seshadri, H. Hepp, and D. J. Slamon. 2003. Quantitative association between HER-2/*neu* and steroid hormone receptors in hormone receptor-positive primary breast cancer. Journal of the National Cancer Institute **95:** 142-153.

Konecny, G. E., Y. G. Meng, M. Untch, H. J. Wang, I. Bauerfeind, M. Epstein, P. Stieber, J. M. Vernes, J. Gutierrez, K. Hong, M. Beryt, H. Hepp, D. J. Slamon, and M. D. Pegram. 2004. Association between HER-2/*neu* and vascular endothelial growth factor expression predicts clinical outcome in primary breast cancer patients. Clinical Cancer Research **10:** 1706-1716.

Kong, F., G. Liu, B. Sun, S. Zhou, A. Zuo, R. Zhao, and D. Liang. 2012. Phosphorylatable short peptide conjugated low molecular weight chitosan for efficient siRNA delivery and target gene silencing. International Journal of Pharmaceutics **422:** 445-453.
Koynova, R., and B. Tenchov. 2010. Cationic lipids: molecular structure/transfection activity relationships and interactions with biomembranes. Topics in Current Chemistry **296:** 51-93.
Kraske, W. V., and D. B. Mountcastle. 2001. Effects of cholesterol and temperature on the permeability of dimyristoylphosphatidylcholine bilayers near the chain melting phase transition. Biochimica et Biophysica Acta **1514:** 159-164.
Kuhn, R., S. Streif, and W. Wurst. 2007. RNA interference in mice. Handbook of Experimental Pharmacology **178:** 149-176.
Kuntsche, J., I. Freisleben, F. Steiniger, and A. Fahr. 2010. Temoporfin-loaded liposomes: physicochemical characterization. European Journal of Pharmaceutical Sciences **40:** 305-315.
Kuntsche, J., J. C. Horst, and H. Bunjes. 2011. Cryogenic transmission electron microscopy (cryo-TEM) for studying the morphology of colloidal drug delivery systems. International Journal of Pharmaceutics **417:** 120-17.
Kurreck, J. 2009. RNA interference: from basic research to therapeutic applications. Angewandte Chemie (International Edition in English) **48:** 1378-1398.
Lakowicz, J. R. 1999. Principles of fluorescence spectroscopy. 2nd ed., Kluwer Academic/Plenum Publishers, USA.
Laouini, A., C. Jaafar-Maalej, I. Limayem-Blouza, S. Sfar, C. Charcosset, and H. Fessi. 2012. Preparation, characterization and applications of liposomes: State of the art. Journal of Colloid Science and Biotechnology **1:** 147-168.
Lavigne, C., and A. R. Thierry. 2007. Specific subcellular localization of siRNAs delivered by lipoplex in MCF-7 breast cancer cells. Biochimie **89:** 1245-1251.
Lax, I., W. H. Burgess, F. Bellot, A. Ullrich, J. Schlessinger, and D. Givol. 1988. Localization of a major receptor-binding domain for epidermal growth factor by affinity labeling. Molecular and Cellular Biology **8:** 1831-1834.
Lee, E. R., J. Marshall, C. S. Siegel, C. Jiang, N. S. Yew, M. R. Nichols, J. B. Nietupski, R. J. Ziegler, M. B. Lane, K. X. Wang, N. C. Wan, R. K. Scheule, D. J. Harris, A. E. Smith, and S. H. Cheng. 1996. Detailed analysis of structures and formulations of cationic lipids for efficient gene transfer to the lung. Human Gene Therapy **7:** 1701-1717.
Lee, Y., S. H. Lee, J. S. Kim, A. Maruyama, X. Chen, and T. G. Park. 2011. Controlled synthesis of PEI-coated gold nanoparticles using reductive catechol chemistry for siRNA delivery. Journal of Controlled Release **155:** 3-10.
Lemmon, M. A. 2009. Ligand-induced ErbB receptor dimerization. Experimental Cell Research **315:** 638-648.
Lemoine, N. R., S. Staddon, C. Dickson, D. M. Barnes, and W. J. Gullick. 1990. Absence of activating transmembrane mutations in the c-erbB-2 proto-oncogene in human breast cancer. Oncogene **5:** 237-239.
LePecq, J. B., and C. Paoletti. 1967. A fluorescent complex between ethidium bromide and nucleic acids. Physical-chemical characterization. Journal of Molecular Biology **27:** 87-106.
Leung, R. K., and P. A. Whittaker. 2005. RNA interference: from gene silencing to gene-specific therapeutics. Pharmacology and Therapeutics **107:** 222-239.
Leventis, R., and J. R. Silvius. 1990. Interactions of mammalian cells with lipid dispersions containing novel metabolizable cationic amphiphiles. Biochimica et Biophysica Acta (BBA) - Biomembranes **1023:** 124-132.
Lewis, C. E., and J. W. Pollard. 2006. Distinct role of macrophages in different tumor microenvironments. Cancer Research **66:** 605-612.

Li, S., W. C. Tseng, D. B. Stolz, S. P. Wu, S. C. Watkins, and L. Huang. 1999. Dynamic changes in the characteristics of cationic lipidic vectors after exposure to mouse serum: implications for intravenous lipofection. Gene Therapy **6:** 585-594.
Li, S. D., and L. Huang. 2006. Gene therapy progress and prospects: non-viral gene therapy by systemic delivery. Gene Therapy **13:** 1313-1319.
Li, S. D., and L. Huang. 2009. Nanoparticles evading the reticuloendothelial system: role of the supported bilayer. Biochimica et Biophysica Acta - Biomembranes **1788:** 2259-2266.
Li, W., and F. C. Jr Szoka. 2007. Lipid-based nanoparticles for nucleic acid delivery. Pharmaceutical Research **24:** 438-449.
Li, Y., L. Zou, Q. Li, B. Haibe-Kains, R. Tian, Y. Li, C. Desmedt, C. Sotiriou, Z. Szallasi, J. D. Iglehart, A. L. Richardson, and Z. C. Wang. 2010. Amplification of LAPTM4B and YWHAZ contributes to chemotherapy resistance and recurrence of breast cancer. Nature Medicine **16:** 214-218.
Li, P., D. Liu, X. Sun, C. Liu, Y. Liu, and N. Zhang. 2011. A novel cationic liposome formulation for efficient gene delivery via a pulmonary route. Nanotechnology **22:** 11 **doi** 10.1088/0957-4484/22/24/245104.
Li, J., Y. Wang, Y. Zhu, and D. Oupický. 2013. Recent advances in delivery of drug-nucleic acid combinations for cancer treatment. Journal of Controlled Release **172:** 589-600.
Liang, Y., H. Gao, S. Y. Lin, J. A. Goss, F. C. Brunicardi, and K. Li. 2010. siRNA-based targeting of cyclin E overexpression inhibits breast cancer cell growth and suppresses tumor development in breast cancer mouse model. PLoS ONE **5:** e12860 **doi** 10.1371/journal.pone.0012860.
Liao, D. J., and R. B. Dickson. 2000. c-Myc in breast cancer. Endocrine-Related Cancer **7:** 143-164.
Lima, R. T., L. M. Martins, J. E. Guimaraes, C. Sambade, and M. H. Vasconcelos. 2004. Specific downregulation of bcl-2 and xIAP by RNAi enhances the effects of chemotherapeutic agents in MCF-7 human breast cancer cells. Cancer Gene Therapy **11:** 309-316.
Lin, P. C., S. Lin, P. C. Wang, and R. Sridhar. 2014. Techniques for physicochemical characterization of nanomaterials. Biotechnology Advances **32:** 711-726.
Linderholm, B., B. Tavelin, K. Grankvist, and R. Henriksson. 1998. Vascular endothelial growth factor is of high prognostic value in node-negative breast carcinoma. Journal of Clinical Oncology **16:** 3121-3128.
Linderholm, B., K. Grankvist, N. Wilking, M. Johansson, B. Travelin, and R. Henriksson. 2000. Correlation of vascular endothelial growth factor content with recurrences, survival, and first relapse site in primary node-positive breast carcinoma after adjuvant treatment. Journal of Clinical Oncology **18:** 1423-1431.
Liu, J., M. A. Carmell, F. V. Rivas, C. G. Marsden, J. M. Thomson, and J. J. Song. 2004a. Argonaute-2 is the catalytic engine of mammalian RNAi. Science **305:** 1437-1441.
Liu, T., J. Q. Yin, B. Shang, Z. Min, H. He, J. Jiang, F. Chen, Y. Zhen, and R. Shao. 2004b. Silencing of hdm2 oncogene by siRNA inhibits p53-dependent human breast cancer. Cancer Gene Therapy **11:** 748-756.
Liu, D. L., J. J. Hu, W. H. Qiao, Z. S. Li, S. B. Zhang, and L. B. Cheng. 2005a. Synthesis of carbamate-linked lipids for gene delivery. Bioorganic and Medicinal Chemistry Letters. **15:** 3147-3150.
Liu, D. L., J. J. Hu, W. H. Qiao, Z. S. Li, S. B. Zhang, and L. B. Cheng. 2005b. Synthesis and characterization of a series of carbamate-linked cationic lipids for gene delivery. Lipids **40:** 83-848.
Liu, X. D., K. A. Howard, M. D. Dong, M. Ø. Andersen, U. L. Rahbek, M. G. Johnsen, O. C. Hansen, F. Besenbacher, and J. Kjems. 2007. The influence of polymeric properties on chitosan/siRNA nanoparticle formulation and gene silencing. Biomaterials **28:** 1280-1288.
Liu, Y., and L. Huang. 2010. Designer lipids advance systemic siRNA delivery. Molecular Therapy **18:** 669-670.
Livak, K. J., and T. D. Schmittgen. 2001. Analysis of relative gene expression data using real-time quantitative PCR and the $2^{-\Delta\Delta CT}$ method. Methods **25:** 402-408.

Lorenzer, C., M. Dirin, A. M. Winkler, V. Baumann, and J. Winkler. 2015. Going beyond the liver: Progress and challenges of targeted delivery of siRNA therapeutics. Journal of Controlled Release **203:** 1-15.
Lundqvist, M., J. Stigler, G. Elia, I. Lynch, T. Cedervall, and K. A. Dawson. 2008. Nanoparticle size and surface properties determine the protein corona with possible implications for biological impacts. Proceedings of the National Academy of Sciences of the United States of America **105:** 14265-14270.
Lungwitz, U., M. Breunig, T. Blunk, and A. Gopferich. 2005. Polyethyleneimine-based nonviral gene delivery systems. European Journal of Pharmaceutics and Biopharmaceutics **60:** 247-266.
Lv, H., S. Zhang, B. Wang, S. Cui, and J. Yan. 2006. Toxicity of cationic lipids and cationic polymers in gene delivery. Journal of Controlled Release **114:** 100-109.
Lynch, I., and K. A. Dawson. 2008. Protein-nanoparticle interactions. Nano Today **3:** 40-47.
Ma, J. B., Y. R. Yuan, G. Meister, Y. Pei, T. Tuschl, and D. J. Patel. 2005a. Structural basis for 5′-end-specific recognition of guide RNA by the *A. fulgidus* Piwi protein. Nature **434:** 666-670.
Ma, Z., J. Li, F. He, A. Wilson, B. Pitt, and S. Li. 2005b. Cationic lipids enhance siRNA-mediated interferon response in mice. Biochemical and Biophysical Research Communications **330:** 755-759.
Mady, M. M. 2004. Serum stability of non-cationic liposomes used for DNA delivery. Romanian Journal of Biophysics **14:** 89-97.
Maeda, H., and Y. Matsumura. 1989. Tumoritropic and lymphotropic principles of macromolecular drugs. Critical Reviews in Therapeutic Drug Carrier Systems **6:** 193-210.
Maitani, Y., S. Igarashi, M. Sato, and Y. Hattori. 2007. Cationic liposome (DC-Chol/DOPE=1:2) and a modified ethanol injection method to prepare liposomes, increased gene expression. International Journal of Pharmaceutics **342:** 33-39.
Mao, S., M. Neu, O. Germershaus, O. Merkel, J. Sitterberg, U. Bakowsky, and T. Kissel. 2006. Influence of polyethylene glycol chain length on the physicochemical and biological properties of poly(ethylene imine)-graft-poly(ethylene glycol) block copolymer/siRNA polyplexes. Bioconjugate Chemistry **17:** 1209-1218.
Mao, S., W. Sun, and T. Kissel. 2010. Chitosan-based formulations for delivery of DNA and siRNA. Advanced Drug Delivery Reviews **62:** 12-27.
Mao, C. Q., J. Z. Du, T. M. Sun, Y. D. Yao, P. Z. Zhang, E. W. Song, and J. Wang. 2011. A biodegradable amphiphilic and cationic triblock copolymer for the delivery of siRNA targeting the acid ceramidase gene for cancer therapy. Biomaterials **32:** 3124-3133.
Mao, Y., Y. Zhang, Q. Qu, M. Zhao, Y. Lou, J. Liu, O. Huang, X. Chen, J. Wu, and K. Shen. 2015. Cancer-associated fibroblasts induce trastuzumab resistance in HER2 positive breast cancer cells. Molecular Biosystems **11:** 1029-1040.
Martinez, L. A., I. Naguibneva, H. Lehrmann, A. Vervisch, T. Tchénio, G. Lozano, and A. Harel-Bellan. 2002. Synthetic small inhibiting RNAs: efficient tools to inactivate oncogenic mutations and restore p53 pathways. Proceedings of the National Academy of Sciences of the United States of America **99:** 14849-14854.
Masson, C., M. Garinot, N. Mignet, B. Wetzer, P. Mailhe, D. Scherman, and M. Bessodes. 2004. pH-sensitive PEG lipids containing orthoester linkers: new potential tools for nonviral gene delivery. Journal of Controlled Release **99:** 423-434.
Mathias, R. A., S. K. Gopal, and R. J. Simpson. 2013. Contribution of cells undergoing epithelial-mesenchymal transition to the tumour microenvironment. Journal of Proteomics **78:** 545-557.
Matranga, C., Y. Tomari, C. Shin, D. P. Bartel, and P. D. Zamore. 2005. Passenger-strand cleavage facilitates assembly of siRNA into AGO2-containing RNAi enzyme complexes. Cell **123:** 607-620.
Mavaddat, N., A. C. Antoniou, D. F. Easton, and M. Garcia-Closas. 2010. Genetic susceptibility to breast cancer. Molecular Oncology **17:** 174-191.
Mayer, L. D., R. Krishna, M. Webb, and M. Bally. 2000. Designing liposomal anticancer drug formulations for specific therapeutic applications. Journal of Liposome Research **10:** 99-115.

Medarova, Z., W. Pham, C. Farrar, V. Petkova, and A. Moore. 2007. *In vivo* imaging of siRNA delivery and silencing in tumors. Nature Medicine **13:** 372-377.
Menard, S., E. Tagliabue, M. Campiglio, and S. M. Pupa. 2000. Role of HER2 gene overexpression in breast carcinoma. Journal of Cellular Physiology **182:** 150-162.
Metzger Filho, O., K. S. Saini, H. A. Azim Jr., and A. Awada. 2012. Prevention and management of major side effects of targeted agents in breast cancer. Critical Reviews in Oncology/Hematology **84:** e79-e85.
Mével, M., N. Kamaly, S. Carmona, M. H. Oliver, M. R. Jorgensen, C. Crowther, F. H. Salazar, P. L. Marion, M. Fujino, Y. Natori, M. Thanou, P. Arbuthnot, J. J. Yaouanc, P. A. Jaffrés, and A. D. Miller. 2010. DODAG; a versatile new cationic lipid that mediates efficient delivery of pDNA and siRNA. Journal of Controlled Release **143:** 222-232.
Meyer, M., A. Philipp, R. Oskuee, C. Schmidt, and E. Wagner. 2008. Breathing life into polycations: functionalization with pH-responsive endosomolytic peptides and polyethylene glycol enables siRNA delivery. Journal of the American Chemical Society **130:** 3272-3273.
Mielke, S., H. Meden, and W. Kuhn. 1998. Expression of the c-erbB-2-encoded oncoprotein p185 (HER-2/*neu*) in pregnancy as a model for oncogene-induced carcinogenesis. Medical Hypotheses **50:** 359-362.
Mintzer, M. A., and E. E. Simanek. 2009. Nonviral vectors for gene delivery. Chemical Reviews **109:** 259-302.
Miyawaki-Shimizu, K., D. Predescu, J. Shimizu, M. Broman, S. Predescu, and A. B. Malik. 2006. siRNA-induced caveolin-1 knockdown in mice increases lung vascular permeability via the junctional pathway. American Journal of Physiology. Lung Cellular and Molecular Physiology. **290:** L405-413.
Moasser, M. M. 2007. The oncogene HER2: its signaling and transforming functions and its role in human cancer pathogenesis. Oncogene **26:** 6469-6487.
Mochizuki, S., N. Kanegae, K. Nishina, Y. Kamikawa, K. Koiwai, H. Masunaga, and K. Sakurai. 2013. The role of the helper lipid dioleoylphosphatidylethanolamine (DOPE) for DNA transfection cooperating with a cationic lipid bearing ethyenediamine. Biochimica et Biophysica Acta **1828:** 412-418.
Molina, M. A., J. Codony-Servat, J. Albanell, F. Rojo, J. Arribas, and J. Baselga. 2001. Trastuzumab (herceptin), a humanized anti-Her2 receptor monoclonal antibody, inhibits basal and activated Her2 ectodomain cleavage in breast cancer cells. Cancer Research **61:** 4744-4749.
Montemurro, F., M. Donadio, M. Clavarezza, S. Redana, M. E. Jacomuzzi, G. Valabrega, S. Danese, G. Vietti-Ramus, A. Durando, M. Venturini, and M. Aglietta. 2006. Outcome of patients with HER2-positive advanced breast cancer progressing during trastuzumab-based therapy. Oncologist **11:** 318-324.
Moreira, J. N., A. Santos, V. Moura, M. C. Pedroso de Lima, and S. Simoes. 2008. Non-viral lipid based nanoparticles for targeted cancer systemic gene silencing. Journal of Nanoscience and Nanotechnology **8:** 2187-2204.
Morrissey, D. V., K. Blanchard, L. Shaw, K. Jensen, J. A. Lockridge, B. Dickinson, J. A. McSwiggen, C. Vargeese, K. Bowman, C. S. Shaffer, B. A. Polisky, and S. Zinnen. 2005. Activity of stabilized short interfering RNA in a mouse model of hepatitis B virus replication. Hepatology **41:** 1349-1356.
Mounkes, L. C., W. Zhong, G. Cipres-Palacin, T. D. Heath, and R. J. Debs. 1998. Proteoglycans mediate cationic liposome-DNA complex-based gene delivery *in vitro* and *in vivo*. The Journal of Biological Chemistry **273:** 26164-26170.
Moy, B., and P. E. Goss. 2006. Lapatinib: current status and future directions in breast cancer. Oncologist **11:** 1047-1057.
Moy, B., and P. E. Goss. 2007. Lapatinib-associated toxicity and practical management recommendations. Oncologist **12:** 756-765.

Mukhopadhyay, P., S. Chakraborty, M. P. Ponnusamy, I. Lakshmanan, M. Jain, and S. K. Batra. 2011. Mucins in the pathogenesis of breast cancer: Implications in diagnosis, prognosis and therapy Biochimica et Biophysica Acta **1815:** 224-240.

Nafisi, S., A. A. Saboury, N. Keramat, J. F. Neault, and H. A. Tajmir-Riahi. 2007. Stability and structural features of DNA intercalation with ethidium bromide, acridine orange and methylene blue. Journal of Molecular Structure **827:** 35-43.

Nahta, R., L. X. Yuan, B. Zhang, R. Kobayashi, and F. J. Esteva. 2005. Insulin-like growth factor-I receptor/Human Epidermal Growth Factor Receptor 2 heterodimerization contributes to trastuzumab resistance of breast cancer cells. Cancer Research **65:** 11118-11128.

Nahta, R., D. Yu, M. C. Hung, G. N. Hortobagyi, and F. J. Esteva. 2006. Mechanisms of disease: understanding resistance to HER2-targeted therapy in human breast cancer. Nature Clinical Practice. Oncology **3:** 269-280.

Nakase, M., M. Inui, K. Okumura, T. Kamei, S. Nakamura, and T. Tagawa. 2005. p53 gene therapy of human osteosarcoma using a transferrin-modified cationic liposome. Molecular Cancer Therapeutics **4:** 625-631.

Nandy, A., S. Gangopadhyay, and A. Mukhopadhyay. 2014. Individualizing breast cancer treatment - The dawn of personalized medicine. Experimental Cell Research **320:** 1-11.

Napoli, C., C. Lemieux, and R. Jorgensen. 1990. Introduction of a chimeric chalcone synthase gene into petunia results in reversible co-suppression of homologous genes *in trans*. Plant Cell **2:** 279-289.

Natali, P. G., M. R. Nicotra, A. Bigotti, I. Venturo, D. J. Slamon, B. M. Fendly, and A. Ullrich. 1990. Expression of the p185 encoded by HER2 oncogene in normal and transformed human tissues. International Journal of Cancer **45:** 457-461.

Natarajan, J. V., A. Darwitan, V. A. Barathi, M. Ang, H. M. Htoon, F. Boey, K. C. Tam, T. T. Wong, and S. S. Venkatraman. 2014. Sustained drug release in nanomedicine: a long-acting nanocarrier-based formulation for glaucoma. ACS Nano **8:** 419-429.

Needham, D., T. J. McIntosh, and D. D. Lasic. 1992. Repulsive interactions and mechanical stability of polymer-grafted lipid membranes. Biochimica et Biophysica Acta **1108:** 40-48.

Negro, A., B. K. Brar, and K. F. Lee. 2004. Essential roles of Her2/erbB2 in cardiac development and function. Recent Progress in Hormone Research **59:** 1-12.

Neu, M., D. Fischer, and T. Kissel. 2005. Recent advances in rational gene transfer vector design based on poly(ethylene imine) and its derivatives. The Journal of Gene Medicine **7:** 992-1009.

Nicholson, K. M., and N. G. Anderson. 2002. The protein kinase B/Akt signalling pathway in human malignancy. Cellular Signalling **14:** 381-395.

Niculescu-Duvaz, D., J. Heyes, and C. J. Springer. 2003. Structure-activity relationship in cationic lipid mediated gene transfection. Current Medicinal Chemistry **10:** 1233-1261.

Nielsen, D. L., M. Andersson, and C. Kamby. 2009. HER2-targeted therapy in breast cancer. Monoclonal antibodies and tyrosine kinase inhibitors. Cancer Treatment Reviews **35:** 121-136.

Nimesh, S., A. Goyal, V. Pawar, S. Jayaraman, P. Kumar, R. Chandra, Y. Singh, and K. C. Gupta. 2006. Polyethylenimine nanoparticles as efficient transfecting agents for mammalian cells. Journal of Controlled Release **110:** 457-468.

Nitta, H., B. D. Kelly, C. Allred, S. Jewell, P. Banks, E. Dennis, and T. M. Grogan. 2016. The assessment of HER2 status in breast cancer: the past, the present, and the future. Pathology International **66:** 313-324.

Nowsheen, S., K. Aziz, P. T. Tran, V. G. Gorgoulis, E. S. Yang, and A. G. Georgakilas. 2014. Epigenetic inactivation of DNA repair in breast cancer. Cancer Letters **342:** 213-222.

Núñez, C., J. L. Capelo, G. Igrejas, A. Alfonso, L. M. Botana, and C. Lodeiro. 2016. An overview of the effective combination therapies for the treatment of breast cancer. Biomaterials **97:** 34-50.

Obata, Y., G. Ciofani, V. Raffa, A. Cuschieri, A. Menciassi, P. Dario, and S. Takeoka. 2010. Evaluation of cationic liposomes composed of an amino acid-based lipid for neuronal transfection. Nanomedicine: Nanotechnology, Biology, and Medicine **6:** 70-77.

Oh, Y. K., and T. G. Park. 2009. siRNA delivery systems for cancer treatment. Advanced Drug Delivery Reviews **61:** 850-862.
Olayioye, M. A. 2001. Update on HER-2 as a target for cancer therapy: intracellular signaling pathways of ErbB2/HER-2 and family members. Breast Cancer Research **3:** 385-389.
Olayioye, M. A., R. M. Neve, H. A. Lane, and N. E. Hynes. 2000. The ErbB signaling network: receptor heterodimerization in development and cancer. The EMBO Journal **9:** 3159-3167.
Oliveras-Ferraros, C., A. Vazquez-Martin, S. Cufí, V. Z. Torres-Garcia, T. Sauri-Nadal, S. D. Barco, E. Lopez-Bonet, J. Brunet, B. Martin-Castillo, and J. A. Menendez. 2011. Inhibitor of apoptosis (IAP) survivin is indispensable for survival of HER2 gene-amplified breast cancer cells with primary resistance to HER1/2-targeted therapies. Biochemical and Biophysical Research Communications **407:** 412-419.
Osborne, M. P. 2000. Breast anatomy and development. ***In.*** Harris, J. R., M. E. Lippman, M. Morrow, C. K. Osborne, ed. Diseases of the breast. Philadelphia: Lippincott Williams & Wilkins; p. 1-14.
Ozben, T. 2006. Mechanisms and strategies to overcome multiple drug resistance in cancer. FEBS Letters **580:** 2903-2909.
Ozpolat, B., A. K. Sood, and G. Lopez-Berestein. 2014. Liposomal siRNA nanocarriers for cancer therapy. Advanced Drug Delivery Reviews **66:** 110-116.
Palchaudhuri, R., and P. J. Hergenrother. 2007. DNA as a target for anticancer compounds: methods to determine the mode of binding and the mechanism of action. Current Opinion in Biotechnology **18:** 497-503.
Palmieri, C., D. K. Patten, A. Januszewski, G. Zucchini, and S. J. Howell. 2014. Breast cancer: Current and future endocrine therapies. Molecular and Cellular Endocrinology **382:** 695-723.
Papahadjopoulos, D., T. M. Allen, A. Gabizon, E. Mayhew, K. Matthay, S. K. Huang, K. D. Lee, M. C. Woodle, D. D. Lasic, C. Redemann, and F. J. Martin. 1991. Sterically stabilized liposomes: improvements in pharmacokinetics and antitumor therapeutic efficacy. Proceedings of the National Academy of Sciences of the United States of America **88:** 11460-11464.
Park, J. W., K. Hong, D. B. Kirpotin, G. Colbern, R. Shalaby, J. Baselga, Y. Shao, U. B. Nielsen, J. D. Marks, D. Moore, D. Papahadjopoulos, and C. C. Benz. 2002. Anti-HER2 immunoliposomes: enhanced efficacy attributable to targeted delivery. Clinical Cancer Research **8:** 1172-1181.
Park, H. S., H. Y. Jung, E. Y. Park, J. Kim, W. J. Lee, and Y. S. Bae. 2004. Cutting edge: direct interaction of TLR4 with NAD(P)H oxidase 4 isozyme is essential for lipopolysaccharide-induced production of reactive oxygen species and activation of NF-kappa B. Journal of Immunology **173:** 3589-3593.
Park, T. G., J. H. Jeong, and S. W. Kim. 2006. Current status of polymeric gene delivery systems. Advanced Drug Delivery Reviews **58:** 467-486.
Park, K., M. Y. Lee, K. S. Kim, and S. K Hahn. 2010. Target specific tumor treatment by VEGF siRNA complexed with reducible polyethylenemine-hyaluronic acid conjugate. Biomaterials **31:** 5258-5265.
Paroo, Z., and D. R. Corey. 2004. Challenges for RNAi *in vivo*. Trends in Biotechnology **22:** 390-394.
Patani, N., L. A. Martin, and M. Dowsett. 2013. Biomarkers for the clinical management of breast cancer: International perspective. International Journal of Cancer **133:** 1-13.
Patil, Y. P., and S. Jadhav. 2014. Novel methods for liposome preparation. Chemistry and Physics of Lipids **177:** 8-18.
Patil, Y. B., S. K. Swaminathan, T. Sadhukha, L. Ma, and J. Panyam. 2010. The use of nanoparticle mediated targeted gene silencing and drug delivery to overcome tumor drug resistance. Biomaterials **31:** 358-365.
Pecot, C. V., G. A. Calin, R. L. Coleman, G. Lopez-Berestein, and A. K. Sood. 2011. RNA interference in the clinic: challenges and future directions. Nature Reviews. Cancer **11:** 59-67.
Pedersen, K., P. D. Angelini, S. Laos, A. Bach-Faig, M. P. Cunningham, C. Ferrer-Ramón, A. Lugue-García, J. García-Castillo, J. L. Parra-Palau, M. Scaltriti, S. Ramón y Cajal, J. Baselga, and

J. Arribas. 2009. A naturally occurring HER2 carboxy-terminal fragment promotes mammary tumor growth and metastasis. Molecular and Cellular Biology **29:** 3319-3331.
Peeters, L., N. N. Sanders, A. Jones, J. Demeester, and S. C. De Smedt. 2007. Post-pegylated lipoplexes are promising vehicles for gene delivery in RPE cells. Journal of Controlled Release **28:** 208-217.
Perche, F., and V. P. Torchilin. 2013. Recent trends in multifunctional liposomal nanocarriers for enhanced tumor targeting. Journal of Drug Delivery **doi** 10.1155/2013/705265.
Perez, E. A. 2008. Cardiac toxicity of ErbB2-targeted therapies: What do we know? Clinical Breast Cancer **8:** S114-S120.
Perou, C. M., T. Sørlie, M. B. Eisen, M. van de Rijn, S. S. Jeffrey, C. A. Rees, J. R. Pollack, D. T. Ross, H. Johnsen, L. A. Akslen, O. Fluge, A. Pergamenschikov, C. Williams, S. X. Zhu, P. E. Lonning, A. L. Borresen-Dale, P. O. Brown, and D. Botstein. 2000. Molecular portraits of human breast tumours. Nature **406:** 747-752.
Perrier, T., P. Saulnier, F. Fouchet, N. Lautram, and J. P. Benoit. 2010. Post-insertion into lipid nanocapsules (LNCs): from experimental aspects to mechanisms. International Journal of Pharmaceutics **396:** 204-209.
Pfaffl, M. W. 2001. A new mathematical model for relative quantification in real-time RT-PCR. Nucleic Acid Research **29:** 2002-2007.
Philipp, A., X. Zhao, P. Tarcha, E. Wagner, and A. Zintchenko. 2009. Hydrophobically modified oligoethylenimines as highly efficient transfection agents for siRNA delivery. Bioconjugate Chemistry **20:** 2055-2061.
Piao, L., H. Li, L. Teng, B. C. Yung, Y. Sugimoto, R. W. Brueggemeier, and R. J. Lee. 2013. Human serum albumin-coated lipid nanoparticles for delivery of siRNA to breast cancer. Nanomedicine: Nanotechnology, Biology, and Medicine **9:** 122-129.
Piché, A., J. Grim, C. Rancourt, J. Gómez-Navarro, J. C. Reed, and D. T. Curici. 1998. Modulation of Bcl-2 protein levels by an intracellular anti-Bcl-2 single-chain antibody increases drug-induced cytotoxicity in the breast cancer cell line MCF-7. Cancer Research **58:** 2134-2140.
Pietras, R. J., J. Arboleda, D. M. Reese, N. Wongvipat, M. D. Pegram, L. Ramos, C. M. Gorman, M. G. Parker, M. X. Sliwkowski, and D. J. Slamon. 1995. HER-2 tyrosine kinase pathway targets estrogen receptor and promotes hormone-independent growth in human breast cancer cells. Oncogene **10:** 2435-2446.
Pille, J. Y., H. Li, E. Blot, J. R. Bertrand, L. L. Pritchard, P. Opolon, A. Maksimenko, H. Lu, J. P. Vannier, J. Soria, C. Malvy, and C. Soria. 2006. Intravenous delivery of anti-RhoA small interfering RNA loaded in nanoparticles of chitosan in mice: safety and efficacy in xenografted aggressive breast cancer. Human Gene Therapy **17:** 1019-1026.
Pinkas-Kramarski, R., L. Soussan, H. Waterman, G. Levkowitz, I. Alroy, L. Klapper, S. Lavi, R. Seger, B. J. Ratzkin, M. Sela, and Y. Yarden. 1996. Diversification of *neu* differentiation factor and epidermal growth factor signaling by combinatorial receptor interactions. The EMBO Journal **15:** 2452-2467.
Pirollo, K. F., and E. H. Chang. 2008. Targeted delivery of small interfering RNA: approaching effective cancer therapies. Cancer Research **68:** 1247-1250.
Place, A. E., S. J. Huh, and K. Polyak. 2011. The microenvironment in breast cancer progression: biology and implications for treatment. Breast Cancer Research **13:** 227-237.
Plank, C., K. Mechtler, F. C. Jr Szoka, and E. Wagner. 1996. Activation of the complement system by synthetic DNA complexes: a potential barrier for intravenous gene delivery. Human Gene Therapy **7:** 1437-1446.
Pohl, F. M., T. M. Jovin, W. Baehr, and J. J. Holbrook. 1972. Ethidium bromide as a cooperative effector of a DNA structure. Proceedings of the National Academy of Sciences of the United States of America **69:** 3805-3809.

Pohlmann, P. R., I. A. Mayer, and R. Mernaugh. 2009. Resistance to trastuzumab in breast cancer. Clinical Cancer Research **15:** 7479-7491.
Polyak, K. 2007. Breast cancer: origins and evolution. The Journal of Clinical Investigation **117:** 3155-3163.
Porras, G., and E. Bezard. 2008. Preclinical development of gene therapy for Parkinson's disease. Experimental Neurology **209:** 72-81.
Porter, P. 2008. "Westernizing" women's risks? Breast cancer in lower-income countries. The New England Journal of Medicine **358:** 213-216.
Pozzi, D., C. Marchini, F. Cardarelli, H. Amenitsch, C. Garulli, A. Bifone, and G. Caracciolo. 2012. Transfection efficiency boost of cholesterol-containing lipoplexes. Biochimica et Biophysica Acta **1818:** 2335-2343.
Pozzi, D., V. Colapicchioni, G. Caracciolo, S. Piovesana, A. L. Capriotti, S. Palchetti, S. Palchetti, S. De Grossi, A. Ricciolo, H. Amenitsch, and A. Laganà. 2014. Effect of polyethyleneglycol (PEG) chain length on the bio-nano-interactions between PEGylated lipid nanoparticles and biological fluids: from nanostructure to uptake in cancer cells. Nanoscale **6:** 2782-2792.
Press, M. F., C. Cordon-Cardo, and D. J. Slamon. 1990. Expression of the HER-2/*neu* protooncogene in normal human adult and fetal tissues. Oncogene **5:** 953-962.
Press, M. F., D. J. Slamon, K. J. Flom, J. Park, J. Y. Zhou, and L. Bernstein. 2002. Evaluation of HER-2/*neu* gene amplification and overexpression: comparison of frequently used assay methods in a molecularly characterized cohort of breast cancer specimens. Journal of Clinical Oncology **20:** 3095-3105.
Pulford, B., N. Reim, A. Bell, J. Veatch, G. Forster, H. Bender, C. Meyerett, S. Hafeman, B. Michel, T. Johnson, A. C. Wyckoff, G. Miele, C. Julius, J. Kranich, A. Schenkel, S. Dow, and M. D. Zabel. 2010. Liposome-siRNA-peptide complexes cross the blood-brain barrier and significantly decrease PrP on neuronal cells and PrP in infected cell cultures. PLoS ONE 5, e11085 **doi** 10.1371/journal.pone.0011085
Ramezani, M., M. Khoshhamdam, A. Dehshahri, and B. Malaekeh-Nikouei. 2009. The influence of size, lipid composition and bilayer fluidity of cationic liposomes on the transfection efficiency of nanolipoplexes. Colloids and Surfaces. B, Biointerfaces **72:** 1-5.
Ramsey, M. R., and N. E. Sharpless. 2006. ROS as a tumour suppressor? Nature Cell Biology **8:** 1213-1215.
Rand, T. A., S. Petersen, F. Du, and X. Wang. 2005. Argonaute 2 cleaves the anti-guide stranded of siRNA during RISC activation. Cell **123:** 621-629.
Rangelov, S., D. Momekova, and M. Almgren. 2010. Structural characterization of lipid-based colloidal dispersions us*in*g cryogenic transmission electron microscopy. ***In.*** Méndez-Vilas, A., and J. Díaz, ed. Microscopy: Science, Technology, Applications and Education, 3. Formatex; p. 1724-1734.
Rao, C. N., and K. Biswas. 2009. Characterization of nanomaterials by physical methods. Annual Review of Analytical Chemistry **2:** 435-462.
Raouf, A., Y. Sun, S. Chatterjee, and P. Basak. 2012. The biology of human breast epithelial progenitors. Seminars in Cell and Developmental Biology **23:** 606-612.
Reinhart, B. J., F. J. Slack, M. Basson, A. E. Pasquinelli, J. C. Bettinger, A. E. Rougvie, H. R. Horvitz, and G. Ruvkun. 2000. The 21-nucleotide let-7 RNA regulates developmental timing in *Caenorhabditis elegans*. Nature **403:** 901-906.
Reischl, D., and A. Zimmer. 2009. Drug delivery of siRNA therapeutics: potentials and limits of nanosystems. Nanomedicine: Nanotechnology, Biology and Medicine **5:** 8-20.
Rejman, J., M. Conese, and D. Hoekstra. 2006. Gene transfer by means of lipo- and polyplexes: role of clathrin and caveole-mediated endocytosis. Journal of Liposome Research **16:** 237-247.
Resnier, P., T. Montier, V. Mathieu, J. P. Benoit, and C. Passirani. 2013. A review of the current status of siRNA nanomedicines in the treatment of cancer. Biomaterials **34:** 6429-6443.

Rivard, N., G. L'Allemain, J. Bartek, and J. Pouyssegur. 1996. Abrogation of p27Kip1 by cDNA antisense suppresses quiescence (G0 state) in fibroblasts. The Journal of Biological Chemistry **271:** 18337-18341.
Rivenbark, A. G., S. M. O'Connor, and W. B. Coleman. 2013. Molecular and cellular heterogeneity in breast cancer - Challenges for personalized medicine. The American Journal of Pathology **183:** 1113-1124.
Rocks, L., and K. A. Dawson. 2014. The interaction between nanoparticles and biological barriers. European Journal of Nanomedicine **6:** 121-122.
Roskoski Jr, R. 2014. The ErbB/HER family of protein-tyrosine kinases and cancer. Pharmacological Research **79:** 34-74.
Ross, J. S., and J. A. Fletcher. 1999. The HER-2/*neu* oncogene: prognostic factor, predictive factor and target for therapy. Seminars in Cancer Biology **9:** 125-138.
Ross, P. C., and S. W. Hui. 1999. Lipoplex size is a major determinant of *in vitro* lipofection efficiency. Gene Therapy **6:** 651-659.
Rubin, I., and Y. Yarden. 2001. The basic biology of HER2. Annals of Oncology **12:** S3-S8.
Rudzinski, W. E., and T. M. Aminabhavi. 2010. Chitosan as a carrier for targeted delivery of small interfering RNA. International Journal of Pharmaceutics **399:** 1-11.
Ruozi, B., D. Belletti, A. Tombesi, G. Tosi, L. Bondioli, F. Forni, and M. A. Vandelli. 2011. AFM, ESEM, TEM, and CLSM in liposomal characterization: a comparative study. International Journal of Nanomedicine **6:** 557-563.
Rusiecki, J. A., T. R. Holford, S. H. Zahm, and T. Zheng. 2005. Breast cancer risk factors according to joint estrogen receptor and progesterone receptor status. Cancer Detection and Prevention **29:** 419-426.
Russo, J., and I. H. Russo. 2004. Development of the human breast. Maturitas **49:** 2-15.
Saini, K. S., H. A. Azim Jr, O. Metzger-Filho, S. Loi, C. Sotiriou, E. de Azambuja, and M. Piccart. 2011. Beyond trastuzumab: New treatment options for HER2-positive breast cancer. The Breast **20:** S20-S27.
Şalva, E., S. Ö. Turan, F. Eren, and J, Akbu. 2015. The enhancement of gene silencing efficiency with chitosan-coated liposome formulations of siRNAs targeting HIF-1α and VEGF. International Journal of Pharmaceutics **478:** 147-154.
Samadikhah, H. R., A. Majidi, M. Nikkhah, and S. Hosseinkhani. 2011. Preparation, characterization, and efficient transfection of cationic liposomes and nanomagnetic cationic liposomes. International Journal of Nanomedicine **6:** 2275-2283.
Santi, S. A., and H. Lee. 2011. Ablation of Akt2 induces autophagy through cell cycle arrest, the downregulation of p70S6K, and the deregulation of mitochondria in MDA-MB231 cells. PLoS ONE **6:** e14614 **doi** 10.1371/journal.pone.0014614.
Sapsford, K. E., K. M. Tyner, B. J. Dair, J. R. Deschamps, and I. L. Medintz. 2011. Analyzing nanomaterial bioconjugates: a review of current and emerging purification and characterization techniques. Analytical Chemistry **83:** 4453-4488.
Schaefer, N. G., B. C. Pestalozzi, A. Knuth, and C. Renner. 2006. Potential use of humanized antibodies in the treatment of breast cancer. Expert Review of Anticancer Therapy **6:** 1065-1074.
Scherr, M., K. Battmer, B. Schultheis, A. Ganser, and M. Elder. 2005. Stable RNA interference as an option for ani-bcr-abl therapy. Gene Therapy **12:** 12-21.
Scherz-Shouval, R., and Z. Elazar. 2007. ROS, mitochondria and the regulation of autophagy. Trends in Cell Biology **17:** 422-427.
Schiffelers, R. M., A. Ansari, J. Xu, Q. Zhou, Q. Tang, G. Storm, G. Molema, P. Y. Lu, P. V. Scaria, and M. C. Woodle. 2004. Cancer siRNA therapy by tumor selective delivery with ligand-targeted sterically stabilized nanoparticle. Nucleic Acids Research **32:** e149 **doi** 10.1093/nar/gnh140.
Schiffelers, R. M., A. J. Mixson, A. M. Ansari, M. H. A. M. Fens, Q. Tang, Q. Zhou, J. Xu, G. Molema, P. Y. Lu, and P. V. Scaria. 2005. Transporting silence: Design of carriers for siRNA to angiogenic endothelium. Journal of Controlled Release **109:** 5-14.

Schmittgen, T. D., and K. J. Livak. 2008. Analyzing real-time PCR data by the comparative C_T method. Nature Protocols **3:** 1101-1108.
Scholz, C., and E. Wagner. 2012. Therapeutic plasmid DNA versus siRNA delivery: Common and different tasks for synthetic carriers. Journal of Controlled Release **161:** 554-565.
Schroeder, A., C. G. Levins, C. Cortez, R. Langer, and D. G. Anderson. 2010. Lipid-based nanotherapeutics for siRNA delivery. Journal of Internal Medicine **267:** 9-21.
Schulze, W. X., L. Deng, and M. Mann. 2005. Phosphotyrosine interactome of the ErbB receptor kinase family. Molecular Systems Biology **doi** 10.1038/msb4100012.
Seliger, B., and R. Kiessling. 2013. The two sides of HER2/*neu*: immune escape versus surveillance. Trends in Molecular Medicine **19:** 677-684.
Sen, K., and M. Mandal. 2013. Second generation liposomal cancer therapeutics: Transition from laboratory to clinic. International Journal of Pharmaceutics **448:** 28-43.
Shah, D., and C. Osipo. 2016. Cancer stem cells and HER2 positive breast cancer: The story so far. Genes and Diseases **doi** 10.1016/j.gendis.2016.02.002.
Sharma, A., and U. S. Sharma. 1997. Liposomes in drug delivery: progress and limitations. International Journal of Pharmaceutics **154:** 123-140.
Shawver, L. K., D. Slamon, and A. Ullrich. 2002. Smart drugs: tyrosine kinase inhibitors in cancer therapy. Cancer Cell **1:** 117-123.
Shekhar, M., R. Pauley, and G. Heppner. 2003. Host microenvironment in breast cancer development: extracellular matrix-stromal cell contribution to neoplastic phenotype of epithelial cells in the breast. Breast Cancer Research **5:** 130-135.
Shi, J., S. Yu, J. Zhu, D. Zhi, Y. Zhao, S. Cui, and S. Zhang. 2016. Carbamate-linked cationic lipids with different hydrocarbon chains for gene delivery. Colloids and Surfaces B: Biointerfaces **141:** 417-422.
Shim, G., M. G. Kim, J. Y. Park, and Y. K. Oh. 2013. Application of cationic liposomes for delivery of nucleic acids. Asian Journal of Pharmaceutical Sciences **8:** 72-80.
Shore, A. N., and J. M. Rosen. 2014. Regulation of mammary epithelial cell homeostasis by lncRNAs. The International Journal of Biochemistry and Cell Biology **54:** 318-330.
Siddiqa, A., L. M. Long, L. Li, R. A. Marciniak, and I. Kazhdan. 2008. Expression of HER-2 in MCF-7 breast cancer cells modulates anti-apoptotic proteins survivin and Bcl-2 via the extracellular signal-related kinase (ERK) and phosphoinositide-3 kinase (PI3K) signalling pathways. BMC Cancer **8:** 129-136.
Silvander, M., M. Johnsson, and K. Edwards. 1998. Effects of PEG-lipids on permeability of phosphatidylcholine/cholesterol liposomes in buffer and in human serum. Chemistry and Physics of Lipids **97:** 15-26.
Simpson, P. T., J. S. Reis-Filho, T. Gale, and S. R. Lakhani. 2005. Molecular evolution of breast cancer. The Journal of Pathology **205:** 248-254.
Singh, M., and M. Ariatti. 2006. A cationic cytofectin with long spacer mediates favourable transfection in transformed human epithelial cells. International Journal of Pharmaceutics **309:** 189-198.
Singh, M., N. Kisoon, and M. Ariatti. 2001. Receptor-mediated gene delivery to HepG2 cells by ternary assemblies containing cationic liposomes and cationized asialoorosomucoid. Drug Delivery **8:** 29-34.
Slamon, D. J., G. M. Clark, S. G. Wong, W. J. Levin, A. Ullrich, and W. L. McGuire. 1987. Human breast cancer: correlation of relapse and survival with amplification of the HER-2/*neu* oncogene. Science **235:** 177-182.
Slamon, D. J., W. Godolphin, L. A. Jones, J. A. Holt, S. G. Wong, D. E. Keith, W. J. Levin, S. G. Stuart, J. Udove, A. Ullrich, and M. F. Press. 1989. Studies of the HER-2/*neu* proto-oncogene in human breast and ovarian cancer. Science **244:** 707-712.
Sledge, G. W., H. S. Rugo, and H. J. Burstein. 2006. The role of angiogenesis inhibition in the treatment of breast cancer. Clinical Advances in Hematology and Oncology **4:** 1-12.

Šmisterová, J., A. Wagenaar, M. C. Stuart, E. Polushkin, G. ten Brinke, R. Hulst, J. B. Engberts, and D. Hoekstra. 2001. Molecular shape of the cationic lipid controls the structure of cationic lipid/dioleylphosphatidylethanolamine-DNA complexes and the efficiency of gene delivery. The Journal of Biological Chemistry **276:** 47615-47622.

Smith, B. A., A. L. Welm, and B. E. Welm. 2012. On the shoulders of giants: A historical perspective of unique experimental methods in mammary gland research. Seminars in Cell and Developmental Biology **23:** 583-590.

Sobel, M., J. Hashimoto, S. P. Arnoczky, and W. H. Bohne. 1992. The microvasculature of the sesamoid complex: its clinical significance. Foot Ankle **13:** 359-363.

Soenen, S. J. H., E. Illyes, D. Vercauteren, K. Braeckmans, Z. Majer, S. C. De Smedt, and M. De Cuyper. 2009. The role of nanoparticle concentration-dependent induction of cellular stress in the internalization of non-toxic cationic magnetoliposomes. Biomaterials **30:** 6803-6813.

Sofia, S. J., V. Premnath, and E. W. Merrill. 1998. Poly(ethylene oxide) grafted to silicon surfaces: Grafting density and protein adsorption. Macromolecules **31:** 5059-5070.

Sonoke, S., T. Ueda, K. Fujiwara, Y. Sato, K. Takagaki, K. Hirabayashi, T. Ohgi, and J. Yano. 2008. Tumor regression in mice by delivery of Bcl-2 small interfering RNA with pegylated cationic liposomes. Cancer Research **68:** 8843-8851.

Sørlie, T., C. M. Perou, R. Tibshirani, T. Aas, S. Geisler, H. Johnsen, T. Hastie, M. B. Eisen, M. van de Rijn, S. S. Jeffrey, T. Thorsen, H. Quish, J. C. Matese, P. O. Brown, D. Botstein, P. E. Lønning, and A. L. Børresen-Dale. 2001. Gene expression patterns of breast carcinomas distinguish tumor subclasses with clinical implications. Proceedings of the National Academy of Sciences of the United States of America **98:** 10869-10874.

Sørlie, T., R. Tibshirani, J. Parker, T. Hastie, J. S. Marron, A. Nobel, S. Deng, H. Johnsen, R. Pesich, S. Geisler, J. Demeter, C. M. Perou, P. E. Lønning, P. O. Brown, A. L. Børresen-Dale, and D. Botstein. 2003. Repeated observation of breast tumor subtypes in independent gene expression data sets. Proceedings of the National Academy of Sciences of the United States of America **100:** 8418-8423.

Sotiriou, C., C. Desmedt, V. Durbecq, L. Dal Lago, M. Lacroix, F. Cardoso, and M. Piccart. 2005. Genomic and molecular classification of breast cancer. ***In.*** Ross, J. S., G. N. Hortobagyi, M. A. Sudbury, ed. Molecular Oncology of Breast Cancer. Jones & Bartlett; p. 81-95.

Spagnou, S., A. D. Miller, and M. Keller. 2004. Lipidic carriers of siRNA: differences in the formulation, cellular uptake, and delivery with plasmid DNA. Biochemistry **43:** 13348-13356.

Spector, N. L., W. Xia, H. Burris 3rd, H. Hurwitz, E. C. Dees, A. Dowlati, B. O'Neil, B. Overmoyer, P. K. Marcom, K. L. Blackwell, D. A. Smith, K. M. Koch, A. Stead, S. Mangum, M. J. Ellis, L. Liu, A. K. Man, T. M. Bremer, J. Harris, and S. Bacus. 2005. Study of the biologic effects of lapatinib, a reversible inhibitor of ErbB1 and ErbB2 tyrosine kinases, on tumor growth and survival pathways in patients with advanced malignancies. Journal of Clinical Oncology **23:** 2502-2512.

Spector, N. L., and K. L. Blackwell. 2009. Understanding the mechanisms behind trastuzumab therapy for Human Epidermal Growth Factor Receptor 2-positive breast cancer. Journal Clinical Oncology **27:** 5838-5847.

Srinivasan, C., and D. J. Burgess. 2009. Optimization and characterization of anionic lipoplexes for gene delivery. Journal of Controlled Release **136:** 62-70.

Sternlicht, M. D. 2006. Key stages in mammary gland development: The cues that regulate ductal branching and morphogenesis. Breast Cancer Research **8:** 201.

Stingl, J. 2011. Estrogen and progesterone in normal mammary gland development and in cancer. Hormones and Cancer **2:** 85-90.

Stingl, J., A. Raouf, P. Eirew, and C. J. Eaves. 2006. Deciphering the mammary epithelial cell hierarchy. Cell Cycle **5:** 1519-1522.

Stoner, M., M. Wormke, B. Saville, I. Samudio, C. Qin, M. Abdelrahim, and S. Safe. 2004. Estrogen regulation of vascular endothelial growth factor gene expression in ZR-75 breast cancer cells through interaction of estrogen receptor alpha and SP proteins. Oncogene **23:** 1052-1063.

Stratford, S., S. Stec, V. Jadhav, J. Seitzer, M. Abrams, and M. Beverly. 2008. Examination of real-time polymerase chain reaction methods for the detection and quantification of modified siRNA. Analytical Biochemistry **379:** 96-104.
Su, Z. Z., M. T. Madireddi, J. J. Lin, C. S. H. Young, S. Kitada, J. C. Reed, N. I. Goldstein, and P. B. Fisher. 1998. The cancer growth suppressor gene mda-7 selectively induces apoptosis in human breast cancer cells and inhibits tumor growth in nude mice. Proceedings of the National Academy of Sciences of the United States of America **95:** 14400-14405.
Sun, T. M., J. Z. Du, Y. D. Yao, C. Q. Mao, S. Dou, S. Y. Huang, P. Z. Zhang, K. W. Leong, E. W. Song, and J. Wang. 2011. Simultaneous delivery of siRNA and paclitaxel via a "two-in-one" micelleplex promotes synergistic tumor suppression. ACS Nano **5:** 1483-1494.
Svoboda, P. 2007. Off-targeting and other non-specific effects of RNAi experiments in mammalian cells. Current Opinion in Molecular Therapeutics **9:** 248-257.
Swami, A., A. Aggarwal, A. Pathak, S. Patnaik, P. Kumar, Y. Singh, and K. C. Gupta. 2007. Imidazolyl-PEI modified nanoparticles for enhanced gene delivery. International Journal of Pharmaceutics **335:** 180-192.
Tack, D. K., F. M. Palmieri, and E. A. Perez. 2004. Anthracycline vs nonanthracycline adjuvant therapy for breast cancer. Oncology **18:** 1367-1376.
Tai, W., R. Mahato, and K. Cheng. 2010a. The role of HER2 in cancer therapy and targeted drug delivery. Journal of Controlled Release **146:** 264-275.
Tai, W., B. Qin, and K. Cheng. 2010b. Inhibition of breast cancer cell growth and invasiveness by dual silencing of HER-2 and VEGF. Molecular Pharmaceutics **7:** 543-556.
Takahashi, A., N. Ohtani, K. Yamakoshi, S. Iida, H. Tahara, K. Nakayama, K. I. Nakayama, T. Ide, H. Saya, and E. Hara. 2006. Mitogenic signalling and the p16INK4a-Rb pathway cooperate to enforce irreversible cellular senescence. Nature Cell Biology **8:** 1291-1297.
Takahashi, Y., M. Nishikawa, and Y. Takakura. 2009. Nonviral vector-mediated RNA interference: its gene silencing characteristics and important factors to achieve RNAi-based gene therapy. Advanced Drug Delivery Reviews **61:** 760-766.
Tan, W. B., S. Jiang, and Y. Zhang. 2007. Quantum-dot based nanoparticles for targeted silencing of HER2/*neu* gene via RNA interference. Biomaterials **28:** 1565-1571.
Tavassoli, F. A., and P. Devilee. 2003. World Health Organization classification of tumours. Pathology and genetics of tumours of the breast and female genital organs. Lyon, France: IARC Press; p. 227-239.
Telesco, S. E., and R. Radhakrishnan. 2009. Atomistic insights into regulatory mechanisms of the HER2 tyrosine kinase domain: a molecular dynamics study. Biophysical Journal **96:** 2321-2334.
Tevaarwerk, A. J., and J. M. Kolesar. 2009. Lapatinib: a small-molecule inhibitor of epidermal growth factor receptor and human epidermal growth factor receptor-2 tyrosine kinases used in the treatment of breast cancer. Clinical Therapeutics **31:** 2332-2348.
Thalla, P. K., A. Contreras-García, H. Fadlallah, J. Barrette, G. De Crescenzo, Y. Merhi, and S. Lerough. 2013. A versatile star PEG grafting method for the generation of nonfouling and nonthrombogenic surfaces. BioMed Research International **doi** 10.1155/2013/962376.
Thery, J. C., J. P. Spano, D. Azria, E. Raymond, and F. P. Llorca. 2014. Resistance to human epidermal growth factor receptor type 2-targeted therapies. European Journal of Cancer **50:** 892-901.
Thiel, K. W., L. I. Hernandez, J. P. Dassie, W. H. Thiel, X. Liu, K. R. Stockdale, A. M. Rothman, F. J. Hernandez, J. O. McNamara II, and P. H. Giangrande. 2012. Delivery of chemo-sensitizing siRNAs to $HER2^{+}$-breast cancer cells using RNA aptamers. Nucleic Acids Research **doi** 10.1093/nar/gks294.
Tirosh, O., Y. Barenholz, J. Katzhender, and A. Priev. 1998. Hydration of polyethylene glycol-grafted liposomes. Biophysical Journal **74:** 1371-1379.
Toi, M., K. Inada, H. Suzuki, and T. Tominaga. 1995. Tumor angiogenesis in breast cancer: its importance as a prognostic indicator and the association with vascular endothelial growth factor expression. Breast Cancer Research and Treatment **36:** 193-204.

Tokunaga, E., E. Oki, K. Nishida, T. Koga, A. Egashira, M. Morita, Y. Kakeji, and Y. Maehara. 2006. Trastuzumab and breast cancer: developments and current status. International Journal of Clinical Oncology **11:** 199-208.
Tophkhane, C., S. Yang, W. Bales, L. Archer, A. Osunkoya, A. D. Thor, and X. Yang. 2007. Bcl-2 overexpression sensitizes MCF-7 cells to genistein by multiple mechanisms. International Journal of Oncology **31:** 867-874.
Torchilin, V. P., V. G. Omelyanenko, M. I. Papisov, A. A. Bogdanov, V. S. Trubetskoy, J. N. Herron, and C. A. Gentry. 1994. Poly(ethyleneglycol) on the liposome surface: on the mechanism of polymer-coated liposome longevity. Biochimica et Biophysica Acta **1195:** 11-20.
Torre, L. A., F. Bray, R. L. Siegel, J. Ferlay, J. L. Tieulent, and A. Jemal. 2015. Global Cancer Statistics, 2012. CA: A Cancer Journal for Clinicians **65:** 87-108.
Tranchant, I., B. Thompson, C. Nicolazzi, N. Mignet, and D. Scherman. 2004. Physicochemical optimisation of plasmid delivery by cationic lipids. Journal of Gene Medicine **6:** 24-35.
Troiber, C., J. C. Kasper, S. Milani, M. Scheible, I. Martin, F. Schaubhut, S. Küchler, J. Rädler, F. C. Simmel, W. Friess, and E. Wagner. 2013. Journal of Pharmaceutics and Biopharmaceutics **84:** 255-264.
Tsai, C. C., S. C. Jain, and H. M. Sobell. 1975. X-ray crystallographic visualization of drug-nucleic acid intercalative binding: structure of an ethidium-dinucleoside monophosphate crystalline complex, Ethidium: 5-iodouridylyl (3'-5') adenosine. Proceedings of the National Academy of Sciences of the United States of America **72:** 628-632.
Tsé, C., A. S. Gauchez, W. Jacot, and P. J. Lamy. 2012. HER2 shedding and serum HER2 extracellular domain: Biology and clinical utility in breast cancer. Cancer Treatment Reviews **38:** 133-142.
Tseng, Y. C., S. Mozumdar, and L. Huang. 2009. Lipid-based systemic delivery of siRNA. Advanced Drug Delivery Reviews **61:** 721-731.
Tuschl, T., P. D. Zamore, R. Lehmann, D. P. Bartel, and P. A. Sharp. 1999. Targeted mRNA degradation by double-stranded RNA *in vitro*. Genes and Development **13:** 3191-3197.
Tzahar, E., H. Waterman, X. Chen, G. Levkowitz, D. Karunagaran, S. Lavi, B. J. Ratzkin, and Y. Yarden. 1996. A hierarchical network of interreceptor interactions determines signal transduction by *neu* differentiation factor/neuregulin and epidermal growth factor. Molecular and Cellular Biology **16:** 5276-5287.
Ullrich, A., L. Coussens, J. S. Hayflick, T. J. Dull, A. Gray, A. W. Tam, J. Lee, Y. Yarden, T. A. Libermann, J. Schlessinger, J. Downward, E. L. V. Mayes, N. Whittle, M. D. Waterfield, and P. H. Seeburg. 1984. Human epidermal growth factor receptor cDNA sequence and aberrant expression of the amplified gene in A431 epidermoid carcinoma cells. Nature **309:** 418-425.
Urban-Klein, B., S. Werth, S. Abuharbeid, F. Czubayko, and A. Aigner. 2005. RNAi-mediated gene-targeting through systemic application of polyethylenimine (PEI)-complexed siRNA *in vivo*. Gene Therapy **12:** 461-466.
ur Rehman, Z., I. S. Zuhorn, and D. Hoekstra. 2013a. How cationic lipids transfer nucleic acids into cells and across cellular membranes: Recent advances. Journal of Controlled Release **166:** 46-56.
ur Rehman, Z., D. Hoekstra, and I. S. Zuhorn. 2013b. Mechanism of polyplex- and lipoplex-mediated delivery of nucleic acids: real-time visualization of transient membrane destabilization without endosomal lysis. ACS Nano **7:** 3767-3777.
Vanderlaag, K. E., S. Hudak, L. Bald, L. Fayadat-Dilman, M. Sathe, J. Grein, and M. J. Janatpour. 2010. Anterior gradient-2 plays a critical role in breast cancer cell growth and survival by modulating cyclin D1, estrogen receptor-alpha and survivin. Breast Cancer Research **12:** R32.
van der Meel, R., M. H. A. M. Fens, P. Vader, W. W. van Solinge, O. Eniola-Adefeso, and R. M. Schiffelers. 2014. Extracellular vesicles as drug delivery systems: Lessons from the liposome field. Journal of Controlled Release **195:** 72-85.
van de Water, F. M., O. C. Boerman, A. C. Wouterse, J. G. P. Peters, F. G. M. Russel, and R. Masereeuw. 2006. Intravenously administered short interfering RNA accumulates in the kidney and

selectively suppresses gene function in renal proximal tubules. Drug Metabolism and Disposition **34:** 1393-1397.
van Gaal, E. V. B., R. van Eijk, R. S. Oosting, R. J. Kok, W. E. Hennink, D. J. A. Crommelin, and E. Mastrobattista. 2011. How to screen non-viral gene delivery systems *in vitro*? Journal of Controlled Release **154:** 218-232.
van Meerloo, J., G. J. Kaspers, and J. Cloos. 2011. Cell sensitivity assays: the MTT assay. Methods in Molecular Biology **731:** 237-245.
van Zijl, F., G. Krupitza, and W. Mikulits. 2011. Initial steps of metastasis: cell invasion and endothelial transmigration. Mutation Research **728:** 23-34.
Verma, I. M., and N. Somia. 1997. Gene therapy – promises, problems and prospects. Nature **389:** 239-242.
Videira, M., R. L. Reis, and M. A. Brito. 2014. Deconstructing breat cancer cell biology and the mechanisms of multidrug resistance. Biochimica et Biophysica Acta **1846:** 312-325.
Villadsen, R., A. J. Fridriksdottir, L. Rønnov-Jessen, T. Gudjonsson, F. Rank, M. A. LaBarge, M. J. Bissell, and O. W. Petersen. 2007. Evidence for a stem cell hierarchy in the adult human breast. The Journal of Cell Biology **177:** 87-101.
Vimala, K., S. Sundarraj, M. V. Sujitha, and S. Kannan. 2012. Curtailing overexpression of E2F3 in breast cancer using siRNA (E2F3)-based gene silencing. Archives of Medical Research **43:** 415-422.
Visvader, J. E. 2009. Keeping abreast of the mammary epithelial hierarchy and breast tumorigenesis. Genes and Development **23:** 2563-2577.
Voduc, K. D., M. C. U. Cheang, S. Tyldesley, K. Gelmon, T. O. Nielsen, and H. Kennecke. 2010. Breast cancer subtypes and the risk of local and regional relapse. Journal of Clinical Oncology **28:** 1684-1691.
Vonarbourg, A., P. Saulnier, C. Passirani, and J. P. Benoit. 2005. Electrokinetic properties of noncharged lipid nanocapsules: influence of the dipolar distribution at the interface. Electrophoresis **26:** 2066-2075.
Vonarbourg, A., C. Passirani, P. Saulnier, and J. P. Benoit. 2006. Parameters influencing the stealthiness of colloidal drug delivery systems. Biomaterials **27:** 4356-4373.
Vu, T., M. X. Sliwkowski, and F. X. Claret. 2014. Individualizing personalized drug combinations to overcome trastuzumab resistance in HER2-positive breast cancer. Biochimica et Biophysica Acta **1846:** 353-365.
Walkey, C. D., and W. C. W. Chan. 2012. Understanding and controlling the interaction of nanomaterials with proteins in a physiological environment. Chemical Society Reviews **41:** 2780-2799.
Wang, J. C. 1974. The degree of unwinding of the DNA helix by ethidium: I. Titration of twisted PM2 DNA molecules in alkaline cesium chloride density gradients. Journal of Molecular Biology **89:** 783-801.
Wang, M., and M. Thanou. 2010. Targeting nanoparticles to cancer. Pharmacological Research **62:** 90-99.
Wang, Y., S. Liu, G. Zhang, C. Zhou, H. Zhu, X. Zhou, L. Quan, J. Bai, and N. Xu. 2005. Knockdown of c-Myc expression by RNAi inhibits MCF-7 breast tumor cells growth *in vitro* and *in vivo*. Breast Cancer Research **7:** R220-R228.
Wang, Y., S. Gao, W. H. Ye, H. S. Yoon, and Y. Y. Yang. 2006. Co-delivery of drugs and DNA from cationic core-shell nanoparticles self-assembled from a biodegradable copolymer. Nature Materials **5:** 791-796.
Wang, Y., L. Miao, A. Satterlee, and L. Huang. 2015. Delivery of oligonucleotides with lipid nanoparticles. Advanced Drug Delivery Reviews **87:** 68-80.
Warren, C. M., and R. Landgraf. 2006. Signaling through ERBB receptors: multiple layers of diversity and control. Cellular Signalling **18:** 923-933.
Wasungu, L., and D. Hoekstra. 2006. Cationic lipids, lipoplexes and intracellular delivery of genes. Journal of Controlled Release **116:** 255-264.

Watson, C. J., and W. T. Khaled. 2008. Mammary development in the embryo and adult: a journey of morphogenesis and commitment. Development **135:** 995-1003.
Weis, S. M., and D. A Cheresh. 2005. Pathophysiological consequences of VEGF-induced vascular permeability. Nature **437:** 497-504.
Weisman, S., D. Hirsch-Lemer, Y. Barenholz, and Y. Talmon. 2004. Nanostructure of cationic lipid-oligonucleotide complexes. Biophysical Journal **87:** 609-614.
Wessman, P., K. Edwards, and D. Mahlin. 2010. Structural effects caused by spray- and freeze-drying of liposomes and bilayer discs. Journal of Pharmaceutical Sciences **99:** 2032-2048.
White, P. J. 2008. Barriers to successful delivery of short interfering RNA after systemic administration. Clinical and Experimental Pharmacology and Physiology **35:** 1371-1376.
Whitehead, K. A., R. Langer, and D. G. Anderson. 2009. Knocking down barriers: advances in siRNA delivery. Nature Reviews Drug Discovery **8:** 129-138.
Wieczorek, M., A. Paczkowska, P. Guzenda, M. Majorek, A. K. Bednarek, and M. Lamparska-Przybysz. 2008. Silencing of Wnt-1 by siRNA induces apoptosis of MCF-7 human breast cancer cells. Cancer Biology and Therapy **7:** 268-274.
Wiese, G. R., and T. W. Healy. 1970. Effect of particle size on colloid stability. Transactions of the Faraday Society **66:** 490-499.
Wirth, T., N. Parker, and S. Ylä-Herttuala. 2013. History of gene therapy. Gene http://dx.doi.org/10.1016/j.gene.2013.03.137.
Wittrup, A., and J. Lieberman. 2015. Knocking down disease: a progress report on siRNA therapeutics. Nature Reviews Genetics **16:** 543-552.
Wolff, A. C., M. E. Hammond, J. N. Schwartz, K. L. Hagerty, D. C. Allred, R. J. Cote, M. Dowsett, P. L. Fitzgibbons, W. M. Hanna, A. Langer, L. M. McShane, S. Paik, M. D. Pegram, E. A. Perez, M. F. Press, A. Rhodes, C. Sturgeon, S. E. Taube, R. Tubbs, G. H. Vance, M. van de Vijver, T. M. Wheeler, and D. F. Hayes. 2007. American Society of Clinical Oncology; College of American Pathologists: American Society of Clinical Oncology/College of American Pathologists guideline recommendations for Human Epidermal Growth Factor Receptor 2 testing in breast cancer. Journal of Clinical Oncology **25:** 118-145.
Wong, L. L., D. Zhang, C. F. Chang, and E. S. C. Koay. 2010. Silencing of the PP2A catalytic subunit causes HER-2/*neu* positive breast cancer cells to undergo apoptosis. Experimental Cell Research **16:** 3387-3396.
Workman, P. 2005. Genomics and the second golden era of cancer drug development. Molecular BioSystems **1:** 17-26.
World Population Prospects (WPP): the 2002 Revision. Population Division of the Department of Economic and Social Affairs of the United Nations Secretariat. Available at: http://esa.un.org/unpp; 2003. Accessed July 27, 2015.
Xia, W., R. J. Mullin, B. R. Keith, L. H. Liu, H. Ma, D. W. Rusnak, G. Owens, K. J. Alligood, and N. L. Spector. 2002. Anti-tumour activity of GW 572016: a dual tyrosine kinase inhibitor blocks EGF activation of EGFR/erbB2 and downstream Erk1/2 and Akt pathways. Oncogene **21:** 6255-6263.
Xia, Y., J. Tian, and X. Chen. 2016. Effect of surface properties on liposomal siRNA delivery. Biomaterials **79:** 56-68.
Xiang, S., H. Tong, Q. Shi, J. C. Fernandes, T. Jin, K. Dai, and X. Zhang. 2012. Uptake mechanisms of non-viral gene delivery. Journal of Controlled Release **158:** 371-378.
Xie, F. Y., Y. Liu, J. Xu, Q. Q. Tang, P. V. Scaria, Q. Zhou, M. C. Woodle, and P. Y. Lu. 2004. Delivering siRNA to animal disease models for validation of novel drug targets *in vivo*. PharmaGenomics **4:** 28-31
Xie, F. Y., M. C. Woodle, and P. Y. Lu. 2006. Harnessing *in vivo* siRNA delivery for drug discovery and therapeutic development. Drug Discovery Today **11:** 67-73.

Xing, X., S. Zhang, J. Y. Chang, S. D. Tucker, H. Chen, L. Huang, and M. C. Hung. 1998. Safety study and characterization of E1A-liposome complex gene-delivery protocol in an ovarian cancer model. Gene therapy **5:** 1538-1544.
Xiong, X. B., and A. Lavasanifar. 2011. Traceable multifunctional micellar nanocarriers for cancer-targeted co-delivery of MDR-1 siRNA and doxorubicin. ACS Nano **5:** 5202-5213.
Xu, Y., S. W. Hui, P. Frederick, and F. C. Szoka Jr. 1999. Physicochemical characterization and purification of cationic lipoplexes. Biophysical Journal **77:** 341-353.
Xu, L., and T. J. Anchordoquy. 2008. Cholesterol domains in cationic lipid/DNA complexes improve transfection. Biochimica et Biophysica Acta **1778:** 2177-2181.
Xu, C. F., and J. Wang. 2015. Delivery systems for siRNA drug development in cancer therapy. Asian Journal of Pharmaceutical Sciences **10:** 1-12.
Yan, X., G. L. Scherphof, and J. A Kamps. 2005. Liposome opsonization. Journal of Liposome Research **15:** 109-139.
Yang, L., Z. Cao, H. Yan, and W. C. Wood. 2003. Coexistence of high levels of apoptotic signaling and inhibitor of apoptosis proteins in human tumor cells: implication for cancer specific therapy. Cancer Research **63:** 6815-6824.
Yang, L., X. H. Peng, Y. A. Wang, X. Wang, Z. Cao, C. Ni, P. Karna, X. Zhang, W. C. Wood, X. Gao, S. Nie, and H. Mao. 2009. Receptor-targeted nanoparticles for *in vivo* imaging of breast cancer. Clinical Cancer Research **15:** 4722-4732.
Yang, X. Z., S. Dou, T. M. Sun, C. Q. Mao, H. X. Wang, and J. Wang. 2011. Systemic delivery of siRNA with cationic lipid assisted PEG-PLA nanoparticles for cancer therapy. Journal of Controlled Release **156:** 203-211.
Yang, S., Y. Chen, R. Ahmadie, and E. A. Ho. 2013a. Advancements in the field of intravaginal siRNA delivery. Journal of Controlled Release 167: 29-39.
Yang, F., W. Huang, Y. Li, S. Liu, M. Jin, Y. Wang, L. Jia, and Z. Gao. 2013b. Anti-tumor effects in mice induced by survivin-targeted siRNA delivered through polysaccharide nanoparticles. Biomaterials **34:** 5689-5699.
Yang, S. Y., Y. Zheng, J. Y. Chen, Q. Y. Zhang, D. Zhao, D. E. Han, and X. J. Chen. 2013c. Comprehensive study of cationic liposomes composed of DC-Chol and cholesterol with different mole ratios for gene transfection. Colloids and Surfaces B: Biointerfaces **101:** 6-13.
Yao, L., J. Daniels, D. Wijesinghe, O. A. Andreev, and Y. K. Reshetnyak. 2013. pHLIP®-mediated delivery of PEGylated liposomes to cancer cells. Journal of Controlled Release **167:** 228-237.
Yarden, Y. 2001. Biology of HER2 and its importance in breast cancer. Oncology **61:** 1-13.
Yarden, Y., and M. X. Sliwkowski. 2001. Untangling the ErbB signaling network. Nature Reviews. Molecular Cell Biology **2:** 127-137.
Yeon, C. H., and M. D. Pegram. 2005. Anti-erbB2 antibody trastuzumab in the treatment of HER2-amplified breast cancer. Investigational New Drugs **23:** 391-409.
Yuan, J. S., A. Reed, F. Chen, and C. N. Stewart Jr. 2006. Statistical analysis of real-time PCR data. BMC Bioinformatics **7**:85 doi:10.1186/1471-2105-7-85.
Zalipsky, S. 1995. Functionalized poly(ethylene glycol) for preparation of biologically relevant conjugates. Bioconjugate Chemistry **6:** 150-165.
Zelnak, A. B., and R. M. O'Regan. 2007. Targeting angiogenesis in advanced breast cancer. BioDrugs **21:** 209-214.
Zelphati, O., L. S. Uyechi, L. G. Barron, and F. C. Szoka Jr. 1998. Effect of serum components on the physico-chemical properties of cationic lipid/oligonucleotide complexes and on their interactions with cells. Biochimica et Biophysica Acta **1390:** 119-133.
Zhang, Y., F. Calon, C. Zhu, R. J. Boado, and W. M. Pardridge. 2003. Intravenous nonviral gene therapy causes normalization of striatal tyrosine hydroxylase and reversal of motor impairment in experimental Parkinsonism. Human Gene Therapy **14:** 1-12.

Zhang, H., F. A. Kolb, L. Jaskiewicz, E. Westhof, and W. Filipowicz. 2004. Single processing center models for human Dicer and bacterial RNase III. Cell **118:** 57-68.
Zhang, Y., E. L. Bradshaw-Pierce, A. Delille, D. L. Gustafson, and T. J. Anchordoquy. 2008. *In vivo* comparative study of lipid/DNA complexes with different *in vitro* serum stability: effects on biodistribution and tumor accumulation. Journal of Pharmaceutical Sciences **97:** 237-250.
Zhang, Y., H. Li, J. Sun, J. Gao, W. Liu, B. Li, Y. Guo, and J. Chen. 2010. DC-Chol/DOPE cationic liposomes: A comparative study of the influence factors on plasmid pDNA and siRNA gene delivery. International Journal of Pharmaceutics **390:** 198-207.
Zhang, X. X., T. J. McIntosh, and M. W. Grinstaff. 2012. Functional lipids and lipoplexes for improved gene delivery. Biochimie **94:** 42-58.
Zhao, Z. X., S. Y Gao, J. C. Wang, C. J. Chen, E. Y. Zhao, W. J. Hou, Q. Feng, L. Y. Gao, X. Y. Liu, L. R. Zhang, and Q. Zhang. 2012. Self-assembly nanomicelles based on cationic mPEG-PLA-b-Polyarginine (R15) triblock copolymer for siRNA delivery. Biomaterials **33:** 6793-6807.
Zhou, B. P., M. C. Hu, S. A. Miller, Z. Yu, W. Xia, S. Y. Lin, and M. C. Hung. 2000. HER-2/*neu* blocks tumor necrosis factor-induced apoptosis via the Akt/NF-kappaB pathway. The Journal of Biological Chemistry **275:** 8027-8031.
Zhou, L., Z. Chen, W. Chi, X. Yang, W. Wang, and B. Zhang. 2012. Mono-methoxy-poly(3-hydroxybutyrate-co-4-hydroxybutyrate)-graft-hyperbranched polyethylenimine copolymers for siRNA delivery. Biomaterials **33:** 2334-2344.
Zhou, L., Z. Chen, F. Wang, X. Yang, and B. Zhang. 2013. Multifunctional triblock co-polymer mP3/4HB-b-PEG-b-lPEI for efficient intracellular siRNA delivery and gene silencing. Acta Biomaterialia **9:** 6019-6031.
Zhou, Y., C. Zhang, and W. Liang. 2014. Development of RNAi technology for targeted therapy - A track of siRNA based agents to RNAi therapeutics. Journal of Controlled Release **193:** 270-281.
Zhu, L., and R. I. Mahato. 2010. Lipid and polymeric carrier mediated nucleic acid delivery. Expert Opinion on Drug Delivery **10:** 1209-1226.
Zidovska, A., H. M. Evans, A. Ahmad, K. K. Ewert, and C. R. Safinya. 2009. The role of cholesterol and structurally related molecules in enhancing transfection of cationic liposome-DNA complexes. The Journal of Physical Chemistry B **113:** 5208-5216.
Zimmermann, T. S., A. C. H. Lee, A. Akinc, B. Bramlage, D. Brumcrot, M. N. Fedoruk, J. Harborth, J. A. Heyes, L. B. Jeffs, M. John, A. D. Judge, K. Lam, K. McClintock, L. V. Nechev, L. R. Palmer, T. Racie, I. Röhl, S. Seiffert, S. Shanmugam, V. Sood, J. Soutschek, I. Toudjarska, A. J. Wheat, E. Yaworski, W. Zedalis, V. Koteliansky, M. Manoharan, H. P. Vornlocher, and I. MacLachlan. 2006. RNAi-mediated gene silencing in non-human primates. Nature **441:** 111-114.
Zintchenko, A., A. Philipp, A. Dehshahri, and E. Wagner. 2008. Simple modifications of branched PEI lead to highly efficient siRNA carriers with low toxicity. Bioconjugate Chemistry **19:** 1448-1455.
Zuhorn, I. S., and D. Hoekstra. 2002. On the mechanism of cationic amphiphile mediated transfection. To fuse or not to fuse: is that the question? The Journal of Membrane Biology **189:** 167-179.
Zuhorn, I. S., V. Oberle, W. H. Visser, J. B. Engberts, U. Bakowsky, E. Polushkin, and D. Hoekstra. 2002. Phase behavior of cationic amphiphiles and their mixtures with helper lipid influences lipoplex shape, DNA translocation, and transfection efficiency. Biophysical Journal **83:** 2096-2108.

APPENDIX A

Chol-T: ^{1}H NMR (250 MHz, CDCl3): δ 0.65 (s, 3H, CCH_3), 0.83 (d, 6H, J = 5.2 Hz, CH(CH_3)$_2$), 0.89 (d, 3H, J = 6.5 Hz, CHCH_3), 2.19 (s, 6H, (CH_3)$_2$NCH$_2$CH$_2$)), 2.30 (t, 2H, J = 6.6 Hz, (CH$_3$)$_2$NCH_2CH$_2$CH$_2$), 3.21 (q, 2H, J = 6.1 Hz, (CH$_3$)$_2$NCH$_2$CH$_2$CH_2NH), 4.46 (m, 1H, Chol-$H_{3\alpha}$), 5.35 (d, 1H, J = 5.3 H, H_6). (HRMS) (M^+) $C_{33}H_{58}N_2O_2$, M*w*: calculated 514.4498, found 514.4490.

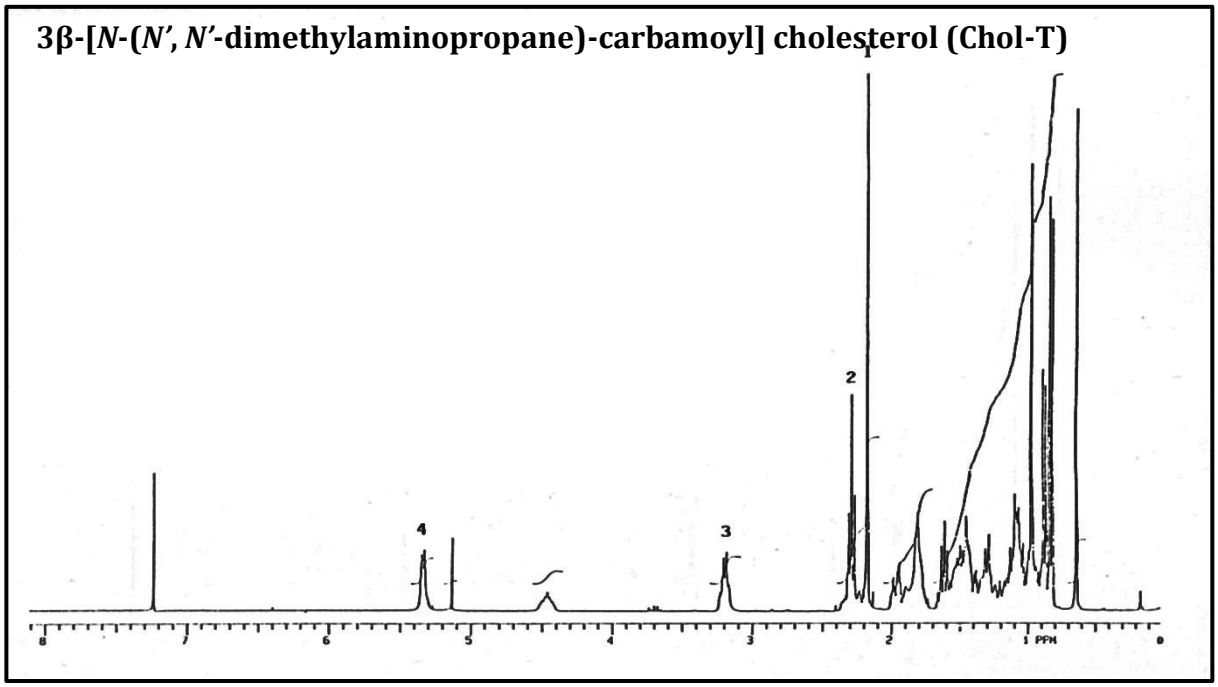

MS04: ^{1}H NMR (300 MHz, DMSO d^6): δ 0.66 (s, 3H, CCH_3), 0.86 (d, 6H, CHCH_3), 0.91 (d, 3H, CHCH_3), 0.99 (s, 3H, CCH_3), 3.88 (bs, 2H, NH_2), 4.38 (m, 1H, Chol-$H_{3\alpha}$), 5.33 (d, 1H, Chol-H_6), 7.93 (s, 1H, N*H*). MS, *m* / *z*, ES-TOF: 445.4358 [M+ H^+], 467.3932 [M + Na^+].

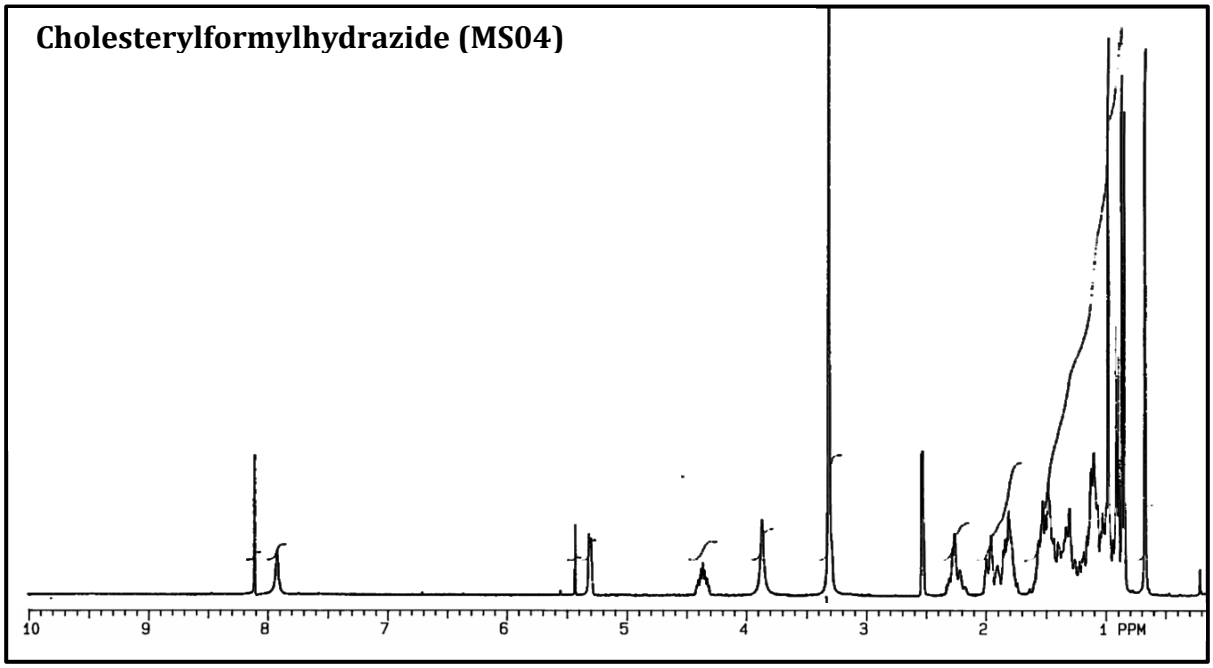

MS08: ^{1}H NMR (300 MHz, DMSO d^{6}): δ 0.64 (s, 3H, CCH_3), 0.83 (d, 6H, CHCH_3), 0.89 (d, 3H, CHCH_3), 0.96 (s, 3H, CCH_3), 4.3 (m, 1H, Chol-$H_{3\alpha}$), 5.34 (d, 1H, Chol-H_6). MS, *m* / *z*, ES-TOF: 545.09 [M+ H^{+}], 567.63 [M + Na^{+}].

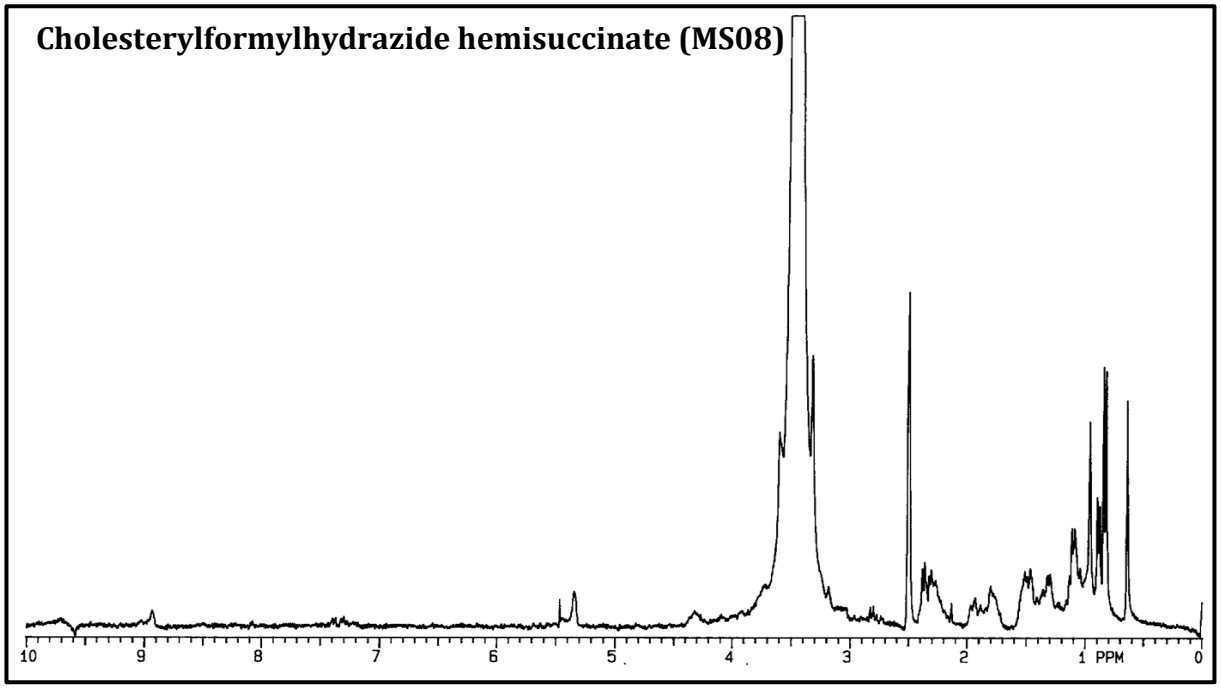

NHS-MS08: ^{1}H NMR (300 MHz, $CDCl_3$): δ 0.68 (s, 3H, CCH_3), 0.87 (d, 6H, CH-CH_3), 1.01 (s, 3H, C-CH_3), 2.72 (s, 2H, CONH-CH_2), 2.82 (bs, succinimide –CH_2CH_2-), 2.92 (d, 2H, OCO-CH_2), 4.54 (m, 1H, Chol-$H_{3\alpha}$), 5.38 (bd, 1H, Chol-H_6).

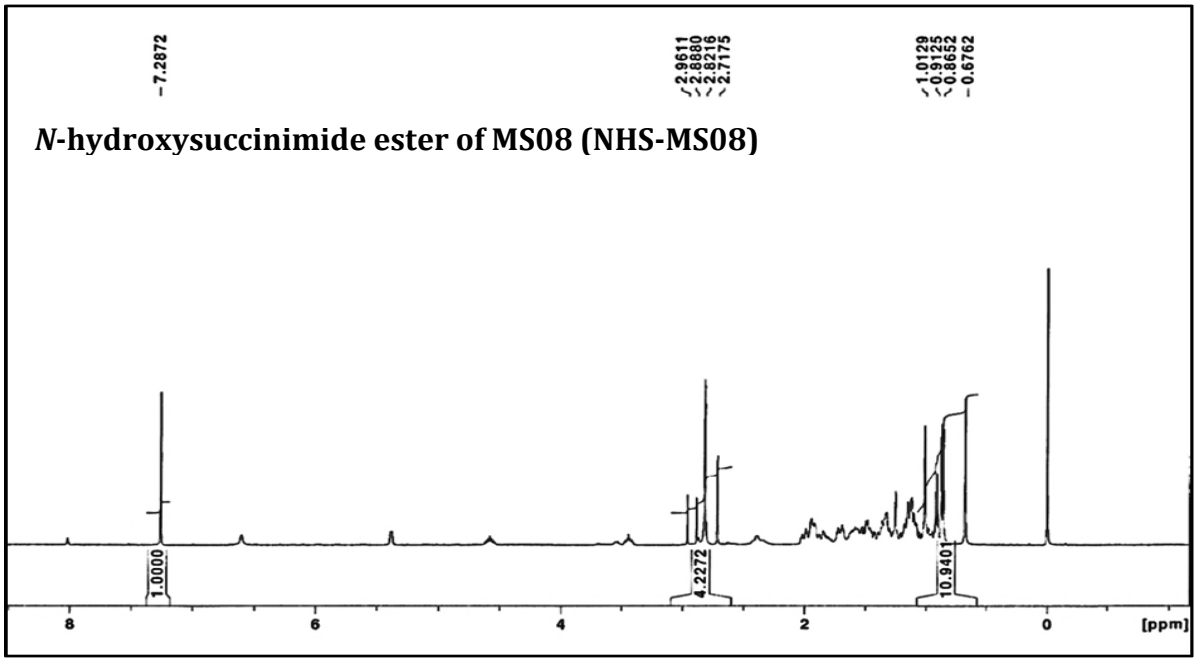

MS09: ^{1}H NMR (300 MHz, $CDCl_3$): δ 0.65 (s, 3H, CC*H*$_3$), 0.84 (d, 6H, CHC*H*$_3$), 0.88 (d, 3H, CHC*H*$_3$), 0.98 (s, 3H, CC*H*$_3$), 2.26 (s, 6H, NC*H*$_3$), 3.28 (q, CH_2CH_2NH), 4.48 (m, 1H, Chol-*H*$_{3\alpha}$), 5.35 (bs, 1H, Chol-*H*$_6$). MS, *m* / *z*, ES-TOF: 629.82 [M+ H^+].

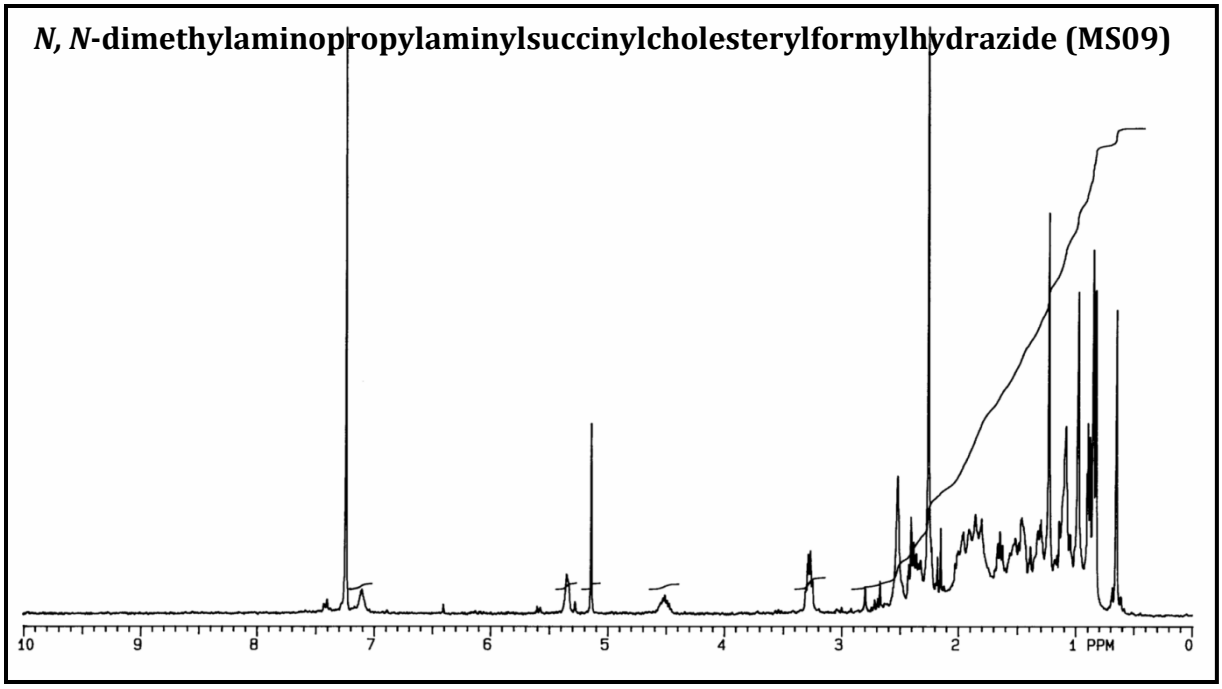

APPENDIX B

Review

Silencing breast cancer using siRNA gene knockdown technology: Potential therapeutic impact and progress in developing non-viral nanocarrier systems

Adhika Balgobind, Mario Ariatti and Moganavelli Singh*****

Department of Biochemistry, Non-Viral Gene Delivery Laboratory, School of Life Sciences, College of Agriculture, Engineering and Science, University of KwaZulu-Natal (Westville Campus), Private Bag X54001, Durban 4000, South Africa; E-Mails: adhikab@gmail.com (A.B); ariattim@ukzn.ac.za (M.A); singhm1@ukzn.ac.za (M.S)

*****Author to whom correspondence should be addressed; E-Mail: singhm1@ukzn.ac.za
Tel.: ; Fax:

Abstract

Breast cancer is prevalent globally as the second leading cause of cancer-related mortality among women, with approximately 1.4 million new cases diagnosed annually. The genetic perturbations associated with this serious public health problem are emerging in the face of intense scientific enquiry thus facilitating its classification, prognostication, and treatment. RNA interference (RNAi) technology, utilizing short interfering RNA (siRNA), has emerged as a novel and potentially powerful approach in the treatment strategy to silence disease-causing genes such as those associated with breast cancer. RNAi is an evolutionarily conserved biological mechanism of post-transcriptional gene silencing mediated by either degradation or translation arrest of target mRNA. In spite of its promise as a novel class of therapy, instability of the therapeutic nucleic acid and its poor cellular uptake have limited its usefulness and application as an ideal clinical therapeutic approach. Nanocarriers have emerged as essential components in siRNA delivery systems and their further development in this role is crucial for the successful achievement of gene silencing based therapeutics. In this review, we highlight research efforts exploring breast cancer therapeutic targets particularly suitable for siRNA strategies, such as angiogenesis, apoptosis, cell cycle regulation, and HER-2/*neu* gene targets. We further explore non-viral nanocarriers based on the use of lipids and polymers which show potential as safe and effective delivery systems.

Keywords: small interfering RNA (siRNA); breast cancer; non-viral gene delivery; lipids; polymers

Research Article

Cationic lipid based nanosystems associated with siRNA: Enhanced HER2/*neu* gene silencing in a breast cancer cell model in the presence of serum

Adhika Balgobind, Mario Ariatti and Moganavelli Singh*****

Department of Biochemistry, Non-Viral Gene Delivery Laboratory, School of Life Sciences, College of Agriculture, Engineering and Science, University of KwaZulu-Natal (Westville Campus), Private Bag X54001, Durban 4000, South Africa; E-Mails: adhikab@gmail.com (A.B); ariattim@ukzn.ac.za (M.A); singhm1@ukzn.ac.za (M.S)

*****Author to whom correspondence should be addressed; E-Mail: singhm1@ukzn.ac.za

Tel.: ; Fax:

Abstract

RNA interference technology, based on the use of siRNA, has emerged as a promising approach in the treatment strategy to suppress disease-causing genes such as those associated with breast cancer (BC). Despite its potential as a form of therapy, instability and poor cellular uptake of the therapeutic nucleic acid have posed daunting challenges. The major hurdle for siRNA-based therapy is the evolution of nontoxic, stable and efficient delivery systems to channel siRNA into target cells. Accordingly, this study assesses the efficacy of two cationic lipid-based delivery systems to deliver intact siRNA which would target the Human Epidermal Growth Factor Receptor 2 (HER2/*neu*) oncogene in a BC cell model.

Two cholesteryl cytofectins, 3β-[*N*-(*N'*, *N'*-Dimethylaminopropane)-carbamoyl] cholesterol (Chol-T) and *N*, *N*-Dimethylaminopropylaminylsuccinylcholesterylformylhydrazide (MS09), were synthesized for the purposes of this study. A series of cationic liposomes were formulated using an equimolar ratio of the respective cytofectins together with the neutral lipid dioleoylphosphatidylethanolamine (DOPE). Sterically stabilized or stealth liposomes contained a 0-5 mol.% 1,2-Distearoyl-*sn*-glycero-3-phosphoethanolamine-N-[methoxy(polyethylene glycol)-2000] (DSPE-PEG_{2000}) grafting.

Cryogenic-transmission electron microscopy (cryo-TEM) and dynamic light scattering measurements revealed that PEGylation generated smaller, defined structures when compared to their non-PEGylated counterparts. The hydrodynamic size ranges of the liposomal formulations and lipoplexes were 65-127 nm and 103-188 nm respectively, with moderate particle size distributions (polydispersity indices were <0.4). Liposomes bound and efficiently compacted siRNA as evidenced in band shift and ethidium bromide intercalation assays respectively, while nuclease digestion assays demonstrated that the degradative effect of serum on lipoplex-associated nucleic acid was minimal.

Cytotoxicity studies, involving the reduction of 3-(4, 5-dimethyl-2-thiazolyl)-2, 5-diphenyl-2H-tetrazolium bromide (MTT), indicated that the siRNA lipoplexes elicited a dose-dependent cytotoxic effect, with cell viability remaining above 50% respectively. Gene expression studies indicated that the Chol-T:DOPE (0% PEG)/siRNA complexes induced the highest HER2/*neu* silencing effect at all tested N/P charge ratios, as observed from the significant fold-increase in gene expression (> 10 000-fold, $P<0.001$). Western blot analysis further confirmed this trend and revealed a dose-dependent decrease in

HER2/*neu* protein expression levels as indicated by a 160.28, 163.89 and 212.80-fold decrease in protein expression relative to the untreated SKBR-3 cells. Furthermore, the most active non-PEGylated Chol-T formulations were less cytotoxic and exceeded the knockdown level of Lipofectamine® 3000 control (4.1-fold decrease). Results suggest that these cytofectin-based cationic liposomes with moderate degree of PEGylation have potential as vectors for trans-gene expression and HER2/*neu* siRNA gene silencing in BC cells.

Keywords: HER2/*neu*, small interfering RNA (siRNA); breast cancer; cationic lipids, PEGylation